



Mass spectrum prediction in non-minimal supersymmetric models

Dissertation
zur Erlangung des wissenschaftlichen Grades
Doctor rerum naturalium
(Dr. rer. nat.)

vorgelegt von

Dipl.-Phys. Alexander Voigt
geboren am 14.08.1984 in Dresden

Institut für Kern- und Teilchenphysik
der Technischen Universität Dresden
2014

Eingereicht am 16.06.2014

Verteidigt am 18.09.2014

1. Gutachter: Prof. Dr. Dominik Stöckinger

2. Gutachter: Prof. Dr. Benjamin Allanach

Abstract

Supersymmetry is an attractive extension of the Standard Model (SM) of particle physics. The minimal supersymmetric extension (MSSM) provides gauge coupling unification, a dark matter candidate particle and can explain the breaking of the electroweak symmetry dynamically. However, it suffers from the little hierarchy and the μ -problem. Non-minimal supersymmetric extensions of the SM with a larger particle content or a higher symmetry can evade the problems of the MSSM. Such models may be well-motivated by Grand Unified Theories (GUTs) and can provide a rich new phenomenology with an extended Higgs sector, exotic particles, additional interactions and a close connection to String Theory. Interesting examples are the Next-to Minimal Supersymmetric Standard Model (NMSSM), which is motivated by the μ -problem, and the Exceptional Supersymmetric Standard Model (E_6 SSM), which is inspired by E_6 GUTs.

For phenomenological investigations of supersymmetric (SUSY) models the pole mass spectrum must be calculated from the fundamental model parameters. This task, however, is non-trivial as the spectrum must be consistent with measured low-energy observables (fine-structure constant, Z boson pole mass, muon decay etc.) as well as electroweak symmetry breaking and potential universality conditions on the soft supersymmetry breaking parameters at the GUT scale. Programs, which calculate the SUSY mass spectrum consistent with constraints of this kind are called spectrum generators.

In this thesis four different contributions to the prediction of mass spectra and model parameters in non-minimal SUSY models are presented. (i) One-loop matching corrections of the E_6 SSM gauge and Yukawa couplings to the SM are calculated to increase the precision of the mass spectrum prediction in the constrained E_6 SSM. (ii) The β -functions of vacuum expectation values (VEVs) are calculated in a general and supersymmetric gauge theory at the one- and two-loop level. The results enable an accurate calculation of the renormalization group running of the VEVs in non-minimal SUSY models. (iii) An NMSSM extension of Softsusy, a spectrum generator for the MSSM, is implemented. It represents a precise alternative to the already existing spectrum generator NMSPEC. (iv) FlexibleSUSY is presented, a general framework which creates a fast, modular and precise spectrum generator for any user-defined SUSY model. It represents a generalization of the hand-written SUSY spectrum generators and allows the study of a large variety of new SUSY models easily with high precision.

Contents

1	Introduction	1
2	Supersymmetry	5
2.1	The minimal supersymmetric standard model (MSSM)	6
2.1.1	Advantages of the MSSM	7
2.1.2	Problems of the MSSM	7
2.2	Non-minimal supersymmetric models	8
2.2.1	Examples for non-minimal models	9
2.2.2	Advantages of non-minimal models	9
2.2.3	Problems of non-minimal models	10
3	Calculation of low-energy gauge and Yukawa couplings in the E_6SSM	13
3.1	Motivation	13
3.2	Calculation of the Yukawa couplings	16
3.3	Implementation into a CE_6 SSM spectrum generator	17
3.4	Numerical evaluation and application	20
3.4.1	Reduced matching scale dependency	20
3.4.2	Parameter scan	21
3.4.3	Parameter space exclusion	23
3.4.4	Updating benchmark points from the literature	25
3.5	Summary and conclusion	26
4	Renormalization of vacuum expectation values	29
4.1	Motivation	29
4.2	Calculation of the VEV counter-term	30
4.2.1	Background field method	30
4.2.2	Lagrangian	32
4.2.3	Renormalization	34
4.2.4	Calculation of the anomalous dimensions	38
4.3	Result for the VEV β -function	39
4.3.1	General gauge theory	39
4.3.2	Kinetic mixing	40
4.3.3	Supersymmetric gauge theory	41
4.4	Application to the MSSM and NMSSM	43
4.4.1	MSSM	43
4.4.2	NMSSM	44
4.5	Summary and conclusion	46

5	Next-to-minimal Softsusy	47
5.1	Motivation for a NMSSM extension of Softsusy	47
5.2	The NMSSM	48
5.3	Physical problem statement	49
5.4	Implementation	51
5.4.1	Class hierarchy	51
5.4.2	Implementation of the β -functions	55
5.4.3	Solving the boundary value problem	57
5.4.4	Calculation of the pole mass spectrum	60
5.5	Tests and comparison to NMSPEC	61
5.6	Summary and conclusion	63
6	FlexibleSUSY – A spectrum generator generator	65
6.1	Motivation	65
6.2	General physical problems	67
6.2.1	Definition of the model	68
6.2.2	Boundary conditions	69
6.2.3	Calculation of pole masses	71
6.3	Implementation	71
6.3.1	Creating the C++ source code	72
6.3.2	Class hierarchy	77
6.3.3	Boundary conditions and the FlexibleSUSY model file	82
6.3.4	Solving the boundary value problem	91
6.3.5	Calculation of the pole masses	95
6.3.6	Summary	96
6.4	Applications	98
6.4.1	Run-time comparison	98
6.4.2	Comparison of Higgs masses in supersymmetric models	100
6.4.3	Influence of loop corrections of different order on the pole mass spectrum	109
6.4.4	Influence of GUT threshold corrections on the Higgs mass	112
6.5	Summary and conclusion	115
7	Summary	117
A	Group invariants	121
B	MSSM field content	123
C	The E_6SSM	125
C.1	Gauge group	125
C.2	Field content	125
C.3	Superpotential	127
C.4	The constrained E_6 SSM	129

C.5	Mass eigenstates	130
C.5.1	Higgs sector	130
C.5.2	Inert Higgs sector	131
C.5.3	Survival Higgs sector	132
C.6	Self-energies	132
C.6.1	W boson	132
C.6.2	Fermions	134
C.7	Gauge coupling threshold corrections	136
D	NMSSM SLHA input template file	139
E	CMSSM speed test SLHA input template file	141
	Bibliography	143

Chapter 1

Introduction

The physics of elementary particles aims for a unified description of the fundamental constituents and forces in the universe. The Standard Model (SM) of particle physics, which was supported by the discovery of a Higgs boson in 2012, is a very successful description of all known particles as well as the electromagnetic, weak and strong interactions. However, the SM does neither describe gravity nor does it contain particles which are candidates for non-baryonic dark matter. In addition, it suffers from the hierarchy problem and fails to correctly explain observations such as the anomalous magnetic moment of the muon for example. Supersymmetric (SUSY) extensions of the SM can provide solutions to all of these problems. Thereby the space-time symmetries are non-trivially extended so that fundamental relations between fermions and bosons arise. A supersymmetric theory must therefore contain as many fermionic degrees of freedom as bosonic ones. For this reason supersymmetric extensions of the SM introduce many new bosonic and fermionic fields, which leads to a rich and interesting phenomenology.

The Minimal Supersymmetric Standard Model (MSSM) has been extensively studied in the past decades. It provides gauge coupling unification, which allows a unification of the three forces, contains a non-baryonic dark matter candidate particle and can explain the origin of the electroweak symmetry breaking. However, the MSSM is not without problems as well: Parameter scenarios which lead to the measured value of the Higgs mass often re-introduce the hierarchy problem. Furthermore, it contains the dimensionful parameter μ , whose value is well-motivated to be of the order of the gauge coupling unification scale, $O(10^{16})$ GeV, as well as of the order of the electroweak scale, $O(10^2)$ GeV. This tension is called the μ -problem.

Non-minimal supersymmetric models with a larger particle content or a higher symmetry can solve the problems of the MSSM. Such models may be well-motivated by Grand Unified Theories (GUTs) and can provide a rich new phenomenology with an extended Higgs sector, exotic particles, additional interactions and close connections to String Theory. Interesting examples are the Next-to Minimal Supersymmetric Standard Model (NMSSM) and the Exceptional Supersymmetric Standard Model (E_6 SSM). The former extends the Higgs sector of the MSSM by an additional singlet field to solve the μ -problem. The E_6 SSM is motivated by E_6 GUTs and provides a matter particle content which fits into fundamental representations of the E_6 . In addition it introduces an extra $U(1)_N$ gauge symmetry, which leads to a new gauge boson Z' .

For phenomenological investigations of supersymmetric models many complicated computations must be performed. Given the Lagrangian of the model, the first step is usually to calculate the pole mass spectrum given a set of fundamental theory input parameters. This mass spectrum can then be used to calculate further observables, such as for example particle decays, cross sections or the dark matter relic density. These observables can be compared with measurements in phenomenological studies to search for allowed and excluded model parameter space regions. The pole masses and the decays may as well be used in event generators and detector simulations to study how decays of SUSY particles manifest in a detector.

The calculation of the pole mass spectrum in a SUSY model is a non-trivial task: The model is required to correctly predict the measured low-energy observables, such as the fine-structure constant, the Z boson pole mass and the muon decay for example. This requirement can be ensured by a matching to the Standard Model, which imposes constraints on the model parameters. Furthermore, the model must contain massive W and Z gauge bosons and fermions. Their mass terms can be generated by a spontaneous breaking of the electroweak symmetry. In order for this symmetry breaking to happen, the scalar Higgs potential must allow for a non-trivial ground state (vacuum expectation value, VEV). This requirement imposes further implicit constraints upon the model parameters, as they must generate a suitably shaped Higgs potential. In addition, in some models further universality conditions on the soft-breaking parameters are imposed at the gauge coupling unification scale. All of these constraints must be fulfilled simultaneously by a consistent set of model parameters. Finding such a set is challenging, but well-suited algorithms exist for this purpose. If a consistent set of parameters is available the pole mass spectrum must be calculated with an appropriate precision, which is of the order or below the experimental uncertainty. For this purpose one- and two-loop corrections have to be taken into account. Programs which search for a consistent set of model parameters and calculate the pole mass spectrum are called spectrum generators.

This thesis makes four contributions to the prediction of mass spectra and $\overline{\text{DR}}$ parameters in non-minimal supersymmetric models.

In Section 3 the calculation of one-loop matching corrections of the $E_6\text{SSM}$ gauge and Yukawa couplings to the SM will be presented, which were unknown so far. These corrections are implemented into an existing $CE_6\text{SSM}$ spectrum generator. It will be shown that their incorporation reduces the unphysical dependence of the pole mass spectrum on the matching scale, which leads to a reduced uncertainty of the predicted mass spectrum. Afterwards, a parameter scan is performed to confront the model with exclusion limits from current experiments.

In Section 4 the β -functions of vacuum expectation values will be calculated in a general and supersymmetric gauge theory in the $\overline{\text{DR}}$ scheme at the one- and two-loop level. These β -functions were known so far only in the MSSM and $E_6\text{SSM}$. The general expressions, however, were unknown. They can be used in spectrum generators for an accurate calculation of the renormalization group running of VEVs.

In Section 5 an extension of the MSSM spectrum generator `Softsusy` will be presented. The extension is able to calculate the $\overline{\text{DR}}$ parameters, the pole mass spectrum and particle mixings in the Z_3 -symmetric and Z_3 -violating NMSSM consistent with

low-energy observables, electroweak symmetry breaking and high-energy universality constraints. This new NMSSM spectrum generator implements the complete two-loop β -functions, one-loop self-energies and tadpoles as well as leading two-loop Higgs mass corrections. Thereby it incorporates many precision corrections, which are neglected in the already existing spectrum generator NMSPEC. This enables, among other things, to estimate the theory uncertainty of the predicted NMSSM mass spectrum by comparing the output of the two programs.

The by-hand programming of a precise spectrum generator for a new SUSY model is a very challenging task, because complicated expressions, such as two-loop β -functions, one-loop self-energies and tadpole diagrams have to be calculated and implemented into a computer program. To simplify this task and to allow studies of a wide range of non-minimal SUSY models to be carried out easily with a high precision, the spectrum generator framework FlexibleSUSY will be presented in Section 6. FlexibleSUSY is a Mathematica package which creates a spectrum generator for any user-defined SUSY model. For this purpose several physical problems must be solved at a general level: (i) A user interface must be created, which allows one to define physical boundary conditions on the model. (ii) Expressions for the mass matrices, self-energies, tadpole diagrams and $\overline{\text{DR}}$ one- and two-loop β -functions must be calculated. (iii) The matching of the SUSY model to the Standard Model via gauge coupling threshold corrections and one-loop Yukawa couplings must be generalized. (iv) General numerical routines must be provided to find the minimum of the (arbitrarily complicated) one-loop effective Higgs potential. (v) An algorithm must be programmed which finds a set of $\overline{\text{DR}}$ model parameters consistent with all user-defined boundary conditions. (vi) The pole masses of all particles must be calculated from the $\overline{\text{DR}}$ parameters with one-loop precision or higher. The technical solutions of these problems will be presented in Section 6.3. In Section 6.4 several physical applications of FlexibleSUSY will be presented, including a comparison of the Higgs mass in four different SUSY models and a study of the influence of GUT threshold corrections. Not only will these applications illustrate physical features of non-minimal SUSY models, but also demonstrate FlexibleSUSY's wide range and simplicity of use. FlexibleSUSY thereby is intended to represent a powerful tool to study a large variety of new SUSY models easily with high precision.

Chapter 2

Supersymmetry

Supersymmetry is the only possibility to non-trivially unify the spacetime symmetries, described by the the Poincaré group, with an internal symmetry [1, 2].¹ The resulting symmetry group is called the Super-Poincaré group. It contains new supersymmetry generators, which transform fermions into bosons and vice versa. Thus, supersymmetry combines fermions and bosons in the same representation of the Super-Poincaré group and requires that each fermion has a bosonic partner with the same mass. Besides unification of the Poincaré and an internal symmetry group, supersymmetry has the following features:

- Due to a non-renormalization theorem [3, 4, 5, 6, 7, 8], scalar self-energies are protected against quadratic divergences. This avoids the so-called “hierarchy problem”, where a large fine-tuning between the bare Higgs mass and its counter-term would be required to create a Higgs pole mass of the measured value of 125.9 GeV [9, 10, 11]. This property is preserved in softly-broken supersymmetric theories [12], if the mass splitting between the heavy fermion and their superpartners is smaller or of the order of the Higgs mass.
- An implementation of local supersymmetry implies an invariance under local coordinate transformations [13]. This provides a connection to Einstein’s theory of General Relativity.

However, exact supersymmetry has not been observed in nature so far, because no superpartners to the Standard Model particles with the same mass have been found [11]. Therefore, if supersymmetry exists in nature, it must be broken. Soft breaking of supersymmetry [12] is an attractive way to increase the masses of the superpartners to hide them from current experimental searches, and at the same time preserve the cancellation of quadratic divergences in scalar self-energies. A drawback of softly breaking supersymmetry is that one introduces $O(100)$ new parameters, which decreases the predictivity of the theory. However, the number of new parameters can be reduced by using well-motivated supersymmetry breaking models, such as the “minimal SuperGRAvity Model of supersymmetry breaking” (mSUGRA) [14], “Gauge Mediated Supersymmetry Breaking” (GMSB) [15, 16, 17] or “Anomaly Mediated Supersymmetry Breaking” (AMSB) [18, 19].

¹Hereby one assumes locality of the interaction, causality, positivity of energy and finiteness of the number of particles.

2.1 The minimal supersymmetric standard model (MSSM)

The Minimal Supersymmetric Standard Model (MSSM) [20] is a $N = 1$ softly broken supersymmetric extension of the Standard Model (SM), with minimal field content. The superfields of the MSSM and their quantum numbers can be found in Table B.1 and Table B.2. To be supersymmetry invariant, each Standard Model spin 1/2 fermion field has a scalar spin 0 superpartner, called sfermion; the spin 1 gauge fields get fermionic superpartners with spin 1/2, called gauginos; and the spin 0 SM Higgs doublet components get fermionic superpartners with spin 1/2, called higgsinos. For anomaly cancellation and due to the analyticity of the superpotential, a second Higgs doublet must be introduced, which generates mass terms for the down-type fermions.

Allowing for all gauge and supersymmetry invariant terms in the superpotential would lead to rapid proton decay due to sfermion exchange [20, 21]. To avoid this R -parity is introduced, which forbids all lepton and baryon number violating terms [22, 6, 23, 24, 25]. The R -parity invariant MSSM superpotential reads

$$\mathcal{W}_{\text{MSSM}} = \mu(H_1 H_2) - y_{ij}^e (H_1 L_i) \bar{E}_j - y_{ij}^d (H_1 Q_i) \bar{D}_j - y_{ij}^u (Q_i H_2) \bar{U}_j, \quad (2.1)$$

where $(AB) = \epsilon_{DE} A^D B^E$ is the invariant product of the fundamental (**2**) representation of $SU(2)$, with $\epsilon_{DE} = -\epsilon_{ED}$. The soft-breaking part of the MSSM Lagrangian has the form

$$\begin{aligned} -\mathcal{L}_{\text{MSSM,soft}} = & + (m_q^2)_{ij} \tilde{q}_{iL}^* \tilde{q}_{jL} + (m_u^2)_{ij} \tilde{u}_{iR}^* \tilde{u}_{jR} + (m_d^2)_{ij} \tilde{d}_{iR}^* \tilde{d}_{jR} + (m_\ell^2)_{ij} \tilde{\ell}_{iL}^* \tilde{\ell}_{jL} \\ & + (m_e^2)_{ij} \tilde{e}_{iR}^* \tilde{e}_{jR} + m_{h_1}^2 |h_1|^2 + m_{h_2}^2 |h_2|^2 + [B\mu(h_1 h_2) + \text{h. c.}] \\ & + \left[(y^e A^e)_{ij} (h_1 \tilde{\ell}_{iL}) \tilde{e}_{jR}^* + (y^d A^d)_{ij} (h_1 \tilde{q}_{iL}) \tilde{d}_{jR}^* \right. \\ & \quad \left. + (y^u A^u)_{ij} (\tilde{q}_{iL} h_2) \tilde{u}_{jR}^* + \text{h. c.} \right] \\ & + \frac{1}{2} \left(M_1 \tilde{B} \tilde{B} + M_2 \tilde{W}^i \tilde{W}^i + M_3 \tilde{g}^a \tilde{g}^a + \text{h. c.} \right). \end{aligned} \quad (2.2)$$

An attractive and often studied supersymmetry breaking model of the MSSM is the so-called “minimal SuperGRAvity model of supersymmetry breaking” (mSUGRA) [14]. It requires all soft-breaking parameters to be real and the unification of all soft-breaking scalar mass parameters $(m_f^2)_{ij}$, all soft-breaking trilinear couplings A_{ij}^f and all gaugino masses M_i at the gauge coupling unification scale M_X :

$$(m_f^2)_{ij}(M_X) = m_0^2 \delta_{ij} \quad (f = q, \ell, u, d, e; i, j = 1, 2, 3), \quad (2.3a)$$

$$A_{ij}^f(M_X) = A_0 \quad (f = u, d, e; i, j = 1, 2, 3), \quad (2.3b)$$

$$M_i(M_X) = M_{1/2} \quad (i = 1, 2, 3). \quad (2.3c)$$

The so constructed variant of the MSSM is called the Constrained MSSM (CMSSM), which has only five free parameters: $\text{sign } \mu$, m_0^2 , $M_{1/2}$, A_0 , $\tan \beta$. Here, the parameter $\tan \beta$ is defined to be the ratio of the vacuum expectation values of the Higgs fields h_2 and h_1 .

2.1.1 Advantages of the MSSM

Besides being a softly broken supersymmetric extension of the Standard Model with a minimal particle content, the MSSM has the following attractive properties:

Gauge coupling unification Due to the new SUSY particles (gauginos, sfermions and the extra Higgs doublet), it is possible that all three gauge couplings unify at the scale $M_X \sim 10^{16}$ GeV. This happens in scenarios where all SUSY particles have masses of the order 1 TeV. In reverse, if one requires gauge coupling unification, one already restricts the allowed MSSM parameter space.

Radiative electroweak symmetry breaking In certain CMSSM scenarios the renormalization group running can lead to a value of $m_{h_2}^2(M_S) < 0$, where M_S is the mass scale of the new SUSY particles. This deforms the Higgs potential such, that the Higgs fields can develop a non-zero ground state, which leads to a spontaneous breaking of the electroweak symmetry (radiative electroweak symmetry breaking).

Dark matter candidate In the MSSM the lightest supersymmetric particle (LSP) is absolutely stable due to the imposed R -parity. In many MSSM scenarios the lightest neutralino $\tilde{\chi}_1^0$ is the LSP. Since it is electrically neutral, it interacts with other matter only via weak interactions and is therefore a candidate for non-baryonic dark matter [26, 27].

2.1.2 Problems of the MSSM

Besides the fact that no superpartner to any of the Standard Model particles has been found so far, the MSSM has several theoretical problems:

The μ -problem The superpotential of the MSSM (2.1) contains the bilinear Higgs coupling term $\mu(H_1 H_2)$ with the parameter μ of dimension of mass. The value of μ must not be zero, because this would lead to very light charginos, which have not been observed by experiment so far [11]. In a Grand Unified Theory (GUT) the superpotential (2.1) is assumed to be generated by some mechanism at the GUT scale M_X , which would lead to a μ value of the order $\mu \sim M_X$. However, in order to make electroweak symmetry breaking possible, μ must be constrained at tree-level by the condition

$$\frac{1}{2}m_Z^2 = \frac{m_{h_1}^2 - m_{h_2}^2 \tan^2 \beta}{\tan^2 \beta - 1} - |\mu|^2. \quad (2.4)$$

Here $m_{h_i}^2$ are the soft-breaking mass parameters of the scalar Higgs doublets h_i and m_Z is the mass of the Z boson. Eq. (2.4) suggests that $\mu \sim m_Z$, as long as there is no large cancellation between the two terms on the right-hand side. This tension between $\mu \sim M_X$ and $\mu \sim m_Z$ is called the μ -problem.

The Higgs mass fine-tuning In the MSSM it is difficult to raise the lightest CP-even Higgs pole mass to the measured value of 125.9 GeV [9, 10, 11]. The reason is that the tree-level Higgs mass is required to be small, because it is constrained by the condition

$$(m_h^{\text{tree}})^2 < \min(m_A^2, m_Z^2)c_{2\beta}^2. \quad (2.5)$$

Since in most MSSM scenarios the mass of the CP-odd Higgs boson, m_A , is larger than m_Z , the tree-level Higgs boson mass must be below m_Z . This means that the CP-even Higgs pole mass can be at maximum

$$(m_h^{\text{pole}})^2 \approx m_Z^2 c_{2\beta}^2 + \Delta m_h^2, \quad (2.6)$$

where Δm_h^2 are loop corrections. Eq. (2.6) implies that, in order to obtain a Higgs pole mass of the order 125.9 GeV, large loop corrections of the order 85 GeV or more are required. Such large loop corrections can be achieved in scenarios where one of the stop masses is much heavier than the top mass. However, such scenarios will automatically re-introduce the hierarchy problem, as discussed above (little hierarchy problem).

Baryon-antibaryon asymmetry In the MSSM the generation of the baryon-antibaryon asymmetry in the universe by a 1st order phase transition is only possible in extreme scenarios [28].

Connection to gravity models Due to its symmetry group and particle content the MSSM allows the connection to a large variety of gravity models with extended gauge groups. However, this also makes the MSSM less predictive, because it does not favor a specific gravity model.

Anomalous magnetic moment of the muon Current fits of the CMSSM parameters to LHC data favor parameter regions with heavy SUSY particles [29]. However, in these regions it is difficult for the CMSSM to correctly predict the measured value of the anomalous magnetic moment of the muon a_μ [30]. The reason is that the required large contributions from the new SUSY particles are usually too small if the mass spectrum is heavy. In the general MSSM, however, it is still possible to simultaneously fulfill all experimental constraints and explain the measured value of a_μ [31, 32].

2.2 Non-minimal supersymmetric models

With non-minimal supersymmetric models all supersymmetric extensions of the SM or the MSSM are denoted, which extend the particle content, introduce extra gauge symmetries, add R -parity violating superpotential terms, or increase the number of SUSY generators ($N > 1$).

2.2.1 Examples for non-minimal models

Most non-minimal SUSY models address the problems of the MSSM by introducing new particles and/or extending the gauge group. Examples for extended models are

- the *Next-to Minimal Supersymmetric Standard Model (NMSSM)* and its variants [33, 34, 35, 36, 37, 38], which introduces an extra gauge singlet superfield S to solve the μ -problem of the MSSM. Furthermore, it can reduce the fine-tuning problem due to extra, positive contributions to the tree-level Higgs mass. However, the model suffers from the so-called domain-wall problem. See Ref. [37] for a detailed review of the NMSSM.
- the *$U(1)'$ -extended Supersymmetric Standard Model (USSM)* and its variants, which extends the NMSSM by an extra $U(1)'$ gauge symmetry to avoid the domain wall problem [39, 40, 41]. It provides an extra Z' gauge boson and a corresponding superpartner.
- the *Exceptional Supersymmetric Standard Model (E_6 SSM)*, which extends the particle content of the USSM such, that the chiral superfields fill complete (27) representations of the E_6 [42]. Since the E_6 is a simple gauge group, the $U(1)'$ quantum numbers of the chiral superfields are automatically predicted. A brief introduction can be found in Appendix C.
- the *Minimal R -symmetric Supersymmetric Standard Model (MRSSM)*, which introduces a continuous R -symmetry in order to solve the supersymmetric flavour problem [43] by suppressing the off-diagonal matrix elements of the sfermion mass matrices [44].

2.2.2 Advantages of non-minimal models

Solution of the μ -problem The NMSSM was invented to solve the μ -problem, i.e. solving the tension between $\mu \sim m_Z$ and $\mu \sim M_X$. It introduces a gauge singlet superfield S with the superpotential

$$\mathcal{W}_{\text{NMSSM}}^{Z_3} = \mathcal{W}_{\text{MSSM}}(\mu = 0) + \lambda S(H_1 H_2) + \frac{\kappa}{3} S^3, \quad (2.7)$$

where the μ -term of the MSSM is explicitly forbidden. Depending on the shape of the Higgs potential, the scalar component of the singlet superfield can have a non-trivial vacuum expectation value v_3 of the order of the TeV scale. This will dynamically generate an effective μ -term $\mu_{\text{eff}} = \lambda v_3 / \sqrt{2}$ of the order of the SUSY scale M_S .

Reduction of the Higgs mass fine-tuning Non-minimal supersymmetric models can attenuate the Higgs mass fine-tuning by increasing its tree-level mass. This avoids the necessity of large loop corrections to the Higgs self-energy, which again avoids the necessity of a large stop mixing. In the NMSSM, for example, the tree-level mass

is enhanced by a positive F -term contribution from the extra scalar, which leads to a maximum pole mass of [37]

$$(m_h^{\text{pole}})^2 \approx m_Z^2 c_{2\beta}^2 + \frac{\lambda^2 v^2}{2} s_{2\beta}^2 + \Delta m_h^2. \quad (2.8)$$

The tree-level Higgs mass is increased further in models which have, in addition to a Higgs singlet, an extra $U(1)'$ gauge symmetry, as in the USSM [39] or E_6 SSM [42]. In these models the tree-level mass gains extra contributions from the D -term of the new $U(1)'$, which leads to a maximum pole mass of

$$(m_h^{\text{pole}})^2 \approx m_Z^2 c_{2\beta}^2 + \frac{\lambda^2 v^2}{2} s_{2\beta}^2 + \frac{m_Z^2}{4} \left(1 + \frac{1}{4} c_{2\beta}\right)^2 + \Delta m_h^2. \quad (2.9)$$

Here the necessary loop corrections can be reduced to $\Delta m_h \approx 78$ GeV for large values of $\tan \beta$ [45].

Baryon-antibaryon asymmetry In NMSSM scenarios it is possible to generate the observed baryon-antibaryon asymmetry with less extreme parameter scenarios than in the MSSM [46].

Connection to gravity models Non-minimal supersymmetric models with larger gauge groups, like $SU(5)$, $SO(10)$ or E_6 and/or a larger field content, which fits into representations of these gauge groups, can provide a close connection to string-inspired supergravity models [47, 48, 49, 42], as for example the heterotic $E_8 \times E_8$ String Theory [50, 51, 52].

2.2.3 Problems of non-minimal models

Domain walls In the scale invariant NMSSM superpotential (2.7) a discrete Z_3 symmetry is imposed by hand to forbid the μ -term. However, such a discrete symmetry can generate phenomenological problems [53]: When the electroweak symmetry is broken in the early universe, regions with different ground states develop, each related by a Z_3 transformation. The borders of these regions are so-called domain walls, which have not been observed in nature. The USSM solves this problem by introducing a continuous $U(1)'$ gauge symmetry and adjusting the $U(1)'$ charges of the superfields such that Z_3 -violating superpotential terms are forbidden.

Incomplete group representations One of the motivations of the E_6 SSM is the unification of all matter fields into complete $(\mathbf{27})$ representations of the E_6 [42]. However, to enable gauge coupling unification two so-called survival Higgs doublets H' and \bar{H}' are added. They originate from incomplete $(\mathbf{27})'$ and $(\overline{\mathbf{27}})'$ representations, thereby spoiling the unification of the all matter fields into complete representations.

The μ' -problem The E_6 SSM solves the μ -problem of the MSSM by forbidding the μ -term and let an effective μ -term be dynamically generated by the VEV of a singlet field. To enable gauge coupling unification, two so-called survival Higgs doublets H' and \bar{H}' are added to the model. They carry opposite $U(1)_N$ charge to ensure anomaly cancellation. However, this allows a superpotential term of the form $\mu'(H'\bar{H}')$ with a coupling μ' with dimension of a mass. The parameter μ' must not be zero to avoid very light charged survival higgsinos. On the other hand, if one assumes the superpotential to be generated by some mechanism at the GUT scale M_X , one would expect μ' to be of the order of M_X . However, to enable gauge coupling unification μ' is required to be of the order 10 TeV. This tension between $\mu' \sim M_X$ and $\mu' \sim 10$ TeV is called the μ' -problem, analogous to the μ -problem of the MSSM.

Chapter 3

Calculation of low-energy gauge and Yukawa couplings in the E_6 SSM

3.1 Motivation

The Exceptional Supersymmetric Standard Model (E_6 SSM) [42] is a supersymmetric gauge theory, which is inspired by Grand Unified Theories (GUTs) with an E_6 gauge symmetry. It solves the μ -problem of the MSSM and can reduce the Higgs mass fine-tuning due to extra contributions to its tree-level mass matrix. The E_6 gauge symmetry is broken at the GUT scale, M_X , to the direct product of the Standard Model gauge group and an extra $U(1)_N$ gauge symmetry

$$E_6 \rightarrow SU(3)_c \times SU(2)_L \times U(1)_Y \times U(1)_N. \quad (3.1)$$

The matter content of the E_6 SSM fills three generations of complete fundamental (27) representations of the E_6 group and is listed in Table C.1. Thereby, it extends the MSSM field content with three generations of Standard Model gauge group singlet fields S_i ($i = 1, 2, 3$), two generations of inert Higgses $H_{1\alpha}, H_{2\alpha}$ ($\alpha = 1, 2$) and three generations of exotic colored fields X_i, \bar{X}_i . Due to the additional $U(1)_N$ gauge symmetry, the E_6 SSM includes an extra vector superfield V_N , which contains a gauge boson B'_μ and its superpartner. Furthermore, two extra survival Higgs doublets H' and \bar{H}' are introduced to ensure gauge coupling unification. A more detailed description of the E_6 SSM can be found in Appendix C.

In Ref. [54] the constrained E_6 SSM (CE_6 SSM) was constructed, which is defined by universality conditions of the soft-breaking parameters at the GUT scale, see Eq. (C.12) in Appendix C.4. The resulting model has the following 12 free parameters

$$\lambda_i, \kappa_i \ (i = 1, 2, 3), \tan \beta, v_3, \mu', B\mu', m_{h'}^2, m_{\bar{h}'}^2. \quad (3.2)$$

The λ_i and κ_i are Yukawa-type superpotential couplings, which couple the third generation singlet field to the Higgs doublets and colored exotics, respectively. See Appendix C.3 for a description of the E_6 SSM superpotential. The mass dimensional superpotential parameter μ' is analogous to the μ -parameter in the MSSM and couples the two survival Higgs doublets. In the E_6 SSM the scalar components of

the third generation Higgs doublets h_{13} , h_{23} and of the scalar s_3 get VEVs v_1 , v_2 , v_3 , respectively. As in the MSSM, the ratio v_2/v_1 is a free parameter and is called $\tan\beta$. The soft-breaking survival Higgs sector parameters $B\mu'$, $m_{h'}^2$ and $m_{\tilde{h}'}^2$ remain unfixed, because this sector originates from the two separate incomplete $(\mathbf{27})'$ and $(\mathbf{27})'$ representations.

Ref. [54] describes a CE_6 SSM spectrum generator, which implements the universality constraints (C.12) to predict the pole masses of the new E_6 SSM particles using a minimal set of parameters. This spectrum generator considers the Standard Model to be an effective theory of the E_6 SSM, where the new E_6 SSM particles have been integrated out. At the same time, the CE_6 SSM is required to correctly predict the masses of the Standard Model (SM) fermions m_f and gauge couplings g_i^{SM} at the Z mass scale m_Z^{pole} . In the spectrum generator [54], this requirement is ensured by using the known SM gauge and Yukawa couplings as low-energy input to predict the E_6 SSM gauge and Yukawa couplings. This prediction has the general form

$$g_i^{\text{E}_6\text{SSM}}(\mu) = g_i^{\text{SM}}(\mu) + \Delta g_i(\mu), \quad (3.3)$$

$$y_f^{\text{E}_6\text{SSM}}(\mu) = y_f^{\text{SM}}(\mu) + \Delta y_f(\mu), \quad (3.4)$$

where $\Delta g_i(\mu)$ and $\Delta y_f(\mu)$ are so-called threshold corrections. These threshold corrections appear when integrating out the heavy E_6 SSM particles and are in general non-zero. The general form of the corrections $\Delta g_i(\mu)$ is well known and may be found in Ref. [55]. The scale μ is the so-called matching scale, at which the transition between the full and the effective theory is performed. The general results in [55] show, that in case only scalars and fermions are integrated out (in the $\overline{\text{MS}}$ scheme), $\Delta g_i(\mu)$ contains only logarithmic terms of the form $\log(\mu/m_i)$.¹ Therefore, $\Delta g_i(\mu)$ is small if all particle masses m_i are degenerate and the matching scale is chosen to be of the order the particle masses.

For simplicity the spectrum generator in Ref. [54] neglects threshold corrections. However, since the CE_6 SSM mass spectrum is usually very split, these corrections are in general non-zero and can even be large. Neglecting them introduces an unphysical dependency of the model parameters on the matching scale μ . This dependency is shown in the upper plot in Figure 3.1, where two sets of the running SM and E_6 SSM gauge couplings are drawn, matched at the scales $T_1 = 500$ GeV and $T_2 = 10$ TeV. One finds that the E_6 SSM gauge couplings at a fixed renormalization scale depend on the chosen value of the matching scale. This effect leads to a dependency of the unification scale M_X (defined in the code as the scale where $g_1(M_X) = g_2(M_X)$) on the chosen matching scale, and a different unification scale will lead to a different particle spectrum at the low-scale. The inclusion of threshold corrections Δg_i reduces this unphysical dependency, as can be seen in the lower plot of Figure 3.1.

In the diploma thesis [56] partial gauge coupling threshold corrections to the renormalization group running have been calculated to avoid the unphysical matching scale dependency. However, the calculated corrections miss contributions from the survival Higgs sector, as well as from the Wino and the SM Higgs. The completed,

¹Integrating out vector bosons would lead to finite, non-logarithmic terms.

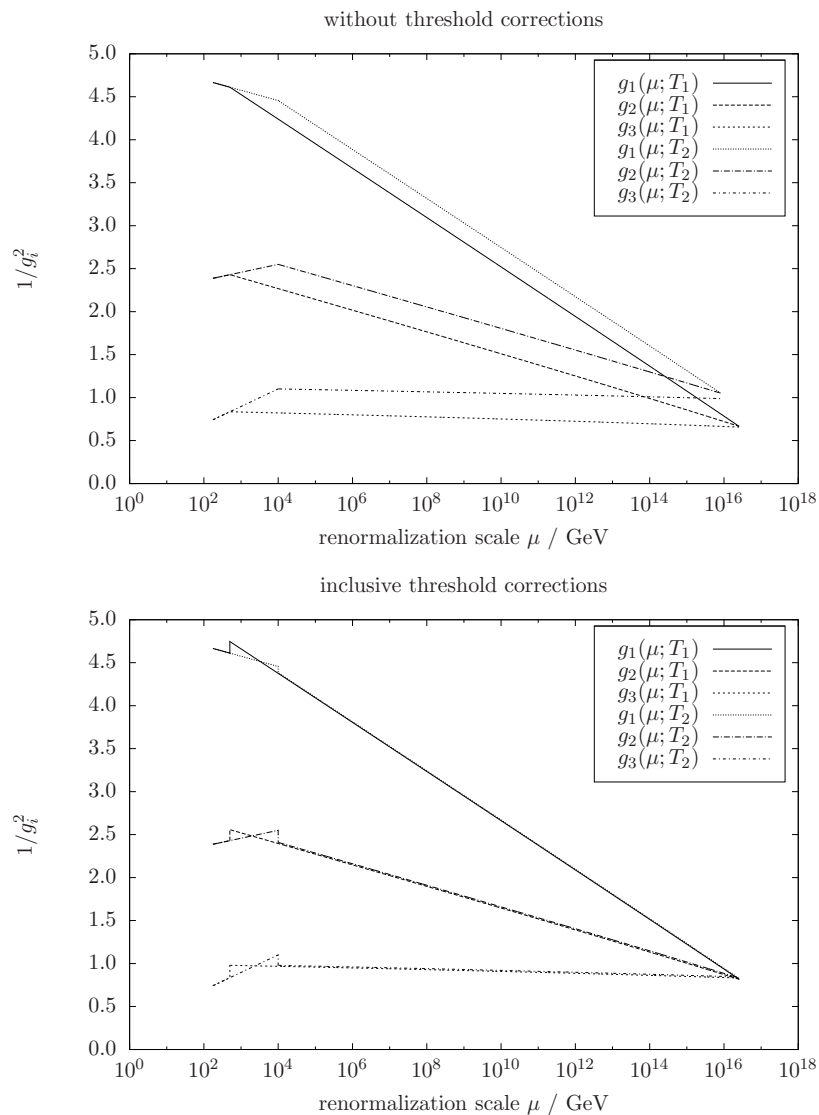


Figure 3.1: Running gauge couplings of the SM and E_6 SSM, matched at two different scales $T_1 = 500$ GeV and $T_2 = 10$ TeV. In the upper plot, without threshold corrections, the unification scale M_X depends on the unphysical matching scale. In the lower plot, where threshold corrections are included, this dependency is reduced significantly.

explicit form of the threshold corrections can be found in Appendix C.7 and have been published in [57]. They are in agreement with the general result presented in [55]. The Yukawa couplings, however, still remained unmatched in the described CE_6 SSM spectrum generator.

Part of this thesis is to calculate the $\overline{\text{DR}}$ Yukawa couplings in the E_6 SSM at the matching scale including one-loop radiative corrections. The procedure of the calculation is described in Section 3.2 and the complete results can be found in Appendix C.6. Section 3.3 describes the implementation of the Yukawa couplings into the existing CE_6 SSM spectrum generator and explains the algorithm used to

calculate the mass spectrum. Finally, an extensive parameter scan is performed to test the CE $_6$ SSM against experimental limits. The results are presented in Section 3.4.

3.2 Calculation of the Yukawa couplings

The Standard Model Yukawa couplings y_f^{SM} have not been measured by experiments directly. Therefore, it is not advantageous to do a matching of the SM Yukawa couplings to the E_6 SSM ones by means of threshold corrections Δy_f . However, the SM fermion masses are known with sufficient precision and are therefore well-suited as input parameters. For this reason the E_6 SSM Yukawa couplings are directly calculated at the matching scale from the known SM fermion masses [11, 58].

The E_6 SSM $\overline{\text{DR}}$ Yukawa couplings $y_f^{\text{E}_6\text{SSM}}$ are related to the third generation SM fermion masses m_f ($f = t, b, \tau$), to the W^\pm boson mass m_W , the left-handed gauge coupling g_2 and $\tan \beta$ as

$$y_t^{\text{E}_6\text{SSM}} = \frac{g_2 m_t}{\sqrt{2} m_W \sin \beta}, \quad y_b^{\text{E}_6\text{SSM}} = \frac{g_2 m_b}{\sqrt{2} m_W \cos \beta}, \quad y_\tau^{\text{E}_6\text{SSM}} = \frac{g_2 m_\tau}{\sqrt{2} m_W \sin \beta}. \quad (3.5)$$

All quantities on the right-hand side of Eq. (3.5) are defined in the $\overline{\text{DR}}$ scheme. The $\overline{\text{DR}}$ masses m_t and m_τ are expressed in terms of the corresponding pole masses as

$$m_f(\mu) = m_f^{\text{pole}} + \Re \hat{\Sigma}_f(p = m_f^{\text{pole}}, \mu), \quad f = t, \tau. \quad (3.6)$$

Here $\hat{\Sigma}_f(p)$ denotes the $\overline{\text{DR}}$ renormalized self-energy of the fermion f in the E_6 SSM and is listed in Appendix C.6.2. The bottom quark pole mass is not known with a high accuracy, because its experimental determination suffers from infra-red sensitivity. However, the $\overline{\text{DR}}$ mass in the 5-flavour QCD $m_b^{(5)}(m_Z^{\text{pole}})$ is known with a higher precision [58]. For this reason the E_6 SSM $\overline{\text{DR}}$ mass m_b is expressed in terms of $m_b^{(5)}(m_Z^{\text{pole}})$ directly as

$$m_b(\mu) = m_b^{(5)}(\mu) + \Re \hat{\Sigma}_b(p = m_b^{(5)}, \mu) - \Re \hat{\Sigma}_b^{(5)}(p = m_b^{(5)}, \mu), \quad (3.7)$$

$$m_b^{(5)}(\mu) = m_b^{(5)}(m_Z^{\text{pole}}) + \beta_{m_b}^{(5)} \log \frac{\mu}{m_Z^{\text{pole}}}, \quad (3.8)$$

$$\beta_{m_b}^{(5)} = -m_b \frac{g_3^2}{2\pi^2}. \quad (3.9)$$

In (3.8) the β -function of $m_b^{(5)}$ is used [59], to shift the mass from m_Z^{pole} to the threshold scale μ . Finally, the $\overline{\text{DR}}$ W^\pm boson mass is calculated from the pole mass via

$$m_W(\mu) = m_W^{\text{pole}} + \Re \hat{\Pi}_{WW,T}(p^2 = (m_W^{\text{pole}})^2, \mu), \quad (3.10)$$

where $\hat{\Pi}_{WW,T}(p^2)$ is the transverse part of the W^\pm boson self-energy, listed in Appendix C.6.1. This allows to express the $\overline{\text{DR}}$ Yukawa couplings in the E_6 SSM as

$$y_t^{E_6SSM} = \frac{g_2 m_t^{\text{pole}}}{\sqrt{2} m_W^{\text{pole}} \sin \beta} \left(1 - \frac{\Re \hat{\Pi}_{WW,T}((m_W^{\text{pole}})^2)}{m_W^{\text{pole}}} + \frac{\Re \hat{\Sigma}_t(m_t^{\text{pole}})}{m_t^{\text{pole}}} \right), \quad (3.11a)$$

$$y_b^{E_6SSM} = \frac{g_2 m_b^{(5)}(m_Z^{\text{pole}})}{\sqrt{2} m_W^{\text{pole}} \cos \beta} \left(1 - \frac{\Re \hat{\Pi}_{WW,T}((m_W^{\text{pole}})^2)}{m_W^{\text{pole}}} + \frac{\Re \hat{\Sigma}_b(m_b^{(5)}) - \Re \hat{\Sigma}_b^{(5)}(m_b^{(5)}) + \beta_{m_b}^{(5)} \log \frac{\mu}{m_Z^{\text{pole}}}}{m_b^{(5)}(m_Z^{\text{pole}})} \right), \quad (3.11b)$$

$$y_\tau^{E_6SSM} = \frac{g_2 m_\tau^{\text{pole}}}{\sqrt{2} m_W^{\text{pole}} \cos \beta} \left(1 - \frac{\Re \hat{\Pi}_{WW,T}((m_W^{\text{pole}})^2)}{m_W^{\text{pole}}} + \frac{\Re \hat{\Sigma}_\tau(m_\tau^{\text{pole}})}{m_\tau^{\text{pole}}} \right). \quad (3.11c)$$

The complete results for the gauge coupling threshold corrections (C.63)–(C.65), the E_6SSM Yukawa couplings (3.11) and the one-loop fermion and W^\pm self-energies (C.37), (C.45) have been published in Ref. [57].

3.3 Implementation into a CE_6SSM spectrum generator

The CE_6SSM spectrum generator presented in [54] is partly based on Softsusy 2.0.5 [60]. As input the program takes the following 8 free CE_6SSM parameters from (3.2), defined in the \overline{DR} scheme:

$$\lambda_i(M_X), \kappa_i(M_X), v_3(Q_{\text{fix}}), \tan \beta(Q_{\text{fix}}). \quad (3.12)$$

The superpotential parameters λ_i and κ_i ($i = 1, 2, 3$) are chosen to be input at the GUT scale M_X , because it is assumed that the superpotential is generated by some breaking mechanism at M_X . The electroweak symmetry breaking (EWSB) parameters v_3 and $\tan \beta$ are input at the fixed low-energy scale Q_{fix} , which is the scale where the EWSB consistency conditions (C.15) are imposed and where the pole mass spectrum is calculated at. In the following Q_{fix} is set to 3 TeV, which is the typical scale of the CE_6SSM particle spectrum. In [54] the survival Higgs parameters μ' , $m_{h'}$, $m_{\bar{h}'}$, $B\mu'$ were not necessary as program input, because they determine only the survival Higgs masses, which decouple from the particle spectrum due to the structure of the RGEs. However, the gauge coupling threshold corrections, given in Appendix C.7, introduce a dependency of the gauge couplings on the survival Higgs masses, and therefore introduce a dependency on the survival Higgs parameters. For this reason these parameters need to be added to the program input. They are defined in the \overline{DR} scheme at the matching scale $\mu = T_{E_6SSM}$

$$\mu'(T_{E_6SSM}), m_{h'}(T_{E_6SSM}), m_{\bar{h}'}(T_{E_6SSM}), B\mu'(T_{E_6SSM}). \quad (3.13)$$

The differential equations, which relate the E_6SSM model parameters at different

renormalization scales are the renormalization group equations (RGEs) [54]. The gauge coupling unification condition (C.14), the soft-breaking parameter universality conditions (C.12), the input parameters at M_X , Q_{fix} and $T_{E_6\text{SSM}}$, (3.12)–(3.13), the matching conditions to the Standard Model (3.3), (3.11) and the EWSB conditions (C.15) then form a boundary value problem. The aim of the spectrum generator is to find sets of model parameters, consistent with all the given constraints, and to calculate the pole mass spectrum for each set.

The algorithm, which searches for a solution of the above mentioned boundary value problem, is a nested fixed-point iteration in combination with an adaptive Runge-Kutta algorithm. It is divided into the following five steps, see Figure 3.2:

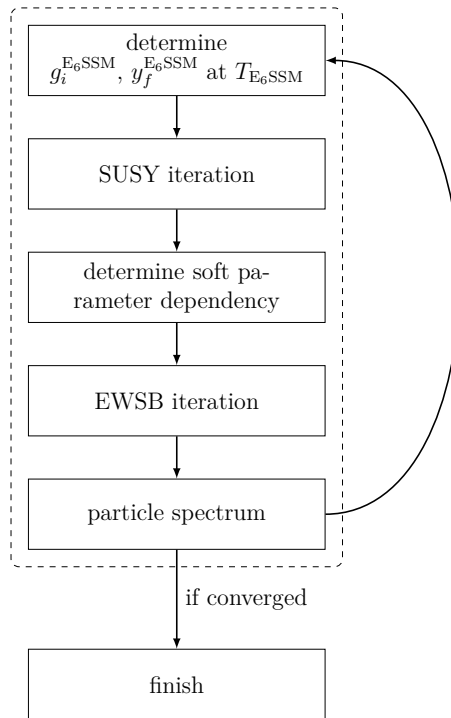


Figure 3.2: CE_6 SSM spectrum calculation algorithm. The dashed box marks the structure of the old spectrum generator presented in [54], which neglects threshold corrections. The inclusion of threshold corrections (in the step 1) made an overall iteration necessary, because the threshold corrections depend on the particle spectrum (calculated in step 5).

1. Determine the E_6 SSM $\overline{\text{DR}}$ gauge and Yukawa couplings, $g_i^{E_6\text{SSM}}, y_f^{E_6\text{SSM}}$:
 - a) Evolve the SM $\overline{\text{MS}}$ gauge and Yukawa couplings, $g_i^{\text{SM}}, y_f^{\text{SM}}$ from their known values at m_Z^{pole} [11] to the intermediate matching scale $T_{E_6\text{SSM}}$ using SM RGEs.
 - b) Convert the SM $\overline{\text{MS}}$ couplings to E_6 SSM $\overline{\text{DR}}$ couplings using the gauge coupling threshold corrections (C.63)–(C.65) and the calculated E_6 SSM Yukawa couplings (3.11). This step is only possible once the full $\overline{\text{DR}}$

mass spectrum is known, i.e. after the first iteration. Hence, in the first iteration, these corrections are neglected and the E_6SSM \overline{DR} gauge and Yukawa couplings are determined as

$$y_f^{E_6SSM}(T_{E_6SSM}) = \frac{y_f^{SM}(T_{E_6SSM})}{\cos \beta} \quad (f = b, \tau), \quad (3.14)$$

$$y_t^{E_6SSM}(T_{E_6SSM}) = \frac{y_t^{SM}(T_{E_6SSM})}{\sin \beta}, \quad (3.15)$$

$$g_i^{E_6SSM}(T_{E_6SSM}) = g_i^{SM}(T_{E_6SSM}) \quad (i = 1, 2, 3). \quad (3.16)$$

2. *SUSY iteration:* Use RGEs to determine all SUSY parameters $(g_i, y_f, \lambda_i, \kappa_i)$ at all scales. This step is independent of soft-breaking parameters, because the β -functions of the SUSY parameters are independent of the soft-breaking parameters [61, 62, 63, 64].

- a) Estimate the values of the Yukawa couplings $\lambda_i(T_{E_6SSM}), \kappa_i(T_{E_6SSM})$ at the matching scale.
- b) Evolve all SUSY parameters from T_{E_6SSM} up to the unification scale M_X , defined as the scale where $g_1(M_X) = g_2(M_X)$, using two-loop E_6SSM RGEs.
- c) Set the Yukawa couplings $\lambda_i(M_X), \kappa_i(M_X)$ to the program input values.
- d) Set $g'_1(M_X) := g_1(M_X)$.
- e) Perform an iteration between M_X and T_{E_6SSM} to obtain values for the SUSY parameters until consistency is reached with the low-energy boundary conditions for $y_f^{E_6SSM}(T_{E_6SSM}), g_i^{E_6SSM}(T_{E_6SSM})$ and the high-energy boundary conditions for $\lambda_i(M_X), \kappa_i(M_X)$.

3. *Determine soft parameter dependency:* Using the high-scale universality conditions (C.12) and the EWSB conditions (C.15) it is possible to express the soft-breaking parameters in the semi-analytic form [54]

$$m_i^2(t) = a_i(t)m_0^2 + b_i(t)M_{1/2}^2 + c_i(t)A_0M_{1/2} + d_i(t)A_0^2, \quad (3.17a)$$

$$A_i(t) = e_i(t)A_0 + f_i(t)M_{1/2}, \quad (3.17b)$$

$$M_i(t) = p_i(t)A_0 + q_i(t)M_{1/2}. \quad (3.17c)$$

The coefficients $a_i(t), \dots, q_i(t)$ depend only on the SUSY parameters and are calculated numerically at the scale $t = \log T_{E_6SSM}/M_X$.

4. *EWSB iteration:* Use the three EWSB conditions (C.15) to fix the values of the universal soft parameters $m_0^2, M_{1/2}$ and A_0 :

- a) The semi-analytic expressions (3.17) are combined with the three tree-level EWSB conditions (C.15) to form three quadratic equations in the universal soft parameters $m_0^2, M_{1/2}$ and A_0 . These three equations are then reduced to one quartic equation.

- b) This quartic equation is then solved numerically, which will yield up to four real solutions $\{m_0^2, M_{1/2}, A_0\}_{i=1,\dots,4}$. Complex solutions are discarded.
 - c) Calculate leading one-loop tadpole corrections to the effective potential and find a minimum iteratively.
5. For each set of $\{m_0^2, M_{1/2}, A_0\}_{i=1,\dots,4}$, the full CE₆SSM particle spectrum is calculated.

The gauge coupling threshold corrections and the determination of the E_6 SSM Yukawa couplings in step 1b depend on the particle spectrum, which is obtained in the step 5. Therefore an iteration over all five steps is performed, until convergent solutions are obtained.

3.4 Numerical evaluation and application

3.4.1 Reduced matching scale dependency

As discussed in Section 3.1, the inclusion of threshold corrections reduces the unphysical dependency of the model parameters on the matching scale. This effect translates to the unification scale M_X , which in turn leads to a stabilization of the pole mass spectrum. This effect is shown in Figure 3.3, where a subset of the CE₆SSM particle spectrum for the parameter point

$$\begin{aligned} \tan \beta(Q_{\text{fix}}) = 35, \quad \lambda_{1,2,3}(M_X) = \kappa_{1,2,3}(M_X) = 0.2, \quad v_3(Q_{\text{fix}}) = 10 \text{ TeV}, \\ \mu'(T_{E_6\text{SSM}}) = m_{h'}(T_{E_6\text{SSM}}) = m_{\bar{h}'}(T_{E_6\text{SSM}}) = 10 \text{ TeV}, \quad B\mu'(T_{E_6\text{SSM}}) = 0 \end{aligned} \quad (3.18)$$

is plotted. The white and the black boxes show the absolute variation of the particle masses when the matching scale $T_{E_6\text{SSM}}$ is varied in the interval $[\frac{1}{2}T_0, 2T_0]$. The scale T_0 is the geometric average of all shown particle masses and has the value $T_0 = 1.9 \text{ TeV}$ for this parameter point. The white boxes show the variation when threshold corrections are neglected, and the black boxes show the variation when threshold corrections are included. One finds that with included threshold corrections (black boxes) the unphysical dependency of the particle masses on the matching scale is significantly smaller than without (white boxes). This reduction effect is largest for gluino mass $m_{\tilde{g}}$ and for the lightest chargino and neutralino masses $m_{\tilde{\chi}_1^\pm}$ and $m_{\tilde{\chi}_1^0}$, respectively. Without threshold corrections these masses vary in the range

$$m_{\tilde{g}}^{\text{w/o TC}} = (691 \dots 1330) \text{ GeV}, \quad (3.19)$$

$$m_{\tilde{\chi}_1^\pm}^{\text{w/o TC}} = (208 \dots 479) \text{ GeV}, \quad (3.20)$$

$$m_{\tilde{\chi}_1^0}^{\text{w/o TC}} = (117 \dots 275) \text{ GeV}, \quad (3.21)$$

which translates to relative errors of 65 %, 83 % and 85 %, respectively. With included threshold corrections the ranges are reduced to

$$m_{\tilde{g}}^{\text{w/ TC}} = (823 \dots 828) \text{ GeV}, \quad (3.22)$$

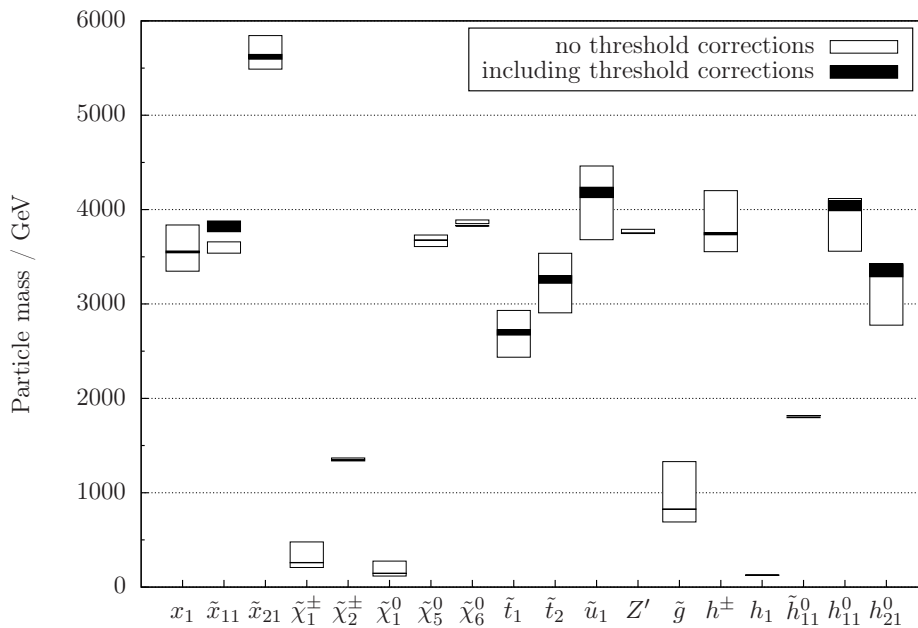


Figure 3.3: CE₆SSM pole mass spectrum for parameter point (3.18). The white and the black boxes show the variation of the particle masses when the matching scale is varied in the interval $[\frac{1}{2}T_0, 2T_0]$, where $T_0 = 1.9$ TeV is the geometric average of all shown particle masses. The black boxes show the error with threshold corrections and the white boxes without.

$$m_{\tilde{\chi}_1^\pm}^{\text{w/ TC}} = (258 \dots 261) \text{ GeV}, \quad (3.23)$$

$$m_{\tilde{\chi}_1^0}^{\text{w/ TC}} = (146 \dots 147) \text{ GeV}, \quad (3.24)$$

which translates to relative errors of 0.7 %, 1.0 % and 1.1 %, respectively. The variation of the remaining pole masses with included threshold corrections in Figure 3.3 is 4 % or less. This remaining variation is formally a two-loop effect. Note that for the lightest first generation exotic squark \tilde{x}_{11} there is no reduction of the scale dependence, but a mass shift. The reason is the non-linear behaviour of the squark mass as a function of the matching scale. In case of \tilde{x}_{11} the function $m_{\tilde{x}_{11}}(T_{\text{E}_6\text{SSM}})$ has a minimum around $T_{\text{E}_6\text{SSM}} \approx T_0$, which leads to an unnatural small error band in case threshold corrections are neglected. One can conclude that the scale variation is not always a good estimation of the theory uncertainty, due to such non-linear effects.

3.4.2 Parameter scan

In order to show the impact of the threshold corrections in a wider range of the CE₆SSM parameter space, a parameter scan over $\tan \beta = 2 \dots 45$ and $\lambda_3 = 0 \dots 3$ is performed in the following. During the scan the superpotential parameters $\lambda_i(M_X)$ and $\kappa_i(M_X)$ parameters are chosen to be universal at the GUT scale,

$$\lambda_1 = \lambda_2 = \lambda_3 = \kappa_1 = \kappa_2 = \kappa_3, \quad (3.25)$$

and the remaining free parameters are fixed to

$$\begin{aligned} v_3(Q_{\text{fix}}) = \mu'(T_{E_6\text{SSM}}) = m_{h'}(T_{E_6\text{SSM}}) = m_{\bar{h}'}(T_{E_6\text{SSM}}) = 10 \text{ TeV}, \\ B\mu'(T_{E_6\text{SSM}}) = 0. \end{aligned} \quad (3.26)$$

The matching scale $T_{E_6\text{SSM}}$ is set to 600 GeV, which is a rough estimate of the expected average size of the pole mass spectrum. Note that the size of $T_{E_6\text{SSM}}$ is only important during an iteration without threshold corrections, because of the dependence of the model parameters on $T_{E_6\text{SSM}}$ in this case.

As described in Section 3.3, for each choice of $(\lambda_3, \tan\beta)$, there exist up to four real solutions for $(m_0, M_{1/2})$ from the electroweak symmetry breaking conditions. Figure 3.4 shows the mapping from the scanned input parameters $(\lambda_3, \tan\beta)$ to all possible output values of $(m_0, M_{1/2})$. The butterfly shape is due to the superposition of all four solutions, where in the overlap region only solution 1 is drawn. In the white

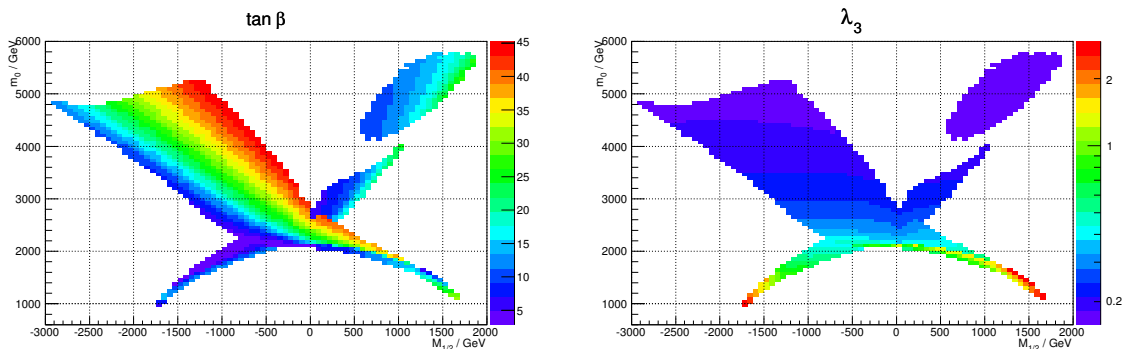


Figure 3.4: Mapping of the input parameters $(\lambda_3, \tan\beta)$ to the output parameters $(m_0, M_{1/2})$. The left panel shows the variation of $\tan\beta$ across the $(m_0, M_{1/2})$ plane. The right panel shows λ_3 as a function of $(m_0, M_{1/2})$.

regions the RG solving algorithm is not able to find a simultaneous solution to the EWSB equations and the unification conditions without producing tachyons. Due to this effect there exists an upper limit on the value of $\tan\beta$ at around 45 [57]. This already places physical constraints on the allowed $(m_0, M_{1/2})$ parameter space.

Figure 3.5 shows the gluino mass $m_{\tilde{g}}$ (upper left panel) and lightest neutralino mass $m_{\tilde{\chi}_1^0}$ (lower left panel) in the scanned parameter space region. The masses vary from 200...2500 GeV for the gluino, and 50...500 GeV for the neutralino. The impact of the threshold corrections on the particle masses is shown in the panels of the right column. There the difference between the mass with and without threshold corrections is drawn for each parameter point. The size of the corrections varies from a few GeV around $M_{1/2} \approx 0$, up to hundreds of GeV around $M_{1/2} \approx -3$ TeV. In the regions with large $M_{1/2}$ these corrections can be up to 40 % of the particle mass. The reason for these large corrections is that large values of $M_{1/2}$ lead to large particle masses. In this case the used matching scale $T_{E_6\text{SSM}} = 600$ GeV is a bad estimate of the average size of the pole mass spectrum. Such a bad guess leads to large threshold corrections, because they contain logarithms of the form $\log(T_{E_6\text{SSM}}/m_i)$.

This translates to a significant mass shift compared to the case without threshold corrections.

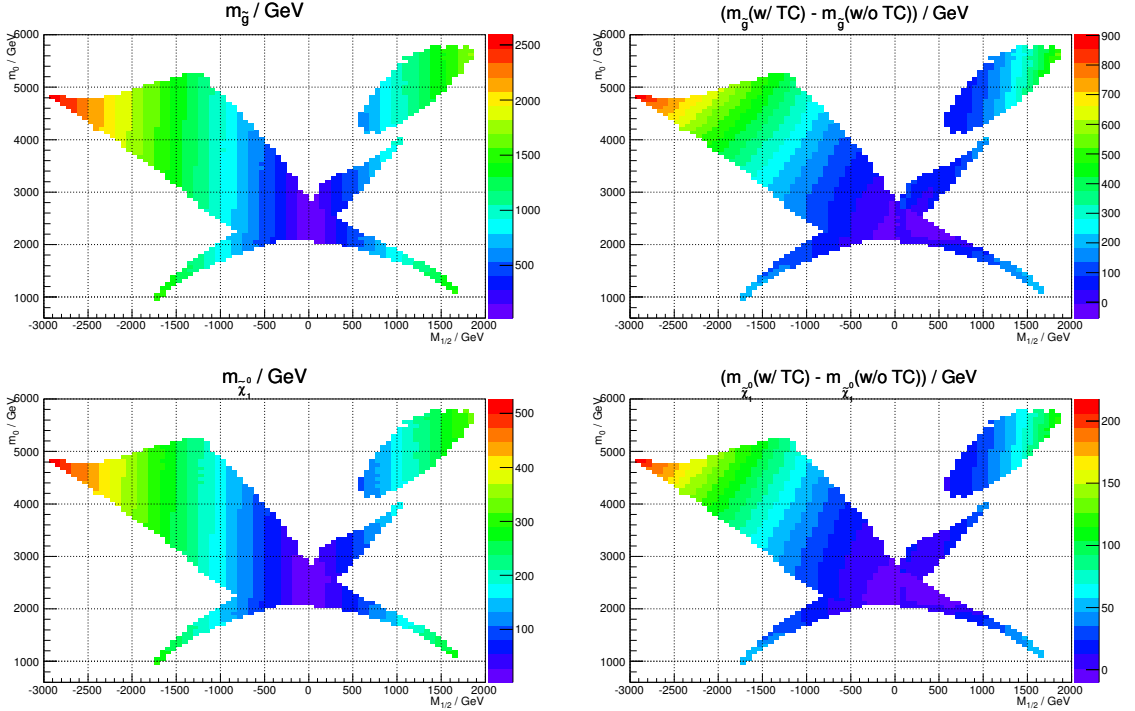


Figure 3.5: Gluino (upper left panel) and lightest neutralino mass (lower left panel) as a function of $(m_0, M_{1/2})$. The right column shows the differences between the masses with and without threshold corrections.

Note that the parameter region with $|M_{1/2}| \lesssim 1.4$ TeV is highly constrained by current LHC experiments, because it leads to a gluino mass of the order or smaller than the current limit of 1.4 TeV [65, 66, 67].

3.4.3 Parameter space exclusion

The improved spectrum generator enables to study the CE₆SSM parameter space with a higher accuracy and to search for experimentally allowed and excluded regions. Figure 3.6 shows the lightest CP-even Higgs pole mass as a function of m_0 and $M_{1/2}$ for the scanned region from Section 3.4.2. Large Higgs masses of $m_h > 126$ GeV can be found for $m_0 \gtrsim 2.5$ TeV and $|M_{1/2}| \gtrsim 500$ GeV, while light Higgses of $m_h < 120$ GeV lie in regions with $m_0 \lesssim 2.2$ TeV. For a more precise determination of the allowed parameter space the following experimental constraints are applied:

$$123.5 \text{ GeV} < m_h < 127.5 \text{ GeV}, \quad (3.27a)$$

$$m_{\tilde{g}} > 1 \text{ TeV}, \quad (3.27b)$$

$$m_{\tilde{t}_1} > 300 \text{ GeV}, \quad (3.27c)$$

$$m_{\tilde{\chi}_1^0}, m_{\tilde{\chi}_1^\pm} > 200 \text{ GeV}, \quad (3.27d)$$

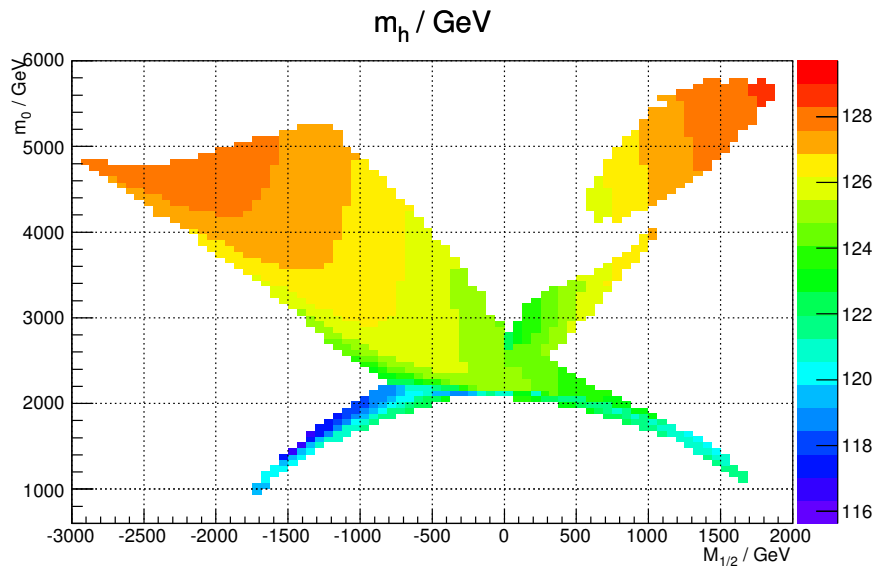


Figure 3.6: Lightest CP-even Higgs pole mass as a function of $(m_0, M_{1/2})$.

$$m_{Z'} > 2.1 \text{ TeV}, \quad (3.27e)$$

$$m_{\tilde{h}_{i0}^0}, m_{\tilde{h}_i^+}, m_{\tilde{h}_{ij}^0}, m_{\tilde{h}_{ij}^\pm} > 100 \text{ GeV}. \quad (3.27f)$$

These constraints are experimental exclusion limits, translated to the CE_6 SSM, at the time of the publication of the here presented analysis in 2012 [57]. A detailed discussion of the constraints placed on the CE_6 SSM by current experiments can be found in [45]. The imposed Higgs mass constraint of $123.5 \text{ GeV} < m_h < 127.5 \text{ GeV}$ is based on the ATLAS and CMS analyses [68, 69] using between 4.6 and 4.9 fb^{-1} of LHC data. Refs. [70, 45] have estimated a lower gluino mass limit of around 850 GeV , based on the first $\approx 5 \text{ fb}^{-1}$ data at $\sqrt{s} = 7 \text{ TeV}$ [71, 72, 73, 74, 75, 76]. The limit was increased to $\approx 1 \text{ TeV}$ by the updated results from the 5.8 fb^{-1} data set with $\sqrt{s} = 7 \text{ TeV}$ [77, 78, 79, 80]. The large lower bound of 2.1 TeV on the Z' mass is taken from the CMS analysis [81], which uses 5 fb^{-1} of collected data. At the time this scan was performed the searches for top and bottom squarks were less advanced. The ATLAS analysis [82] excludes top squarks with a mass smaller than 310 GeV , if the lightest neutralino mass is in the range $115 \dots 230 \text{ GeV}$. For the sbottom quark a lower bound of the same order applies [83]. All the here scanned parameter points pass these light squark mass limits, because the chosen value of $v_3 = 10 \text{ TeV}$ leads to sfermion masses of the order 1 TeV or larger. The lower bounds on the light neutralino, chargino and inert fermions and sfermions are based on the scenarios discussed in [84, 85, 86, 87].

Figure 3.7 shows the allowed and excluded CE_6 SSM parameter regions when the constraints (3.27) are imposed. The mass limits for the Higgs and the gluino are most constraining, see Figure 3.5 and 3.6 for reference. The reason is that the CE_6 SSM usually predicts a light gluino with a mass of the order $M_3 \sim 0.7M_{1/2}$. The high exclusion limit on the gluino mass of 1 TeV therefore leads to a high lower bound on

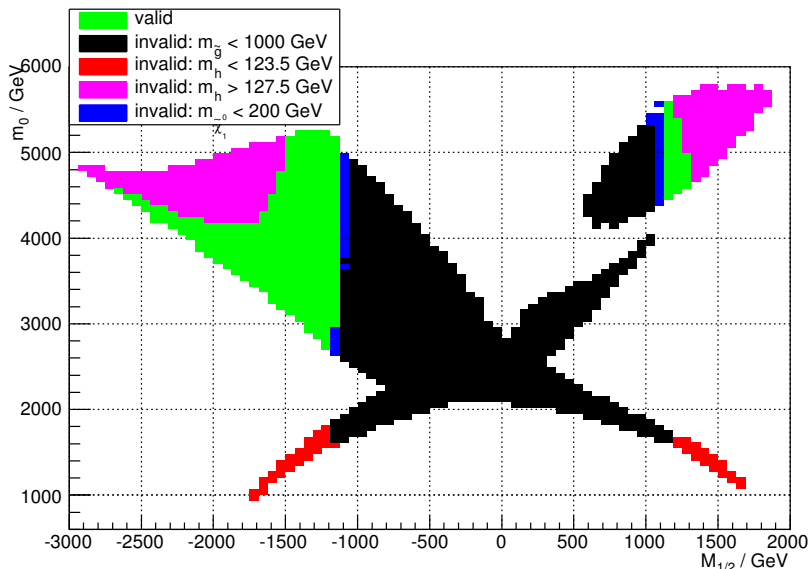


Figure 3.7: Allowed and excluded regions of the CE₆SSM parameter space using the constraints from (3.27).

$M_{1/2}$. The parameter regions with $m_0 \lesssim 1.8$ TeV predict a light Higgs mass below 123.5 GeV and are therefore excluded as well. However, there is still a large region around $m_0 \approx 3 \dots 5$ TeV and $M_{1/2} \approx -(1 \dots 2.5)$ TeV, where all constraints are passed and where the Higgs mass is consistent with the discovery.

3.4.4 Updating benchmark points from the literature

The implemented threshold corrections allow to update the pole mass spectrum of the CE₆SSM benchmark points proposed in [54, 88, 45], where these corrections were missing. Table 3.1 lists all benchmark points together with the reported gluino mass (without threshold corrections) and the recalculated one including threshold corrections. For the recalculation the survival Higgs sector parameters were set to

$$\mu' = m_{h'} = m_{\tilde{h}'} = 10 \text{ TeV}, \quad (3.28)$$

except for points marked with ^a or ^b, where the survival Higgs masses were varied until a self-consistent solution was found.

One finds that for most of the light benchmark points BMA–BME [88] and BM1–BM6 [54] the gluino mass is reduced. When the current LHC limit of $m_{\tilde{g}} \lesssim 1.4$ TeV [67] is applied, all these light benchmark points are excluded. From the five heavy benchmark points HBM1–HBM5 [45], only HBM2 and HBM3 pass the gluino mass limit. However, these points predict light exotic quarks with masses of 368 GeV and 521 GeV, respectively. Current LHC searches for vector-like quarks with charge $-1/3$ constrain the exotic quark mass to be larger than 590 GeV [89] or 645 GeV [90]. Therefore, HBM2 and HBM3 would be excluded by these searches. However, the incorporation of threshold corrections does not change the qualitative properties

$m_{\tilde{g}} / \text{GeV}$	BMA	BMB	BMC	BMD	BME	
without thresholds	336	330	353	327	338	
including thresholds	224	269 ^b	260	230	203 ^b	
$m_{\tilde{g}} / \text{GeV}$	BM1	BM2	BM3	BM4	BM5	BM6
without thresholds	350	673	362	642	338	805
including thresholds	322	613 ^a	275	423 ^a	190	825
$m_{\tilde{g}} / \text{GeV}$	HBM1	HBM2	HBM3	HBM4	HBM5	
without thresholds	984	1352	1659	1129	1001	
including thresholds	1090	1494	1886	827	1067	

Table 3.1: Comparison of the originally reported gluino mass and the gluino mass including threshold corrections for previously published CE_6 SSM benchmarks. The survival Higgs sector parameters were chosen to be $\mu' = m_{h'} = m_{\tilde{h}'} = 10 \text{ TeV}$ for all points, except those marked ^a where we used $\mu' = m_{h'} = m_{\tilde{h}'} = 100 \text{ TeV}$ to evade tachyonic problems with convergence and ^b where they were increased to 10^4 TeV .

of all these points. In particular the lightest CP-even Higgs pole mass changes only in the sub-GeV range and remains in the signal region of 125 GeV for HBM1–HBM5.

3.5 Summary and conclusion

In Ref. [54] a spectrum generator for the CE_6 SSM was presented, which calculates the E_6 SSM mass spectrum from high-scale and low-scale input parameters. However, this spectrum generator neglects threshold corrections to the gauge and Yukawa couplings, which introduces an unphysical dependence of the model parameters and the mass spectrum on the matching scale. In the diploma thesis [56], partial gauge coupling threshold corrections were calculated and implemented into the spectrum generator.

In this thesis the gauge coupling threshold corrections were completed and are listed in Appendix C.7. Furthermore, the full E_6 SSM Yukawa couplings have been calculated at the one-loop level from known Standard Model fermion masses and m_W^{pole} , see Section 3.2. Full expressions for these corrections have been provided and they have been implemented into the CE_6 SSM spectrum generator.

The impact of these corrections has been studied, using the improved spectrum generator. The pole mass spectrum shows a significant reduction of the matching scale dependency up to 80 % relative to the particle mass. The largest reduction has been found for the gluino and the lightest neutralino and chargino masses. Since these particles are light, they are especially important for setting limits on the CE_6 SSM parameter space, which again emphasizes the necessity for the implemented corrections.

A consequence of the threshold corrections is that they introduce a connection between the particle spectrum from the $(\mathbf{27})_i$ representations and the survival Higgs

sector $(\mathbf{27})'$ and $(\overline{\mathbf{27}})'$. In former studies [54, 88, 45], without threshold corrections, the survival Higgs sector decoupled from the rest of the spectrum. To take this new connection into account, the parameters μ' , $m_{h'}$, $m_{\bar{h}'}$, $B\mu'$ had to be added to the list of input parameters for the spectrum generator.

Furthermore, a parameter scan over λ_3 and $\tan\beta$ was performed using the improved CE_6SSM spectrum generator. Experimental constraints were applied to search for allowed and excluded parameter regions. It was found that the lower limits on the gluino and the Higgs mass are most constraining and exclude already large regions of the m_0 – $M_{1/2}$ parameter space. However, there are still large regions where the model passes all experimental bounds and can predict the discovered Higgs mass.

Finally, the mass spectrum of previously proposed CE_6SSM benchmark points [54, 88, 45] has been recalculated with the improved spectrum generator. All of these points are already excluded by current gluino and vector-like quark searches at the LHC [65, 89, 90].

In conclusion, the calculation of threshold corrections and Yukawa couplings has shown to be valuable, because it significantly improves the precision of the predicted low-energy CE_6SSM particle spectrum by reducing the theory uncertainty from the unphysical matching scale. The studied CE_6SSM parameter regions show that the qualitative features of the CE_6SSM do not change by the inclusion of these corrections. The complete results for the gauge and Yukawa coupling threshold corrections, as well as the here presented numerical studies have been published in [57].

It must be noted that the CE_6SSM is still an attractive, predictive and experimentally viable SUSY model. However, further LHC studies might exclude larger regions of the CE_6SSM parameter space, making it possible to distinguish between several non-minimal SUSY models.

Chapter 4

Renormalization of vacuum expectation values

4.1 Motivation

The Standard Model of particle physics [91, 92, 93] as well as many attractive extensions, such as the MSSM [20], use spontaneous breaking of the local gauge invariance to generate mass terms for the vector bosons and fermions of the theory [94, 95, 96, 97]. For this purpose scalar fields φ_a are introduced together with a scalar potential which allows for a non-trivial minimum. These scalar fields are then shifted by the constants v_a (the vacuum expectation values, VEVs)

$$\varphi_a \rightarrow \varphi_a + v_a, \tag{4.1}$$

where v_a can be adjusted to the minimum of the scalar potential. Finally, a gauge fixing is introduced, which breaks the local gauge invariance to allow to quantize the theory.

During loop calculations in the quantized theory divergences appear, which can be removed consistently via renormalization [98, 99, 100, 101, 102, 103]. Thereby all parameters and fields of the theory are multiplied by so-called renormalization constants Z_i , such that the symmetry of the Lagrangian is preserved. This procedure is called multiplicative renormalization transformation. The renormalization constants can be adjusted such that all divergences are absorbed at each loop level (perturbative renormalization).

The VEV in Eq. (4.1) is renormalized by a renormalization constant Z_{v_a} , which is decomposed as $Z_{v_a} = 1 + \delta v_a/v_a$. The quantity δv_a is called VEV counter-term and in general depends on the chosen gauge fixing [104].

For some applications, for example in spectrum generators for supersymmetric models, the β -function of v_a is required. It is used to calculate the renormalization group equations, which are solved numerically to relate the model parameters at different renormalization scales. For convenience, these spectrum generators use $\overline{\text{DR}}$ renormalized parameters [105, 106] and use a R_ξ gauge fixing [98, 99], because it avoids mixings between gauge and goldstone bosons. However, β_{v_a} has not been known in a general gauge theory with R_ξ gauge. So far it has been calculated only in the MSSM at the one-loop [107] and leading two-loop level [62], as well as in the

E_6 SSM at the one-loop level [57], see Table 4.1.

Model	$\beta_v^{(1)}$	$\beta_v^{(2)}$
MSSM	known [107]	only $O(g^2 Y^2)$ known [62]
E_6 SSM	known [57]	unknown
general gauge theory	unknown	unknown
general supersymmetric gauge theory	unknown	unknown

Table 4.1: Status of the calculation of β_v at the one- and two-loop level for different gauge theories.

In the following, the VEV counter-term δv_a is calculated in a general gauge theory with R_ξ gauge fixing in the $\overline{\text{MS}}$ renormalization scheme at the one- and two-loop level. The β -function of v_a can then be directly computed from the counter-term δv_a . The result is applied to a general supersymmetric gauge theory in Wess–Zumino gauge in the $\overline{\text{DR}}$ renormalization scheme. The VEV β -functions complement the well-known one- and two-loop β -functions for general gauge theories and general supersymmetric gauge theories [108, 109, 110, 61, 62, 111]. Furthermore, the results will allow to implement the one- and two-loop $\overline{\text{DR}}$ VEV β -functions into spectrum generators for general supersymmetric models, such as SARAH/SPheno [112, 113] and FlexibleSUSY [114].

4.2 Calculation of the VEV counter-term

4.2.1 Background field method

As discussed above, to generate mass terms for gauge bosons and fermions, one introduces scalar fields φ_a into the invariant Lagrangian \mathcal{L}_{inv} and couples them to the fields. Furthermore, a gauge invariant and renormalizable scalar potential $V(\varphi_a)$, which allows for a non-trivial minimum is added to \mathcal{L}_{inv} . The scalar fields are then shifted by a constant, v_a , (the vacuum expectation value, VEV)

$$\varphi_a \rightarrow \varphi_a + v_a, \quad (4.2)$$

where v_a can be set to the minimum of the scalar potential. After shifting the field Eq. (4.2), the Lagrangian is still invariant under both local and global gauge transformations, as long as the combination $(\varphi_a + v_a)$ transforms as a whole.

The most general renormalization transformation of the combination $(\varphi_a + v_a)$ can then be written in the following two equivalent forms

$$\varphi_a + v_a \rightarrow \sqrt{\overline{Z}}_{ab} \varphi_b + v_a + \delta v_a, \quad (4.3a)$$

$$\rightarrow \sqrt{\overline{Z}}_{ab} (\varphi_b + v_b + \delta \bar{v}_b), \quad (4.3b)$$

from which one can deduce $\delta v_a = (\sqrt{\overline{Z}} - 1)_{ab} v_b + \sqrt{\overline{Z}}_{ab} \delta \bar{v}_b$. Writing the renormalization

transformation in the form (4.3b) has the advantage that the appearing counter-term $\delta\bar{v}_b$ characterizes to what extent v_b renormalizes differently from the corresponding scalar field φ_b .

In a theory with global (rigid) gauge invariance, the combination $(\varphi_a + v_a)$ transforms as a whole under the global gauge transformation. For this reason, in such a theory the extra counter-term $\delta\bar{v}_a$ is forbidden by the global gauge symmetry, because it would introduce a deviation from the combined transformation of $(\varphi_a + v_a)$ and therefore violate the symmetry. However, if the theory is not globally gauge invariant, the extra counter-term $\delta\bar{v}_a$ is not forbidden by the symmetry and is in general non-vanishing.

For quantization of a gauge theory a gauge fixing is required [115, 116]. In QED and QCD, the typical gauge fixing terms have the form [117, 118]

$$\mathcal{L}_{\text{f.p.}+\text{g.f.}}^{\text{QCD}} = s \left[\bar{c}^A \left(F_{\text{QCD}}^A + \frac{\xi}{2} B^A \right) \right], \quad F_{\text{QCD}}^A = \partial^\mu V_\mu^A, \quad (4.4a)$$

$$\mathcal{L}_{\text{g.f.}}^{\text{QCD}} = -\frac{1}{2\xi} F_{\text{QCD}}^A F_{\text{QCD}}^A = -\frac{1}{2\xi} (\partial^\mu V_\mu^A)(\partial^\nu V_\nu^A), \quad (4.4b)$$

$$\mathcal{L}_{\text{f.p.}}^{\text{QCD}} = -\bar{c}^A \square c^A - gf^{ABC} (\partial^\mu \bar{c}^A) V_\mu^B c^C. \quad (4.4c)$$

The fields V^A represent the gauge bosons, c^A are Faddeev-Popov ghosts and \bar{c}^A are anti-ghost fields. The Nakanishi-Lautrup auxiliary fields B^A can be eliminated by their equations of motion. The gauge fixings (4.4) break local gauge invariance, because $\mathcal{L}_{\text{g.f.}}^{\text{QCD}}$ is no longer invariant under

$$V_\mu^A \rightarrow V_\mu^A + \partial_\mu \alpha^A(x) - gf^{ABC} V_\mu^B \alpha^C(x). \quad (4.5)$$

However, global gauge invariance, where $\partial_\mu \alpha^A = 0$, remains intact. In spontaneously broken gauge theories R_ξ gauge fixings are used, which have the form¹

$$\mathcal{L}_{\text{f.p.}+\text{g.f.}}^{R_\xi} = s \left[\bar{c}^A \left(F_{R_\xi}^A + \frac{\xi}{2} B^A \right) \right], \quad F_{R_\xi}^A = \partial^\mu V_\mu^A + ig\xi\xi' v_a T_{ab}^A \varphi_b, \quad (4.6a)$$

$$\mathcal{L}_{\text{g.f.}}^{R_\xi} = -\frac{1}{2\xi} F_{R_\xi}^A F_{R_\xi}^A = -\frac{1}{2\xi} \left(\partial^\mu V_\mu^A + ig\xi\xi' v_a T_{ab}^A \varphi_b \right)^2, \quad (4.6b)$$

$$\mathcal{L}_{\text{f.p.}}^{R_\xi} = -\bar{c}^A \square c^A - gf^{ABC} (\partial^\mu \bar{c}^A) V_\mu^B c^C - g^2 \xi \xi' \bar{c}^A c^B v_a T_{ab}^A T_{bc}^B (\varphi + v)_c. \quad (4.6c)$$

In contrast to the covariant QCD gauge (4.4), the R_ξ gauge (4.6) breaks even global invariance (for $\xi \neq 0$). The reason is that $F_{R_\xi}^A$ is not written in terms of the combination $(\varphi_a + v_a)$, but contains φ_a and v_a separately. Therefore, in theories with R_ξ gauges, the extra counter-term $\delta\bar{v}_a$ is not forbidden by symmetry and is in general non-vanishing.

The counter-term $\delta\bar{v}_a$ can be calculated in an elegant way with the aid of scalar background fields, as used in [119]. The idea is to introduce classical real scalar

¹The parameter ξ' is introduced to preserve the non-mixing of gauge and goldstone bosons at the loop-level. At the tree-level one has $\xi' = 1$.

background fields $\hat{\varphi}_a$ and corresponding shifts \hat{v}_a into \mathcal{L}_{inv} . The gauge transformation of the combination $(\hat{\varphi}_a + \hat{v}_a)$ is defined to be the same as the one of the scalar field φ_a . This allows to formulate a global gauge invariant gauge fixing function F_{bg}^A as

$$F_{\text{bg}}^A = \partial^\mu V_\mu^A + ig\xi\xi' (\hat{\varphi} + \hat{v})_a T_{ab}^A \varphi_b. \quad (4.7)$$

As a consequence, the resulting gauge fixing Lagrangian

$$\mathcal{L}_{\text{f.p.}+\text{g.f.}}^{\text{bg}} = s \left[\bar{c}^A \left(F_{\text{bg}}^A + \frac{\xi}{2} B^A \right) \right] \quad (4.8)$$

breaks local gauge invariance, but leaves global gauge invariance intact. As explained above, due to the global gauge symmetry the extra VEV counter-term $\delta\bar{v}_a$ is forbidden and must vanish. Another important property of the modified gauge fixing function (4.7) is that it reproduces the conventional R_ξ gauge fixing (4.6a), because the classical fields $\hat{\varphi}_a$ have to be set to zero for the calculation of the Green functions. In this case the shift \hat{v}_a of the background field is equivalent to the shift v_a of the scalar field.

In summary, this background field formalism has the advantage that one can calculate the VEV counter-term in a global gauge invariant theory where $\delta\bar{v}_a = 0$. The obtained results are equivalent to the case with the conventional R_ξ gauge fixing (4.6a), because the classical background fields are set to zero at the end.

4.2.2 Lagrangian

In the following calculation a general gauge theory with a simple gauge group and gauge coupling g is considered. The renormalizable, locally gauge invariant Lagrangian is written in terms of real scalar fields φ_a , Weyl 2-spinors ψ_p and gauge fields V^A . The indices a , p and A run over the gauge group representation space of the scalar, spinor and vector fields, respectively. In the notation of [108, 109, 110, 120] the Lagrangian reads

$$\begin{aligned} \mathcal{L}_{\text{inv}} = & -\frac{1}{4} F_{\mu\nu}^A F^{A\mu\nu} + \frac{1}{2} (D_\mu \varphi)_a (D^\mu \varphi)_a + i\psi_p^\alpha \sigma_{\alpha\dot{\alpha}}^\mu (D_\mu^\dagger \bar{\psi}^{\dot{\alpha}})_p \\ & - \frac{1}{2!} m_{ab}^2 \varphi_a \varphi_b - \frac{1}{3!} h_{abc} \varphi_a \varphi_b \varphi_c - \frac{1}{4!} \lambda_{abcd} \varphi_a \varphi_b \varphi_c \varphi_d \\ & - \frac{1}{2} \left[(m_f)_{pq} \psi_p^\alpha \psi_{q\alpha} + \text{h.c.} \right] - \frac{1}{2} \left[Y_{pq}^a \psi_p^\alpha \psi_{q\alpha} \varphi_a + \text{h.c.} \right]. \end{aligned} \quad (4.9)$$

The appearing covariant derivatives D_μ and the field strength tensor $F_{\mu\nu}^A$, have the form

$$D_\mu \varphi_a = \left(\delta_{ab} \partial_\mu + ig T_{ab}^A V_\mu^A \right) \varphi_b, \quad (4.10a)$$

$$D_\mu \psi_{p\alpha} = \left(\delta_{pq} \partial_\mu + igt_{pq}^A V_\mu^A \right) \psi_{q\alpha}, \quad (4.10b)$$

$$F_{\mu\nu}^A = \partial_\mu V_\nu^A - \partial_\nu V_\mu^A - gf^{ABC} V_\mu^B V_\nu^C. \quad (4.10c)$$

The generators T_{ab}^A of the gauge transformation for the scalars are chosen to be antisymmetric and purely imaginary, while the generators t_{pq}^A for the spinors are hermitian. The symbols f^{ABC} are the structure constants of the simple gauge group.

As described above, real scalar background fields $\hat{\varphi}_a$ together with constant shifts \hat{v}_a are introduced. The gauge transformation of the combination $(\hat{\varphi}_a + \hat{v}_a)$ is defined to be the same as for the scalar field φ_a . The Lagrangian with background fields and shifts is then obtained by replacing in (4.9)

$$\varphi_a \rightarrow \varphi_a^{\text{eff}} = \varphi_a + \hat{\varphi}_a + \hat{v}_a. \quad (4.11)$$

To establish a gauge fixing and quantize the theory, Faddeev-Popov ghost fields c^A , anti-ghost fields \bar{c}^A , as well as the Nakanishi-Lautrup auxiliary field B^A are introduced. Furthermore one defines BRST transformations for all fields. For the vector fields, the spinors, ghosts, anti-ghosts and the Nakanishi-Lautrup field the standard definitions are used [121, 122, 116]

$$sV_\mu^A = \partial_\mu c^A - gf^{ABC}V_\mu^B c^C, \quad (4.12)$$

$$s\psi_{p\alpha} = -igc^A t_{pq}^A \psi_{q\alpha}, \quad (4.13)$$

$$sc^A = \frac{1}{2}gf^{ABC}c^B c^C, \quad (4.14)$$

$$s\bar{c}^A = B^A, \quad sB^A = 0. \quad (4.15)$$

In order to leave the physics content of the theory unchanged, the background fields $\hat{\varphi}_a$ need to transform as BRST doublet with another background field \hat{q}_a [123, 124]

$$s\hat{\varphi}_a = \hat{q}_a, \quad s\hat{q}_a = 0. \quad (4.16)$$

The scalar fields φ_a^{eff} are required to transform homogeneously, which leads to

$$s\varphi_a^{\text{eff}} = -igT_{ab}^A c^A \varphi_b^{\text{eff}}. \quad (4.17)$$

This implies the transformation for the scalar fields to read

$$s\varphi_a = -igT_{ab}^A c^A \varphi_b^{\text{eff}} - \hat{q}_a. \quad (4.18)$$

To fix the gauge a global gauge invariant R_ξ gauge is used with the gauge fixing function

$$F_{\text{bg}}^A = \partial^\mu V_\mu^A + ig\xi\xi' (\hat{\varphi} + \hat{v})_a T_{ab}^A \varphi_b. \quad (4.19)$$

The Lagrangian for the Faddeev-Popov ghosts and the gauge fixing is then given by

$$\mathcal{L}_{\text{f.p.}+\text{g.f.}} = s \left[\bar{c}^A \left(F_{\text{bg}}^A + \frac{\xi}{2} B^A \right) \right]. \quad (4.20)$$

After eliminating the Nakanishi-Lautrup auxiliary field B^A by its equations of motion,

Eq. (4.20) evaluates to

$$\begin{aligned}
 \mathcal{L}_{\text{f.p.}+\text{g.f.}} = & -\frac{1}{2\xi}(\partial^\mu V_\mu^A)(\partial^\nu V_\nu^A) - \bar{c}^A \square c^A - gf^{ABC}(\partial^\mu \bar{c}^A)V_\mu^B c^C \\
 & - ig\xi'(\partial^\mu V_\mu^A)(\hat{\varphi} + \hat{v})_a T_{ab}^A \varphi_b - ig\xi\xi' \bar{c}^A \hat{q}_a T_{ab}^A (\varphi + \hat{\varphi} + \hat{v})_b \\
 & - g^2 \xi \xi' \bar{c}^A c^B (\hat{\varphi} + \hat{v})_a T_{ab}^A T_{bc}^B (\varphi + \hat{\varphi} + \hat{v})_c \\
 & + \frac{1}{2} g^2 \xi \xi'^2 (\hat{\varphi} + \hat{v})_a T_{ab}^A \varphi_b (\hat{\varphi} + \hat{v})_c T_{cd}^A \varphi_d.
 \end{aligned} \tag{4.21}$$

Finally, sources K for the non-linear BRST transformations are introduced

$$\mathcal{L}_{\text{ext}} = K_{\varphi_a} s\varphi_a + K_{V_\mu^A} sV_\mu^A + K_{c^A} sc^A + [K_{\psi_p} s\psi_p + \text{h.c.}]. \tag{4.22}$$

They allow to formulate relations between Green functions which originate from the BRST invariance, so-called Slavnov-Taylor identities [125, 126, 98, 99, 127, 101, 102, 103, 128]. The full BRST invariant Lagrangian with background fields is then given by

$$\mathcal{L}_{\text{tot}} = \mathcal{L}_{\text{inv}}|_{\varphi \rightarrow \varphi^{\text{eff}}} + \mathcal{L}_{\text{f.p.}+\text{g.f.}} + \mathcal{L}_{\text{ext}}. \tag{4.23}$$

4.2.3 Renormalization

The renormalization of the general gauge theory with background fields from Section 4.2.2 proceeds as in the case without background fields [98, 99, 100, 101, 102, 103]. The most general renormalization transformation for the aforementioned setup is given by the general solution of

1. the Slavnov-Taylor identity, which expresses the BRST invariance on the level of Green functions,
2. the gauge condition, which fixes the dependency of the Nakanishi-Lautrup field B^A and
3. the Ward identity, which expresses the global gauge invariance.

Note that the Ward identity from 3. is a result of the preserved global gauge invariance and provides additional information on the counter-term structure of the theory. The resulting general renormalization transformation is given by

1. Parameter renormalization, where all parameters $p \in \{g, \xi, \xi', m_{ab}^2, h_{abc}, \lambda_{abcd}, (m_f)_{pq}, Y_{pq}^a\}$ renormalize as $p \rightarrow Z_p p = p + \delta p$. A counter-term $\delta \hat{v}$ for the shift \hat{v} is forbidden by the global Ward identity.
2. Field renormalization, where all fields transform multiplicatively with corresponding \sqrt{Z} factors and the BRST sources with inverse \sqrt{Z} factors. In particular, the renormalization transformations of the scalars, the background fields and the source K_{φ_a} read

$$\varphi_a \rightarrow \sqrt{Z} \varphi_a, \tag{4.24a}$$

$$(\hat{\varphi} + \hat{v})_a \rightarrow \sqrt{\hat{Z}}_{ab} \sqrt{\hat{Z}}_{bc} (\hat{\varphi} + \hat{v})_c, \quad (4.24b)$$

$$\hat{q}_a \rightarrow \sqrt{\hat{Z}}_{ab} \sqrt{\hat{Z}}_{bc} \hat{q}_c, \quad (4.24c)$$

$$K_{\varphi_a} \rightarrow \left(\sqrt{\hat{Z}}^{-1} \right)_{ba} K_{\varphi_b}. \quad (4.24d)$$

Furthermore, only theories are considered that possess a symmetry (at the operator dimension 4 level), which restricts the field renormalizations of the scalar fields to be diagonal, i.e.

$$\sqrt{\hat{Z}}_{ab} \rightarrow \sqrt{\hat{Z}}(a) \delta_{ab} \quad \text{and} \quad \sqrt{\hat{Z}}_{ab} \rightarrow \sqrt{\hat{Z}}(a) \delta_{ab}. \quad (4.25)$$

Such a symmetry is present in most models. For example in the MSSM and NMSSM it is given by the Peccei-Quinn symmetry [129]. In the E₆SSM the extra $U(1)_N$ gauge symmetry takes this role [42].

Equivalence to the standard approach

In a general gauge theory, without background fields, the general renormalization transformation of the scalar fields φ_a including shifts read

$$\varphi_a + v_a \rightarrow \sqrt{\hat{Z}}_{ab} \varphi_b + v_a + \delta v_a, \quad (4.26)$$

see Eq. (4.3a). In the modified setup with background fields, the effective scalar field φ_a^{eff} renormalizes as

$$\varphi_a^{\text{eff}} \rightarrow \sqrt{\hat{Z}}_{ab} \left(\varphi_b + \sqrt{\hat{Z}}_{bc} (\hat{\varphi} + \hat{v})_c \right). \quad (4.27)$$

Since the classical background field is set to zero at the end, these two approaches are equivalent and it holds

$$v_a = \hat{v}_a \quad \text{and} \quad \delta v_a = \left(\sqrt{\hat{Z}} \sqrt{\hat{Z}} - 1 \right)_{ab} v_b. \quad (4.28)$$

Eq. (4.28) shows the advantages of the background field method: First, the VEV counter-term is expressed in terms of the field renormalization constants $\sqrt{\hat{Z}}$ and $\sqrt{\hat{Z}}$ of the scalar and the background field, respectively. Since $\sqrt{\hat{Z}}$ and $\sqrt{\hat{Z}}$ are of mass dimension zero, they are at most logarithmically divergent. Second, the mass dimension of δv_a stems only from the direct proportionality to v_a . Third, $\sqrt{\hat{Z}}$ is well known at the one- and two-loop level [120, 108].

The unknown field renormalization $\sqrt{\hat{Z}}$ of the background field can be calculated directly from renormalizing the unphysical two-point Green function $\Gamma_{\hat{q}_a, K_{\varphi_b}}$. The reason is that the renormalization transformation, applied to the Lagrangian of the

(a) $\Gamma_{\varphi_b, c^A, K_{\varphi_a}} = gT_{ab}^A$, (b) $\Gamma_{\varphi_b, \hat{q}_a, \bar{c}^A} = \xi \xi' g T_{ab}^A$,

(c) $\Gamma_{\hat{q}_a, K_{\varphi_b}} = -i \left(\sqrt{\hat{Z}} - 1 \right)_{ba} = -\frac{i}{2} \delta \hat{Z}_{ba}^{(1)} + O(\hbar^2)$

Figure 4.1: Feynman rules necessary for the calculation of $\sqrt{\hat{Z}}$.

BRST sources \mathcal{L}_{ext} , yields with (4.24c) and (4.24d)

$$\mathcal{L}_{\text{ext}} = -K_{\varphi_a} \hat{q}_a + \dots \xrightarrow{\text{RT}} -K_{\varphi_a} \sqrt{\hat{Z}}_{ab} \hat{q}_b + \dots \quad (4.29)$$

This leads to a counter-term Feynman rule for the \hat{q}_a - K_{φ_b} two-point function, which is only proportional $(\sqrt{\hat{Z}} - 1)$, see Figure 4.1(c). Choosing a renormalization scheme then fixes the divergent and the finite parts of $\sqrt{\hat{Z}}$. Furthermore, there are only two Feynman rules which couple \hat{q}_a and K_{φ_b} to propagating fields: $\Gamma_{\varphi_b, c^A, K_{\varphi_a}}$ and $\Gamma_{\varphi_b, \hat{q}_a, \bar{c}^A}$, see Figure 4.1(a) and 4.1(b). These two Feynman rules are both proportional to the gauge coupling g . In addition, $\Gamma_{\varphi_b, \hat{q}_a, \bar{c}^A}$ depends on the gauge fixing parameter ξ . As a consequence, the field renormalization $\sqrt{\hat{Z}}$ of the background field is proportional to g^2 and gauge dependent. This leads automatically to a gauge dependence of δv_a and β_{v_a} .

Determination of β_v from δv

The β -function of the VEV describes the dependency of the renormalized v on the renormalization scale μ . It is defined as

$$\beta_v = \mu \frac{\partial v}{\partial \mu}. \quad (4.30)$$

It can be determined from the fact that the bare VEV, $v_0 = \mu^{-\epsilon} \sqrt{Z_v} v$, is independent of the renormalization scale μ

$$0 = \mu \frac{dv_0}{d\mu} \quad (4.31)$$

$$\Leftrightarrow 0 = \epsilon \sqrt{Z_v} v - \sum_p \beta_p \left[\partial_p \sqrt{Z_v} \right] v - \sqrt{Z_v} \beta_v. \quad (4.32)$$

Here the index p runs over all theory parameters. Expanding the field renormalization and the β -function in powers of \hbar

$$\sqrt{Z_v} = \mathbf{1} + \frac{1}{2} \sum_{n=1} \hbar^n \delta Z_v^{(n)}, \quad (4.33a)$$

$$\beta_v = \sum_{n=0} \hbar^n \beta_v^{(n)}, \quad (4.33b)$$

yields for the β -function of the VEV

$$\beta_v^{(0)} = \epsilon v, \quad (4.34a)$$

$$\beta_v^{(1)} = - \sum_p \beta_p^{(0)} \frac{1}{2} [\partial_p \delta Z_v^{(1)}] v, \quad (4.34b)$$

$$\beta_v^{(2)} = - \sum_p \beta_p^{(0)} \frac{1}{2} [\partial_p \delta Z_v^{(2)}] v - \sum_p \beta_p^{(1)} \frac{1}{2} [\partial_p \delta Z_v^{(1)}] v - \frac{1}{2} \delta Z_v^{(1)} \beta_v^{(1)}. \quad (4.34c)$$

From Eq. (4.28) one finds $\sqrt{Z_v} = \sqrt{Z} \sqrt{\hat{Z}}$ and the above equations reduce to

$$\beta_{v_a}^{(0)} = \epsilon v_a, \quad (4.35a)$$

$$\beta_{v_a}^{(1)} = - \sum_p \beta_p^{(0)} \partial_p \left[\frac{1}{2} (\delta Z_{ab}^{(1)} + \delta \hat{Z}_{ab}^{(1)}) \right] v_b, \quad (4.35b)$$

$$\begin{aligned} \beta_{v_a}^{(2)} = & - \sum_p \beta_p^{(0)} \partial_p \left[\frac{1}{2} (\delta Z_{ab}^{(2)} + \delta \hat{Z}_{ab}^{(2)}) \right] v_b - \sum_p \beta_p^{(1)} \partial_p \left[\frac{1}{2} (\delta Z_{ab}^{(1)} + \delta \hat{Z}_{ab}^{(1)}) \right] v_b \\ & - \frac{1}{2} [\delta Z_{ab}^{(1)} + \delta \hat{Z}_{ab}^{(1)}] \beta_{v_b}^{(1)}. \end{aligned} \quad (4.35c)$$

The Eqs. (4.35) can be written in a simpler form in terms of the anomalous dimensions of the scalar and background fields. These are defined as [130]

$$\gamma_{ab}(\mathbf{S}) = \left(\mu \partial_\mu \sqrt{Z_{ac}^{-1}} \right) \sqrt{Z_{cb}}, \quad \hat{\gamma}_{ab}(\mathbf{S}) = \left(\mu \partial_\mu \sqrt{\hat{Z}_{ac}^{-1}} \right) \sqrt{\hat{Z}_{cb}}. \quad (4.36)$$

By using the loop-expansions (4.33), the different loop orders of the anomalous dimension of the scalar field read

$$\gamma_{ab}^{(0)}(\mathbf{S}) = 0, \quad (4.37a)$$

$$\gamma_{ab}^{(1)}(\mathbf{S}) = - \sum_p \beta_p^{(0)} \partial_p \frac{1}{2} \delta Z_{ab}^{(1)}, \quad (4.37b)$$

$$\gamma_{ab}^{(2)}(\mathbf{S}) = - \sum_p \beta_p^{(0)} \partial_p \frac{1}{2} \delta Z_{ab}^{(2)} - \sum_p \beta_p^{(1)} \partial_p \frac{1}{2} \delta Z_{ab}^{(1)} - \frac{1}{2} \delta Z_{ac}^{(1)} \gamma_{cb}^{(1)}(\mathbf{S}). \quad (4.37c)$$

The expansion for the background field is analogue. This yields the β -function of the VEV in terms of the anomalous dimensions

$$\beta_{v_a}^{(n)} = \left[\gamma_{ab}^{(n)}(\mathbf{S}) + \hat{\gamma}_{ab}^{(n)}(\mathbf{S}) \right] v_b. \quad (4.38)$$

Note that Eq. (4.38) is valid for arbitrary loop orders $n \geq 0$.

In summary, the here used formalism with scalar background fields allows to express the β -function of the VEV (4.38) in terms of the anomalous dimensions of the scalar and the background fields. The former are well known in a general gauge theory at the one- and two-loop level. The latter can be directly calculated from the counter-term $\delta\hat{Z}$, which renormalizes the unphysical Green function $\Gamma_{\hat{q},K_\varphi}$. The results for $\gamma(S)$ and $\hat{\gamma}(S)$ will be given in the next section.

4.2.4 Calculation of the anomalous dimensions

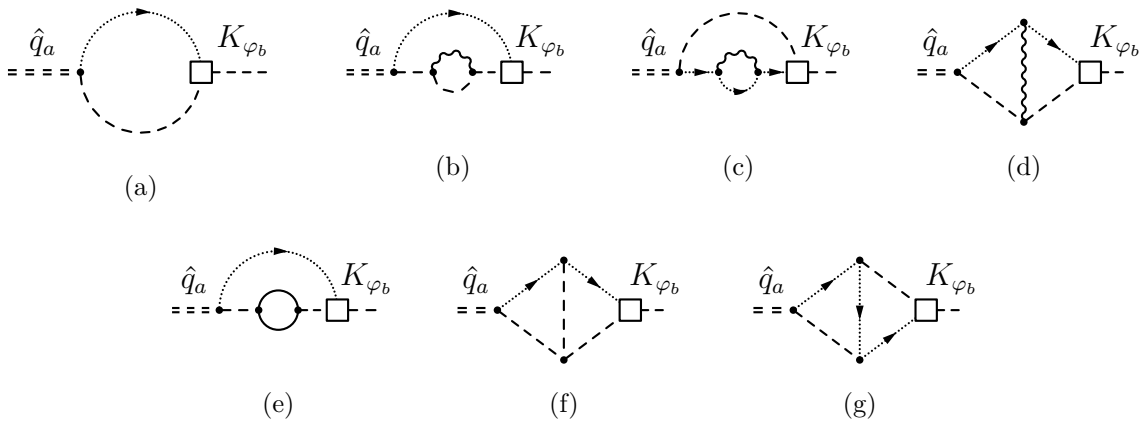


Figure 4.2: All relevant graphs for the determination of the one- and two-loop corrections to $\Gamma_{\hat{q}_a, K_{\varphi_b}}$. Graph 4.2(a) is of order $O(g^2)$; graphs 4.2(b)–4.2(d) are $O(g^4)$ -contributions; graph 4.2(e) is of order $O(g^2YY^\dagger)$; graphs 4.2(f)–4.2(g) are power-counting finite.

As explained in Section 4.2.3, the field renormalization $\delta\hat{Z}_{ab}$ can be directly calculated from renormalizing the unphysical two-point function $\Gamma_{\hat{q}_a, K_{\varphi_b}}$. At the one-loop level there is only one Feynman diagram contributing to $\Gamma_{\hat{q}_a, K_{\varphi_b}}$, see Figure 4.2(a). In the $\overline{\text{MS}}$ renormalization scheme one obtains for $\delta\hat{Z}_{ab}$

$$\delta\hat{Z}_{ab}^{(1)} = \frac{1}{(4\pi)^2} 2g^2 \xi \xi' C_{ab}^2(S) \Delta, \quad (4.39)$$

where $\Delta = 1/\epsilon - \gamma_E + \ln 4\pi$ is the regularized divergence in $D = 4 - 2\epsilon$ dimensions. The quadratic Casimir $C_{ab}^2(S)$ of the scalar representation is defined in Appendix A. From Eq. (4.37b) one then obtains the one-loop anomalous dimension of the background field in the $\overline{\text{MS}}$ scheme

$$\hat{\gamma}_{ab}^{(1)}(S) = \frac{1}{(4\pi)^2} 2g^2 \xi \xi' C_{ab}^2(S). \quad (4.40a)$$

Note that $\hat{\gamma}_{ab}^{(1)}(S)$ is gauge dependent.

At the two-loop level there are four diagrams that contribute a divergence to $\Gamma_{\hat{q}_a, K_{\varphi_b}}$, see Figure 4.2. The diagrams 4.2(b)–4.2(d) are of the order $O(g^4)$, and the diagram 4.2(e) contributes at the order $O(g^2 Y Y^\dagger)$. The remaining two diagrams 4.2(f)–4.2(g) are finite and do therefore not contribute to $\delta \hat{Z}_{ab}^{(2)}$. Using Eq. (4.37c) one obtains the two-loop anomalous dimension of the background field in the $\overline{\text{MS}}$ scheme

$$\hat{\gamma}_{ab}^{(2)}(S) = \frac{\xi \xi'}{(4\pi)^4} \left\{ g^4 \left[2(1 + \xi) C_{ac}^2(S) C_{cb}^2(S) + \frac{7 - \xi}{2} C_2(G) C_{ab}^2(S) \right] - 2g^2 C_{ac}^2(S) Y_{cb}^2(S) \right\}. \quad (4.40b)$$

Here $C_2(G)$ is the quadratic Casimir operator of the group in the representation of the gauge field and $Y_{cb}^2(S)$ is a group invariant proportional to Yukawa coupling squared, see Appendix A.

The anomalous dimension $\gamma_{ab}(S)$ of the scalar in a general gauge theory is well known at the one- and two-loop level in the $\overline{\text{MS}}$ scheme [120, 108]. In terms of the group invariants of Appendix A they read

$$\gamma_{ab}^{(1)}(S) = \frac{1}{(4\pi)^2} \left[g^2 (3 - \xi) C_{ab}^2(S) - Y_{ab}^2(S) \right], \quad (4.41a)$$

$$\begin{aligned} \gamma_{ab}^{(2)}(S) = \frac{1}{(4\pi)^4} \left\{ g^4 C_{ab}^2(S) \left[\left(\frac{35}{3} - 2\xi - \frac{1}{4} \xi^2 \right) C_2(G) - \frac{10}{6} S_2(F) - \frac{11}{12} S_2(S) \right] \right. \\ \left. - \frac{3}{2} g^4 C_{ac}^2(S) C_{cb}^2(S) + \frac{3}{2} H_{ab}^2(S) + \bar{H}_{ab}^2(S) - \frac{10}{2} g^2 Y_{ab}^{2F}(S) - \frac{1}{2} \Lambda_{ab}^2(S) \right\}. \end{aligned} \quad (4.41b)$$

4.3 Result for the VEV β -function

4.3.1 General gauge theory

Using the decomposition of β_v in terms of the anomalous dimensions, Eq. (4.38), and the one- and two-loop expressions for $\gamma(S)$ and $\hat{\gamma}(S)$, Eqs. (4.40) and (4.41), one obtains the β -function of the VEV in a general gauge theory with R_ξ gauge fixing in the $\overline{\text{MS}}$ scheme

$$\beta_{v_a}^{(1)} = \frac{1}{(4\pi)^2} \left[g^2 (3 - \xi + 2\xi \xi') C_{ab}^2(S) - Y_{ab}^2(S) \right] v_b, \quad (4.42a)$$

$$\begin{aligned} \beta_{v_a}^{(2)} = \frac{1}{(4\pi)^4} \left\{ g^4 C_{ab}^2(S) \left[\left(\frac{35}{3} - 2\xi - \frac{1}{4} \xi^2 + \frac{7 - \xi}{2} \xi \xi' \right) C_2(G) - \frac{10}{6} S_2(F) - \frac{11}{12} S_2(S) \right] \right. \\ \left. + g^4 \left[2\xi \xi' (1 + \xi) - \frac{3}{2} \right] C_{ac}^2(S) C_{cb}^2(S) - \frac{1}{2} \Lambda_{ab}^2(S) \right\} \end{aligned}$$

$$+ \frac{3}{2} H_{ab}^2(S) + \bar{H}_{ab}^2(S) - \frac{10}{2} g^2 Y_{ab}^{2F}(S) - 2\xi\xi' g^2 C_{ac}^2(S) Y_{cb}^2(S) \Big\} v_b. \quad (4.42b)$$

Note that these β -functions are gauge dependent.

4.3.2 Kinetic mixing

The calculated anomalous dimensions Eqs. (4.40) and (4.41) are valid for gauge theories with a simple gauge group G . Refs. [131, 132, 133] have generalized $\gamma(S)$ to a semisimple product group of the form

$$G = \left(\times_{k \in I} G_k \right) \times \left(\times_{a \in J} U(1)_a \right). \quad (4.43)$$

Here, G_k are simple groups and I, J are finite subsets of \mathbb{N} . For gauge groups of the form (4.43) kinetic mixing of the $U(1)$ field strength tensors can occur, if $|J| > 1$. In this case the Lagrangian for the abelian gauge field mixing reads

$$\mathcal{L}_{\text{kin.}} = -\frac{1}{4} \sum_{a, b \in J} F_{a, \mu\nu} \Xi_{ab} F_b^{\mu\nu}, \quad (4.44)$$

with a non-diagonal matrix Ξ . To take the effect of kinetic mixing in $\hat{\gamma}(S)$ into account, the approach in [132, 133] is followed. Here, the matrix Ξ is absorbed into a redefinition of the abelian gauge fields, which leads to a matrix-valued gauge coupling \hat{g}_{ab}

$$\hat{g}_{ab} = \sum_{c \in J} \delta_{ac} g'_c \sqrt{\Xi_{cb}^{-1}}. \quad (4.45)$$

Here g'_c denotes the abelian gauge coupling corresponding to the group $U(1)_c$. This approach allows to provide substitution rules for the gauge coupling dependent terms in $\hat{\gamma}(S)$, in order to account for the kinetic mixing.

At the one-loop level $\hat{\gamma}^{(1)}$ receives no correction from kinetic mixing, because the ghost and anti-ghost fields are not affected by the mixing. The same holds for the $O(g^2 Y Y^\dagger)$ contribution in $\hat{\gamma}^{(2)}$ at the two-loop level. The terms of the form $g^4 C_2(G) C^2(S)$ receive no correction as well, because the abelian gauge fields do not couple to ghost and anti-ghost fields. The only non-vanishing contribution appears in the $g^4 C^2(S) C^2(S)$ term and has its origin in diagram 4.2(b). The corresponding substitution rule reads

$$g^4 C^2(S) C^2(S) \xrightarrow{\text{kin. mix } \hat{\gamma}} \left[\sum_{k \in I} g_k^2 C_{G_k}^2(S) + \sum_{a \in J} W_a(S) W_a(S) \right] \times \left[\sum_{k \in I} g_k^2 C_{G_k}^2(S) + \sum_{a \in J} g_a'^2 Q_a^2(S) \right], \quad (4.46)$$

with

$$W_a(S) = \sum_{b \in J} Q_b(S) \hat{g}_{ba}. \quad (4.47)$$

Here g_k is the non-abelian gauge coupling that corresponds to the simple group G_k . The $Q_a(S)$ are the charges of the scalar field with respect to the abelian groups $U(1)_a$. Finally, $C_{G_k}^2(S)$ represents the quadratic Casimir of the group G_k in the representation of the scalar field.

4.3.3 Supersymmetric gauge theory

The VEV β -functions (4.42) are valid in a general gauge theory and are given in the $\overline{\text{MS}}$ renormalization scheme. In this section the results are converted to a $N = 1$ supersymmetric gauge theory in Wess-Zumino gauge, in the supersymmetry preserving renormalization scheme $\overline{\text{DR}}$ [105, 106]. For the conversion the following steps have to be performed:

1. The field content of the theory must involve complex scalars φ_a and corresponding superpartner Weyl spinors ψ_p in the same representation of the gauge group. Furthermore, for each vector field V^A a corresponding gaugino Weyl spinor λ^A is introduced, which transforms in the adjoint representation of the gauge group.
2. The Yukawa-type coupling structure between the Weyl fermions ψ_p , gauginos λ^A and complex scalars φ_a is restricted by supersymmetry to be

$$\frac{1}{2} \left[Y_{pq}^a \psi_p^\alpha \psi_{q\alpha} \varphi_a + \text{h. c.} \right] \xrightarrow{\text{gaugino}} -\sqrt{2}g \left[\bar{\lambda}_{\dot{\alpha}}^A \bar{\psi}_p^{\dot{\alpha}} T_{pa}^A \varphi_a + \text{h. c.} \right]. \quad (4.48)$$

Besides these Yukawa-type gaugino interactions, further Yukawa terms without gauginos may originate from the superpotential.

3. The anomalous dimensions $\hat{\gamma}(S)$ and $\gamma(S)$ must be rewritten in terms of complex scalars and the contribution from the gauginos must be taken into account.
4. The resulting expression for $\gamma(S)$ and $\hat{\gamma}(S)$ must then be converted from the $\overline{\text{MS}}$ to the supersymmetry preserving $\overline{\text{DR}}$ renormalization scheme. This conversion can be done by using transition counter-terms for the model parameters [134] and fields [135].

Applying all of the above steps yields for the one- and two-loop anomalous dimensions of the complex scalar fields in a supersymmetric theory in the $\overline{\text{DR}}$ scheme

$$\gamma_{ab}^{(1)}(S) \Big|_{\text{SUSY}}^{\overline{\text{DR}}} = \frac{1}{(4\pi)^2} \left[g^2 (1 - \xi) C_{ab}^2(S) - \frac{1}{2} Y_{apq}^* Y_{bpq} \right], \quad (4.49a)$$

$$\begin{aligned}
 \gamma_{ab}^{(2)}(\mathbf{S}) \Big|_{\text{SUSY}}^{\overline{\text{DR}}} &= \frac{1}{(4\pi)^4} \left\{ g^4 \left[\left(\frac{9}{4} - \frac{5}{3}\xi - \frac{1}{4}\xi^2 \right) C_2(\mathbf{G}) - S_2(\mathbf{S}) \right] C_{ab}^2(\mathbf{S}) \right. \\
 &\quad - 2g^4 C_{ac}^2(\mathbf{S}) C_{cb}^2(\mathbf{S}) + \frac{1}{2} Y_{arc}^* Y_{rpq} Y_{pqd}^* Y_{bcd} \\
 &\quad \left. + g^2 \left[C_{ac}^2(\mathbf{S}) Y_{cpq}^* Y_{bpq} - 2Y_{apq}^* C_{pr}^2(\mathbf{S}) Y_{brq} \right] \right\}. \quad (4.49b)
 \end{aligned}$$

For the anomalous dimensions of the complex scalar background fields the same procedure must be applied. However, the conversion from the $\overline{\text{MS}}$ to the $\overline{\text{DR}}$ scheme in the last step is trivial, because no diagram contributing to $\delta\hat{Z}$ leads to a difference between the two schemes. From this property the transition counter-terms for the background field renormalization \hat{Z} and for ξ' can be derived as a by-product:

$$\delta\hat{Z}^{(1),\text{trans}} = 0, \quad (4.50)$$

$$\delta Z_{\xi'}^{(1),\text{trans}} = -\delta Z_g^{(1),\text{trans}} + \frac{1}{2} \delta Z_V^{(1),\text{trans}} = \frac{1}{(4\pi)^2} \frac{g^2}{3} C_2(\mathbf{G}). \quad (4.51)$$

Here $\delta Z_g^{(1),\text{trans}}$ and $\delta Z_V^{(1),\text{trans}}$ denote the transition counter-terms for the gauge coupling and the gauge field, respectively [134, 135]. The one- and two-loop anomalous dimensions of the background field then read

$$\hat{\gamma}_{ab}^{(1)}(\mathbf{S}) \Big|_{\text{SUSY}}^{\overline{\text{DR}}} = \frac{1}{(4\pi)^2} 2g^2 \xi \xi' C_{ab}^2(\mathbf{S}), \quad (4.52a)$$

$$\begin{aligned}
 \hat{\gamma}_{ab}^{(2)}(\mathbf{S}) \Big|_{\text{SUSY}}^{\overline{\text{DR}/\overline{\text{MS}}}} &= \frac{\xi \xi'}{(4\pi)^4} \left\{ g^4 \left[\frac{7-\xi}{2} C_2(\mathbf{G}) C_{ab}^2(\mathbf{S}) - 2(1-\xi) C_{ac}^2(\mathbf{S}) C_{cb}^2(\mathbf{S}) \right] \right. \\
 &\quad \left. - g^2 C_{ac}^2(\mathbf{S}) Y_{cpq}^* Y_{bpq} \right\}. \quad (4.52b)
 \end{aligned}$$

Using the decomposition (4.38) of β_v in terms of $\gamma(\mathbf{S})$ and $\hat{\gamma}(\mathbf{S})$ one obtains for the VEV β -function

$$\beta_{v_a}^{(1)} \Big|_{\text{SUSY}}^{\overline{\text{DR}}} = \frac{1}{(4\pi)^2} \left[g^2 (1-\xi + 2\xi\xi') C_{ab}^2(\mathbf{S}) - \frac{1}{2} Y_{apq}^* Y_{bpq} \right] v_b, \quad (4.53)$$

$$\begin{aligned}
 \beta_{v_a}^{(2)} \Big|_{\text{SUSY}}^{\overline{\text{DR}}} &= \frac{1}{(4\pi)^4} \left\{ g^4 \left[\left(\frac{9}{4} - \frac{5}{3}\xi - \frac{1}{4}\xi^2 + \frac{7-\xi}{2}\xi\xi' \right) C_2(\mathbf{G}) - S_2(\mathbf{S}) \right] C_{ab}^2(\mathbf{S}) \right. \\
 &\quad - g^4 [2\xi\xi' (1-\xi) + 2] C_{ac}^2(\mathbf{S}) C_{cb}^2(\mathbf{S}) + \frac{1}{2} Y_{arc}^* Y_{rpq} Y_{pqd}^* Y_{bcd} \\
 &\quad \left. + g^2 [1 - \xi\xi'] C_{ac}^2(\mathbf{S}) Y_{cpq}^* Y_{bpq} - 2g^2 Y_{apq}^* C_{pr}^2(\mathbf{S}) Y_{brq} \right\} v_b. \quad (4.54)
 \end{aligned}$$

4.4 Application to the MSSM and NMSSM

4.4.1 MSSM

The MSSM [20] contains two scalar $SU(2)$ Higgs doublets h_1 and h_2 with hypercharges $Y_{h_1}/2 = -Y_{h_2}/2 = -1/2$, respectively. The complete field content and the superpotential of the MSSM can be found in Appendix B. The neutral components of the Higgs doublets are shifted by VEVs v_1 and v_2 as

$$h_1 = \begin{pmatrix} h_1^0 \\ h_1^- \end{pmatrix} \rightarrow \begin{pmatrix} \frac{v_1}{\sqrt{2}} + h_1^0 \\ h_1^- \end{pmatrix}, \quad h_2 = \begin{pmatrix} h_2^+ \\ h_2^0 \end{pmatrix} \rightarrow \begin{pmatrix} h_2^+ \\ \frac{v_2}{\sqrt{2}} + h_2^0 \end{pmatrix}. \quad (4.55)$$

In this convention the one-loop anomalous dimensions of the MSSM Higgs doublets and their corresponding background fields read

$$(4\pi)^2 \gamma_{\text{MSSM}}^{(1),\overline{\text{DR}}} (h_2) = (1 - \xi) \left(\frac{3}{20} g_1^2 + \frac{3}{4} g_2^2 \right) - N_c \text{Tr} (y^u y^{u\dagger}), \quad (4.56a)$$

$$(4\pi)^2 \gamma_{\text{MSSM}}^{(1),\overline{\text{DR}}} (h_1) = (1 - \xi) \left(\frac{3}{20} g_1^2 + \frac{3}{4} g_2^2 \right) - N_c \text{Tr} (y^d y^{d\dagger}) - \text{Tr} (y^e y^{e\dagger}), \quad (4.56b)$$

$$(4\pi)^2 \hat{\gamma}_{\text{MSSM}}^{(1),\overline{\text{DR}}} (h_2) = 2\xi\xi' \left(\frac{3}{20} g_1^2 + \frac{3}{4} g_2^2 \right), \quad (4.56c)$$

$$(4\pi)^2 \hat{\gamma}_{\text{MSSM}}^{(1),\overline{\text{DR}}} (h_1) = 2\xi\xi' \left(\frac{3}{20} g_1^2 + \frac{3}{4} g_2^2 \right). \quad (4.56d)$$

In the above expressions g_1 is the GUT normalized gauge coupling of the $U(1)_Y$ and is defined as $g_1 = \sqrt{5/3} g_Y$. At the two-loop level one obtains

$$(4\pi)^4 \gamma_{\text{MSSM}}^{(2),\overline{\text{DR}}} (h_2) = -\frac{207}{200} g_1^4 - \frac{9}{20} g_1^2 g_2^2 - \left(3 + \frac{5}{2} \xi + \frac{3}{8} \xi^2 \right) g_2^4 \quad (4.57a)$$

$$- \left(\frac{4}{15} g_1^2 + \frac{16}{3} g_3^2 \right) N_c \text{Tr} (y^u y^{u\dagger}) \\ + N_c \text{Tr} (y^u y^{d\dagger} y^d y^{u\dagger}) + 3N_c \text{Tr} (y^u y^{u\dagger} y^u y^{u\dagger}),$$

$$(4\pi)^4 \gamma_{\text{MSSM}}^{(2),\overline{\text{DR}}} (h_1) = -\frac{207}{200} g_1^4 - \frac{9}{20} g_1^2 g_2^2 - \left(3 + \frac{5}{2} \xi + \frac{3}{8} \xi^2 \right) g_2^4 \quad (4.57b)$$

$$- \left(-\frac{2}{15} g_1^2 + \frac{16}{3} g_3^2 \right) N_c \text{Tr} (y^d y^{d\dagger}) - \frac{6}{5} g_1^2 \text{Tr} (y^e y^{e\dagger}) \\ + 3N_c \text{Tr} (y^d y^{d\dagger} y^d y^{d\dagger}) + N_c \text{Tr} (y^d y^{u\dagger} y^u y^{d\dagger}) + 3 \text{Tr} (y^e y^{e\dagger} y^e y^{e\dagger}),$$

$$(4\pi)^4 \hat{\gamma}_{\text{MSSM}}^{(2),\overline{\text{DR}}} (h_2) = -\xi\xi' \left\{ \left(\frac{3}{10} g_1^2 + \frac{3}{2} g_2^2 \right) [N_c \text{Tr} (y^u y^{u\dagger})] + \mathcal{R}_{\text{MSSM}} \right\}, \quad (4.57c)$$

$$(4\pi)^4 \hat{\gamma}_{\text{MSSM}}^{(2),\overline{\text{DR}}} (h_1) = -\xi\xi' \left\{ \left(\frac{3}{10} g_1^2 + \frac{3}{2} g_2^2 \right) [N_c \text{Tr} (y^d y^{d\dagger}) + \text{Tr} (y^e y^{e\dagger})] + \mathcal{R}_{\text{MSSM}} \right\}, \quad (4.57d)$$

with the abbreviation

$$\mathcal{R}_{\text{MSSM}} = (1 - \xi) \frac{9}{2} \left(\frac{1}{100} g_1^4 + \frac{1}{10} g_1^2 g_2^2 + \frac{1}{4} g_2^4 \right) - 3 \frac{7 - \xi}{4} g_2^4. \quad (4.58)$$

An important application of the results (4.56)–(4.58) is the β -function of $\tan \beta$. The latter is a MSSM input parameter, which is defined as

$$\tan \beta = \frac{v_2}{v_1}. \quad (4.59)$$

At the n -loop level its β -function is given by

$$\frac{\beta_{\tan \beta}^{(n)}}{\tan \beta} = \gamma^{(n)}(h_2) - \gamma^{(n)}(h_1) + \hat{\gamma}^{(n)}(h_2) - \hat{\gamma}^{(n)}(h_1). \quad (4.60)$$

Using the anomalous dimensions from (4.56) and (4.57) one obtains at the one- and two-loop level

$$\frac{\beta_{\tan \beta, \text{MSSM}}^{(1), \overline{\text{DR}}}}{\tan \beta} = -\frac{1}{(4\pi)^2} \left[N_c \text{Tr} (y^u y^{u\dagger}) - N_c \text{Tr} (y^d y^{d\dagger}) - \text{Tr} (y^e y^{e\dagger}) \right], \quad (4.61a)$$

$$\begin{aligned} \frac{\beta_{\tan \beta, \text{MSSM}}^{(2), \overline{\text{DR}}}}{\tan \beta} = & \frac{1}{(4\pi)^4} \left\{ - \left(\frac{4}{15} g_1^2 + \frac{16}{3} g_3^2 \right) N_c \text{Tr} (y^u y^{u\dagger}) \right. \\ & + \left(-\frac{2}{15} g_1^2 + \frac{16}{3} g_3^2 \right) N_c \text{Tr} (y^d y^{d\dagger}) + \frac{6}{5} g_1^2 \text{Tr} (y^e y^{e\dagger}) \\ & \left. + 3N_c \text{Tr} (y^u y^{u\dagger} y^u y^{u\dagger}) - 3N_c \text{Tr} (y^d y^{d\dagger} y^d y^{d\dagger}) - 3 \text{Tr} (y^e y^{e\dagger} y^e y^{e\dagger}) \right\} \\ & + \frac{1}{(4\pi)^2} \xi \xi' \left(\frac{3}{10} g_1^2 + \frac{3}{2} g_2^2 \right) \frac{\beta_{\tan \beta, \text{MSSM}}^{(1), \overline{\text{DR}}}}{\tan \beta}, \end{aligned} \quad (4.61b)$$

Note that $\tan \beta$ is gauge-independent at the one-loop level, because the ξ -dependent terms from $\hat{\gamma}^{(1)}(h_1)$ and $\hat{\gamma}^{(1)}(h_2)$ cancel. The reason is that the two Higgs doublets have the same $SU(2)_L$ and $U(1)_Y$ quantum numbers, up to a sign. At the two-loop level this cancellation does not happen and, thus, $\tan \beta$ is gauge-dependent.

4.4.2 NMSSM

In the NMSSM [37] one introduces a gauge singlet superfield S in addition to the MSSM Higgs doublets, see Section 5.2. Due to the shape of the scalar NMSSM potential, its scalar component s can acquire a non-zero vacuum expectation value v_3 . Therefore, s is shifted by its VEV as

$$s \rightarrow \frac{v_3}{\sqrt{2}} + s, \quad (4.62)$$

and one obtains for the one-loop anomalous dimensions of the Higgs fields

$$\gamma_{\text{NMSSM}}^{(1),\overline{\text{DR}}}(h_{1,2}) = \gamma_{\text{MSSM}}^{(1),\overline{\text{DR}}}(h_{1,2}) - \frac{1}{(4\pi)^2} |\lambda|^2, \quad (4.63a)$$

$$\gamma_{\text{NMSSM}}^{(1),\overline{\text{DR}}}(s) = -\frac{1}{(4\pi)^2} 2 \left(|\lambda|^2 + |\kappa|^2 \right), \quad (4.63b)$$

$$\hat{\gamma}_{\text{NMSSM}}^{(1),\overline{\text{DR}}}(h_{1,2}) = \hat{\gamma}_{\text{MSSM}}^{(1),\overline{\text{DR}}}(h_{1,2}), \quad (4.63c)$$

$$\hat{\gamma}_{\text{NMSSM}}^{(1),\overline{\text{DR}}}(s) = 0. \quad (4.63d)$$

At the two-loop level one obtains

$$\gamma_{\text{NMSSM}}^{(2),\overline{\text{DR}}}(h_2) = \gamma_{\text{MSSM}}^{(2),\overline{\text{DR}}}(h_2) + \frac{|\lambda|^2}{(4\pi)^4} \left[2|\kappa|^2 + 3|\lambda|^2 + N_c \text{Tr} \left(y^d y^{d\dagger} \right) + \text{Tr} \left(y^e y^{e\dagger} \right) \right], \quad (4.64a)$$

$$\gamma_{\text{NMSSM}}^{(2),\overline{\text{DR}}}(h_1) = \gamma_{\text{MSSM}}^{(2),\overline{\text{DR}}}(h_1) + \frac{|\lambda|^2}{(4\pi)^4} \left[2|\kappa|^2 + 3|\lambda|^2 + N_c \text{Tr} \left(y^u y^{u\dagger} \right) \right], \quad (4.64b)$$

$$\hat{\gamma}_{\text{NMSSM}}^{(2),\overline{\text{DR}}}(h_2) = -\frac{\xi\xi'}{(4\pi)^4} \left\{ \left(\frac{3}{10} g_1^2 + \frac{3}{2} g_2^2 \right) \left[N_c \text{Tr} \left(y^u y^{u\dagger} \right) + |\lambda|^2 \right] + \mathcal{R}_{\text{NMSSM}} \right\}, \quad (4.64c)$$

$$\hat{\gamma}_{\text{NMSSM}}^{(2),\overline{\text{DR}}}(h_1) = -\frac{\xi\xi'}{(4\pi)^4} \left\{ \left(\frac{3}{10} g_1^2 + \frac{3}{2} g_2^2 \right) \left[N_c \text{Tr} \left(y^d y^{d\dagger} \right) + \text{Tr} \left(y^e y^{e\dagger} \right) + |\lambda|^2 \right] \right. \\ \left. + \mathcal{R}_{\text{NMSSM}} \right\}, \quad (4.64d)$$

$$(4\pi)^4 \gamma_{\text{NMSSM}}^{(2),\overline{\text{DR}}}(s) = 8|\kappa|^4 + 8|\kappa|^2 |\lambda|^2 + 4|\lambda|^4 - \left(\frac{6}{5} g_1^2 + 6g_2^2 \right) |\lambda|^2 \\ + 2|\lambda|^2 \left[N_c \text{Tr} \left(y^d y^{d\dagger} \right) + \text{Tr} \left(y^e y^{e\dagger} \right) + N_c \text{Tr} \left(y^u y^{u\dagger} \right) \right], \quad (4.64e)$$

$$\hat{\gamma}_{\text{NMSSM}}^{(2),\overline{\text{DR}}}(s) = 0. \quad (4.64f)$$

with $\mathcal{R}_{\text{NMSSM}} = \mathcal{R}_{\text{MSSM}}$. Since γ_{NMSSM} and $\hat{\gamma}_{\text{NMSSM}}$ are of mass dimension zero, they gain extra contributions, compared to the MSSM, only from the dimensionless NMSSM superpotential couplings λ and κ . Therefore, Eqs. (4.63)–(4.64) are valid for both the Z_3 -symmetric and the Z_3 -violating NMSSM.

Since the NMSSM Higgs doublet quantum numbers are the same as in the MSSM, the one-loop β -functions of $\tan \beta$ are the same in both models

$$\beta_{\tan \beta, \text{NMSSM}}^{(1),\overline{\text{DR}}} = \beta_{\tan \beta, \text{MSSM}}^{(1),\overline{\text{DR}}}. \quad (4.65)$$

For this reason $\beta_{\tan \beta, \text{NMSSM}}^{(1),\overline{\text{DR}}}$ is gauge-independent, as in the MSSM. The two-loop β -function for $\tan \beta$ receives an extra contribution from the additional NMSSM Yukawa-

coupling λ

$$\frac{\beta_{\tan\beta,\text{NMSSM}}^{(2),\overline{\text{DR}}}}{\tan\beta} = \frac{\beta_{\tan\beta,\text{MSSM}}^{(2),\overline{\text{DR}}}}{\tan\beta} + \frac{|\lambda|^2}{(4\pi)^2} \frac{\beta_{\tan\beta,\text{MSSM}}^{(1),\overline{\text{DR}}}}{\tan\beta}. \quad (4.66)$$

Here, as in the MSSM, $\beta_{\tan\beta,\text{NMSSM}}^{(2),\overline{\text{DR}}}$ is gauge-dependent, because the ξ -dependent terms do not cancel in (4.60).

4.5 Summary and conclusion

The β -function of the vacuum expectation value was calculated in a general gauge theory with R_ξ gauge fixing in the $\overline{\text{MS}}$ renormalization scheme at the one- and two-loop level. The result was converted to a general supersymmetric gauge theory in Wess-Zumino gauge in the $\overline{\text{DR}}$ scheme. These results complement the well-known one- and two-loop β -functions and anomalous dimensions for general gauge theories and general supersymmetric gauge theories [108, 109, 110, 61, 62, 111]. The calculation was performed in an elegant scheme with scalar background fields, as used in [119]. The description of the calculation and the here presented results have been published in [63, 64].

The calculated generic one- and two-loop VEV β -functions were specialized to the MSSM and NMSSM. This made it possible to implement the prior unknown MSSM $O(g^4)$ contributions from (4.57) and (4.61b) into the Softsusy version 3.4.0. In addition, the here presented full NMSSM VEV β -functions (4.63)–(4.66) were implemented into the NMSSM extension of Softsusy in version 3.4.0 [136].

Shortly after the publication of the generic results presented here, the expressions for $\gamma(\text{S})$ and $\hat{\gamma}(\text{S})$ (4.49)–(4.52) were implemented by the SARAH developers into SARAH version 4.0.0 [137]. They can now be used to calculate the $\overline{\text{DR}}$ β -function of the VEVs in any supersymmetric model in R_ξ gauge. These β -functions are of special importance for general spectrum generators such as SARAH/SPheno [112, 113] and FlexibleSUSY [114]. These programs impose boundary conditions for the running $\overline{\text{DR}}$ model parameters (gauge and Yukawa couplings, VEVs, soft-breaking parameters, etc.) at different renormalization scales. The so defined boundary value problem is solved iteratively by numerically integrating the renormalization group equations and imposing the boundary conditions. For this procedure the $\overline{\text{DR}}$ β -functions of all model parameters (including the VEVs) need to be known. Before the here presented general results were known, the VEV β -functions were incomplete in these spectrum generators. This gap is herewith closed.

Chapter 5

Next-to-minimal Softsusy

5.1 Motivation for a NMSSM extension of Softsusy

As discussed in Section 2.2, the Next-to Minimal Supersymmetric Standard Model (NMSSM) is a well-motivated and experimentally viable model [138, 139, 140, 141, 31, 142, 143, 144], which can solve the μ -problem of the MSSM and can reduce the lightest Higgs mass fine-tuning due to additional, positive contributions from the extra scalar field.

To study the properties of the NMSSM and confront the model with experimental data a spectrum generator is needed, which calculates the pole masses and the couplings of the NMSSM particles given a set of theory input parameters. By the end of 2013 NMSPEC [145] was the only publicly available out-of-the-box spectrum generator for the NMSSM. Besides NMSPEC, the Mathematica package SARA [146, 137] can create a NMSSM spectrum generator by generating Fortran code, which is then integrated into SPheno [147, 148]. In 2008 the SUSY Les Houches Accord (SLHA) was extended [149] to include the NMSSM. It provides a well-defined interface to pass the spectrum generator output to programs which calculate further observables such as decays, the dark matter relic density, etc.

Due to the recent focus of the community on the NMSSM [31, 138, 139, 140, 141, 142, 143, 144, 150, 151, 152, 153, 154], it was decided to extend the MSSM spectrum generator Softsusy [60, 155, 156, 136] to enable the calculation of the NMSSM mass spectrum. Having another NMSSM spectrum generator can help to find bugs and to estimate the theory uncertainty of the pole mass spectrum prediction, because different spectrum generators usually use different levels of approximations [157, 158].

Part of this thesis was to implement the NMSSM into Softsusy, in collaboration with B. C. Allanach, P. Athron, L. C. Tunstall and A. G. Williams. For this it was necessary to re-design the Softsusy class hierarchy, implement the one- and two-loop β -functions of all NMSSM parameters as well as mass matrices, one-loop self-energies, one-loop tadpoles and EWSB conditions. Furthermore, the SLHA input and output interface needed to be extended according to the specification [149]. Finally, the full NMSSM implementation was systematically tested against existing NMSSM spectrum generators.

This chapter is organized as follows: In Section 5.2 the NMSSM field content and the Lagrangian is briefly described. Section 5.3 explains the physical boundary con-

ditions imposed on the model and the task of the spectrum generator. In Section 5.4 it is described in detail how the physical problems are solved at the C++ source code level and Section 5.5 lists the tests performed to validate the output and discusses differences to NMSPEC. In addition a brief comparison of the lightest CP-even Higgs pole mass between Softsusy and NMSPEC is performed to illustrate the precision of the Higgs mass prediction in different parameter regions.

5.2 The NMSSM

The Next-to Minimal Supersymmetric Standard Model (NMSSM) extends the MSSM field content, listed in Table B.1, by an extra gauge singlet superfield S in the $(\mathbf{1}, \mathbf{1}, 0)$ representation of the $SU(3)_c \times SU(2)_L \times U(1)_Y$ gauge group. Its (complex) scalar component is denoted by s , and the fermionic (Weyl spinor) component by \tilde{s} . Since all its charges are zero, it does not couple via gauge interaction. It couples to other matter fields only via additional superpotential terms. The most general renormalizable R -parity conserving NMSSM superpotential reads

$$\mathcal{W}_{\text{NMSSM}} = \mathcal{W}_{\text{MSSM}} + \lambda S(H_1 H_2) + \frac{\kappa}{3} S^3 + \frac{\mu'}{2} S^2 + \xi_F S, \quad (5.1)$$

with $\mathcal{W}_{\text{MSSM}}$ from Eq. (2.1). However, this general superpotential does not solve the μ -problem, since the μ -term $\mu(H_1 H_2)$ is still contained in $\mathcal{W}_{\text{MSSM}}$. Therefore a Z_3 -symmetry is imposed, which forbids all superpotential terms with dimensionful couplings. The resulting Z_3 -symmetric NMSSM superpotential is then given by

$$\mathcal{W}_{\text{NMSSM}}^{Z_3} = \mathcal{W}_{\text{MSSM}}(\mu = 0) + \lambda S(H_1 H_2) + \frac{\kappa}{3} S^3. \quad (5.2)$$

When the scalar component of S acquires a non-zero vacuum expectation value

$$s \rightarrow \frac{v_3}{\sqrt{2}} + s, \quad (5.3)$$

an effective μ -term with the value $\mu_{\text{eff}} = \lambda v_3 / \sqrt{2}$ is generated dynamically. In the NMSSM supersymmetry is softly broken by the following additional Lagrangian:

$$\mathcal{L}_{\text{NMSSM,soft}} = \mathcal{L}_{\text{NMSSM,soft}}^{Z_3} + \mathcal{L}_{\text{NMSSM,soft}}^{\tilde{Z}_3}, \quad (5.4)$$

$$\mathcal{L}_{\text{NMSSM,soft}}^{Z_3} = \mathcal{L}_{\text{MSSM,soft}}(B\mu = 0) - \left[\lambda A^\lambda s(h_1 h_2) + \frac{\kappa}{3} A^\kappa s^3 + \text{h. c.} \right] - m_s^2 |s|^2, \quad (5.5)$$

$$\mathcal{L}_{\text{NMSSM,soft}}^{\tilde{Z}_3} = - \left[B\mu(h_1 h_2) + \frac{m_s^2}{2} s^2 + \xi_S s + \text{h. c.} \right]. \quad (5.6)$$

The $\mathcal{L}_{\text{NMSSM,soft}}^{Z_3}$ part contains all breaking terms present in the Z_3 -invariant NMSSM, while $\mathcal{L}_{\text{NMSSM,soft}}^{\tilde{Z}_3}$ contains all explicitly Z_3 -violating contributions. The soft-breaking terms of the MSSM, $\mathcal{L}_{\text{MSSM,soft}}$, were given in Eq. (2.2).

The mixing of the gauge eigenstates to mass eigenstates is analogous to the MSSM,

except for an extended neutralino and Higgs sector. The fermionic component of the singlet superfield mixes with the bino, the neutral wino and the two neutral higgsinos to five neutralinos $\tilde{\chi}_i^0$. In the CP-conserving NMSSM the real component of the scalar singlet mixes with the real parts of the neutral Higgs doublet components to three CP-even Higgs bosons h_i . The imaginary part of the singlet mixes with the imaginary parts of the neutral Higgs doublet components to two CP-odd Higgs bosons A_i and a Goldstone boson. A broad review of the phenomenology of the NMSSM can be found in [37].

5.3 Physical problem statement

Goal of a NMSSM spectrum generator is to numerically calculate the pole masses and couplings of the SUSY particles, given numerical values for the NMSSM parameters. All model parameters of the Z_3 -symmetric and Z_3 -violating NMSSM are listed in Table 5.1. The first row shows the gauge and Yukawa couplings as well as the

	Z_3 -NMSSM	\tilde{Z}_3 -NMSSM
SM input	$g_1, g_2, g_3, y_u, y_d, y_e, v$	$g_1, g_2, g_3, y_u, y_d, y_e, v$
EWSB output	$\kappa, v_3 ^2, m_s^2$	$ \mu ^2, B\mu, \xi_S$
User input (general)	$m_q^2, m_u^2, m_d^2, m_\ell^2, m_e^2, m_{h_1}^2, m_{h_2}^2,$ $A^e, A^d, A^u, A^\lambda, A^\kappa,$ $M_1, M_2, M_3,$ $\lambda, \tan \beta, \text{sign } v_3$	$m_q^2, m_u^2, m_d^2, m_\ell^2, m_e^2, m_{h_1}^2, m_{h_2}^2,$ $A^e, A^d, A^u, A^\lambda, A^\kappa,$ $M_1, M_2, M_3,$ $\lambda, \tan \beta, \text{sign } \mu,$ $\kappa, v_3, m_s^2, \mu', m_s'^2, \xi_F$
User input (mSUGRA)	$m_0^2, A_0, M_{1/2},$ $\lambda, \tan \beta, \text{sign } v_3$	$m_0^2, A_0, M_{1/2},$ $\lambda, \tan \beta, \text{sign } \mu,$ $\kappa, v_3, m_s^2, \mu', m_s'^2, \xi_F$

Table 5.1: Model parameters of the Z_3 -symmetric and Z_3 -violating NMSSM. The first row contains the gauge and Yukawa couplings and the VEV $v = \sqrt{v_1^2 + v_2^2}$, which have all a Standard Model correspondence. The second row shows parameters chosen to be fixed by the EWSB conditions. In the third row the remaining free NMSSM parameters are listed. The last row contains the reduced parameter set in a mSUGRA-inspired scenario.

combination of VEVs $v = \sqrt{v_1^2 + v_2^2}$. These parameters have a direct correspondence to their Standard Model equivalents. In the second row parameters are listed which are chosen to be fixed by the electroweak symmetry breaking conditions, see below. The third segment of the table contains all remaining free parameters, such as soft-breaking squared masses, soft-breaking trilinear scalar couplings, soft-breaking linear terms, soft-breaking gaugino masses, superpotential parameters and VEVs. The last segment shows a reduced set of NMSSM parameters in a mSUGRA-inspired soft-breaking scenario, see below.

Since the NMSSM is a (only softly-broken) supersymmetric model, it is convenient to define all model parameters in the supersymmetry preserving $\overline{\text{DR}}$ renormalization scheme [105, 106]. Thereby, the model parameters become renormalization scale dependent quantities, which is expressed by the renormalization group equations

$$\mu \frac{\partial p}{\partial \mu} = \beta_p. \quad (5.7)$$

Here p denotes a model parameter and μ is the renormalization scale. On the right-hand side of Eq. (5.7) stands the β -function of the parameter p , which is known in a general softly broken supersymmetric model up to the two-loop level [159, 160, 161, 134, 162, 61, 132, 63, 64].

In the NMSSM only parameter choices are experimentally allowed, with which the known low-energy precision observables are correctly predicted. This includes in particular the known Standard Model fermion masses m_f , the electromagnetic and strong couplings $\alpha_{\text{e.m.}}(m_Z^{\text{pole}})$ and $\alpha_s(m_Z^{\text{pole}})$, the muon decay constant G_F and the Z boson pole mass m_Z^{pole} [11]. Such valid parameter choices can be ensured by using the Standard Model observables as input to determine the NMSSM $\overline{\text{DR}}$ gauge and Yukawa couplings g_i and y_f as well as the combined VEV v at the low-energy scale.

Furthermore, spontaneous breaking of the electroweak symmetry is required to occur in the NMSSM to generate mass terms for the W and Z bosons as well as for the quarks and leptons. This is possible in many NMSSM parameter regions, where the Higgs potential, V_{Higgs} , allows non-zero ground states v_1 , v_2 and v_3 for the three scalar fields h_1^0 , h_2^0 and s , respectively. To ensure this, the following three electroweak symmetry breaking consistency conditions must be fulfilled:

$$\frac{\partial V_{\text{Higgs}}}{\partial v_i} = 0 \quad i = 1, 2, 3. \quad (5.8)$$

These conditions are usually imposed at the SUSY scale M_S , which is the typical scale of the SUSY particle masses and is often defined as

$$M_S = \sqrt{m_{\tilde{t}_1} m_{\tilde{t}_2}}. \quad (5.9)$$

Here $m_{\tilde{t}_1}$ and $m_{\tilde{t}_2}$ are the $\overline{\text{DR}}$ masses of the two stops. The three EWSB equations (5.8) can be used to fix three NMSSM parameters. In the Z_3 -symmetric model, these are chosen to be $\kappa(M_S)$, $|v_s(M_S)|^2$ and $m_s^2(M_S)$. In the Z_3 -violating model $|\mu(M_S)|^2$, $B\mu(M_S)$ and ξ_S are chosen for this purpose, see the second row in Table 5.1.

Often, further conditions on the soft-breaking parameters are imposed. In the well-motivated mSUGRA-inspired scenario for example the universality constraints

$$(m_f^2)_{ij}(M_X) = m_0^2 \delta_{ij} \quad (f = q, \ell, u, d, e; i, j = 1, 2, 3), \quad (5.10a)$$

$$m_{h_1}^2(M_X) = m_{h_2}^2(M_X) = m_0^2, \quad (5.10b)$$

$$A_{ij}^f(M_X) = A_0 \quad (f = u, d, e; i, j = 1, 2, 3), \quad (5.10c)$$

$$A^f(M_X) = A_0 \quad (f = \lambda, \kappa), \quad (5.10d)$$

$$M_i(M_X) = M_{1/2} \quad (i = 1, 2, 3) \quad (5.10e)$$

at the gauge coupling unification scale M_X are demanded. These constraints reduce the number of free NMSSM parameters drastically. One obtains 6 free parameters in the Z_3 -symmetric, and 12 in the Z_3 -violating model, see the last segment in Table 5.1.

All together, the (i) matching of the gauge and Yukawa couplings to the Standard Model parameters at the low-energy scale, the (ii) EWSB consistency conditions at the SUSY scale and the (iii) mSUGRA-inspired constraints at the unification scale form a set of boundary conditions on the model parameters at three different scales. The renormalization group equations (5.7) together with all of the above conditions form a boundary value problem. Task of the NMSSM spectrum generator is to find a set of model parameters consistent with all boundary conditions and to calculate the pole mass spectrum for this parameter set.

The widely used approach to solve such boundary value problems is to iteratively use the renormalization group running to run with the model parameters to the boundary condition scales and impose the constraints [163]. This so-called fixed-point iteration is already used in Softsusy's MSSM implementation. To adapt it to the NMSSM case it is necessary to implement the β -functions of all model parameters. For the calculation of the gauge and Yukawa couplings from the known Standard Model observables the SUSY particle threshold corrections must be implemented as well. To impose the EWSB conditions at the loop level the Higgs tadpoles diagrams are necessary. Finally, for the calculation of the pole mass spectrum the mass matrices and self-energies of all particles need to be implemented. The implementation details will be given in the following section.

5.4 Implementation

To solve the boundary value problem described in Section 5.3 the $\overline{\text{DR}}$ β -functions of all NMSSM parameters have to be implemented. To allow for a flexible usage (exchangeability, extendability, reuse) of the NMSSM parameters and their β -functions they are put into C++ classes with well-defined interfaces. However, to implement the NMSSM a re-design of Softsusy's class hierarchy was necessary, which is described in the following.

5.4.1 Class hierarchy

MSSM class hierarchy

In Softsusy prior to version 3.6.0 the MSSM class hierarchy was structured as shown in the UML class diagram in Figure 5.1. At the top of the hierarchy is the abstract base class `RGE`, which defines the interface for the RGE running via the `runto()` function. At the level of the `RGE` interface, the running parameters are treated as a vector (`DoubleVector`) of real numbers. The pure virtual methods `set()`, `display()` and `beta()` are to be implemented by the derived class to set and return the parameter vector and the corresponding β -functions. The `runto()` user interface function integrates

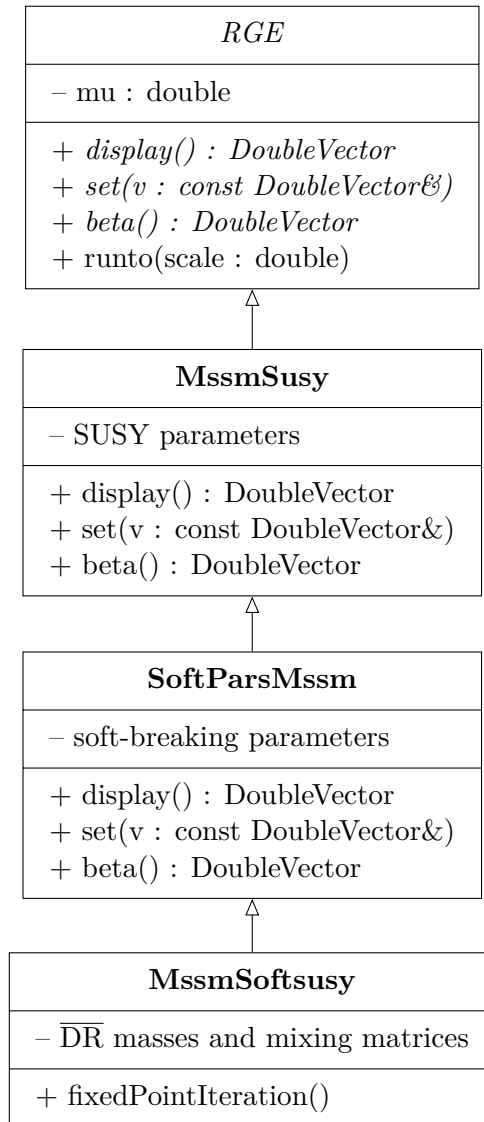


Figure 5.1: MSSM class hierarchy in Softsusy.

the renormalization group equations from the current scale (stored in the member variable `mu`) to the given new scale using a Runge-Kutta algorithm with dynamic step size. This allows a “running” of the parameters between different scales.

In a supersymmetric theory with soft breaking, the β -functions of the supersymmetric parameters (gauge couplings, superpotential parameters and vacuum expectation values) are independent of the soft-breaking parameters [159, 160, 161, 134, 162, 61, 132, 63, 64]. This property is reflected in Softsusy’s class hierarchy by putting the supersymmetric MSSM parameters into the `MssmSusy` class, which directly inherits from `RGE` and implements all virtual functions. The soft-breaking parameters are contained in `SoftParsMssm`, which inherits from `MssmSusy`. It overwrites the virtual `RGE` interface functions to implement the soft-breaking β -functions in terms of the SUSY parameters in the base class and the soft-breaking parameters themselves.

At the bottom of the hierarchy stands the MSSM model class `MssmSoftsusy`, which implements all mass matrices, self-energies, tadpoles and electroweak symmetry breaking conditions. The `fixedPointIteration()` function organizes the iteration between the high and low scales and calculates the pole mass spectrum.

New NMSSM class hierarchy

To implement the NMSSM in Softsusy the old class structure in Figure 5.1 had to be re-designed with the following requirements:

1. The old MSSM class hierarchy should be preserved for backward compatibility.
2. The class hierarchy should reflect the fact that the β -functions of the supersymmetric parameters are independent of the soft-breaking parameters. This can be done by making the class of soft-breaking β -functions a derived class of the class of supersymmetric parameters.
3. As much MSSM code as possible (β -functions, mass matrices, self-energies, tadpoles) should be reused in order to avoid code duplication. This simplifies the code maintenance and reduces the size of the executable. The extra NMSSM contributions should be added on top of the existing MSSM expressions.

To implement the NMSSM in Softsusy and at the same time fulfill the above requirements, `SoftParsMssm` and `MssmSoftsusy` were converted into the class templates `SoftPars<T>` and `Softsusy<T>`, respectively, which inherit from their template parameters, see Figure 5.2. This technique is called policy-based design [164]. The template parameter of `SoftPars<T>` is intended to be the class of SUSY parameters. This allows to exchange the SUSY parameter base class, i.e. it is possible to calculate the MSSM soft-breaking β -functions with a different set of SUSY parameters. The template parameter of `Softsusy<T>` is the class of soft-breaking parameters. This allows to calculate the MSSM mass matrices and self-energies using a different set of model parameters. With this approach it is possible to

1. restore the old MSSM class hierarchy, Figure 5.1, by defining the following type abbreviations:

```
typedef SoftPars<MssmSusy> SoftParsMssm;
typedef Softsusy<SoftParsMssm> MssmSoftsusy;
```

2. implement the NMSSM soft-breaking β -functions in terms of the supersymmetric NMSSM parameters,
3. and reuse the existing MSSM expressions (β -functions, mass matrices, self-energies, etc.) in the implementation of the NMSSM ones.

The NMSSM class hierarchy is now constructed as shown in Figure 5.3: First, the class of supersymmetric NMSSM parameters, `NmssmSusy`, inherits from `MssmSusy`

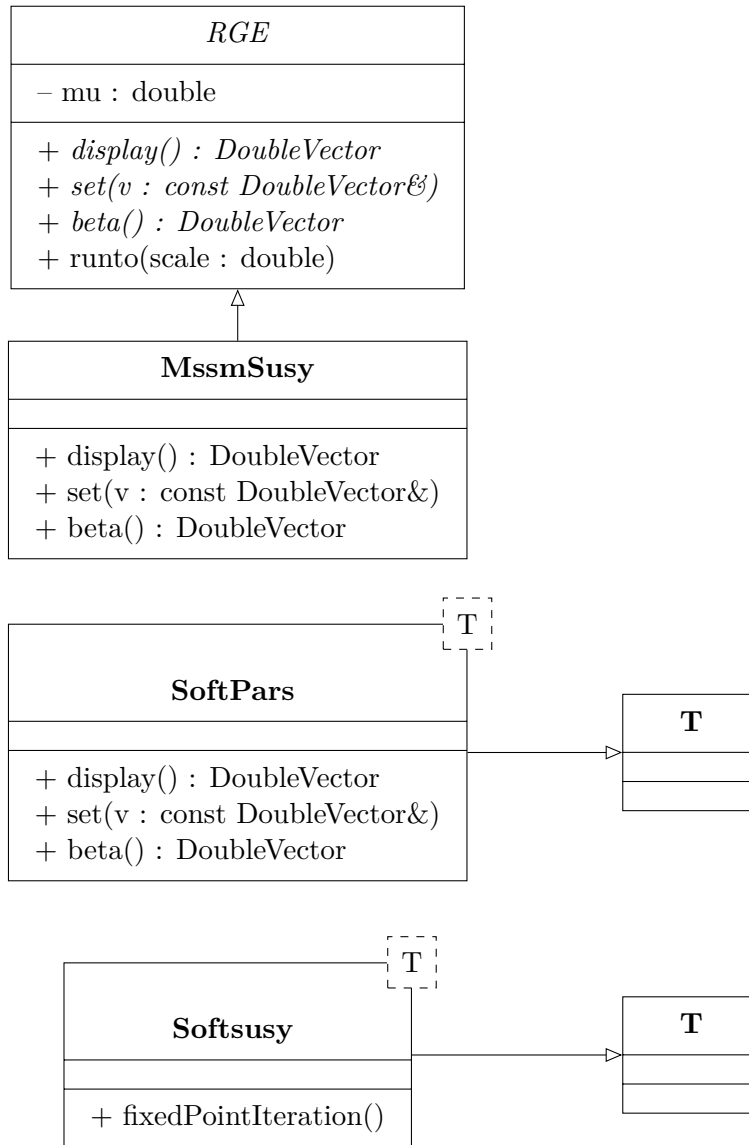


Figure 5.2: Generalized class hierarchy in Softsusy 3.6.0.

to reuse the β -functions of the supersymmetric MSSM parameters. Afterwards, `SoftPars<NmssmSusy>` is instantiated, which contains the MSSM soft-breaking β -functions, using the supersymmetric NMSSM parameters. Then, the class of soft-breaking NMSSM parameters, `SoftParsNmssm`, is created which inherits from `SoftPars<NmssmSusy>`. It implements the NMSSM soft-breaking β -functions, reusing the MSSM ones from its parent class by adding the extra NMSSM contributions. Afterwards, the class template `Softsusy<SoftParsNmssm>` is instantiated, which contains the MSSM mass matrices and self-energies, now written in terms of the NMSSM parameters. Finally, the NMSSM model class, `NmssmSoftsusy`, is created which implements the NMSSM mass matrices and self-energies in terms of the ones from the parent class, i.e. in terms of the MSSM ones.

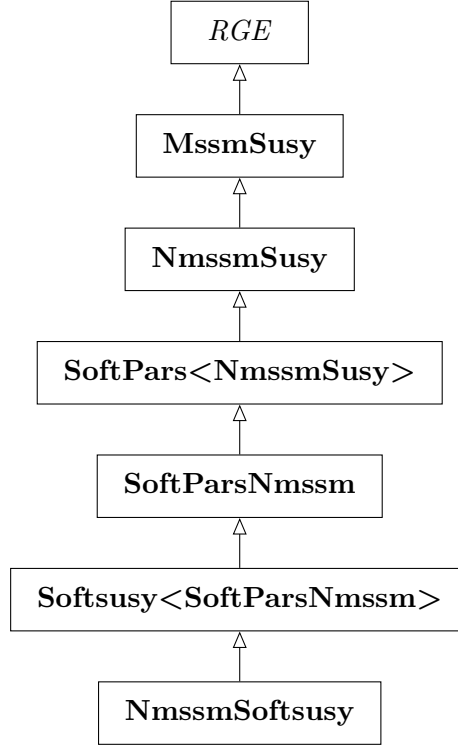


Figure 5.3: NMSSM class hierarchy in Softsusy 3.6.0.

5.4.2 Implementation of the β -functions

After having re-designed the class hierarchy it was possible to implement the general NMSSM β -functions in terms of the MSSM ones. The expressions were obtained from the known one- and two-loop level results for general softly broken supersymmetric theories [61, 62, 63, 64].

SUSY parameters

The β -functions of the SUSY parameters (gauge and Yukawa couplings, superpotential parameters and VEVs) were implemented into `NmssmSusy` on top of the existing MSSM expression in the parent class. The extra NMSSM contributions read at the one-loop level

$$(4\pi)^2 \beta_{g_i}^{(1)} = 0, \quad (5.11)$$

$$(4\pi)^2 \beta_{y_f}^{(1)} = |\lambda|^2 y_f, \quad f = u, d, e, \quad (5.12)$$

$$(4\pi)^2 \beta_\lambda^{(1)} = \lambda \left(3 \operatorname{Tr}(y_d y_d^\dagger) + 3 \operatorname{Tr}(y_u y_u^\dagger) + \operatorname{Tr}(y_e y_e^\dagger) + 2|\kappa|^2 + 4|\lambda|^2 - \frac{3g_1^2}{5} - 3g_2^2 \right), \quad (5.13)$$

$$(4\pi)^2 \beta_\kappa^{(1)} = 6\kappa(|\kappa|^2 + |\lambda|^2), \quad (5.14)$$

$$(4\pi)^2 \beta_\mu^{(1)} = 2\mu|\lambda|^2, \quad (5.15)$$

$$(4\pi)^2 \beta_{\mu'}^{(1)} = 4\mu'(|\kappa|^2 + |\lambda|^2), \quad (5.16)$$

$$(4\pi)^2 \beta_{\xi_F}^{(1)} = 2\xi_F(|\kappa|^2 + |\lambda|^2), \quad (5.17)$$

$$(4\pi)^2 \beta_{v_i}^{(1)} = -v_i |\lambda|^2, \quad i = 1, 2, \quad (5.18)$$

$$(4\pi)^2 \beta_{v_3}^{(1)} = -2v_3(|\kappa|^2 + |\lambda|^2). \quad (5.19)$$

In Eq. (5.13) the symbol g_1 denotes the GUT normalized gauge coupling of the $U(1)_Y$ and is defined as $g_1 = \sqrt{5/3} g_Y$. The full two-loop expressions can be found in [136]. For the implementation of the one- and two-loop VEV β -functions Eqs. (5.18)–(5.19) the results obtained in Section 4.4.2 Eq. (4.63) were used.

Soft-breaking parameters

The extra NMSSM contributions for the soft-breaking parameters were implemented into `SoftParsNmssm` class on top of the existing MSSM expressions in the parent class. They read at the one-loop level

$$(4\pi)^2 \beta_{T_{y_f}}^{(1)} = |\lambda|^2 y_f (A^f + 2A^\lambda), \quad (T_{y_f})_{ij} = (y_f)_{ij} A_{ij}^f, \quad f = u, d, e, \quad (5.20)$$

$$(4\pi)^2 \beta_{T_\lambda}^{(1)} = \lambda A^\lambda \left(3 \text{Tr}(y_d y_d^\dagger) + \text{Tr}(y_e y_e^\dagger) + 3 \text{Tr}(y_u y_u^\dagger) + 12|\lambda|^2 - \frac{3g_1^2}{5} - 3g_2^2 \right) \\ + 6\lambda \text{Tr}(y_d^\dagger y_d A^d) + 2\lambda \text{Tr}(y_e^\dagger y_e A^e) + 6\lambda \text{Tr}(y_u^\dagger y_u A^u) + 2|\kappa|^2 \lambda (2A^\kappa + A^\lambda) \\ + \frac{6}{5} g_1^2 M_1 \lambda + 6g_2^2 M_2 \lambda, \quad T_\lambda = \lambda A^\lambda, \quad (5.21)$$

$$(4\pi)^2 \beta_{T_\kappa}^{(1)} = 6\kappa \left[|\lambda|^2 (A^\kappa + 2A^\lambda) + 3|\kappa|^2 A^\kappa \right], \quad T_\kappa = \kappa A^\kappa, \quad (5.22)$$

$$(4\pi)^2 \beta_{B\mu}^{(1)} = 2\lambda m_s'^2 \kappa^* + 6|\lambda|^2 B\mu + 4\mu |\lambda|^2 A^\lambda, \quad (5.23)$$

$$(4\pi)^2 \beta_{m_s'^2}^{(1)} = 8(\kappa \lambda^* B\mu + \mu' |\kappa|^2 A^\kappa + \mu' |\lambda|^2 A^\lambda) + 4m_s'^2 (2|\kappa|^2 + |\lambda|^2), \quad (5.24)$$

$$(4\pi)^2 \beta_{\xi_S}^{(1)} = 2 \left[\kappa A^\kappa (m_s'^2)^* + \mu' m_s'^2 \kappa^* + 2\mu' \lambda^* B\mu + 2\lambda A^\lambda (B\mu)^* \right. \\ \left. + (|\kappa|^2 + |\lambda|^2) \xi_S + 2\xi_F (|\kappa|^2 A^\kappa + |\lambda|^2 A^\lambda) \right. \\ \left. + 2\lambda \mu^* (m_{h_1}^2 + m_{h_2}^2) + 2m_s'^2 \kappa \mu'^* \right], \quad (5.25)$$

$$(4\pi)^2 \beta_{M_i}^{(1)} = 0, \quad i = 1, 2, 3, \quad (5.26)$$

$$(4\pi)^2 \beta_{m_f^2}^{(1)} = 0, \quad f = q, \ell, u, d, e, \quad (5.27)$$

$$(4\pi)^2 \beta_{m_{h_1}^2}^{(1)} = (4\pi)^2 \beta_{m_{h_2}^2}^{(1)} = 2 \left[|\lambda|^2 (m_{h_1}^2 + m_{h_2}^2 + m_s^2) + |\lambda A^\lambda|^2 \right], \quad (5.28)$$

$$(4\pi)^2 \beta_{m_s^2}^{(1)} = 4 \left[|\lambda|^2 (m_{h_1}^2 + m_{h_2}^2 + m_s^2) + 3m_s^2 |\kappa|^2 + |\kappa A^\kappa|^2 + |\lambda A^\lambda|^2 \right], \quad (5.29)$$

The full two-loop expressions were published in [136].

5.4.3 Solving the boundary value problem

The implemented NMSSM β -functions can now be used to solve the boundary value problem described in Section 5.3. The algorithm, which solves the boundary value problem is shown in Figure 5.4 and works as follows:

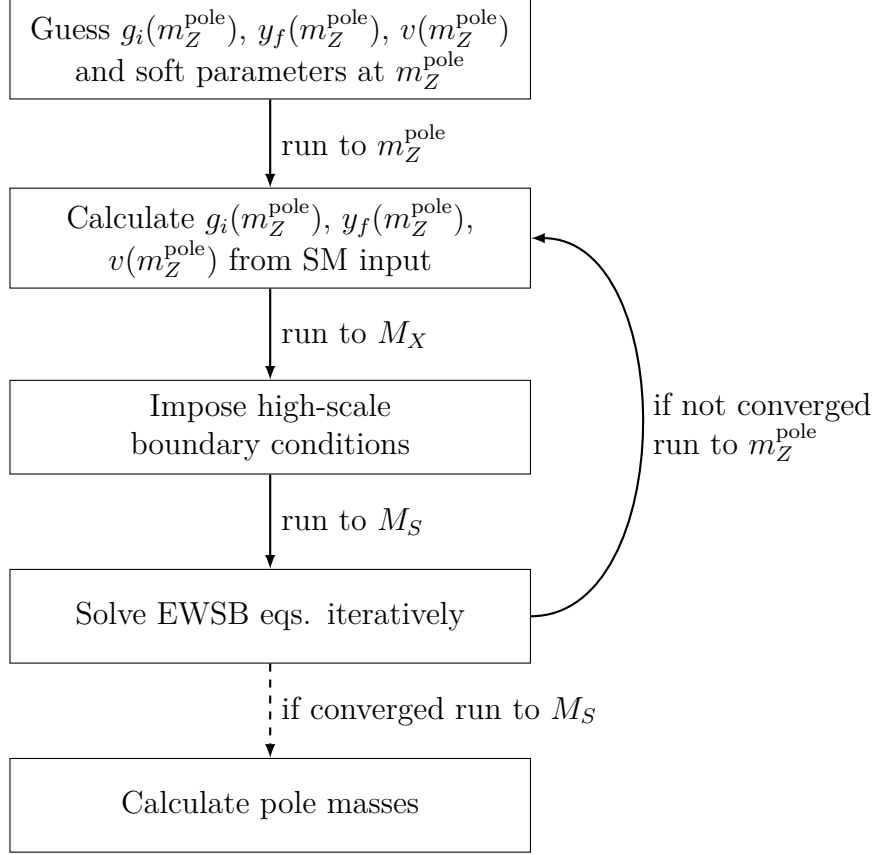


Figure 5.4: Algorithm to calculate the pole mass spectrum in Softsusy.

Initial guess of the model parameters:

1. Set the initial scale to m_t^{pole} .
2. Calculate the Standard Model gauge couplings $g_i^{\text{SM}}(m_t^{\text{pole}})$ in the $\overline{\text{MS}}$ scheme from the known values $g_1^{\text{SM}}(m_Z^{\text{pole}})$, $g_2^{\text{SM}}(m_Z^{\text{pole}})$, $g_3^{\text{SM}}(m_t^{\text{pole}})$ [11]. Set NMSSM gauge couplings g_i to the Standard Model ones

$$g_i(m_t^{\text{pole}}) = g_i^{\text{SM}}(m_t^{\text{pole}}) \quad (i = 1, 2, 3), \quad (5.30)$$

thereby ignoring threshold corrections.

3. Set the NMSSM VEV v to the Standard Model value of 246.22 GeV. Afterwards, the NMSSM Yukawa couplings are estimated from the running Standard

Model fermion masses [11] as

$$y_u = \frac{\sqrt{2}}{v_2} \text{diag}(2.4 \cdot 10^{-3}, 1.27, 165.0) \text{ GeV}, \quad (5.31)$$

$$y_d = \frac{\sqrt{2}}{v_1} \text{diag}(4.75 \cdot 10^{-3}, 0.104, 4.2) \text{ GeV}, \quad (5.32)$$

$$y_e = \frac{\sqrt{2}}{v_1} \text{diag}(5.10998902 \cdot 10^{-4}, 0.105658357, 1.77699) \text{ GeV}. \quad (5.33)$$

4. Run the SUSY parameters to the guessed high-energy scale $M_X = 2 \cdot 10^{16}$ GeV.
5. Impose the high-scale constraint by overwriting the values of the NMSSM parameters. According to the user's choice, this might be the mSUGRA constraint Eq. (5.10), where the soft-breaking parameters are set to the universal values m_0 , $M_{1/2}$ and A_0 .
6. Run all model parameters to the low-energy scale m_Z^{pole} .
7. Solve the EWSB equations (5.8) at the tree-level by setting $\{\kappa, |v_3|^2, m_s^2\}$ or $\{|\mu|^2, B\mu, \xi_S\}$ in the Z_3 - or \bar{Z}_3 -NMSSM, respectively.
8. Calculate the $\overline{\text{DR}}$ mass spectrum.

After this initial parameter guess all NMSSM model parameters are initialized and the actual fixed-point iteration, which solves the boundary value problem can be started.

Fixed-point iteration:

1. Run all model parameters to the low-energy scale m_Z^{pole} .
 - a) Calculate the $\overline{\text{DR}}$ mass spectrum.
 - b) Calculate the $\overline{\text{DR}}$ NMSSM gauge couplings $g_i(m_Z^{\text{pole}})$ ($i = 1, 2, 3$) from the known Standard Model couplings $\alpha_{\text{e.m.}}(m_Z^{\text{pole}})$, $\alpha_s(m_Z^{\text{pole}})$ and the muon decay constant G_F , including threshold and radiative corrections.
 - c) Calculate the $\overline{\text{DR}}$ Yukawa couplings $y_f(m_Z^{\text{pole}})$ ($f = u, d, e$) from the known SM fermion masses, using radiative corrections. Afterwards, the NMSSM VEV $v(m_Z^{\text{pole}})$ is calculated in the $\overline{\text{DR}}$ scheme as

$$v(m_Z^{\text{pole}}) = \frac{2m_Z(m_Z^{\text{pole}})}{\sqrt{3g_1^2(m_Z^{\text{pole}})/5 + g_2^2(m_Z^{\text{pole}})}}, \quad (5.34)$$

where $m_Z(m_Z^{\text{pole}})$ is the $\overline{\text{DR}}$ mass of the Z boson at the scale m_Z^{pole} , which is re-calculated in each iteration from the known pole mass. Note that the gauge coupling g_1 is GUT normalized. It is related to the hypercharge coupling of $U(1)_Y$ via $g_Y = \sqrt{3/5} g_1$.

2. Run all model parameters to the GUT scale M_X .
 - a) Calculate the gauge coupling β -functions β_{g_1} and β_{g_2} at the two-loop level and re-calculate M_X as

$$M'_X = M_X \exp\left(\frac{g_2(M_X) - g_1(M_X)}{\beta_{g_1} - \beta_{g_2}}\right). \quad (5.35)$$

The scale M'_X is used as new GUT scale in the next iteration.

- b) Impose the high-scale constraint by overwriting the values of the NMSSM parameters. According to the user's choice, this might be the mSUGRA constraint Eq. (5.10), where the soft-breaking parameters are set to the universal values m_0 , $M_{1/2}$ and A_0 .
3. Run all model parameters to the SUSY scale M_S .
 - a) Calculate the $\overline{\text{DR}}$ mass spectrum.
 - b) Re-calculate the SUSY-scale as

$$M_S = \sqrt{m_{\tilde{t}_1} m_{\tilde{t}_2}}, \quad (5.36)$$

where $m_{\tilde{t}_1}$ and $m_{\tilde{t}_2}$ are the $\overline{\text{DR}}$ stop masses (squark flavour mixing is ignored).

- c) Solve the EWSB equations (5.8) iteratively at the loop level by varying $\{\kappa, |v_3|^2, m_s^2\}$ or $\{|\mu|^2, B\mu, \xi_S\}$ in the Z_3 - or \tilde{X}_3 -NMSSM, respectively. The iteration stops if the equations

$$\frac{\partial V_{\text{Higgs}}^{\text{tree}}}{\partial v_i} - t_i = 0 \quad (i = 1, 2, 3) \quad (5.37)$$

are fulfilled. Here t_i are the full one-loop tadpole diagrams with external CP-even Higgs gauge eigenstates. By default leading two-loop contributions of the order $O(y_t^4 + y_t^2 y_b^2 + y_b^4 + y_\tau^4 + y_t^2 g_3^2 + y_b^2 g_3^2)$ from Refs. [165, 166] are added.

4. If the relative deviation between the SUSY particles of the current and the previous iteration is larger than the accuracy goal (set in the SLHA input file), and the maximum number of iterations is not yet reached, then go to step 1. Otherwise, stop the iteration.

If the iteration has converged, all NMSSM parameters are consistent with the EWSB conditions, low-energy data and all user-supplied boundary conditions and are known at any scale between m_Z^{pole} and M_X .¹

¹In Chapter 6 a generalization of the algorithm described here is presented, which can handle towers of effective field theories with an arbitrary number of intermediate scales and boundary conditions.

5.4.4 Calculation of the pole mass spectrum

If a set of NMSSM parameters consistent with all boundary conditions has been found the pole mass spectrum can be calculated. This is explained in the following.

The pole mass of a field is an observable and does not depend on the renormalization scheme or the gauge fixing. It is therefore a well-suited spectrum generator output quantity that can be passed to decay calculators or event generators. The pole mass of a field is defined to be the momentum p for which the full propagator of the field has a pole. For the general case of field multiplets this requirement is equivalent to finding values p_i for which the equations

$$0 = \det \left(p_i^2 \mathbf{1} - M_\varphi + M_{\varphi,1L}(p_i^2) \right) \quad \text{for scalars/vectors } \varphi, \text{ or} \quad (5.38a)$$

$$0 = \det \left(p_i \mathbf{1} - M_\xi + M_{\xi,1L}(p_i^2) \right) \quad \text{for Dirac/Majorana fermions } \xi \quad (5.38b)$$

are fulfilled. Here M_φ and M_ξ are the mass matrices of a scalar/vector field φ and a Dirac/Majorana fermion ξ , respectively. In the $\overline{\text{DR}}$ scheme, in which the NMSSM is renormalized, the mass matrix one-loop corrections $M_{f,1L}(p^2)$ have the form

$$\text{scalar } \phi: \quad M_{\phi,1L}(p^2) = \hat{\Sigma}_\phi(p^2), \quad (5.39a)$$

$$\text{vector } V: \quad M_{V,1L}(p^2) = \hat{\Sigma}_{V,T}(p^2), \quad (5.39b)$$

$$\text{Dirac fermion } \psi: \quad M_{\psi,1L}(p^2) = \hat{\Sigma}_\psi^S(p^2) + \hat{\Sigma}_\psi^R(p^2)M_\psi + M_\psi \hat{\Sigma}_\psi^L(p^2), \quad (5.39c)$$

$$\begin{aligned} \text{Majorana fermion } \chi: \quad M_{\chi,1L}(p^2) = & \frac{1}{2} \left\{ \hat{\Sigma}_\chi^S(p^2) + \hat{\Sigma}_\chi^{S,T}(p^2) + \left[\hat{\Sigma}_\chi^{L,T}(p^2) + \hat{\Sigma}_\chi^R(p^2) \right] M_\chi \right. \\ & \left. + M_\chi \left[\hat{\Sigma}_\chi^L(p^2) + \hat{\Sigma}_\chi^{R,T}(p^2) \right] \right\}. \end{aligned} \quad (5.39d)$$

Here $\hat{\Sigma}_f$ is the real part of the $\overline{\text{DR}}$ renormalized one-loop self-energy of field f . The left-, right- and unpolarized parts of the fermion self-energies are denoted as $\hat{\Sigma}_f^{L,R,S}$, and $\hat{\Sigma}_{V,T}$ is the transverse part the vector boson self-energy. By default leading two-loop contributions of the order $O(y_t^4 + y_t^2 y_b^2 + y_b^4 + y_\tau^4 + y_t^2 g_3^2 + y_b^2 g_3^2)$ to the CP-even and CP-odd Higgs self-energies are added [166, 167, 168].

If a consistent set of NMSSM parameters is available, the Eqs. (5.38) can be solved numerically for all NMSSM Dirac fermions (quarks, leptons, charginos), Majorana fermions (neutralinos, gluino), scalars (squarks, sleptons, Higgs bosons) and vector bosons (W^\pm , Z). For this purpose the $\overline{\text{DR}}$ mass matrices M_φ and M_ξ are calculated numerically from the $\overline{\text{DR}}$ model parameters. Afterwards, the full loop-corrected mass matrices ($M_f - M_{f,1L}(p_i^2)$) must be diagonalized to obtain the pole masses. However, since the loop corrections are momentum dependent an iteration over the p_i has to be performed in principle. This is done in the Higgs sector to obtain a precise pole mass prediction. For the other fields the iteration is replaced by a faster approximation, which is correct at the one-loop level but neglects higher order terms. Here the full loop-corrected mass matrices are diagonalized N times, where N is the size of the multiplet. For the i th field in the multiplet the momentum p_i is set to the $\overline{\text{DR}}$ mass m_i . The i th eigenvalue is then an approximation of the pole mass m_i^{pole} . Thereby

two-loop terms of the form

$$\left[(m_i^{\text{pole}})^2 - m_i^2 \right] \frac{\partial M_{f,1L}(p^2)}{\partial p^2} \Big|_{p^2=m_i^2} \quad (5.40)$$

are neglected.

The diagonalization of the mass matrices can lead to negative mass eigenvalues. In case of fermions, the masses can be defined as positive by a suitable complex phase transformation of the mixing matrices. However, in the scalar sector negative squared mass eigenvalues inevitably result in tachyons. During the fixed-point iteration such tachyonic states are avoided by taking the square root of the magnitude of the eigenvalues. If these tachyons still occur after the fixed-point iteration has converged, the parameter point is marked as unphysical and an error flag is set.

5.5 Tests and comparison to NMSPEC

To validate all implemented expressions extensive cross-checks have been performed. The β -functions for both the Z_3 -symmetric and Z_3 -violating NMSSM are analytically compared against the expressions given in [37] in the third family approximation. Furthermore, the mass matrices, EWSB conditions, full one- and two-loop β -functions as well as the complete one-loop self-energies and tadpoles were systematically compared with a Z_3 - and \bar{X}_3 -NMSSM spectrum generator, created by FlexibleSUSY, and were found to agree within double machine precision (16 digits). The overall spectrum of pole masses was compared with NMSPEC [145] and found to agree within 2–4% on average.² These deviations mainly stem from the following differences between Softsusy and NMSPEC:

- NMSPEC uses a third-family approximation, where all Standard Model Yukawa couplings are set to zero, except for y_t , y_b and y_τ . Softsusy on the other hand does not set any Yukawa couplings to zero and takes family mixing via the CKM matrix into account.
- Softsusy implements the full one-loop self-energies and tadpoles to calculate the pole mass spectrum. NMSPEC neglects for example electroweak contributions in the sfermion self-energies.
- As low-energy scale M_{low} NMSPEC uses the definition

$$M_{\text{low}} = \sqrt[4]{(m_q^2)_{33}(m_u^2)_{33}}. \quad (5.41)$$

At this scale the SM gauge and Yukawa couplings, the Higgs wave function renormalization constants, as well as third generation squark and slepton pole

²For parameter points with fine-tuning the deviation can be much larger (up to 50%). The reason is that for such points the spectrum is highly sensitive to the values of the input parameters. This has the consequence that small numerical differences during the computation can lead to a completely different spectrum.

masses are calculated [145]. Softsusy calculates the gauge and Yukawa couplings at m_Z^{pole} and all pole masses at the SUSY scale $M_S = \sqrt{m_{\tilde{t}_1} m_{\tilde{t}_2}}$.

- The SUSY scale is defined in NMSPEC as

$$M_S^{\text{NMSPEC}} = \frac{1}{2} \sqrt{2(m_q^2)_{11} + (m_u^2)_{11} + (m_d^2)_{11}}. \quad (5.42)$$

The here appearing soft-breaking squared mass matrices of the squarks, m_f^2 , are assumed to be diagonal and degenerate in the first two generations. At this scale NMSPEC defines the input parameter λ and the EWSB output parameters κ , v_3 and m_s^2 (in the $\overline{\text{DR}}$ scheme). Softsusy on the other hand allows to define λ either at the scale $M_S = \sqrt{m_{\tilde{t}_1} m_{\tilde{t}_2}}$, or at the high-energy scale M_X . The EWSB output parameters are always defined at M_S .

To illustrate the size of the deviations of the predicted pole masses between Softsusy 3.4.1 and NMSPEC 4.2.1 a parameter scan over $\tan\beta$ in the Z_3 -symmetric NMSSM is performed. A mSUGRA-inspired scenario with large universal parameters $m_0 = M_{1/2} = -A_0 = 5$ TeV is chosen to produce spectra with heavy Higgses with a masses of the order 120 GeV. The superpotential parameter λ is set to 0.1 at the SUSY scale and the sign of the VEV v_3 is chosen to be positive. Figure 5.5 shows the lightest CP-even Higgs pole mass as a function of $\tan\beta$ in the range $2 \dots 50$. The

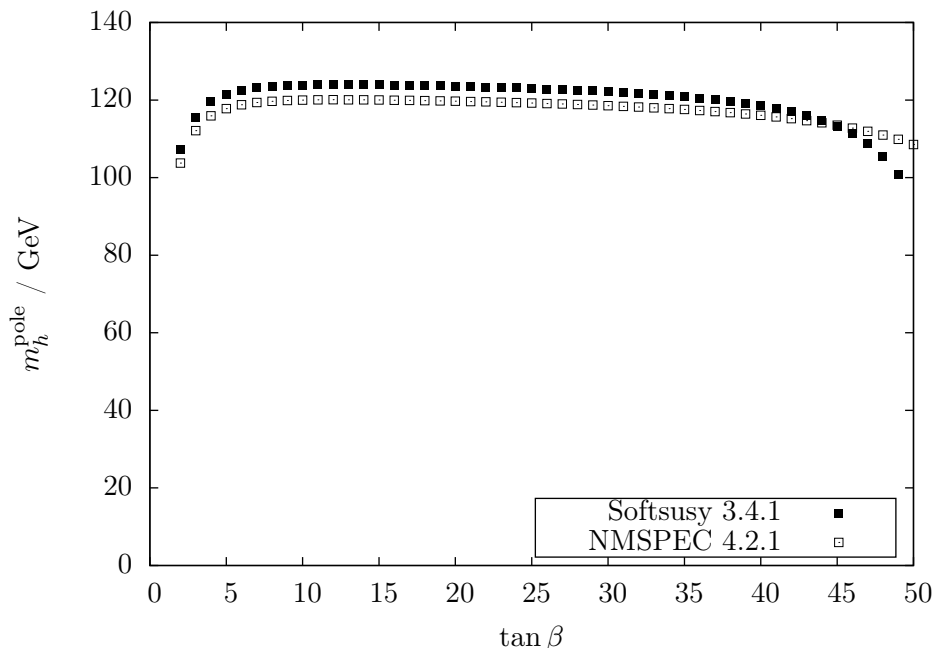


Figure 5.5: Lightest CP-even Higgs pole mass in the Z_3 -NMSSM as a function of $\tan\beta$. The plot shows the prediction with Softsusy 3.4.1 and NMSPEC 4.2.1. The chosen Z_3 -NMSSM parameter point has $m_0 = M_{1/2} = -A_0 = 5$ TeV, $\lambda(M_S) = 0.1$ and sign $v_3 = +1$.

used SLHA input file is listed in Appendix D. One finds that for $\tan\beta = 2 \dots 47$ the

two spectrum generators predict the same Higgs pole mass within 2–3% deviation. For larger values, $\tan\beta > 47$, the deviations can rise to 10%. In these parameter regions the Higgs loop corrections are more sensitive to small numeric deviations. Here the differing input scales for λ plus the various approximations used by Softsusy and NMSPEC lead to a significantly different Higgs mass prediction. At $\tan\beta = 50$ Softsusy’s loop corrections lead to a tachyonic Higgs. Overall, this emphasizes again the benefit of having several NMSSM spectrum generators for comparison.

5.6 Summary and conclusion

The increasing lower mass limits on new SUSY particles from current LHC experiments and the discovery of a Higgs boson of 125.9 GeV decrease the attractiveness of the MSSM as an extension of the Standard Model. Currently the NMSSM becomes more popular as it can relax the Higgs mass fine-tuning and is less experimentally constrained.

By the end of 2013 NMSPEC was the only out-of-the-box NMSSM spectrum generator, which could calculate the pole masses of the new NMSSM particles. In the past, having various spectrum generators at hand has been proven useful for the SUSY community, because different spectrum generators use different levels of approximations, which can result in very different pole mass predictions in some parameter regions.

Part of this thesis was to help extending the MSSM spectrum generator Softsusy, to calculate the pole mass spectrum of the Z_3 -symmetric and Z_3 -violating NMSSM as well. This NMSSM extension was released in version 3.4.0 [136]. To make this extension possible Softsusy’s class hierarchy was re-designed and extended. The new NMSSM classes implement the full two-loop $\overline{\text{DR}}$ β -functions, as well as complete mass matrices, one-loop self-energies and tadpoles plus leading two-loop contributions to the CP-even and CP-odd Higgs self-energies and tadpoles. The resulting NMSSM spectrum generator was extensively tested against both NMSPEC and automatically generated C++ code, created by FlexibleSUSY.

In Section 5.5 it was shown that there are NMSSM parameter regions where the predicted lightest CP-even Higgs pole mass can be very different between NMSPEC and Softsusy. The main reason is a high sensitivity of the mass spectrum on the input parameters in these regions. This emphasizes the benefit of having several NMSSM spectrum generators for comparison to estimate the precision of the spectrum prediction.

Chapter 6

FlexibleSUSY – A spectrum generator generator

6.1 Motivation

As discussed in Section 2, the Minimal Supersymmetric Standard Model (MSSM) has some theoretical problems, such as the Higgs mass fine-tuning and the μ -problem. Non-minimal models can solve these problems by introducing new particles or extending the gauge group and provide a rich phenomenology at the TeV scale.

To study the properties of non-minimal supersymmetric models, spectrum generators are necessary, which calculate the pole masses of the new SUSY particles numerically, given a set of theory input parameters. The calculated pole mass spectrum can then be transferred to programs which calculate further observables, such as cross sections, branching ratios, the dark matter relic density and detection rates etc. These observables can then be used in experimental data analysis to search for supersymmetric particles. For a review of some available computational tools for SUSY phenomenology see for example [169].

To create a spectrum generator one needs the Lagrangian and the field content of the model and derive the RGEs, mass matrices, self-energies, tadpoles and electroweak symmetry breaking (EWSB) conditions. The derivation of these expressions can be carried out algebraically with the Mathematica package SARAH [112, 113, 146, 137]. Here the user specifies the gauge group, the fields and their quantum numbers, additional discrete symmetries, the superpotential and the mixing to mass eigenstates. Since version 3.2 [146] SARAH can convert these expressions to Fortran code, which can be incorporated into SPheno [147, 148] to obtain a complete spectrum generator for the given SUSY model.

However, the so generated spectrum generator has some disadvantages:

- Due to the large variety and complexity of supersymmetric models it is likely that the user wants to adapt the generated spectrum generator source code to his own needs. However, the SARAH generated Fortran code is not very modular. For example, it is not possible exchange the boundary conditions easily at the Fortran code level. The reason is that in the generated `RunRGE` function, which integrates the RGEs to run between the high-, SUSY and low-energy scales, the used boundary condition functions are hard-coded:

```

! SUSY boundary condition function
Subroutine BoundarySUSY(gA,gB)
  Real(dp),Intent(in)::gA(:)
  Real(dp),Intent(out)::gB(:)
  ...
End Subroutine BoundarySUSY

! high-scale boundary condition function
Subroutine BoundaryHS(gA,gB)
  Real(dp),Intent(in)::gA(:)
  Real(dp),Intent(out)::gB(:)
  ...
End Subroutine BoundaryHS

Subroutine RunRGE(kont, delta0, g1A, g1C, mGUT)
  Integer,Intent(inout)::kont
  Real(dp),Intent(in)::delta0
  Real(dp),Intent(inout)::g1A(57)
  Real(dp),Intent(out)::g1C(213),mGUT
  ...
  ! explicit call to BoundarySUSY
  Call BoundarySUSY(g1A,g1B)
  ...
  ! explicit call to BoundaryHS
  Call BoundaryHS(g1B,g1C)
  ...
End Subroutine RunRGE

```

Due to this structure, it is not easily possible to exchange the boundary condition functions by user-supplied Fortran routines. The user has to either (i) directly modify the generated boundary condition functions and recompile, or (ii) replace the explicit function calls to `BoundarySUSY` and `BoundaryHS` by calls to his own routines and recompile, or (iii) try to express the boundary conditions in the SPheno model file `sheno.m`, which might not always be possible.

- The run-time of the spectrum generator is around 0.2–1.0 s for the CMSSM, see Section 6.4.1. This is rather slow, compared to hand-written CMSSM spectrum generators SPheno and Softsusy, which run approximately between 0.05–0.3 s and 0.1–0.2 s, respectively. Having a fast spectrum generator is especially important when performing parameter scans, because the dimension of the parameter space can be quite large (5 parameters in the CMSSM¹, 6 in the Z_3 -NMSSM², 12 in the \tilde{X}_3 -NMSSM³, 12 in the CE_6 SSM⁴).
- The algorithm, which solves the boundary value problem is a (nested) fixed-

¹Free CMSSM parameters: m_0^2 , $M_{1/2}$, A_0 , $\tan\beta$, $\text{sign}\mu$

²In the Z_3 -symmetric NMSSM the following minimal parameter set can be chosen [136]: m_0^2 , $M_{1/2}$, A , $\tan\beta$, λ , $\text{sign}v_3$, (κ , $|v_3|^2$, m_S^2 are output of the EWSB equations)

³In the Z_3 -violating NMSSM the following minimal parameter set can be chosen [136]: m_0^2 , $M_{1/2}$, A_0 , $\tan\beta$, λ , κ , v_3 , ξ_F , μ' , m'_S , m_S^2 , $\text{sign}\mu$ ($|\mu|^2$, $B\mu$, ξ_S are output of the EWSB equations)

⁴See Eq. (3.2).

point iteration together with an adaptive Runge-Kutta algorithm to integrate the RGEs. The convergence properties of this fixed-point iteration strongly depend on the chosen input parameters and it might happen that the algorithm does not converge.

- In some models, for example the supersymmetric type-I see-saw model [170, 171, 172, 173], one would like to integrate out particles at some intermediate scale between the weak and the GUT scale. To study such models one has to construct a tower of effective field theories, which are matched at the intermediate scale. However, the SARAH generated Fortran code does not define an interface for such a tower construction.

In this thesis the spectrum generator framework FlexibleSUSY was developed, which represents an alternative to SARAH/SPheno with additional features. It provides Mathematica meta code, which generates spectrum generators for any supersymmetric model in C++. It uses SARAH to generate algebraic expressions for the RGEs, mass matrices, self-energies, tadpoles and EWSB conditions and converts them to C++ classes, which are then automatically combined to a spectrum generator. FlexibleSUSY's design goals are:

- The generated C++ code should be modular, in order to allow the user to modify, extend and reuse the code easily. This is achieved by using the object orientation features of C++, see Section 6.3.2.
- The compiled C++ code should be as fast as possible and at least as fast as hand-written spectrum generators. This is achieved by using the linear algebra package Eigen [174], which exploits C++ expression template techniques to generate well-optimizable code, see Section 6.4.1.
- It provides an interface for alternative boundary value problem solvers, in order to study parameter space regions where the standard fixed-point iteration does not converge. This is achieved by designing the code structure such that different solvers can be used at run-time. The standard fixed-point iteration solver can already be generated automatically. As an alternative a lattice solver prototype already exists for the CMSSM as a proof of concept.
- An interface for a tower of effective field theories should be provided at the C++ level.

6.2 General physical problems

To create a spectrum generator for a arbitrary SUSY model the physical and technical questions, which had to be solved in the NMSSM extension of Softsusy or the CE₆SSM spectrum generator have to be generalized. They are explained in the following.

6.2.1 Definition of the model

The physical starting point for the spectrum generator is the definition of the model. FlexibleSUSY currently considers only supersymmetric gauge theories with soft breaking. Such models are defined by

1. *The symmetry group.* This includes the $N = 1$ Super-Poincaré group and the gauge group. Since the model must include the Standard Model at low energies, only semisimple product groups are considered which contain the Standard Model gauge group $SU(3)_c \times SU(2)_L \times U(1)_Y$ as factor. This allows to directly identify the strong, left-handed and hypercharge gauge couplings needed for a matching to the Standard Model.
2. *The fields and their representations with respect to the symmetry group.* Here only chiral and vector superfield representations of the Super-Poincaré group are considered, which contain fields with spin 0, 1/2 and 1. Fields with spin 3/2 or 2, such as the gravitino and the graviton are explicitly excluded. The field representations with respect to the gauge group defines their gauge transformations and charges. The representations with respect to the full symmetry group of the model fixes the Kähler potential and therefore the gauge interactions. Furthermore, the charges need to be chosen such that the theory is free of gauge anomalies.

FlexibleSUSY requires that the model contains at least the known Standard Model fermions (quarks and leptons), gauge bosons (photon, W^\pm , Z , gluon) and a Higgs boson.

3. *The superpotential and the soft supersymmetry breaking terms.* Only power counting renormalizable superpotentials and soft-breaking Girardello-Grisaru terms of the form [12] are considered.
4. *The spontaneous gauge symmetry breaking scheme.* The breaking scheme must be such that only $SU(3)_c \times U(1)_{em}$ remains as an exact symmetry in order to obtain a massless gluon and photon. All other gauge group factors must be broken to produce massive gauge bosons for phenomenological reasons.
5. *The field mixings to mass eigenstates.* Only mixings are allowed which do not violate the low-energy symmetry of the model. These are the Lorentz group and the $SU(3)_c \times U(1)_{em}$ gauge group. This implies that only fields with the same spin, color and electromagnetic charge can be mixed.
6. *The regularization and renormalization scheme.* In FlexibleSUSY all model parameters are renormalized in the supersymmetry, gauge and Poincaré symmetry preserving $\overline{\text{DR}}$ scheme [105, 106].

A so-defined SUSY model can be directly matched to the Standard Model at low energies, because it contains all known matter fields and gauge bosons. Since the Lagrangian and the mixing to mass eigenstates is defined completely, the mass matrices,

EWSB conditions, Feynman rules, one-loop self-energies and tadpole diagrams can be calculated automatically for all fields. Furthermore, in such a model the β -functions of all parameters are known up to the two-loop level [61, 132, 63, 64].

SARAH [112, 146, 137], a Mathematica package for supersymmetric models, allows a user to define such a model. It can calculate mass matrices, EWSB conditions, Feynman rules, one-loop self-energies and tadpole diagrams algebraically with Mathematica. FlexibleSUSY uses all these SARAH generated expressions to create a spectrum generator for the given model, which numerically calculates the model parameters, the pole mass spectrum and mixing matrices of all fields.

6.2.2 Boundary conditions

In most SUSY models some of the parameters are fixed by explicit or implicit conditions. For example in the MSSM the gauge and Yukawa couplings are usually chosen such that they match the known Standard Model values at the Z mass scale. Usually many more conditions are imposed at other scales. Therefore, FlexibleSUSY is designed to allow for an arbitrary number of boundary conditions at any scale. However, two constraints are of particular phenomenological importance and will always be imposed: The matching of the gauge and Yukawa couplings to the Standard Model and the electroweak symmetry breaking.

Matching to the Standard Model

Any phenomenologically viable SUSY model is required to correctly predict the measured low-energy observables. This includes in particular the known Standard Model fermion masses m_f , the gauge boson masses m_W^{pole} and m_Z^{pole} and the electromagnetic and strong couplings $\alpha_{\text{e.m.}}^{\text{SM}}(m_Z^{\text{pole}})$ and $\alpha_s^{\text{SM}}(m_Z^{\text{pole}})$. As in the case of the NMSSM extension of Softsusy and the CE₆SSM spectrum generator, these parameters are well suited to be input at the low scale to determine the gauge and Yukawa couplings (if they exist) of the SUSY model.

For this purpose the quarks, leptons and W^\pm and Z bosons of the Standard Model must be identified. This identification is done by the user in the SARAH model file. The four input quantities m_W^{pole} , m_Z^{pole} , $\alpha_{\text{e.m.}}^{\text{SM}}(m_Z^{\text{pole}})$ and $\alpha_s^{\text{SM}}(m_Z^{\text{pole}})$ can then be used to determine the three gauge couplings g_i of the $SU(3)_c \times SU(2)_L \times U(1)_Y$ symmetry group. This first requires the calculation of the gauge coupling threshold corrections $\Delta\alpha_i(\mu)$ to determine the electromagnetic and strong couplings e and g_3 in the SUSY model via

$$\alpha_{\text{e.m.}}(\mu) = \frac{\alpha_{\text{e.m.}}^{\text{SM}}(\mu)}{1 - \Delta\alpha_{\text{e.m.}}(\mu)} \quad \Rightarrow \quad e(\mu) = \sqrt{4\pi\alpha_{\text{e.m.}}(\mu)}, \quad (6.1)$$

$$\alpha_s(\mu) = \frac{\alpha_s^{\text{SM}}(\mu)}{1 - \Delta\alpha_s(\mu)} \quad \Rightarrow \quad g_3(\mu) = \sqrt{4\pi\alpha_s(\mu)}. \quad (6.2)$$

The general form of $\Delta\alpha_i(\mu)$ is well known [55] and depends on the renormalization scale μ , the field representations and the masses. Afterwards, the Weinberg angle θ_W

must be calculated to relate e to g_1 and g_2 via

$$g_1(\mu) = N_{\text{GUT}} \frac{e(\mu)}{\cos \theta_W(\mu)}, \quad (6.3)$$

$$g_2(\mu) = \frac{e(\mu)}{\sin \theta_W(\mu)}. \quad (6.4)$$

Here N_{GUT} is a possible GUT normalization of the coupling g_1 to allow the embedding of the SM gauge group into a simple GUT gauge group. The calculation of θ_W is model specific and depends on the photon– Z mixing. In case of an extended Higgs sector and/or additional neutral gauge bosons the determination of θ_W is non-trivial.

The known masses of the quarks and leptons as well as the CKM matrix can in general be used to calculate the SM-like Yukawa couplings of the SUSY model at the low-energy scale. Special care must be taken when determining the bottom and top quark Yukawa couplings, because they strongly influence the spectrum for large $\tan \beta$ and the prediction of the Higgs pole mass, respectively.

Electroweak symmetry breaking

As discussed above, the SUSY model is required to spontaneously break the electroweak symmetry by a Higgs mechanism. For this the scalar Higgs potential, V_{Higgs} , is required to allow for a non-zero ground state (vacuum expectation value, VEV) of one or more electrically and color neutral spin 0 Higgs bosons. This is ensured by the electroweak symmetry breaking consistency conditions, which have the form

$$\frac{\partial V_{\text{Higgs}}}{\partial v_i} = 0 \quad \forall i. \quad (6.5)$$

Here $i = 1, \dots, N$ enumerates all non-zero VEVs v_i . These N conditions can be fulfilled by adjusting N model parameters, the so-called EWSB output parameters. In the CMSSM for example these are chosen to be μ and $B\mu$, while in the Z_3 -symmetric NMSSM κ , $|v_3|^2$ and m_s^2 are used. At the loop level the Higgs potential receives radiative corrections. To let the sum of all tree-level and loop tadpole diagrams vanish, it is convenient to minimize the loop-corrected Higgs potential. The EWSB consistency conditions then take the form

$$\frac{\partial V_{\text{Higgs}}^{\text{tree}}}{\partial v_i} - t_i = 0, \quad (6.6)$$

where t_i is the tadpole diagram of i th gauge eigenstate Higgs field. Since the tadpole diagrams contain the masses of the SUSY particles, which depend on the EWSB output parameters, Eq. (6.6) must be solved iteratively.

Further boundary conditions

In constrained SUSY models, such as the CMSSM or CE₆SSM further conditions on the soft-breaking parameters are imposed at the GUT scale M_X . These models

use mSUGRA scenarios where all soft-breaking squared masses, gaugino masses and trilinear couplings are universal at M_X . Here the GUT scale is defined to be the scale where the (GUT normalized) gauge couplings g_1 and g_2 unify. Since such constrained models are often studied, FlexibleSUSY provides a mechanism to determine the GUT scale and impose constraints of this kind.

Boundary value problem

Just as in the case of the CE₆SSM and NMSSM spectrum generators described in Sections 3 and 5 all here listed constraints together with the β -functions of all model parameters form a boundary value problem. Even more general constructions are conceivable, where a tower of effective theories is constructed which are matched at intermediate scales between m_Z^{pole} and M_X . To solve such general boundary value problems, taking towers of effective theories and an arbitrary number of constraints into account, FlexibleSUSY provides a generalization of Algorithm 5.4, which will be explained in Section 6.3.2.

6.2.3 Calculation of pole masses

Having solved the above described boundary value problem it is possible to calculate the pole mass spectrum. This means finding values for the momenta p_i for which the full propagators of the fields have a pole. It is equivalent to finding values p_i such that the equations

$$0 = \det \left(p_i^2 \mathbf{1} - M_\varphi + M_{\varphi,L}(p_i^2) \right) \quad \text{for scalars/vectors } \varphi, \text{ or} \quad (6.7a)$$

$$0 = \det \left(p_i \mathbf{1} - M_\xi + M_{\xi,L}(p_i^2) \right) \quad \text{for Dirac/Majorana fermions } \xi \quad (6.7b)$$

are fulfilled. Here M_f is the tree-level mass matrix and $M_{f,L}$ contains loop corrections from the self-energy of field f . In the $\overline{\text{DR}}$ scheme the form of the loop corrections $M_{f,L}$ for the here considered spin 0, 1/2 and 1 fields is well known at the one-loop level. The general form was already given in Section 5.4.4 and can be directly applied to the SUSY models considered here.

6.3 Implementation

Goal of FlexibleSUSY is to create a fast and modular spectrum generator for a user-defined SUSY model, which numerically solves the given boundary value problem and calculates the pole mass spectrum. This is done in the following way: At first the β -functions, mass matrices, self-energies, tadpoles and EWSB equations are calculated algebraically with SARAH. These algebraic expressions are then converted to C++ form and are written to C++ classes. The created classes are finally combined at the C++ level to form a complete spectrum generator, which is then compiled to a single executable.

To achieve the design goals from Section 6.1, the generated C++ classes implement well-defined interfaces for the model parameters, β -functions, boundary conditions, etc. This allows to easily modify, extend, exchange and reuse the generated code. Furthermore, the algebraic expressions for the β -functions are written at the C++ level in terms of the matrix and vector classes provided by Eigen [174]. Eigen uses C++ expression templates [175] to formulate the matrix operations such that they can be well optimized by the compiler. This results in very well optimized code with a short execution time. In addition multi-threading is used to calculate the pole mass spectrum, which further decreases the run-time of the spectrum generator on multi-core CPUs.

This chapter is structured as follows: Section 6.3.1 describes how the algebraic expressions for the β -functions, mass matrices, self-energies etc. are obtained from SARAH and converted to C++ form. In Section 6.3.2 the C++ class structure is explained, which allows for the flexible usage. Section 6.3.3 describes how a user can define boundary conditions on the model parameters and how the gauge and Yukawa couplings are obtained from the Standard Model values at the low-energy scale. Sections 6.3.4 and 6.3.5 explain the algorithm to solve the user-defined boundary value problem and the calculation of the pole mass spectrum.

6.3.1 Creating the C++ source code

To build the spectrum generator, FlexibleSUSY requires the following information:

- A SARAH model file must be available, which defines the SUSY model. Here the user has to provide the gauge group, the field content, the superpotential and the mixing to mass eigenstates. A detailed description of how to write such a model file can be found in [137] or in the manual shipped with each SARAH package. Note that SARAH already provides plenty of predefined model files for the most common models, as for example the MSSM (and variants), NMSSM (Z_3 -conserving and -violating version) and USSM. FlexibleSUSY ships additional model files for the E_6 SSM and a MSSM extension with right-handed neutrinos.
- A FlexibleSUSY model file must be created, which defines the input parameters, the boundary conditions at the high-, SUSY and low-energy scale and the EWSB output parameters. See Section 6.3.3 for a detailed description on how to create such a model file. Note that FlexibleSUSY already is distributed with examples for often studied SUSY models such as the MSSM, NMSSM (Z_3 -conserving and -violating version), USSM and E_6 SSM.

Configuration and build

When this information is available, FlexibleSUSY can be configured and build with the following three commands

```
./createmodel --name=<model>
./configure --with-models=<model>
make
```

where `<model>` is the user-defined name of the SUSY model. The `createmodel` script will create a sub-directory `<model>/` with a makefile module (`module.mk`), the FlexibleSUSY model file (`FlexibleSUSY.m`) and the Mathematica start script (`start.m`). The latter will invoke Mathematica to start the code generation. The `configure` script checks the build environment (compilers, installed SARAH version, available Mathematica version, Eigen library, etc.) and creates the `Makefile`. Finally, `make` will start the code generation and finally compiles all source code files. After the compilation has finished, the spectrum generator can be run with the command

```
./models/<model>/run_<model>.x \
  --slha-input-file=<input-file> --slha-output-file=<output-file>
```

This will calculate the pole mass spectrum and the model parameters for the parameter point given in the SLHA input file `<input-file>` and write the result to the output file `<output-file>` in SLHA format [176, 149].

Code generation

When `make` is called, a Mathematica kernel is started and the start script in the model directory `<model>/start.m` is loaded, which starts the C++ code generation. This code generation is described in the following and is illustrated in Figure 6.1.

At first, SARAH is loaded and `SARAH‘Start["<model>"]` is called. This loads the SARAH model file, where the gauge symmetry group, the particles, their mass eigenstate mixings and the superpotential are defined. Afterwards, FlexibleSUSY is loaded and `FlexibleSUSY‘MakeFlexibleSUSY[]` is called. This function starts the code generation:

1. The β -functions are calculated algebraically by calling `SARAH‘CalcRGEs[]`. These β -functions are then split into two sets: β -functions for SUSY parameters (gauge couplings, VEVs and superpotential parameters) and β -functions for soft-breaking parameters (soft squared masses, soft-breaking gaugino masses and trilinear, bilinear and linear soft-breaking scalar couplings). This splitting is physically motivated, because the β -functions of the SUSY parameters do not depend on soft-breaking parameters due to the general structure of the RGEs [159, 160, 161, 134, 162, 61, 132, 63, 64]. Therefore, the RGEs of the SUSY parameters can in principle be solved independently from the soft-breaking ones.

This property is also reflected in the generated C++ code, as will be explained in Section 6.3.2: The SUSY parameters and their β -functions are stored in the class `<model>_susy_parameters`. The soft-breaking model parameters, together with their β -functions are stored in the class `<model>_soft_parameters`. The

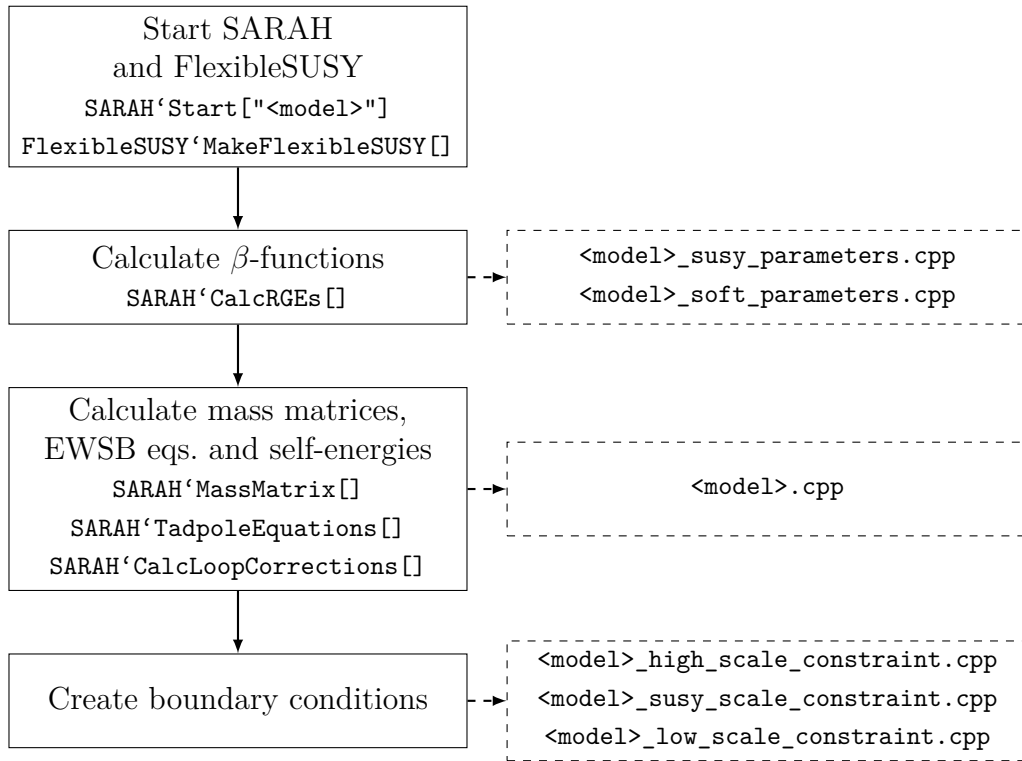


Figure 6.1: FlexibleSUSY C++ code generation program flow.

dependence of the soft-breaking parameters on the SUSY parameters is realized via inheritance, see Figure 6.2, where `<model>_soft_parameters` inherits from `<model>_susy_parameters`. In this way, the class `<model>_soft_parameters` can implement the soft-breaking β -functions in terms of the all parameters, while the class `<model>_susy_parameters` is independent of the soft-breaking ones.

2. The mass matrices are calculated by calling `SARAH'MassMatrix[<particle>]` for each mass eigenstate `<particle>`. The obtained expression is converted into a C++ member function of the model class. For example, the mass matrix for the CP-even Higgs `hh` in the MSSM is converted to

```

Eigen::Matrix<double,2,2> MSSM::get_mass_matrix_hh() const
{
    Eigen::Matrix<double,2,2> mass_matrix_hh;

    mass_matrix_hh(0,0) = mHd2 + AbsSqr(Mu)
        + 0.225*Sqr(g1)*Sqr(vd) + 0.375*Sqr(g2)*Sqr(vd)
        - 0.075*Sqr(g1)*Sqr(vu) - 0.125*Sqr(g2)*Sqr(vu);
    mass_matrix_hh(0,1) = -0.5*BMu - 0.5*Conj(BMu)
        - 0.15*vd*vu*Sqr(g1) - 0.25*vd*vu*Sqr(g2);
    mass_matrix_hh(1,0) = mass_matrix_hh(0,1);
    mass_matrix_hh(1,1) = mHu2 + AbsSqr(Mu)
        - 0.075*Sqr(g1)*Sqr(vd) - 0.125*Sqr(g2)*Sqr(vd)
        + 0.225*Sqr(g1)*Sqr(vu) + 0.375*Sqr(g2)*Sqr(vu);
}
  
```

```

    return mass_matrix_hh;
}

```

For each mass matrix a corresponding diagonalization function is created, which calculates the \overline{DR} mass eigenstates and the mixing matrices. For the CP-even Higgs this function looks like

```

void MSSM::calculate_Mhh()
{
    const auto mass_matrix_hh(get_mass_matrix_hh());
    fs_diagonalize_hermitian(mass_matrix_hh, Mhh, ZH);

    if (Mhh.minCoeff() < 0.)
        problems.flag_tachyon(hh);
    else
        problems.unflag_tachyon(hh);

    Mhh = AbsSqrt(Mhh);
}

```

For mass matrices of size 4×4 or smaller, the function `fs_diagonalize_hermitian()` uses Eigen's `SelfAdjointEigenSolver` to diagonalize the mass matrix. For larger matrices, LAPACK's diagonalization functions are used for speed reasons. After the diagonalization the function checks for tachyons and takes the square root of the mass eigenstate vector `Mhh`.

3. The tree-level electroweak symmetry breaking equations are calculated by calling `SARAH::TadpoleEquations[]`. FlexibleSUSY tries to solve them analytically for the user-defined set of EWSB output parameters. If an analytic solution can be found, the result is written to the `solve_ewsb_tree_level()` function of the model class.⁵ In the CMSSM, for example, where μ and $B\mu$ are chosen as EWSB output, the function which solves the EWSB equations has the form

```

int MSSM::solve_ewsb_tree_level()
{
    int error = 0;

    const double old_BMu = BMu;
    const double old_Mu = Mu;

    BMu = (0.05*(-20*mHd2*vd*vu + 20*mHu2*vd*vu
        - 3*Power(vd,3)*vu*Sqr(g1) + 3*vd*Power(vu,3)*Sqr(g1)
        - 5*Power(vd,3)*vu*Sqr(g2) + 5*vd*Power(vu,3)*Sqr(g2)))
        / (Sqr(vd) - Sqr(vu));
}

```

⁵In case multiple solutions are found, which differ by a sign only, the free sign is added to the list of input parameters. This is the case in the CMSSM for example, where the EWSB conditions fix only $|\mu|^2$ and sign μ remains free.

```

Mu = LOCALINPUT(SignMu)*Sqrt((-mHd2*vd) + vu*BMu
- 0.075*Power(vd,3)*Sqr(g1) - 0.125*Power(vd,3)*Sqr(g2)
+ 0.075*vd*Sqr(g1)*Sqr(vu)
+ 0.125*vd*Sqr(g2)*Sqr(vu))/vd);

const bool is_finite = std::isfinite(BMu)
&& std::isfinite(Mu);

if (!is_finite) {
  BMu = old_BMu;
  Mu = old_Mu;
  error = 1;
}

return error;
}

```

If no analytic solution can be found, an iterative algorithm is used to solve the EWSB conditions numerically. The algorithm tries to find the root of the EWSB equations (6.6) simultaneously using GNU GSL's `gsl_multiroot_fsolver_hybrid` [177]. If no solution can be found the multi-dimensional GSL root-finder with dynamic step size `gsl_multiroot_fsolver_hybrids` is used. If this method fails as well the Broyden method `gsl_multiroot_fsolver_broyden` is tried finally.

4. The one-loop self-energies, tadpole diagrams and Feynman Rules are calculated by calling `SARAH::CalcLoopCorrections[]`. The obtained expressions are converted to C++ functions and are written to the model class. For example, the CP-even Higgs self-energy function in the MSSM has the form

```

std::complex<double> MSSM::self_energy_hh(double p,
unsigned g01, unsigned g02) const
{
  std::complex<double> result;

  result += 4*B0(p, MVWm, MVWm)*Conj(CpUhhconjVWmVWm(g02))
    *CpUhhconjVWmVWm(g01);
  result += 4*A0(MVWm)*CpUhhUhhconjVWmVWm(g01, g02);
  ...

  return result * oneOver16PiSqr;
}

```

The first argument of the function is the momentum of the external Higgs field. The second and third arguments are the mass eigenstate indices of the external Higgs fields ($i = 1, 2$). The function then successively adds all one-loop diagrams that contribute to the self-energy. For instance, the first diagram in the above example is a W -boson loop with two propagators and is written in terms of the $B_0(p, m_W, m_W)$ Passarino-Veltman function [178], which are defined in the convention of [179].

5. As last step, FlexibleSUSY creates classes for the three user-defined boundary conditions at the high-, SUSY and low-energy scale. All of these classes implement the common `Constraint` interface, which defines the abstract properties of a boundary condition. See Section 6.3.3 for the implementation details.

6.3.2 Class hierarchy

To allow for a flexible usage (reuseability, extendability, exchangeability) of the model information the generated code is structured in C++ classes with well-defined interfaces. For this purpose two main class hierarchies are created:

1. The model class hierarchy, which contains the model parameters, β -functions, mass matrices, EWSB equations, tadpoles and self-energies. Most of this information is provided by SARAH. Among the expressions mentioned here only the parameters, which are chosen to be output of the EWSB equations are defined in the FlexibleSUSY model file.
2. The RGE solver class hierarchy, which connects the model class hierarchy with the boundary conditions at an abstract level. The later established concrete connection with the user-defined boundary conditions defines the actual boundary value problem at the C++ level.

These two C++ class hierarchies are described in the following. The concrete model-specific definitions of the boundary conditions will be explained afterwards in Section 6.3.3.

Model class hierarchy

The model class hierarchy describes in essence four properties of the SUSY model from Section 6.2: The model parameters, the β -functions, the electroweak symmetry breaking and the calculation of the pole mass spectrum. It is illustrated in the UML diagram in Figure 6.2.

At the top of the hierarchy is the `Beta_function` interface class. Its purpose is to define the `run_to()` function, which integrates the RGEs up to a given scale, using a Runge-Kutta method with adaptive step size. To provide this functionality, three virtual interface functions need to be implemented by the derived class: (i) The `get()` function, which returns all model parameters in form of a vector, (ii) the corresponding `set()` function, which sets all model parameters, given the vector of parameters, and (iii) the `beta()` function, which returns all β -functions in form of a vector. The `run_to()` function uses these three interface functions to implement the Runge-Kutta algorithm. For the concrete implementation Softsusy's `numerics` module is used [60], slightly adapted to the data types used in FlexibleSUSY.

The model parameters and their β -functions are contained in the first and second derived class in the hierarchy. The first derived class, `<model>_susy_parameters`, contains the SUSY parameters and implements the three interface functions `get()`, `set()` and `beta()`. Thus, the `<model>_susy_parameters` class has already implemented

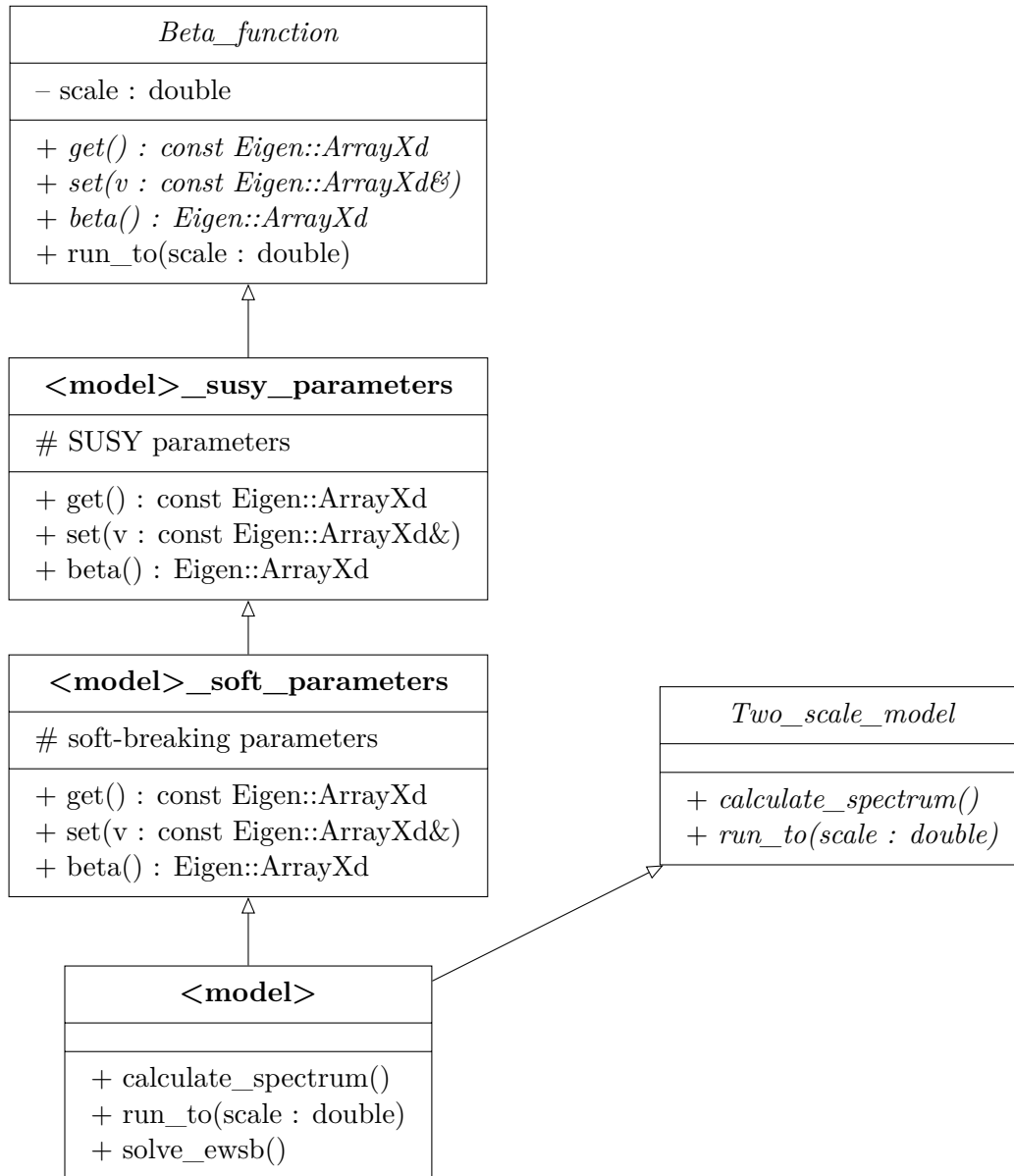


Figure 6.2: Model class hierarchy.

the complete `Beta_function` interface, and can therefore already be used on its own. The second derived class is `<model>_soft_parameters`, which contains all soft-breaking parameters. It inherits directly from `<model>_susy_parameters` and extends the interface functions by the soft-breaking parameters. As a consequence the function `<model>_soft_parameters::run_to()` integrates the RGEs of *all* model parameters.

The bottom of the hierarchy is formed by the so-called model class `<model>`. It inherits from the `<model>_soft_parameters` class in order to have access to all model parameters. At the same time it implements the `Two_scale_model` interface, which is used for communication with the boundary condition solver `RGFlow`. This interface defines a `calculate_spectrum()` and a `run_to()` function. The model class imple-

ments the `run_to()` function simply by calling `<model>_soft_parameters::run_to()`. The `calculate_spectrum()` function uses the generated mass matrices and self-energies to calculate the pole mass spectrum, see Section 6.3.5.

In summary, the so defined model class hierarchy contains all information about the SUSY model from Section 6.2, except for the boundary conditions. It already has a lot of potential for being reused:

- The class of SUSY parameters, `<model>_susy_parameters`, can be used independently of the soft-breaking parameters and the model class. In particular, it can be used to run the SUSY parameters to any scale by using the `run_to()` function. This is especially useful in models where the boundary value problem must be solved for the SUSY parameters first, ignoring the soft-breaking parameters. This is the case in the CE_6SSM , for example.
- The class of soft-breaking parameters, `<model>_soft_parameters`, can be used independently of the model class. It contains all model parameters, including the SUSY parameters, and also implements the `run_to()` function.
- The model class `<model>` contains all information about the model parameters, the electroweak symmetry breaking and is able to calculate the pole mass spectrum. It is completely independent of the RGE solver class and the boundary conditions. It can be used for example to study pure low-energy models, which do not impose boundary conditions at different scales.

RGE solver class hierarchy

The RGE solver class hierarchy connects the model class hierarchy (`Two_scale_model` interface) with the boundary conditions (`Constraint` interface) and the boundary condition solver `RGF1ow`. Thereby it defines a constrained SUSY model completely at an abstract level. It is illustrated in Figure 6.3. In the standard “two-scale” implementation the `RGF1ow` class solves the boundary value problem iteratively by running the model parameters to the various scales, defined by constraints, and impose the boundary conditions by calling the `apply()` member function. In detail it works as described in Algorithm 6.1. This algorithm is a generalization of the procedures described in [163] for the CMSSM and in Section 5.4.3 for the NMSSM.⁶ It is widely implemented in SUSY spectrum generators [60, 136, 147, 146, 137, 180, 181, 182]. To use the RGE solver at the C++ level, the user has to provide the following classes:

- One or more model classes, which implement the `Two_scale_model` interface. See the model class hierarchy implementation in the previous section.
- One or more model boundary conditions (constraints), which implement the `Constraint` interface. The interface defines a `get_scale()` function, which should

⁶The two-scale algorithm described in Algorithm 6.1 is a fixed-point iteration of the form $x_{n+1} = f(x_n)$ ($n = 0, 1, 2, \dots$), where x_n is the vector of model parameters after the n th iteration. The function f is the integration of the RGEs and the imposition of the boundary conditions.

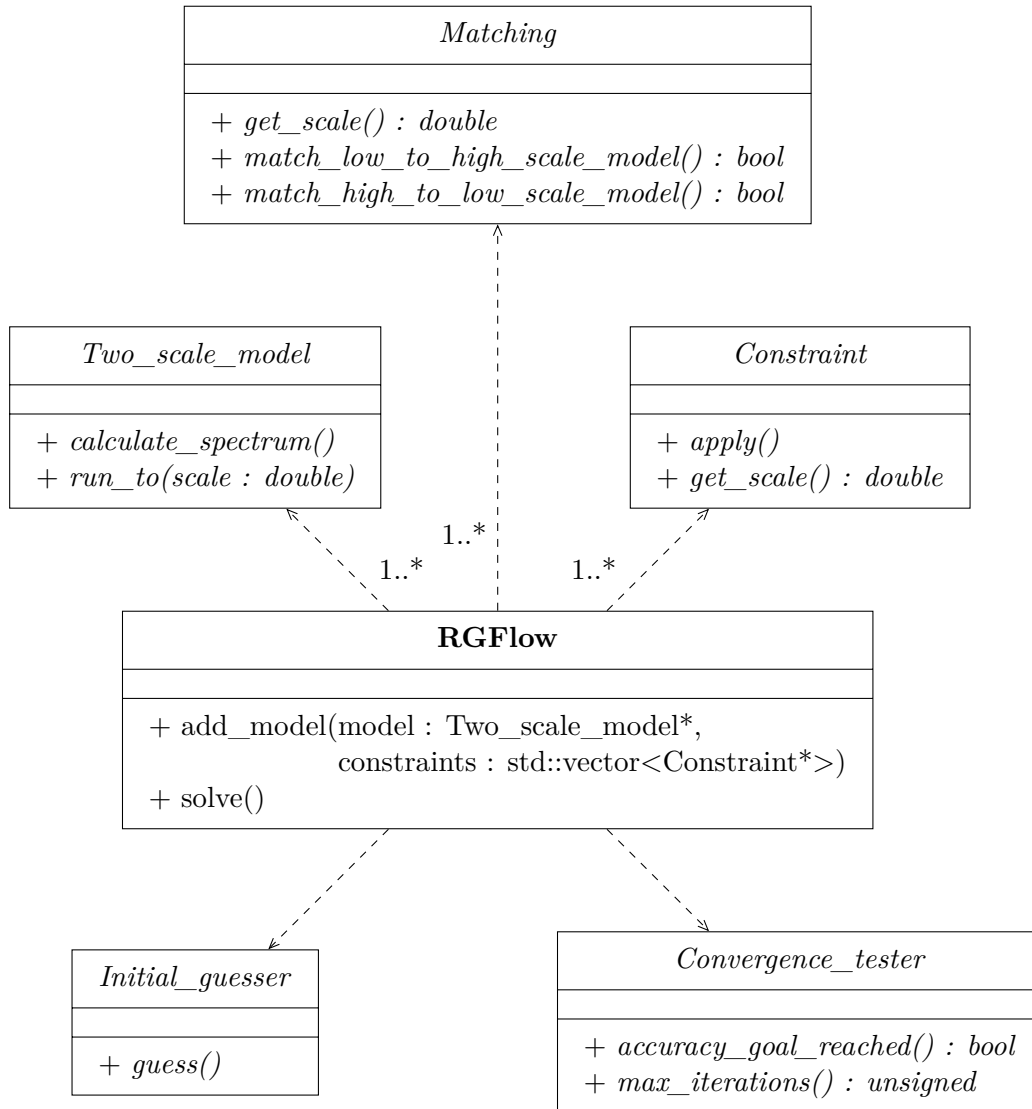


Figure 6.3: Class hierarchy of the two-scale boundary value problem solver `RGFlow`.

return the renormalization scale where the constraint is supposed to be imposed, and an `apply()` function, which imposes the constraint.

- If more than one model should be used, a matching condition class, implementing the `Matching` interface, must be given. It defines the interface functions `match_low_to_high_scale_model()` and `match_high_to_low_scale_model()`, which convert the parameters of the low-energy (high-energy) model to parameters of the high-energy (low-energy) model. An example of such a parameter matching are the E_6 SSM gauge coupling threshold corrections given in Appendix C.7.
- A convergence tester, which implements the `Convergence_tester` interface. Its `accuracy_goal_reached()` function should implement a convergence measure and must return true if convergence is achieved. FlexibleSUSY creates a default

Algorithm 6.1 Two-scale iteration in `RGFlow::solve()`

Assume there is a tower of m models $\mathcal{M}_1, \dots, \mathcal{M}_m$ and corresponding constraints \mathcal{C}_{ij} , where $i = 1, \dots, m$ is the model index and $j = 1, \dots, c_i$ labels the constraints for model i . Calling the `solve()` function starts the following iteration:

1. *Initial guess*: Call the `guess()` function of the initial guesser.
 2. While not maximum number of iterations reached and the convergence tester method `accuracy_goal_reached()` returns false, do
 - a) *Run the tower up*: For each model $i = 1$ to m do
 - I For each constraint $j = 1$ to c_i do
 - A. get the scale μ of constraint \mathcal{C}_{ij} : $\mu \leftarrow \mathcal{C}_{ij}.\text{get_scale}()$
 - B. run model \mathcal{M}_i to scale μ : $\mathcal{M}_i.\text{run_to}(\mu)$
 - C. impose the constraint: $\mathcal{C}_{ij}.\text{apply}()$
 - II If $i < m$, then match model \mathcal{M}_i to \mathcal{M}_{i+1} :
 $\mathcal{M}_i.\text{match_low_to_high_scale_model}()$
 - b) *Run the tower down*: For each model $i = m$ to 1 do
 - I For each constraint $j = c_i$ to 1 do
 - A. get the scale μ of constraint \mathcal{C}_{ij} : $\mu \leftarrow \mathcal{C}_{ij}.\text{get_scale}()$
 - B. run model \mathcal{M}_i to scale μ : $\mathcal{M}_i.\text{run_to}(\mu)$
 - C. impose the constraint: $\mathcal{C}_{ij}.\text{apply}()$
 - II If $i > 1$, then match model \mathcal{M}_i to \mathcal{M}_{i-1} :
 $\mathcal{M}_i.\text{match_high_to_low_scale_model}()$
 3. If the convergence tester method `accuracy_goal_reached()` still returns false, throw an exception of type `NoConvergenceError`.
-

convergence tester for each model, which compares the maximum relative deviation of the $\overline{\text{DR}}$ mass spectrum between two consecutive iterations against a threshold. The value of the threshold can be set in the in the SLHA input file or directly in the class constructor.

- Optional: An initial guesser, which implements the `Initial_guesser` interface. Its `guess()` function should set the model parameters to guessed values, which are not too far away from the real solution.

Note that, when FlexibleSUSY's Mathematica interface is used, see Section 6.3.3, the model class, three boundary conditions (at the low-, SUSY and high-energy scale), a convergence tester and an initial guesser are created automatically. The above description is only relevant for users which want to build their own model at the C++ level.

In summary, the RGE solver class hierarchy plugs together the SUSY model and the boundary conditions, thereby defining a *constrained* model completely at an abstract level. The `solve()` method of the `RGFlow` class tries to find a solution for the so-defined boundary value problem using a fixed-point iteration. It is a generalization of the procedures used in the CMSSM and NMSSM with the additional possibility to specify a tower of models (effective field theories) with matching conditions and an arbitrary number of constraints. An advantage of this hierarchy is that `RGFlow` depends only on abstract interfaces. This allows the user to easily exchange the models and constraints during run-time. This so-called run-time polymorphism is an advantage of object-oriented programming languages, like C++, over statically typed languages, such as Fortran.

6.3.3 Boundary conditions and the FlexibleSUSY model file

In the previous sections it was described how the C++ code for a user-supplied non-constrained SUSY model is created and structured. This section explains how a user can define boundary conditions at the Mathematica (meta code) level via a FlexibleSUSY model file.

After the `createmodel` script has been executed, see Section 6.3.1, the configuration file for the SUSY model can be found in `<model>/FlexibleSUSY.m`. In this model file the user can specify (i) the model input parameters, (ii) the EWSB output parameters and (iii) three boundary conditions at the low-, SUSY and high-energy scale. In the following the various model file options are explained on the basis of the CMSSM. The application to other models is straightforward. The FlexibleSUSY model file for the CMSSM reads

Source code listing 6.1: FlexibleSUSY model file for the CMSSM

```
FSmodelName = "MSSM"; (* model name *)

MINPAR = {
  {1, m0},
  {2, m12},
  {3, TanBeta},
  {4, Sign[\[Mu]]},
  {5, Azero}
};

EXTPAR = {};

EWSBOutputParameters = { B[\[Mu]], \[Mu] };

HighScale = g1 == g2;

HighScaleFirstGuess = 2.0 10^16;

HighScaleInput = {
  {T[Ye], Azero*Ye},
  {T[Yd], Azero*Yd},
```

```

    {T[Yu], Azero*Yu},
    {mHd2, m0^2},
    {mHu2, m0^2},
    {mq2, UNITMATRIX[3] m0^2},
    {ml2, UNITMATRIX[3] m0^2},
    {md2, UNITMATRIX[3] m0^2},
    {mu2, UNITMATRIX[3] m0^2},
    {me2, UNITMATRIX[3] m0^2},
    {MassB, m12},
    {MassWB, m12},
    {MassG, m12}
};

SUSYScale = Sqrt[M[Su[1]]*M[Su[6]]];

SUSYScaleFirstGuess = Sqrt[m0^2 + 4 m12^2];

SUSYScaleInput = {};

LowScale = SM[MZ];

LowScaleFirstGuess = SM[MZ];

LowScaleInput = {
    {Yu, Automatic},
    {Yd, Automatic},
    {Ye, Automatic},
    {vd, 2 MZDRbar Cos[ArcTan[TanBeta]]
        / Sqrt[GUTNormalization[g1]^2 g1^2 + g2^2]},
    {vu, 2 MZDRbar Sin[ArcTan[TanBeta]]
        / Sqrt[GUTNormalization[g1]^2 g1^2 + g2^2]}
};

InitialGuessAtLowScale = {
    {vd, SM[vev] Cos[ArcTan[TanBeta]]},
    {vu, SM[vev] Sin[ArcTan[TanBeta]]},
    {Yu, Automatic},
    {Yd, Automatic},
    {Ye, Automatic}
};

InitialGuessAtHighScale = {
    {\[Mu], 1.0},
    {B\[Mu]}, 0.0}
};

UseHiggs2LoopMSSM = True;
EffectiveMu = \[Mu];

OnlyLowEnergyFlexibleSUSY = False; (* default *)

```

The variable `FSModelName` contains the name of the FlexibleSUSY model. It is set to "MSSM" in this case.

All (non-Standard Model) model input parameters are specified in the variables `MINPAR` and `EXTPAR` in form of a list. The elements of these lists are two-component lists, where the first entry is the index of the parameter in the `MINPAR` or `EXTPAR` block of the SLHA input file, respectively. See [176, 149] for the definition of the SLHA format. The second entry in the list is the name of the input parameter. In the above example the five free CMSSM parameters m_0 , $M_{1/2}$, $\tan\beta$, $\text{sign}\mu$ and A_0 are defined as input, see Section 2.1. When the spectrum generator is run, these parameters are read from the `MINPAR` block of the SLHA input file. This block has the form

Block	MINPAR	# Input parameters
1	125.	# m0
2	500.	# m12
3	10.	# TanBeta
4	1	# SignMu
5	0	# Azero

where the first column contains the SLHA indices, and the second column contains the corresponding input parameter values.

The model parameters, which shall be used as output of the electroweak symmetry breaking conditions (6.6), are set in the variable `EWSBOutputParameters`. When the `solve_ewsb()` method of the model class is called, these parameters will be adjusted such that the EWSB conditions (6.6) are fulfilled. In the CMSSM these are chosen to be the superpotential parameter μ and the corresponding soft-breaking parameter $B\mu$.⁷⁸

Furthermore, the user can specify parameter boundary conditions at three different scales: low-, SUSY and high-energy scale. These scales are defined with variables `LowScale`, `SUSYScale` and `HighScale`. The values of these variables can be set to:

- a fixed numerical value, such as $2.0 \cdot 10^{-14}$
- a predefined fixed scale, such as a pole mass of a Standard Model particle, for example `SM[MZ]`, `SM[MW]`, `SM[MH]`, `SM[MTOP]`, `SM[MBOTTOM]`, etc.
- an expression evaluated at run-time, for example `Sqrt[M[Su[1]]*M[Su[6]]]`. Here `M[Su[1]]` is the $\overline{\text{DR}}$ mass of the lightest, and `M[Su[6]]` the mass of the heaviest up-type squark (see the SARAH model file for the definition of the particle names).
- a condition of the form `<lhs> == <rhs>`, where `<lhs>` and `<rhs>` are expressions

⁷In the MSSM the EWSB conditions fix only $|\mu|$ and leave the sign of μ unfixed. FlexibleSUSY recognizes such cases and introduces the sign of μ as free model input parameter.

⁸Care should be taken when choosing dimensionless model parameters as EWSB output. The reason is that these parameters in general affect the running of *all* other model parameters. This can lead to a very unstable iteration. However, there are cases where a dimensionless parameter has little impact on the RG flow, as for example κ in the Z_3 -symmetric NMSSM. Such parameters may therefore be chosen as EWSB output.

of model parameters. An example for such a condition is the definition of the gauge coupling unification scale, defined as the scale where $g_1 == g_2$.

Furthermore, for each scale there is an initial guess variable, which defines the first guess of the scale. For the three constraints these are `HighScaleFirstGuess`, `SUSYScaleFirstGuess` and `LowScaleFirstGuess`. These variables may have either fixed numerical values, predefined pole mass scales (such as `SM[MZ]`, `SM[MW]`, `SM[MH]`, `SM[MTOP]`, `SM[MBOTTOM]`, etc.), or expressions of input parameters.

The exact form of the three constraints is set in the variables `HighScaleInput`, `SUSYScaleInput` and `LowScaleInput`. These variables contain lists of settings, applied at the corresponding scale. A setting can be any of the following:

- A two-component list of the form `{parameter, value}`. This defines an assignment of the `value` to the `parameter` at the considered scale. `value` can be either (i) a fixed numerical value, (ii) a predefined fixed value, such as a mass of a Standard Model particle (`SM[MZ]`, `SM[MW]`, `SM[MH]`, `SM[MTOP]`, `SM[MBOTTOM]`, `MZDRbar`, `MWDRbar`), or (iii) an expression of input parameters. As an alternative, `value` can be read from a special “input block” from an input file in SLHA-2 format [149]. In this case, it must be written as `LHInput[value]`. Example:

```
SUSYScaleInput = {
  {mHd2, m0^2},
  {mHu2, LHInput[mHu2]}
};
```

Here the parameter `mHd2` is set to the value of `m0^2`, where `m0` is a model input parameter read from the `MINPAR` block. The parameter `mHu2` is set to the value given in the `MSOFTIN` block, entry 22 [149]. The SLHA-2 input block names and entry numbers can be defined in the SARAH model file `parameters.m`, see [112].

For the Standard Model Yukawa couplings Y_u , Y_d , Y_e the special value `Automatic` is allowed. This will trigger the automatic calculation of the Yukawa couplings from the known Standard Model quark and lepton masses, see below.

- The special symbol `FSMinimize[parameters, function]` can be used to adjust the model parameters given in the list `parameters`, such that the scalar `function` is minimal. Example:

```
FSMinimize[{vd, vu},
  (SM[MZ] - Pole[M[VZ]])^2
  / STANDARDDEVIATION[MZ]^2 +
  (SM[MH] - Pole[M[hh[1]]])^2
  / STANDARDDEVIATION[MH]^2]
```

Here, the model parameters `vu` and `vd` are varied until the function

$$\chi^2(v_d, v_u) = \frac{(\text{SM}[\text{MZ}] - m_Z^{\text{pole}})^2}{\sigma_{m_Z}^2} + \frac{(\text{SM}[\text{MH}] - m_h^{\text{pole}})^2}{\sigma_{m_h}^2} \quad (6.8)$$

is minimal. The constants `SM[MZ]`, `SM[MH]`, σ_{m_Z} and σ_{m_h} are defined in the file `src/ew_input.hpp` and have the values [11]

$$\text{SM}[\text{MZ}] = 91.1876, \quad \text{SM}[\text{MH}] = 125.9, \quad (6.9)$$

$$\sigma_{m_Z} = 0.0021, \quad \sigma_{m_h} = 0.4. \quad (6.10)$$

- The special symbol `FSFindRoot[parameters, functions]` can be used to adjust the model parameters given in the list `parameters`, until a root of the vector-valued function is found. Example:

```
FSFindRoot [{vd, vu},
            {SM[MZ] - Pole[M[VZ]], SM[MH] - Pole[M[h h [1]]}]}
```

In this example the parameters `vu` and `vd` are varied until the vector-valued function

$$f(v_d, v_u) = \begin{pmatrix} \text{SM}[\text{MZ}] - m_Z^{\text{pole}} \\ \text{SM}[\text{MH}] - m_h^{\text{pole}} \end{pmatrix} \quad (6.11)$$

is zero in each component.

Please note that it might not always be possible to find a minimum or a root of the above functions. Especially the correct prediction of the lightest CP-even Higgs mass by just varying v_u and v_d might fail in most of the CMSSM parameter regions. However, the above examples illustrate how function minimization and root finding can be used in principle to determine model parameters.

In the above example the high-scale is defined to be the GUT scale, where the gauge couplings of $U(1)_Y$ and $SU(2)_L$ unify⁹:

```
HighScale = g1 == g2;
```

The settings in `HighScaleInput` are precisely the mSUGRA boundary conditions from Eq. (2.3). In addition to the boundary condition definitions above, FlexibleSUSY automatically calculates the gauge couplings g_1 , g_2 and g_3 at the low-scale from known Standard Model input $\alpha_{\text{e.m.}}(m_Z^{\text{pole}})$, $\alpha_s(m_Z^{\text{pole}})$, m_Z^{pole} , m_W^{pole} . The details of this calculation can be found in the next section. The SUSY scale is special in FlexibleSUSY, because it is the scale where the EWSB conditions (6.5) are solved and the pole mass spectrum is eventually calculated. In a model without squark flavour mixing this scale is usually defined to be $\sqrt{m_{\tilde{t}_1} m_{\tilde{t}_2}}$.

Finally, the user can define an initial guess for the model parameters at the low and high scale, using the variables `InitialGuessAtLowScale` and `InitialGuessAtHighScale`,

⁹Note that FlexibleSUSY GUT normalizes all gauge couplings, so that the gauge coupling unification condition takes the simple form $g_1(M_X) = g_2(M_X)$. A consequence is that in the calculation of the VEVs v_u and v_d from m_Z and $\tan\beta$ at the low-energy scale the GUT-normalization of g_1 has to be taken into account.

respectively. Non-guessed parameters will be initialized to zero, except for the gauge couplings, which are initialized automatically at the low-energy scale from the known Standard Model parameters. The initial guess for the Yukawa couplings can be done automatically by setting the corresponding value to `Automatic`, see the example above.

For a precise prediction of the CP-even and -odd Higgs pole masses, FlexibleSUSY allows one to add leading two-loop contributions to the Higgs self-energies and tadpoles. For MSSM-like models¹⁰ these corrections can be enabled by setting in the model file `UseHiggs2LoopMSSM = True`; and by defining the effective μ -term in `EffectiveMu`. This will add the zero-momentum corrections of the order $O(y_t^4 + y_t^2 y_b^2 + y_b^4 + y_\tau^4)$ and $O(y_t^2 g_3^2 + y_b^2 g_3^2)$ from [165, 166, 167, 183, 184]. For NMSSM-like models¹¹ the two-loop contributions are enabled by setting `UseHiggs2LoopNMSSM = True`; and by again defining the effective μ -term. In the NMSSM one might set `EffectiveMu = \[\Lambda] vS / Sqrt[2]`, for example. This will add the the zero-momentum corrections of the order $O(y_t^2 g_3^2 + y_b^2 g_3^2)$ from [168], plus MSSM-like contributions of the order $O(y_t^4 + y_t^2 y_b^2 + y_b^4 + y_\tau^4)$ [166, 167]. Note that two-loop corrections from matter fields absent from the MSSM and NMSSM are not included automatically.

It is possible to create a pure low-energy model, which has only a low-scale and SUSY-scale constraint, but no high-energy scale is defined. Such a model can be created by setting `OnlyLowEnergyFlexibleSUSY = True` in the model file. Here all model parameters, which are not specified in `MINPAR`, `EXTPAR` or `EWSBOutputParameters`, are read from the corresponding input blocks of the SLHA input file [149] and are set at the SUSY scale.

Calculation of the gauge couplings at the low-scale

At the low-energy scale, the $\overline{\text{DR}}$ gauge couplings $g_i(m_Z^{\text{pole}})$ of the SUSY model are calculated automatically from the known Standard Model $\overline{\text{MS}}$ parameters $\alpha_{\text{e.m.}}^{\text{SM}(5),\overline{\text{MS}}}(m_Z^{\text{pole}})$, $\alpha_s^{\text{SM}(5),\overline{\text{MS}}}(m_Z^{\text{pole}})$ ¹² and the W and Z boson pole masses m_Z^{pole} and m_W^{pole} [11]. This is done by first converting the SM $\overline{\text{MS}}$ parameters to $\overline{\text{DR}}$ parameters of the SUSY model

$$\alpha_{\text{e.m.}}(m_Z^{\text{pole}}) = \frac{\alpha_{\text{e.m.}}^{\text{SM}(5),\overline{\text{MS}}}(m_Z^{\text{pole}})}{1 - \Delta\alpha_{\text{e.m.}}^{\text{SM}}(m_Z^{\text{pole}}) - \Delta\alpha_{\text{e.m.}}^{\text{susy}}(m_Z^{\text{pole}})}, \quad (6.12)$$

$$\alpha_s(m_Z^{\text{pole}}) = \frac{\alpha_s^{\text{SM}(5),\overline{\text{MS}}}(m_Z^{\text{pole}})}{1 - \Delta\alpha_s^{\text{SM}}(m_Z^{\text{pole}}) - \Delta\alpha_s^{\text{susy}}(m_Z^{\text{pole}})}, \quad (6.13)$$

¹⁰Here a model is MSSM-like if (i) its superpotential is approximately given by (2.1), (ii) it implements R -parity conservation, and (iii) contains two CP-even and CP-odd Higgs bosons, where one CP-odd Higgs boson may be a Goldstone boson, all with an MSSM-like coupling to t , b and τ .

¹¹Here, a model is NMSSM-like if (i) its superpotential is approximately given by (5.1), (ii) it implements R -parity conservation, and (iii) contains three CP-even and CP-odd Higgs bosons, where one or two CP-odd Higgs bosons may be Goldstone bosons, all with an NMSSM-like coupling to t , b and τ .

¹² $\alpha_{\text{e.m.}}^{\text{SM}(5),\overline{\text{MS}}}(m_Z^{\text{pole}})$ and $\alpha_s^{\text{SM}(5),\overline{\text{MS}}}(m_Z^{\text{pole}})$ denote the electromagnetic and strong couplings in the $\overline{\text{MS}}$ scheme in the Standard Model including only 5 quark flavours.

where

$$\Delta\alpha_{\text{e.m.}}^{\text{SM}}(\mu) = \frac{\alpha_{\text{e.m.}}}{2\pi} \left[\frac{1}{3} - \frac{16}{9} \log \frac{m_t}{\mu} \right], \quad (6.14)$$

$$\Delta\alpha_{\text{e.m.}}^{\text{susy}}(\mu) = \frac{\alpha_{\text{e.m.}}}{2\pi} \left[- \sum_{\text{susy particle } i} F_i T_i \log \frac{m_i}{\mu} \right], \quad (6.15)$$

$$\Delta\alpha_s^{\text{SM}}(\mu) = \frac{\alpha_s}{2\pi} \left[-\frac{2}{3} \log \frac{m_t}{\mu} \right], \quad (6.16)$$

$$\Delta\alpha_s^{\text{susy}}(\mu) = \frac{\alpha_s}{2\pi} \left[\frac{1}{2} - \sum_{\text{susy particle } i} F_i T_i \log \frac{m_i}{\mu} \right] \quad (6.17)$$

are threshold corrections. The constant T_i is the Dynkin index of the representation of SUSY particle i with respect to the gauge group, and F_i is a particle type-specific constant [55]

$$F_i = \begin{cases} 2/3 & \text{if particle } i \text{ is a Majorana fermion,} \\ 4/3 & \text{if particle } i \text{ is a Dirac fermion,} \\ 1/6 & \text{if particle } i \text{ is a real scalar,} \\ 1/3 & \text{if particle } i \text{ is a complex scalar.} \end{cases} \quad (6.18)$$

For $\alpha_{\text{e.m.}}^{\text{SM}(5),\overline{\text{MS}}}(m_Z^{\text{pole}})$ and $\alpha_s^{\text{SM}(5),\overline{\text{MS}}}(m_Z^{\text{pole}})$ FlexibleSUSY uses internally [11]

$$\alpha_{\text{e.m.}}^{\text{SM}(5),\overline{\text{MS}}}(m_Z^{\text{pole}}) = 1/127.944, \quad (6.19)$$

$$\alpha_s^{\text{SM}(5),\overline{\text{MS}}}(m_Z^{\text{pole}}) = 0.1185. \quad (6.20)$$

From $\alpha_{\text{e.m.}}(m_Z^{\text{pole}})$ and $\alpha_s(m_Z^{\text{pole}})$ in the $\overline{\text{DR}}$ scheme the electromagnetic and strong coupling constants are then calculated as

$$e(m_Z^{\text{pole}}) = \sqrt{4\pi\alpha_{\text{e.m.}}(m_Z^{\text{pole}})}, \quad (6.21)$$

$$g_3(m_Z^{\text{pole}}) = \sqrt{4\pi\alpha_s(m_Z^{\text{pole}})}. \quad (6.22)$$

To obtain the gauge couplings g_1 and g_2 , the $\overline{\text{DR}}$ Weinberg angle θ_W is calculated in the given SUSY model from the corresponding expression set in `DependenceNum` in the SARAH model file. In the MSSM it is given by

$$\theta_W(m_Z^{\text{pole}}) = \arcsin \sqrt{1 - \left(\frac{m_W(m_Z^{\text{pole}})}{m_Z(m_Z^{\text{pole}})} \right)^2}, \quad (6.23)$$

while in a model with a Higgs triplet the relation has the form

$$\theta_W(m_Z^{\text{pole}}) = \arcsin \sqrt{1 - \frac{m_W^2(m_Z^{\text{pole}}) - g_2^2 v_T^2}{m_Z^2(m_Z^{\text{pole}})}}. \quad (6.24)$$

At run-time, the $\overline{\text{DR}}$ W and Z boson masses m_W and m_Z , appearing in (6.23)–(6.24), are calculated from the corresponding pole masses as

$$m_W^2(m_Z^{\text{pole}}) = (m_W^{\text{pole}})^2 + \Re \Pi_{WW}^T(p^2 = (m_W^{\text{pole}})^2, \mu = m_Z^{\text{pole}}), \quad (6.25)$$

$$m_Z^2(m_Z^{\text{pole}}) = (m_Z^{\text{pole}})^2 + \Re \Pi_{ZZ}^T(p^2 = (m_Z^{\text{pole}})^2, \mu = m_Z^{\text{pole}}). \quad (6.26)$$

For the pole masses, FlexibleSUSY uses $m_W^{\text{pole}} = 80.404$ GeV and $m_Z^{\text{pole}} = 91.1876$ GeV [11]. Finally, the expressions for the $U(1)_Y$ and $SU(2)_L$ gauge couplings g_1 and g_2 in terms of θ_W are used to calculate $g_1(m_Z^{\text{pole}})$ and $g_2(m_Z^{\text{pole}})$. In the MSSM, for example, one has

$$g_1(m_Z^{\text{pole}}) = N_{\text{GUT}} \frac{e(m_Z^{\text{pole}})}{\cos \theta_W(m_Z^{\text{pole}})}, \quad (6.27)$$

$$g_2(m_Z^{\text{pole}}) = \frac{e(m_Z^{\text{pole}})}{\sin \theta_W(m_Z^{\text{pole}})}, \quad (6.28)$$

where the GUT normalization prefactor for g_1 has the value $N_{\text{GUT}} = \sqrt{5/3}$.

Calculation of the Yukawa couplings at the low-scale

In case the user has chosen to let FlexibleSUSY calculate the $\overline{\text{DR}}$ Yukawa couplings y_u, y_d, y_e automatically, they are determined from the known Standard Model fermion masses [11] as follows: At first, the mass matrices of the up- and down-type fermions u_i, d_i, e_i ($i = 1, 2, 3$) are calculated with the help of SARAH's `MassMatrix[]` function. Thereby it is assumed that these matrices are expressed in terms the Yukawa couplings. FlexibleSUSY then tries to invert these expressions to obtain the Yukawa coupling matrices in terms of the fermion mass matrices. In the MSSM, for example, the result is in the SLHA convention

$$y_u(m_Z^{\text{pole}}) = \frac{\sqrt{2} m_u^T}{v_u}, \quad y_d(m_Z^{\text{pole}}) = \frac{\sqrt{2} m_d^T}{v_d}, \quad y_e(m_Z^{\text{pole}}) = \frac{\sqrt{2} m_e^T}{v_d}. \quad (6.29)$$

In FlexibleSUSY version 1.0.0, flavour mixing is neglected, which leads to diagonal mass matrices $(m_f)_{ij} = m_{f_i} \delta_{ij}$ ($f = u, d, e$). At the Z mass scale these fermion mass matrices are composed as

$$m_u = \text{diag}(m_u, m_c, m_t(m_Z^{\text{pole}})), \quad (6.30a)$$

$$m_d = \text{diag}(m_d, m_s, m_b(m_Z^{\text{pole}})), \quad (6.30b)$$

$$m_e = \text{diag}(m_e, m_\mu, m_\tau(m_Z^{\text{pole}})), \quad (6.30c)$$

where the masses of the first two generations are directly read from the `SMINPUTS` block of the SLHA input file [176]. The 3rd generation quark masses m_t , m_b and m_τ are calculated in the $\overline{\text{DR}}$ scheme from the SLHA user input quantities m_t^{pole} , $m_b^{\text{SM},\overline{\text{MS}}}(m_Z^{\text{pole}})$, $m_\tau^{\text{SM},\overline{\text{MS}}}(m_Z^{\text{pole}})$. The calculation of the top quark $\overline{\text{DR}}$ mass reads

$$m_t(\mu) = m_t^{\text{pole}} + \Re \Sigma_t^S(m_t^{\text{pole}}) + m_t^{\text{pole}} \left[\Re \Sigma_t^L(m_t^{\text{pole}}) + \Re \Sigma_t^R(m_t^{\text{pole}}) + \Delta m_t^{(1),\text{qcd}} + \Delta m_t^{(2),\text{qcd}} \right]. \quad (6.31)$$

Here $\Sigma_f^{L,R}$ denote the left- and right-handed part of the self-energy of fermion f , and Σ_f^S is the unpolarized part. In Eq. (6.31) QCD corrections are omitted from the self-energies. The separated one- and two-loop QCD corrections $\Delta m_t^{(1),\text{qcd}}$ and $\Delta m_t^{(2),\text{qcd}}$ have the form [185]

$$\Delta m_t^{(1),\text{qcd}} = -\frac{g_3^2}{12\pi^2} \left[5 - 3 \log \left(\frac{m_t^2}{\mu^2} \right) \right], \quad (6.32)$$

$$\Delta m_t^{(2),\text{qcd}} = \left(\Delta m_t^{(1),\text{qcd}} \right)^2 - \frac{g_3^4}{4608\pi^4} \left[396 \log^2 \left(\frac{m_t^2}{\mu^2} \right) - 1476 \log \left(\frac{m_t^2}{\mu^2} \right) - 48\zeta(3) + 2011 + 16\pi^2(1 + \log 4) \right]. \quad (6.33)$$

The $\overline{\text{DR}}$ mass of the bottom quark is calculated from the known Standard Model $\overline{\text{MS}}$ mass as [58, 176]

$$m_b(\mu) = \frac{m_b^{\text{SM},\overline{\text{DR}}}(\mu)}{1 - \Delta m_b(m_b^{\text{SM},\overline{\text{MS}}})}, \quad (6.34)$$

$$\Delta m_b(\mu) = \Re \Sigma_b^{S,\text{heavy}}(\mu)/m_b + \Re \Sigma_b^{L,\text{heavy}}(\mu) + \Re \Sigma_b^{R,\text{heavy}}(\mu), \quad (6.35)$$

$$m_b^{\text{SM},\overline{\text{DR}}}(\mu) = m_b^{\text{SM},\overline{\text{MS}}}(\mu) \left(1 - \frac{\alpha_s}{3\pi} - \frac{23}{72} \frac{\alpha_s^2}{\pi^2} + \frac{3g_2^2}{128\pi^2} + \frac{13g_Y^2}{1152\pi^2} \right). \quad (6.36)$$

Note that Eq. (6.34) resums $\tan \beta$ -enhanced loop corrections. Finally, the τ $\overline{\text{DR}}$ mass is calculated as

$$m_{\tau,\text{susy}}^{\overline{\text{DR}}}(\mu) = m_{\tau,\text{SM}}^{\overline{\text{DR}}}(\mu) + \Re \Sigma_\tau^{S,\text{heavy}}(m_{\tau,\text{SM}}^{\overline{\text{MS}}}) + m_{\tau,\text{SM}}^{\overline{\text{DR}}}(\mu) \left[\Re \Sigma_\tau^{L,\text{heavy}}(m_{\tau,\text{SM}}^{\overline{\text{MS}}}) + \Re \Sigma_\tau^{R,\text{heavy}}(m_{\tau,\text{SM}}^{\overline{\text{MS}}}) \right], \quad (6.37)$$

$$m_{\tau,\text{SM}}^{\overline{\text{DR}}}(\mu) = m_\tau^{\text{SM},\overline{\text{MS}}}(\mu) \left(1 - 3 \frac{g_Y^2 - g_2^2}{128\pi^2} \right). \quad (6.38)$$

In the equations above, the QCD and photon contributions to the bottom and τ self-energies are omitted, which is indicated by the “heavy” keyword. For the conversion of the fermion masses from the $\overline{\text{MS}}$ to the $\overline{\text{DR}}$ scheme the Yukawa coupling conversion given in [134] is used and it is assumed that the VEV is defined in the $\overline{\text{DR}}$ scheme.

6.3.4 Solving the boundary value problem

In the previous sections it was described how the user can specify a SUSY model and supply boundary conditions (constraints) for the model parameters at three different renormalization scales. From this information the Mathematica meta code creates a model class hierarchy and three constraint classes. After these have been created, the actual spectrum generator is set up, which combines the classes to solve the boundary value problem. This combined setup is shown in source code listing 6.2.

Source code listing 6.2: Combining all spectrum generator components: model class, constraints and boundary condition solver

```

<model> model;
<model>_input_parameters input;

std::vector<Constraint*> constraints = {
    new <model>_high_scale_constraint(input),
    new <model>_susy_scale_constraint(input),
    new <model>_low_scale_constraint(input)
};

RGFlow solver;
solver.add_model(&model, constraints);
solver.solve();

model.calculate_spectrum();

```

At first, an instance of the model class `<model>` and the input parameters structure is created. Afterwards, a vector of pointers to `Constraint` classes is defined and filled with the three user-supplied boundary conditions. Then, the boundary value problem solver `RGFlow` is created and the model and the constraints are registered via a call to `add_model()`. When the `solve()` method is called, the solver tries to find a solution to the given boundary value problem by iteratively running between the three scales and imposing the boundary conditions (by calling the `apply()` function of each constraint). If a solution was found, the `solve()` routine returns and the `calculate_spectrum()` function is called, which calculates the pole mass spectrum.

The general algorithm hidden in the `solve()` function was described in Section 6.3.2, Algorithm 6.1. For the concrete CMSSM example, given in source code listing 6.1, it proceeds as follows (see Figure 6.4):

Initial guess of the model parameters:

1. Set initial scale to m_t^{pole} .
2. Calculate the Standard Model gauge couplings $g_i^{\text{SM}}(m_t^{\text{pole}})$ in the $\overline{\text{MS}}$ scheme from the known values $g_1^{\text{SM}}(m_Z^{\text{pole}})$, $g_2^{\text{SM}}(m_Z^{\text{pole}})$, $g_3^{\text{SM}}(m_t^{\text{pole}})$ [11]. Set MSSM gauge couplings g_i to the Standard Model ones

$$g_i(m_t^{\text{pole}}) = g_i^{\text{SM}}(m_t^{\text{pole}}) \quad (i = 1, 2, 3). \quad (6.39)$$

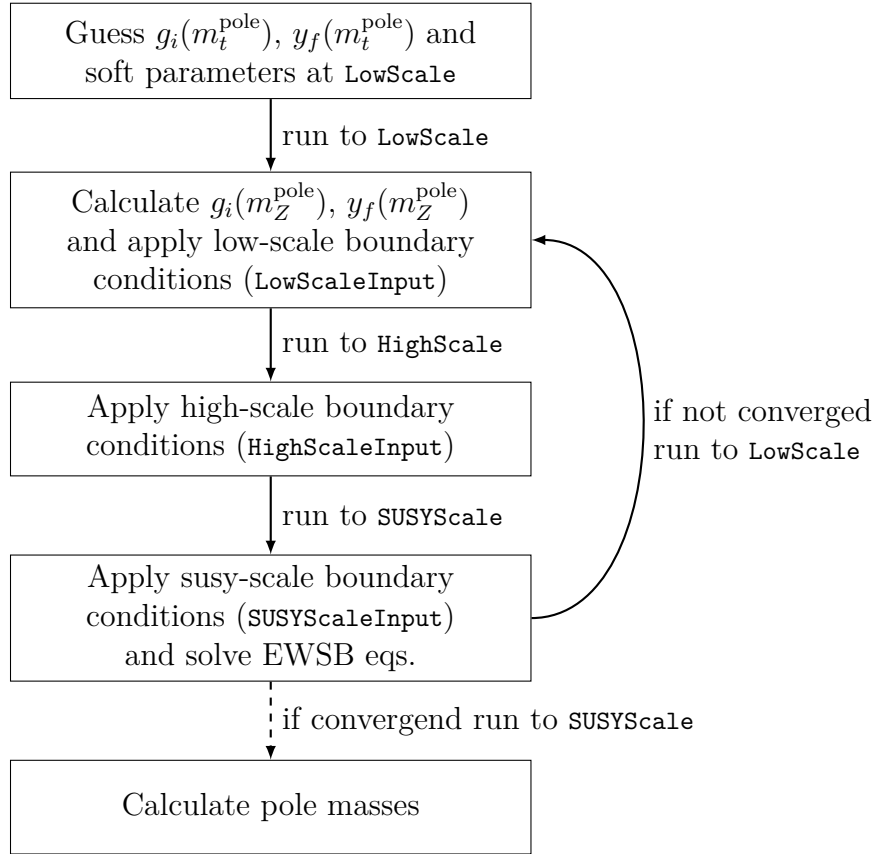


Figure 6.4: Iterative two-scale algorithm to calculate the spectrum.

3. Impose user-defined low-scale constraint (`LowScaleInput`):

$$v_1 = \frac{v}{\sqrt{1 + \tan^2 \beta}}, \quad v_2 = \frac{v \tan \beta}{\sqrt{1 + \tan^2 \beta}}. \quad (6.40)$$

Here $\tan \beta$ is an input parameter, defined in the $\overline{\text{DR}}$ scheme, and is read from the SLHA input file. The appearing Standard Model VEV v is set to 246.22 GeV. Afterwards, the Yukawa couplings are guessed automatically from the running Standard Model fermion masses [11] as

$$y_u(m_Z^{\text{pole}}) = \frac{\sqrt{2}}{v_2} \text{diag}(2.4 \cdot 10^{-3}, 1.27, 165.0) \text{ GeV}, \quad (6.41)$$

$$y_d(m_Z^{\text{pole}}) = \frac{\sqrt{2}}{v_1} \text{diag}(4.75 \cdot 10^{-3}, 0.104, 4.2) \text{ GeV}, \quad (6.42)$$

$$y_e(m_Z^{\text{pole}}) = \frac{\sqrt{2}}{v_1} \text{diag}(5.10998902 \cdot 10^{-4}, 0.105658357, 1.77699) \text{ GeV}. \quad (6.43)$$

4. Run the SUSY parameters to the high-scale guess $M_X = 2 \cdot 10^{16}$ GeV (`HighScaleFirstGuess`).

5. Impose the mSUGRA high-scale constraint on the soft-breaking MSSM parameters (`HighScaleInput`):

$$A_{ij}^f(M_X) = A_0 \quad (f = u, d, e; i, j = 1, 2, 3), \quad (6.44a)$$

$$m_{h_i}^2(M_X) = m_0^2 \quad (i = 1, 2), \quad (6.44b)$$

$$m_f^2(M_X) = m_0^2 \mathbf{1} \quad (f = q, \ell, d, u, e), \quad (6.44c)$$

$$M_i(M_X) = M_{1/2} \quad (i = 1, 2, 3), \quad (6.44d)$$

where A_0 , m_0 and $M_{1/2}$ are the universal soft-breaking input parameters, read from the SLHA input file. The soft-breaking scalar squared mass terms of the MSSM are denoted in (6.44) as $m_{h_i}^2$ and m_f^2 . The M_i are the gaugino masses and A_{ij}^f are the soft-breaking trilinear scalar couplings. Afterwards, the initial guess of the remaining model parameters (defined in `InitialGuessAtHighScale`) is imposed:

$$\mu(M_X) = 1, \quad B\mu(M_X) = 0. \quad (6.45)$$

6. Run all model parameters to the low-energy scale m_Z^{pole} (`LowScaleFirstGuess`).
7. Solve the EWSB conditions (6.5) at the tree-level by choosing $\mu(m_Z^{\text{pole}})$ and $B\mu(m_Z^{\text{pole}})$ suitably.
8. Calculate the $\overline{\text{DR}}$ mass spectrum.

At this point all model parameters are initialized and the actual fixed-point iteration can be started.

Fixed-point iteration:

1. Run all model parameters to the low-energy scale m_Z^{pole} (`LowScale`).
- a) Calculate the $\overline{\text{DR}}$ mass spectrum.
- b) Calculate the $\overline{\text{DR}}$ gauge couplings $g_i(m_Z^{\text{pole}})$ ($i = 1, 2, 3$) from the known Standard Model values $\alpha_{\text{e.m.}}(m_Z^{\text{pole}})$, $\alpha_s(m_Z^{\text{pole}})$, m_W^{pole} and m_Z^{pole} including threshold corrections, as described in Section 6.3.3.
- c) Impose the user-defined low-scale constraint (`LowScaleInput`): (i) Calculate the Yukawa couplings $y_f(m_Z^{\text{pole}})$ ($f = u, d, e$) as described in Section 6.3.3 and (ii) calculate the VEVs as

$$v_1(m_Z^{\text{pole}}) = \frac{2m_Z(m_Z^{\text{pole}}) \cos \beta}{\sqrt{3g_1^2/5 + g_2^2}}, \quad (6.46a)$$

$$v_2(m_Z^{\text{pole}}) = \frac{2m_Z(m_Z^{\text{pole}}) \sin \beta}{\sqrt{3g_1^2/5 + g_2^2}}. \quad (6.46b)$$

Here $m_Z(m_Z^{\text{pole}})$ is the $\overline{\text{DR}}$ mass of the Z boson at the scale m_Z^{pole} , which is re-calculated in each iteration as shown in Eq. (6.26). In Eqs. (6.46) $\cos\beta$ and $\sin\beta$ are obtained from $\tan\beta$ in the $\overline{\text{DR}}$ scheme. As a result, the calculated VEVs v_i are defined in the $\overline{\text{DR}}$ scheme.

2. Run parameters to the GUT scale M_X (`HighScale`).
 - a) Calculate the gauge coupling β -functions β_{g_1} and β_{g_2} up to the two-loop level and re-calculate the scale as

$$M'_X = M_X \exp\left(\frac{g_2(M_X) - g_1(M_X)}{\beta_{g_1} - \beta_{g_2}}\right). \quad (6.47)$$

The scale M'_X is used as new GUT scale in the next iteration.

- b) Impose the mSUGRA high-scale constraint (`HighScaleInput`) from Eqs. (6.44).
3. Run all model parameters to the SUSY scale M_S (`SUSYScale`).
 - a) Calculate the $\overline{\text{DR}}$ mass spectrum.
 - b) Re-calculate the SUSY scale as

$$M_S = \sqrt{m_{\tilde{u}_1} m_{\tilde{u}_6}}, \quad (6.48)$$

where $m_{\tilde{u}_1}$ and $m_{\tilde{u}_6}$ are the $\overline{\text{DR}}$ masses of the lightest and heaviest up-type squark, respectively. Note that this is a non-standard definition, which is used here due to the allowed squark flavour mixing. However, since the pole masses are renormalization scale independent quantities, their dependence on the definition of M_S is of two-loop order or higher.

- c) Solve the EWSB conditions (6.6) at the loop level by varying $\mu(M_S)$ and $B\mu(M_S)$. In the here discussed CMSSM model file `UseHiggs2LoopMSSM` is set to `True`, which triggers the inclusion of leading two-loop tadpole contributions of the order $O(y_t^4 + y_t^2 y_b^2 + y_b^4 + y_t^2 g_3^2 + y_b^2 g_3^2)$ [165, 166].
4. If the relative deviation between the SUSY particle $\overline{\text{DR}}$ masses of the current and the previous iteration is larger than the accuracy goal (set in the SLHA input file), and the maximum number of iterations is not yet reached, then go to step 1. Otherwise, stop the iteration.

If the iteration has converged, all model parameters are consistent with the EWSB conditions, low-energy data and the user-supplied mSUGRA boundary conditions at any scale between m_Z^{pole} and M_X . In this case FlexibleSUSY runs all model parameters to the SUSY scale and calculates the pole mass spectrum by calling the `calculate_spectrum()` function, see the next section.

Note that the above described algorithm is exactly the procedure described in [163] for the CMSSM. The special feature of FlexibleSUSY is that the C++ classes, used in the above algorithm, are generated automatically from a user-supplied model file.

This allows an immediate application of the algorithm to other, non-minimal models. Furthermore, FlexibleSUSY's boundary value problem solver `RGFlow` is generalized to handle a tower of effective theories with an arbitrary number of constraints as described in Section 6.3.2.

6.3.5 Calculation of the pole masses

In the previous sections it was described how the user can set up a SUSY model and define boundary conditions for the model parameters at the meta code level. From this information C++ code is generated and a boundary value problem solver is used to find a set of model parameters consistent with the so-defined constraints. The final step is to calculate the pole mass spectrum and the corresponding mixing matrices. This is done in the `calculate_spectrum()` function and is described in the following.

As explained in Section 5.4.4 the (physical) pole mass is defined to be the momentum for which the full propagator of the field under consideration has a singularity. For general case of particle multiplets it means to find values p_i for which the Eqs. (5.38) are fulfilled. This can be achieved by diagonalizing the full loop-corrected mass matrix

$$M_{f,\text{full}}(p_i^2) = M_f - M_{f,1L}(p_i^2) \quad i = 1, \dots, N, \quad (6.49)$$

where M_f is the tree-level $\overline{\text{DR}}$ mass matrix of field f and $M_{f,1L}(p_i^2)$ contains self-energy loop corrections. However, since the loop corrections are by themselves momentum dependent an iteration over the p_i must be performed, where the mass eigenvalues of the previous iteration are used as momenta to calculate the loop corrections. If this iterative procedure converges, the eigenvalues of the full loop-corrected mass matrix are the pole masses.

However, this iterative procedure can be very time-consuming, because it must be performed for each field in the multiplet, i.e. N times. In case of N_{it} iterations, the loop correction matrix must be calculated $N_{\text{it}}N$ times. Each matrix entry again involves the calculation of a self-energy, which requires the evaluation of $O(50)$ Feynman diagrams with complicated vertices and loop functions. All together, to calculate the pole masses of a particle multiplet $N_{\text{it}}N^3$ self-energies need to be calculated.

For this reason FlexibleSUSY provides two alternative pole mass calculation algorithms with a lower precision but a shorter run-time. The algorithm to be used can be selected in the model file `<model>/FlexibleSUSY.m` for each particle multiplet. They work as follows:

- **LowPoleMassPrecision:** This algorithm has the lowest precision, but also the shortest run-time. Here the full mass matrix $M_{f,\text{full}}^{\text{low}}$ is calculated exactly once as

$$\forall i, j : (M_{f,\text{full}}^{\text{low}})_{ij} = (M_{f,\text{full}}(p^2 = m_{f_i}m_{f_j}))_{ij}, \quad (6.50)$$

where m_{f_i} is the i th $\overline{\text{DR}}$ mass eigenvalue of the tree-level mass matrix M_f . The

matrix $M_{f,\text{full}}^{\text{low}}$ is diagonalized and the eigenvalues are interpreted as pole masses $m_{f_i}^{\text{pole}}$. Thereby two-loop terms of the form

$$\left[(m_{f_k}^{\text{pole}})^2 - m_{f_i} m_{f_j} \right] \frac{\partial M_{f,1L}(p^2)}{\partial p^2} \Big|_{p^2=m_{f_i} m_{f_j}} \quad (6.51)$$

are neglected. This approximation leads to significant deviations from the true pole masses if the $\overline{\text{DR}}$ mass spectrum of the multiplet is very split or the loop corrections are very large. With this method the self-energy of field f needs to be calculated only N^2 times.

- **MediumPoleMassPrecision** (default): This algorithm calculates the pole masses with medium precision and has a medium execution time. Here the full mass matrix $M_{f,\text{full}}^{\text{medium}}$ is calculated N times as

$$(M_{f,\text{full}}^{\text{medium}})^{(k)}_{ij} = (M_{f,\text{full}}(p^2 = m_{f_k}^2))_{ij}, \quad k = 1, \dots, N, \quad (6.52)$$

where m_{f_k} is the k th $\overline{\text{DR}}$ mass eigenvalue of the tree-level mass matrix M_f . Afterwards, each mass matrix $(M_{f,\text{full}}^{\text{medium}})^{(k)}$ is diagonalized and its k th eigenvalue is interpreted as pole mass $m_{f_k}^{\text{pole}}$. Thereby for the k th eigenvalue two-loop terms of the form

$$\left[(m_{f_k}^{\text{pole}})^2 - m_{f_k}^2 \right] \frac{\partial M_{f,1L}(p^2)}{\partial p^2} \Big|_{p^2=m_{f_k}^2} \quad (6.53)$$

are neglected. This approximation leads to significant deviations from the true pole masses if the loop corrections are large. Note that this algorithm is used in Softsusy to calculate the pole masses of the non-Higgs fields, see Section 5.4.4. For this method the self-energy of field f needs to be calculated N^3 times.

Besides these two approximations, FlexibleSUSY also provides the precise calculation of the spectrum via iterations over the momenta p_i . This algorithm is selected by choosing **HighPoleMassPrecision**. Here the full mass matrix $M_{f,\text{full}}^{\text{high}}$ is diagonalized N times, as in the case of **MediumPoleMassPrecision**, resulting in N pole masses $m_{f_k}^{\text{pole}}$ ($k = 1, \dots, N$). Afterwards, the diagonalization is repeated, this time using the calculated pole masses $m_{f_k}^{\text{pole}}$ for the momentum calculation $p^2 = (m_{f_k}^{\text{pole}})^2$. This iteration stops if convergence is reached.

6.3.6 Summary

To calculate the pole mass spectrum of a general SUSY model several non-trivial tasks have to be performed: First, the model must be defined and the β -functions, mass matrices, self-energies and tadpole diagrams must be calculated. In addition the model must be matched to the Standard Model and electroweak symmetry breaking

must be ensured. Further user-defined boundary conditions might be imposed at the GUT or weak scales.

In the previous sections it was shown that FlexibleSUSY can create a complete, modular C++ spectrum generator automatically, given a SARAH and FlexibleSUSY model file. Depending on the user's choice it includes boundary conditions for the matching to the Standard Model and the electroweak symmetry breaking as well as high-scale conditions for GUT models. A generalized boundary condition solver is provided, which tries to find a set of model parameters consistent with all given constraints, even supporting towers of effective theories. Finally, the pole mass spectrum can be calculated using the full one-loop self-energies of all particles. In addition leading two-loop Higgs mass corrections can be added automatically for MSSM- and NMSSM-like models. Thereby FlexibleSUSY represents a powerful tool to study a large variety of non-minimal SUSY models with high precision and great flexibility.

6.4 Applications

6.4.1 Run-time comparison

One of the design goals of FlexibleSUSY is a short run-time. In this section the run-time of two FlexibleSUSY-generated CMSSM spectrum generators (a flavour-violating and a non-flavour-violating variant) are compared to the hand-written spectrum generators Softsusy [60], SPheno [147, 148] and to SARAH’s automatically generated SPhenoMSSM [137, 146].

From studying and profiling the source code of Softsusy and SPheno, two major speed bottlenecks can be identified:

1. *Calculation of the β -functions:* The dominant part (approximately 60% or more) of the run-time is used for the calculation of two-loop β -functions. The reason is the complicated structure, which involves $O(500)$ additions of products of up to five $(3, 3)$ -matrices. For an average CMSSM parameter point with a mass precision goal of 0.01% the β -functions have to be calculated $O(500)$ times during the full fixed-point iteration.
2. *Calculation of the pole masses:* The second most time-consuming part (approximately 20–30%) is the calculation of the pole masses and especially the self-energies. The reason is that the self-energy matrices have to be calculated multiple times, where each matrix entry involves the evaluation of Passarino-Veltman loop functions and complicated vertices (especially the scalar four-point vertices).

FlexibleSUSY uses the following two techniques to address these two bottlenecks:

1. *Fast linear algebra via Eigen:* FlexibleSUSY expresses the β -functions in terms of the fixed-size `Matrix` class provided by the linear algebra package Eigen [174]. Eigen exploits C++ expression templates to remove temporary objects and enable lazy evaluation. It supports explicit vectorization and avoids dynamic memory allocation. These features in combination allow the compiler to generate very fast code for the calculation of the β -functions.
2. *Multi-threading:* The optimization of the pole mass calculation is difficult. However, modern CPUs provide multiple cores, which can be used to parallelize certain calculations. By default FlexibleSUSY calculates each pole mass in a separate thread, allowing the operating system to distribute these calculations among several cores. The overhead of creating and joining these threads is negligible compared to the time needed to calculate a single pole mass.

In the following, the run-times of two sets of CMSSM spectrum generators are compared:

- FlexibleSUSY-NoFV (version 1.0.0), Softsusy (version 3.4.0) and SPheno (version 3.2.4). All of these spectrum generators disable flavour violation.

- FlexibleSUSY-FV (version 1.0.0) and SPhenoMSSM (generated with SARAH 4.1.0 and linked against SPheno 3.2.4), which are both based on SARAH's MSSM model file. FlexibleSUSY-FV uses the configuration file given in source code listing 6.1. These two automatically generated spectrum generators both allow flavour violation and are therefore a bit slower than the ones above.

The source codes of FlexibleSUSY and Softsusy are compiled with g++ 4.8.0 and Intel ifort 13.1.3 20130607. SPheno and SPhenoMSSM are compiled with Intel ifort 13.1.3 20130607 only.¹³ For the comparison $2 \cdot 10^4$ random CMSSM parameter points are generated, with $m_0 \in [50, 1000]$ GeV, $M_{1/2} \in [50, 1000]$ GeV, $\tan \beta \in [1, 100]$, $\text{sign } \mu \in \{-1, +1\}$ and $A_0 \in [-1000, 1000]$ GeV. For every point a MINPAR block in SLHA format is created and appended to the SLHA input template file listed in Appendix E. The resulting SLHA file is passed to each spectrum generator and the (wall-clock) time is measured until the program stops. To measure the influence of the number of cores, the study is done on three different architectures: (i) On an Intel Core2 Duo (P8600) where only one core is enabled, (ii) on an Intel Core2 Duo (P8600) where two cores are enabled and (iii) on a machine with two Intel Xeon CPUs (L5640) with six physical cores each. The run-time distributions for the three architecture types can be found in Figure 6.5. In Table 6.1 the average run-times are listed.

	Intel Core2 Duo (P8600, 1 core, 2.40 GHz)	Intel Core2 Duo (P8600, 2 cores, 2.40 GHz)	2 × Intel Xeon (L5640, 6 cores 2.27 GHz)
FlexibleSUSY-NoFV 1.0.0	0.086 s	0.079 s	0.060 s
SPheno 3.2.4	0.119 s	0.114 s	0.101 s
Softsusy 3.4.0	0.175 s	0.171 s	0.147 s
FlexibleSUSY-FV 1.0.0	0.150 s	0.113 s	0.074 s
SPhenoMSSM 4.1.0	0.415 s	0.401 s	0.370 s

Table 6.1: Average CMSSM spectrum generator run-time (in seconds) for random parameter points. The first three rows list spectrum generators which do not allow flavour violation. The 4th and 5th row show automatically generated spectrum generators which allow flavour violation.

One finds that under both the non-flavour violating spectrum generators (rows 1–3 in Table 6.1), as well as under the flavour violating ones (4th and 5th row), FlexibleSUSY is significantly fastest. Compared to SPheno, FlexibleSUSY-NoFV is a factor 1.4–1.7 faster, and compared to Softsusy around a factor 2–2.5. Compared to the automatically generated spectrum generator SPhenoMSSM, FlexibleSUSY-FV is faster by a factor 2.8–5. One of the main reasons for the long run-time of SPhenoMSSM is the long calculation time of the β -functions, as can be seen from

¹³Intel's ifort compiler is used, because it decreases the run-time of SPheno and SPhenoMSSM by approximately a factor 1.5, compared to gfortran 4.8.0.

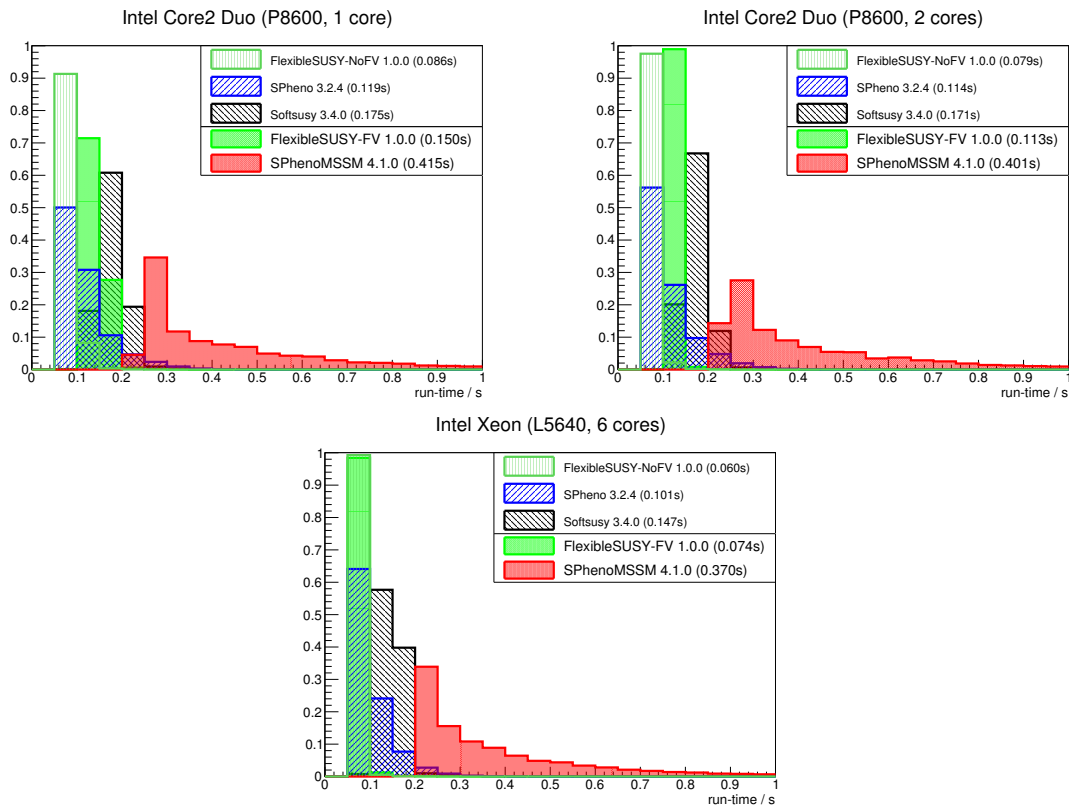


Figure 6.5: Run-time distributions of different CMSSM spectrum generators for random parameter points on different architectures. The top row shows the run-time on an Intel Core2 Duo (P8600) with one (left panel) and two (right panel) cores enabled. In the plot at the bottom a machine with two Intel Xeon CPUs (L5640) with six physical cores each is used. For each spectrum generator the average run-time is given in brackets.

the long tail in the distributions in Figure 6.1. At this point FlexibleSUSY benefits a lot from Eigen’s well-optimizable matrix expressions, resulting in sharp peaks in the run-time distributions. One also finds that increasing the number of CPU cores decreases FlexibleSUSY’s run-time. The reason is that each pole mass is calculated in a separate thread, which lets FlexibleSUSY benefit from multi-core CPUs.

6.4.2 Comparison of Higgs masses in supersymmetric models

As a small application of FlexibleSUSY’s ability to create spectrum generators for user-defined SUSY models, parameter scans in four different constrained models are presented. The considered models are the CMSSM, the NMSSM, the USSM and the E_6 SSM. Studying these models successively is particularly interesting, because each model adds additional particles or symmetries to the predecessor: The NMSSM adds a singlet field, the USSM adds another $U(1)'$ gauge symmetry and the E_6 SSM adds further matter fields to complete the $(\mathbf{27})_i$ representations. All of these models use a mSUGRA-inspired soft supersymmetry breaking scenario at the GUT scale M_X with

the universal soft-breaking sfermion mass m_0 , a universal gaugino mass $M_{1/2}$ and a universal trilinear scalar coupling A_0 . Furthermore, all contain a down-type and an up-type Higgs doublet with VEVs v_1 and v_2 , respectively. Since the combination $v = \sqrt{v_1^2 + v_2^2}$ is fixed by the measured Z mass, only the ratio of the Higgs VEVs $\tan\beta = v_2/v_1$ is a free parameter in all of these models.

In the following the lightest CP-even Higgs pole mass is studied in these four models as a function of $\tan\beta$ and m_0 in the range $\tan\beta = 1 \dots 50$ and $m_0 = 0 \dots 10$ TeV. All other common parameters are set to $M_{1/2} = A_0 = 5$ TeV. The thereby studied parameter region yields heavy spectra with SUSY masses of the order $O(1$ TeV). Depending on the model, the lightest CP-even Higgs boson pole mass varies between 93 and 135 GeV in these regions. For a precise Higgs mass prediction, the leading two-loop Higgs self-energy and tadpole corrections described in Section 6.3.3 are enabled in each model.

CMSSM

For the parameter scan in the CMSSM, the model file from Section 6.3.3 is used. It defines the mSUGRA constraint (2.3) at the GUT scale, which leaves the 5 free input parameters m_0 , $M_{1/2}$, A_0 , $\tan\beta(m_Z^{\text{pole}})$ and $\text{sign}\mu$. The parameters $|\mu(M_S)|$, $B\mu(M_S)$ are chosen to be output of the EWSB conditions at the SUSY scale. The lightest CP-even Higgs pole mass as a function of the scanned parameters m_0 and $\tan\beta$ is shown in Figure 6.6.

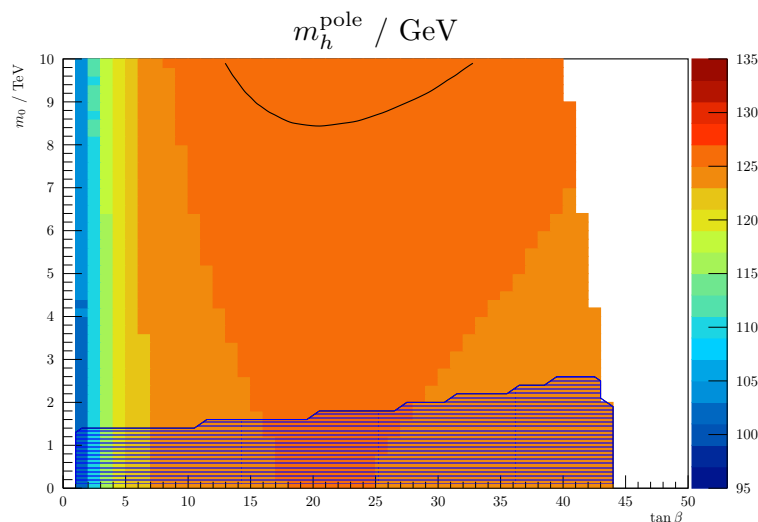


Figure 6.6: Lightest CP-even Higgs pole mass in the CMSSM as a function of m_0 and $\tan\beta$. The parameter point uses $M_{1/2} = A_0 = 5$ TeV and $\text{sign}\mu = +1$. The measured value of $m_h^{\text{pole}} = 125.9$ GeV can be found on the black contour line. In the shaded area the LSP is a charged particle.

Only in the region $\tan\beta = 1 \dots 44$ GeV physical solutions to all the boundary conditions can be found. For $\tan\beta \gtrsim 44$ the CP-odd and charged Higgs bosons

become tachyonic. As can be seen from Eq. (2.6) increasing $\tan\beta$ and keeping m_0 fixed increases the tree-level mass contribution, which is approximately given by $m_Z c_{2\beta}$. The slope of $c_{2\beta}$ as a function of $\tan\beta$ is very steep in the range $1 \dots 5$, thereby leading to a rapidly increasing Higgs mass. However, increasing $\tan\beta$ also decreases the top Yukawa coupling, given by $y_t = \sqrt{2}m_t/v_2$. This leads to decreasing Higgs self-energy loop corrections and therefore to a slowly decreasing Higgs pole mass for $\tan\beta \gtrsim 25$. For constant $\tan\beta$ increasing m_0 raises the stop masses, which leads to larger self-energy loop corrections and therefore to a large Higgs mass.

Large CP-even Higgs masses of the order 126 GeV are achieved in regions with large $m_0 \sim 8 \dots 10$ TeV and $\tan\beta \sim 10 \dots 35$. Small values of $\tan\beta \lesssim 3$ lead to very light Higgs masses of $m_h^{\text{pole}} \lesssim 110$ GeV. The measured value of $m_h^{\text{pole}} = 125.9$ GeV lies on the black contour line in the region with $m_0 > 8$ TeV. It is remarkable that even for $m_0 = 0$ parameter points with a large Higgs mass of up to 125 GeV can be found. The reason is the large value of $M_{1/2}$, which generates large gaugino masses at the GUT scale that significantly influence the RG running of the soft-breaking squared Higgs masses. However, such CMSSM parameter regions with $m_0 \lesssim 2$ TeV contain charged LSPs (usually the lightest down-type slepton) and are therefore ruled out. In Figure 6.6 these areas are shaded.

As conclusion, the measured value of the Higgs pole mass significantly constrains the allowed CMSSM parameter space. For the here studied region values of $m_0 > 8$ TeV and $\tan\beta$ between $10 \dots 35$ are preferred. The SUSY spectra in this region contain gluinos, neutralinos and charginos with masses in the range $3 \dots 10$ TeV and very heavy sfermions with masses of the order $7 \dots 12$ TeV. These points thereby suffer from a large splitting between the top and stop masses, which re-introduces the hierarchy problem as discussed in Section 2.1.2.

NMSSM

For the scan in the Z_3 -symmetric NMSSM the superpotential (5.2) is used, together with the mSUGRA boundary conditions from Eq. (5.10). This model has the five input parameters m_0 , $M_{1/2}$, A_0 , $\tan\beta(m_{\tilde{Z}}^{\text{pole}})$ and $\lambda(M_X)$ plus the sign of the VEV v_3 . As EWSB output the parameters $\kappa(M_S)$, $|v_3(M_S)|$, $m_s^2(M_S)$ are chosen. The lightest CP-even Higgs mass as a function of m_0 and $\tan\beta$ is shown in Figure 6.7 for two different values of $\lambda(M_X)$ and $A_0 = \pm 5$ TeV. The plots in the left column use $\lambda(M_X) = 0.1$, and in the right column $\lambda(M_X) = 0.2$. In the upper row, the universal trilinear coupling A_0 is set to 5 TeV, and in the lower row it is set to -5 TeV.

Similarly to the CMSSM, for fixed m_0 the Higgs mass shows a steep slope as a function of $\tan\beta$ for small values of $\tan\beta$. The reason is again the tree-level contribution of the form $m_Z c_{2\beta}$, which rises with $\tan\beta$. Furthermore, as shown in Eq. (2.8), in the NMSSM the Higgs mass gains an additional positive contribution at the tree-level from an F -term. This term is proportional to $s_{2\beta}$ and has therefore a strong influence for small $\tan\beta$. However, in Figure 6.7 one finds that for $A_0 = 5$ TeV (upper row) small values of $\tan\beta$ lead to CP-even Higgs tachyons, resulting in unphysical points. The situation is almost inverted for negative A_0 , where large values of $\tan\beta$ lead to tachyonic CP-even Higgs bosons. Furthermore, the overall Higgs mass found in

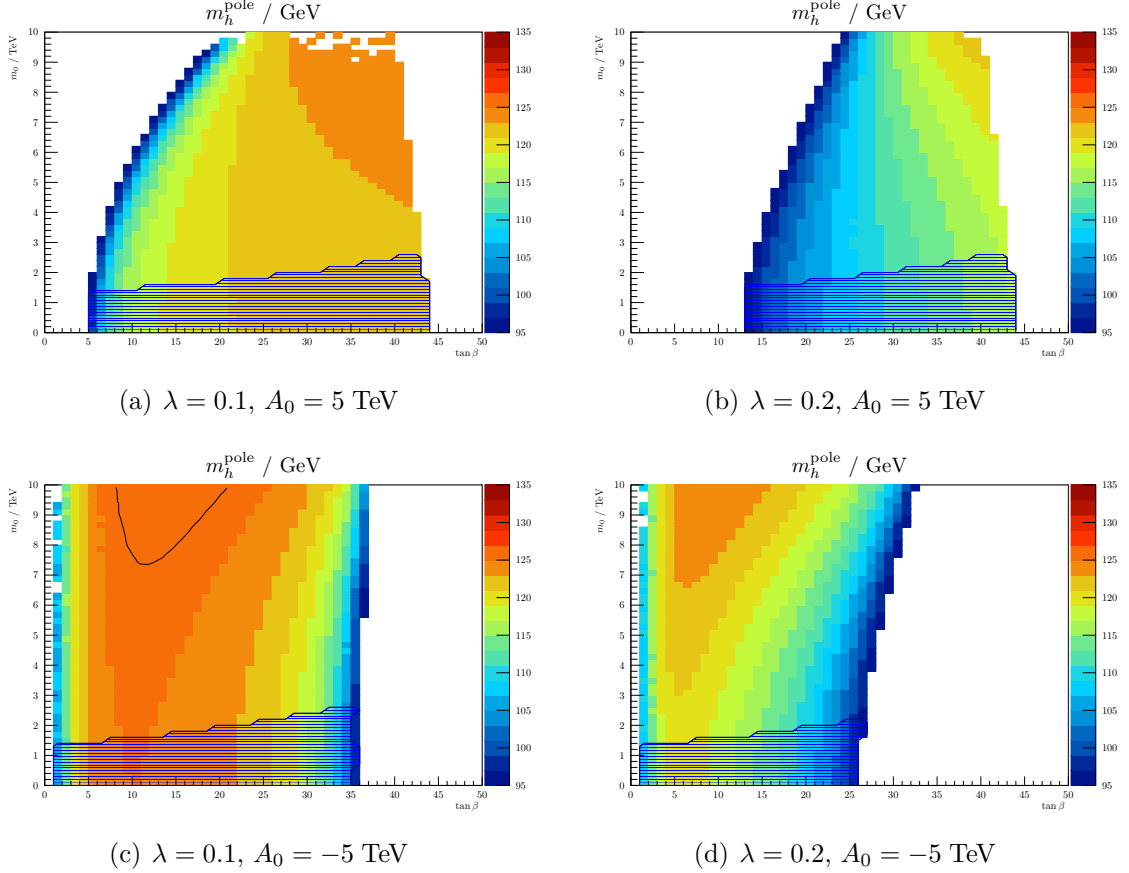


Figure 6.7: Lightest CP-even Higgs pole mass in the NMSSM as a function of m_0 and $\tan\beta$. The parameter point uses $M_{1/2} = \pm A_0 = 5 \text{ TeV}$ and $\text{sign } v_3 = +1$. The measured value of $m_h^{\text{pole}} = 125.9 \text{ GeV}$ can only be achieved for $\lambda(M_X) = 0.1$ and $A_0 = -5 \text{ TeV}$ and is drawn with a black contour line. In the shaded area the LSP is a charged particle.

the scanned parameter regions is rather small compared to the CMSSM. The reason for these phenomena is the mixing with the singlet field. Including this mixing, the lightest CP-even tree-level mass is approximately given by [186, 37]

$$(m_h^{\text{tree}})^2 \approx m_Z^2 c_{2\beta}^2 + \frac{\lambda^2 v^2}{2} s_{2\beta}^2 - \frac{\lambda^2 v^2}{2\kappa^2} \left[\lambda - s_{2\beta} \left(\kappa + \frac{A^\lambda}{\sqrt{2}v_3} \right) \right]^2. \quad (6.54)$$

The last term, which comes from the mixing with the singlet is a negative Higgs mass contribution proportional to $\lambda^2 v^2$, which can be more significant for larger λ (right column). This term is the major origin for the overall small NMSSM Higgs masses and the increased appearance of Higgs tachyons found in this parameter scan. It can in principle be minimized by adjusting A^λ accordingly. However, in the here studied NMSSM variant A^λ is fixed to A_0 at the GUT scale. Relaxing this constraint can lead to larger Higgs masses. Large Higgs masses with $m_h^{\text{pole}} \geq 125 \text{ GeV}$ are only achieved

for $\lambda(M_X) = 0.1$ and $A_0 = -5$ TeV. Parameter points which lead to the measured value of 125.9 GeV lie on the black contour line. Also in the NMSSM it is possible to achieve large Higgs masses of up to 125 GeV with $m_0 = 0$. However, such points are again ruled out due to charged LSPs and are marked by the shaded area.

Thus, the experimentally allowed parameter space of the here studied NMSSM is highly constrained by the measured value of the Higgs pole mass. In the studied region negative values of A_0 are preferred as they increase the stop mass splitting and reduce the singlet mixing, which in combination raises the lightest Higgs pole mass. A less constrained NMSSM variant, where A^λ is a free input parameter can lead to larger Higgs masses and would therefore be less sensitive to experimental constraints.

USSM

The third model considered here is the USSM [39, 40, 41], which extends the general NMSSM by an extra $U(1)'$ gauge symmetry. A discrete Z_3 symmetry, as introduced by hand in the NMSSM, is not imposed on the USSM superpotential. The $U(1)'$ charges of the superfields are chosen to be the same as the $U(1)_N$ charges in the E₆SSM, see Table C.1, including the GUT normalization $1/\sqrt{40}$. Due to the chosen $U(1)'$ charges the USSM superpotential is the same as the in the Z_3 -symmetric NMSSM and reads

$$\mathcal{W}_{\text{USSM}} = \lambda S(H_1 H_2) - y_{ij}^e(H_1 L_i)\bar{E}_j - y_{ij}^d(H_1 Q_i)\bar{D}_j - y_{ij}^u(Q_i H_2)\bar{U}_j. \quad (6.55)$$

A possible gauge-kinetic mixing term is omitted from the Lagrangian. At the GUT scale the following mSUGRA-inspired boundary conditions on the soft-breaking parameters are imposed:

$$(m_f^2)_{ij}(M_X) = m_0^2 \delta_{ij} \quad (f = q, \ell, u, d, e; i, j = 1, 2, 3), \quad (6.56a)$$

$$A_{ij}^f(M_X) = A_0 \quad (f = u, d, e; i, j = 1, 2, 3), \quad (6.56b)$$

$$A^\lambda(M_X) = A_0, \quad (6.56c)$$

$$M_i(M_X) = M_{1/2} \quad (i = 1, 2, 3, 4). \quad (6.56d)$$

Furthermore, gauge coupling unification is enforced by setting the $U(1)'$ gauge coupling $g'(M_X)$ to the value of $g_1(M_X) = g_2(M_X)$ at the GUT scale. As output of the three EWSB equations the soft squared Higgs masses $m_{h_1}^2(M_S)$, $m_{h_2}^2(M_S)$ and $m_s^2(M_S)$ are chosen. This variant of the USSM can therefore be called a non-universal Higgs mass model (NUHM). It has six free parameters: m_0 , $M_{1/2}$, A_0 , $\tan\beta(m_Z^{\text{pole}})$, $\lambda(M_X)$, $v_3(M_S)$.

The lightest CP-even Higgs pole mass as a function of m_0 and $\tan\beta$ is shown in Figure 6.8 for $v_3 = 10$ TeV and three different choices of $\lambda(M_X)$. In the white regions with large $\tan\beta$ no simultaneous solution to all boundary conditions with a non-tachyonic mass spectrum can be found. It is remarkable that even low values of $m_0 < 100$ GeV lead to large Higgs masses of the order 130 GeV in the scanned parameter region. The reason is the positive D -term contribution from the extra

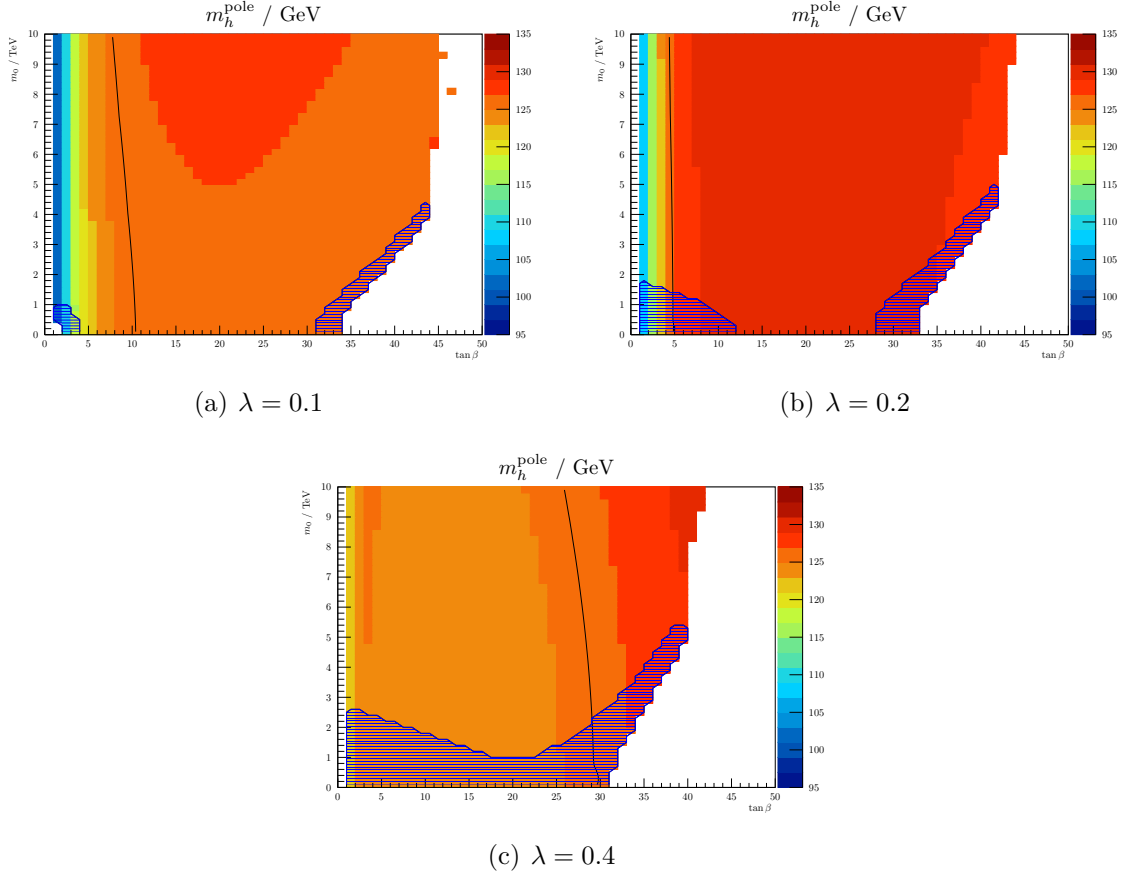


Figure 6.8: Lightest CP-even Higgs pole mass in the USSM as a function of m_0 and $\tan\beta$ for three different choices of $\lambda(M_X)$. The parameter point uses $M_{1/2} = A_0 = 5$ TeV and $v_3 = 10$ TeV. The measured value of $m_h^{\text{pole}} = 125.9$ GeV can be found on the black contour line. In the shaded regions the LSP is a charged particle.

$U(1)'$ gauge symmetry to the tree-level Higgs mass

$$(m_h^{\text{tree}})^2 \approx m_Z^2 c_{2\beta}^2 + \frac{\lambda^2 v^2}{2} s_{2\beta}^2 + \frac{m_Z^2}{4} \left(1 + \frac{1}{4} c_{2\beta}\right)^2. \quad (6.57)$$

This last term contains a $\tan\beta$ -independent part, which increases the tree-level Higgs mass by approximately $m_Z/2$, and a $\tan\beta$ -dependent part, which raises the Higgs mass further in regions with large $\tan\beta$. For $\lambda = 0.1$ there is a relatively large area between $\tan\beta = 10 \dots 45$ and with low values of $m_0 \lesssim 5$ TeV, in which the predicted Higgs masses are of the order 126 GeV or larger. A value of $\lambda = 0.2$ leads to large regions with masses of the order 130 GeV. For higher values of λ the mixing with the singlet gains more influence, which reduces the Higgs mass again. This effect has already been seen in the NMSSM above, see Eq. (6.54) and Figure 6.7.

An interesting property of the additional $U(1)'$ gauge symmetry in the USSM is that the sfermion masses gain extra positive D -term contributions. In the case

of $\lambda = 0.1 \dots 0.2$ this leads to parameter regions with $m_0 = 0$ where the lightest slepton is heavier than the lightest neutralino, resulting in neutral LSPs. However, for $\tan \beta \lesssim 10$ or $\tan \beta \gtrsim 30$ charged LSPs can still appear.

The parameter scans performed here have shown that the USSM predicts large Higgs masses of the order 125 ... 131 GeV easily due to the extra D -term contribution to the tree-level mass. As a consequence, the constraints imposed upon the USSM parameter space from the measured Higgs mass are therefore significantly weaker than in the CMSSM and NMSSM.

E₆SSM

The last model studied here is a constrained variant of the E₆SSM with non-universal soft Higgs masses [187]. A brief introduction to the general E₆SSM is given in Appendix C. For the parameter scan the superpotential

$$\begin{aligned} \mathcal{W}_{\text{E}_6\text{SSM}} = & \lambda_3 S_3(H_{13}H_{23}) - y_{ij}^e(H_{13}L_i)\bar{E}_j - y_{ij}^d(H_{13}Q_i)\bar{D}_j - y_{ij}^u(Q_iH_{23})\bar{U}_j \\ & + \kappa_{ij}S_3(X_i\bar{X}_j) + \lambda_{\alpha\beta}S_3(H_{1\alpha}H_{2\beta}) + \mu'(H'\bar{H}') \end{aligned} \quad (6.58)$$

is used, with $i, j = 1, 2, 3$ and $\alpha, \beta = 1, 2$. At the GUT scale, M_X , the following mSUGRA-inspired constraints on the soft-breaking parameters are imposed:

$$(m_f^2)_{ij}(M_X) = m_0^2 \delta_{ij} \quad (f = q, \ell, u, d, e, x, \bar{x}; i, j = 1, 2, 3), \quad (6.59a)$$

$$(m_s^2)_{\alpha\beta}(M_X) = m_0^2 \delta_{\alpha\beta} \quad (\alpha, \beta = 1, 2), \quad (6.59b)$$

$$(m_{h_p}^2)_{\alpha\beta}(M_X) = m_0^2 \delta_{\alpha\beta} \quad (\alpha, \beta = 1, 2; p = 1, 2), \quad (6.59c)$$

$$m_{h'}^2(M_X) = m_0^2, \quad (6.59d)$$

$$m_{\bar{h}'}^2(M_X) = m_0^2, \quad (6.59e)$$

$$A_{ij}^f(M_X) = A_0 \quad (f = u, d, e, \kappa; i, j = 1, 2, 3), \quad (6.59f)$$

$$A_3^\lambda(M_X) = A_{\alpha\beta}^\lambda(M_X) = A_0 \quad (\alpha, \beta = 1, 2), \quad (6.59g)$$

$$M_i(M_X) = M_{1/2} \quad (i = 1, 2, 3, 4). \quad (6.59h)$$

In addition, the singlet couplings are set to the universal values λ and κ at the GUT scale:

$$\lambda_3(M_X) = \lambda(M_X), \quad (6.60a)$$

$$\lambda_{\alpha\beta}(M_X) = \lambda(M_X)\delta_{\alpha\beta}, \quad (6.60b)$$

$$\kappa_{ij}(M_X) = \kappa(M_X)\delta_{ij}. \quad (6.60c)$$

Furthermore, to ensure gauge coupling unification the extra $U(1)_N$ gauge coupling is set to the value of $g_1(M_X) = g_2(M_X)$ at the GUT scale. As output of the EWSB equations the soft-breaking squared Higgs masses $m_{h_{13}}^2(M_S)$, $m_{h_{23}}^2(M_S)$ and $m_{s_3}^2(M_S)$ are chosen. This leaves the parameters m_0 , $M_{1/2}$, A_0 , $\tan \beta(m_Z^{\text{pole}})$, $\lambda(M_X)$, $\kappa(M_X)$, $v_3(M_S)$, $\mu'(M_S)$ and $B\mu'(M_S)$ unfixed, which are treated as input.

Figure 6.9 shows the lightest CP-even Higgs pole mass as a function of m_0 and

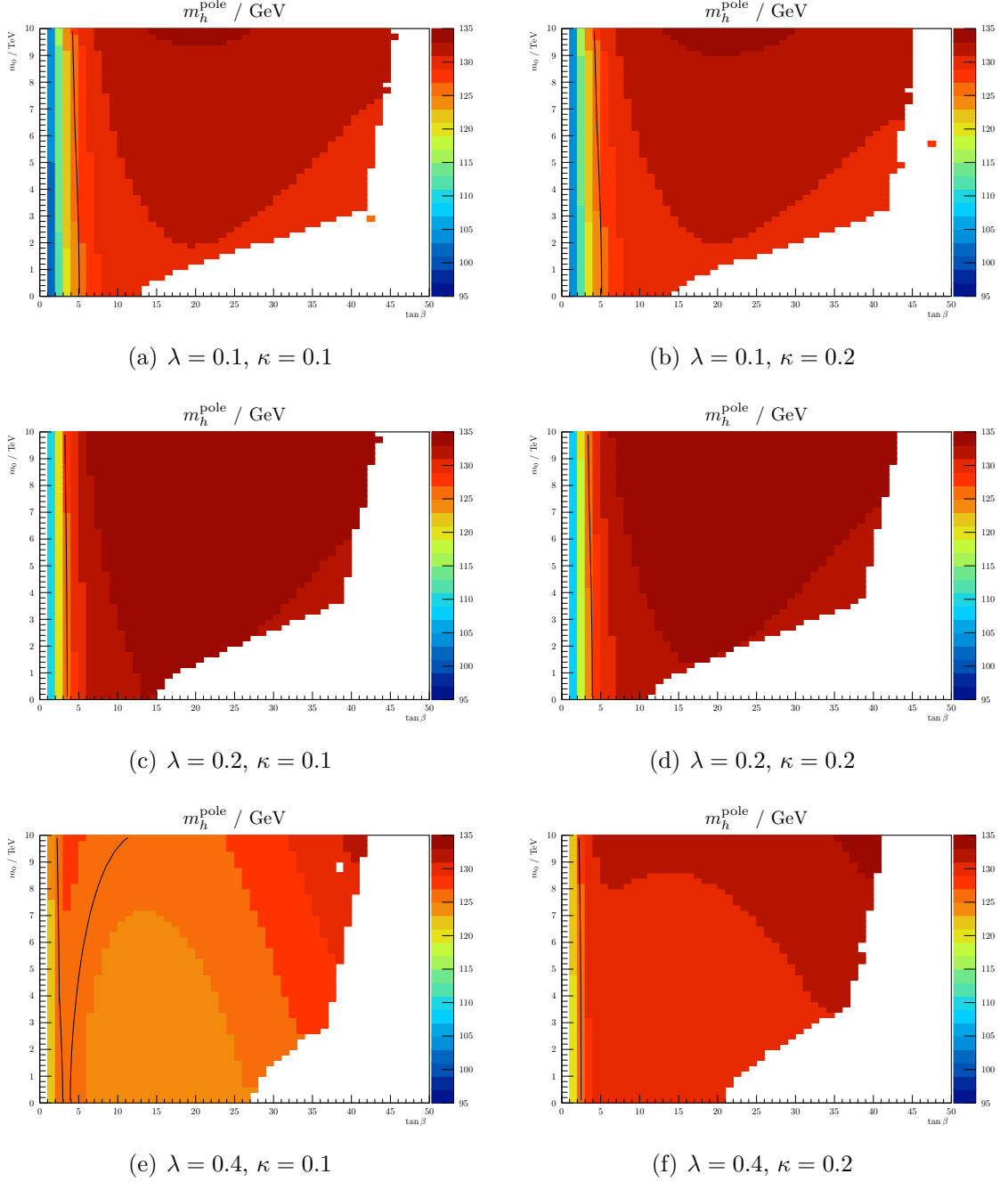


Figure 6.9: Lightest CP-even Higgs pole mass in the semi-constrained E_6 SSM as a function of m_0 and $\tan\beta$. The parameter point uses $M_{1/2} = A_0 = 5$ TeV and $v_3 = \mu' = B\mu' = 10$ TeV. The measured value of $m_h^{\text{pole}} = 125.9$ GeV can be found on the black contour line.

$\tan\beta$ for different values of the universal couplings $\lambda(M_X)$ and $\kappa(M_X)$. The input parameters $v_3(M_S)$, $\mu'(M_S)$ and $B\mu'(M_S)$ are set to 10 TeV. Physical points can be found between $\tan\beta = 1 \dots 15$ for low values of m_0 , and between $\tan\beta = 1 \dots 45$

for high values of m_0 . Outside this region the large top and bottom Yukawa couplings drive the soft squared sfermion masses negative, which results in tachyonic sfermions.¹⁴ As can be seen from Figure 6.9, the studied parameter space leads to overall very large Higgs masses of $m_h^{\text{pole}} = 125 \dots 135$ GeV. Smaller masses are only achieved for values of $\tan \beta \lesssim 5$. The main reason for the large Higgs masses is the extra D -term contribution from the $U(1)_N$, analogous to the USSM. In addition, the extra matter fields present in the E_6 SSM influence the renormalization group equation of λ , which results in a larger value of $\lambda(M_S)$ than in the USSM [45]. This leads to an additional enhancement of the F -term contribution to m_h^{tree} .

Analogous to the USSM, the sfermion masses gain extra D -term contribution from the additional $U(1)_N$ gauge group. This leads to parameter points with $m_0 = 0$, which contain a heavy Higgs of the order 130 GeV or more, but which are not excluded by charged LSPs. However, while in the USSM charged LSPs still appear for small or very large $\tan \beta$, in the E_6 SSM parameter regions studied here the LSP is always the neutralino. The reason is the extra matter, which contributes to the gaugino mass β -functions and thereby leads lighter neutralinos than in the USSM.

Similarly to the USSM, the NUHM E_6 SSM is less constrained by the experimentally measured Higgs mass than the CMSSM and NMSSM. However, the E_6 SSM in general predicts a gluino which is significantly lighter than the squarks [54, 88, 70, 45]. This imposes a strong constraint on the allowed parameter space due to the large gluino mass bounds extracted from the LHC data [70, 45].

Conclusions

The lightest Higgs pole mass was studied in the four different SUSY models CMSSM, NMSSM, USSM and the E_6 SSM, as a function of the common input parameters $\tan \beta$ and m_0 . The additional common free parameters $M_{1/2}$ and A_0 were set to 5 TeV to allow for heavy gauginos and a large stop mass splitting. The remaining free parameters of the individual models were chosen to be of the order of the TeV scale to produce heavy spectra. The obtained values for the Higgs mass in the scanned parameter region demonstrate that

- the USSM and E_6 SSM predict CP-even Higgs pole masses which are significantly larger than in the CMSSM and NMSSM. The main reason is the positive contribution from the extra $U(1)$ D -term. Beyond that the extra matter fields in the E_6 SSM can lead to a larger value of $\lambda(M_S)$, which increases the influence of the F -term contribution for low values of $\tan \beta$.
- For the here studied parameter region the NMSSM predicts Higgs masses which are smaller or of the order of the CMSSM values. The reason is a reduction

¹⁴Note that in the CE_6 SSM there exists an upper bound on $\tan \beta$ of around 45 [57]. The reason is that for high $\tan \beta$ the top and bottom Yukawa couplings become equal at the SUSY scale, which makes it difficult to generate a large splitting between the soft Higgs masses, as required for EWSB. However, this effect does not occur in the here considered variant of the E_6 SSM, because the soft Higgs masses are output of the EWSB equations and are automatically chosen to be as large as required.

of the tree-level Higgs mass due to mixing with the singlet field. This mixing can be avoided by choosing A^λ differently from A_0 at the GUT scale in order to suppress the negative term in Eq. (6.54).

Furthermore, the parameter scans demonstrate that FlexibleSUSY is able to create spectrum generators for the here studied minimal and non-minimal SUSY models and can be used to do extensive parameter scans. The lightest CP-even Higgs pole mass can be predicted for each parameter point at the one-loop and leading two-loop level. This enables to constrain the allowed parameter space of non-minimal SUSY models by the measured value of $m_h^{\text{pole}} = 125.9$ GeV, as shown above.

6.4.3 Influence of loop corrections of different order on the pole mass spectrum

In this section the influence of the loop order in the β -functions, self-energies, tadpoles and threshold corrections on the pole mass spectrum is examined with FlexibleSUSY for two different SUSY models. The purpose is to illustrate the size of the loop effects and demonstrate how they can be studied with FlexibleSUSY.

The first model considered here is the flavour-violating CMSSM, which was introduced in Section 6.4.2. It has five the free input parameters m_0 , $M_{1/2}$, A_0 , $\tan\beta$ and sign μ , which are for the purpose of illustration set to

$$m_0 = 125 \text{ GeV}, \quad M_{1/2} = A_0 = 500 \text{ GeV}, \quad \tan\beta = 10, \quad \text{sign } \mu = +1, \quad (6.61)$$

in the following. This CMSSM parameter point results in a spectrum with light SUSY particles of 0.2...1.2 TeV and a light CP-even Higgs of 113 GeV. To study the influence of different loop orders on the SUSY particle masses a spectrum generator for the CMSSM is created with FlexibleSUSY using the model file from Section 6.3.3. The loop orders used in the self-energies, tadpoles, β -functions and low-scale threshold corrections can be selected in the `FlexibleSUSY` block in the SLHA input file. The default is

Block	FlexibleSUSY
4	2 # pole mass loop order
5	2 # EWSB loop order
6	2 # beta-functions loop order
7	1 # threshold corrections (0 = disabled, 1 = enabled)

Switch number 4 defines the loop order of the self-energies used to calculate the pole mass spectrum from the $\overline{\text{DR}}$ model parameters. FlexibleSUSY provides full one-loop self-energies for each field in any SUSY model. These one-loop self-energies can be enabled by setting switch 4 to 1. In the MSSM and NMSSM additional leading two-loop contributions to the CP-even and CP-odd Higgs bosons can be added by setting the switch to 2 (default). Switch 5 selects the loop order of the effective Higgs potential used for the electroweak symmetry breaking. Here full one-loop Higgs tadpole diagrams are provided by FlexibleSUSY. Leading two-loop contributions are

available in the MSSM and NMSSM. The switch 6 selects the β -function loop order and switch 7 enables/disables the gauge and Yukawa coupling threshold corrections.

Figure 6.10 shows three excerpts of the CMSSM pole mass spectrum for the parameter point given in (6.61). In 6.10(a) the β -function loop order is set to 1

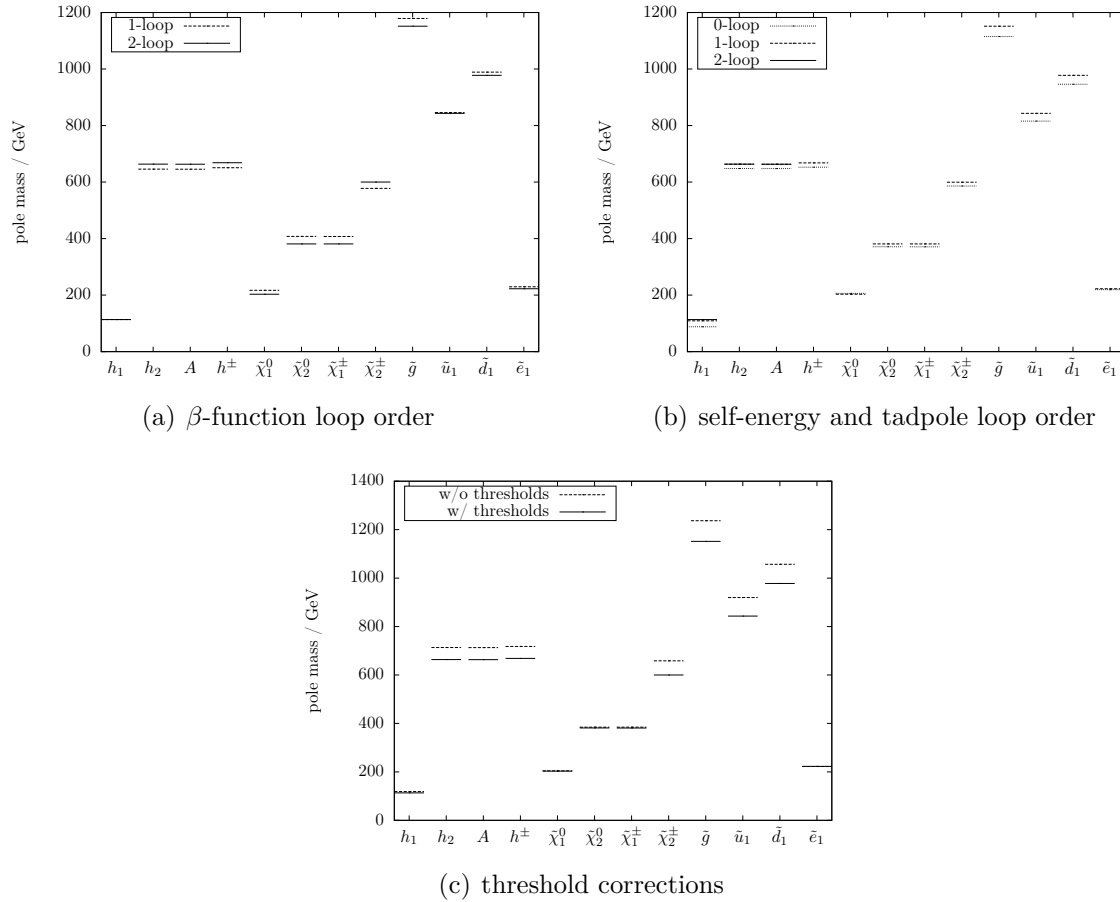


Figure 6.10: Influence of loop corrections of different order on the pole mass spectrum in the CMSSM. The parameter point uses $m_0 = 125$ GeV, $M_{1/2} = A_0 = 500$ GeV, $\tan \beta = 10$ and $\text{sign } \mu = +1$.

(dashed lines) and 2 (solid lines). One finds that the difference in the pole mass spectrum between one- and two-loop β -functions can be up to 25 GeV. The largest effect is found for the gluino. The reason is that its mass is given by M_3 at the tree-level, and the renormalization group running of M_3 depends on the strong coupling constant g_3 . Since g_3 is of the order $O(1)$ at the low-scale, the contribution of the two-loop β -function to the running of M_3 is not negligible. The lightest Higgs mass is insensitive to the β -function loop order and changes only by 0.03 GeV. The main reason is that after the electroweak symmetry breaking the tree-level mass is independent of the soft-breaking squared Higgs masses and is mainly given by $m_Z c_{2\beta}$. Since m_Z and $c_{2\beta}$ are fixed at the scale m_Z^{pole} , which is in usually close to M_S , the contribution of the two-loop β -functions to their running is subdominant.

Figure 6.10(b) shows the CMSSM mass spectrum when the self-energy and tadpole loop orders are set simultaneously to 0 (dotted lines), 1 (dashed lines) and 2 (solid lines), respectively. Thereby, zero-loop order corresponds to the $\overline{\text{DR}}$ mass spectrum. The largest mass difference between the zero-loop and one-loop self-energy corrections can be found for the gluino and squark masses, where dominant self-energy contributions of the order $O(g_3^2)$ appear. The one-loop correction for the lightest CP-even Higgs mass is of the order 20 GeV and the leading two-loop correction amounts for further 4 GeV. It is well known that these large loop corrections stem mainly from top and stop diagrams of the order $O(y_t^2)$, which are enhanced by a large top-stop mass splitting. The size of these corrections emphasizes the necessity to include two-loop Higgs self-energy and tadpole contributions to achieve a precise Higgs pole mass prediction.

In Figure 6.10(c) the influence of threshold corrections to the gauge and Yukawa couplings at the low-scale on the mass spectrum is shown. One finds that neglecting these corrections can lead to mass shifts of up to 80 GeV. The largest effect can again be found for the gluino and the squarks, which are influenced by large threshold corrections to α_s due to the large gauge coupling g_3 . The influence on the lightest CP-even Higgs mass is also not negligible: It is decreased by 5 GeV when threshold corrections are added. This change is mainly due to decreased stop loop corrections to the Higgs self-energy. On the one hand the threshold corrections decrease the top Yukawa coupling by 4 %. On the other hand the change in the gauge couplings at the low scale changes the value of the GUT scale, which leads to 8 % smaller stop masses for this parameter point. These two effects in combination lead to a significantly decreased Higgs pole mass.

The second model considered here is the Z_3 -symmetric NMSSM, which was used in Section 6.4.2 before. Compared to the CMSSM it has the additional free parameter $\lambda(M_X)$, which is set to 0.1 in the following. The parameters m_0 , $M_{1/2}$, A_0 , $\tan\beta$ and $\text{sign}\mu$ are set to the values given in (6.61). For the parameter point studied here the mass spectrum of the NMSSM is similar to that of the CMSSM, except for the modified Higgs sector. Figure 6.11 shows an excerpt of the NMSSM mass spectrum for three different self-energy and tadpole loop orders. Similarly to the CMSSM, one finds that the largest loop contributions appear for the gluino and the squarks due to the $O(g_3^2)$ enhancement. The one-loop contribution to the lightest CP-even Higgs is 23 GeV and the two-loop corrections are around 4.5 GeV. This shows again that two-loop corrections are necessary to predict the Higgs pole mass with sufficient precision. Note again, that leading two-loop Higgs self-energy and tadpole contributions can be added automatically for any MSSM- and NMSSM-like model in FlexibleSUSY, see Section 6.3.3.

Conclusions

The influence of different loop orders in the β -functions, self-energies, tadpoles and threshold corrections on the pole mass spectrum was quantified in the CMSSM and NMSSM for parameter points with light spectra. The size of the one-loop contributions to the pole masses were found to be up to 80 GeV. The leading two-loop

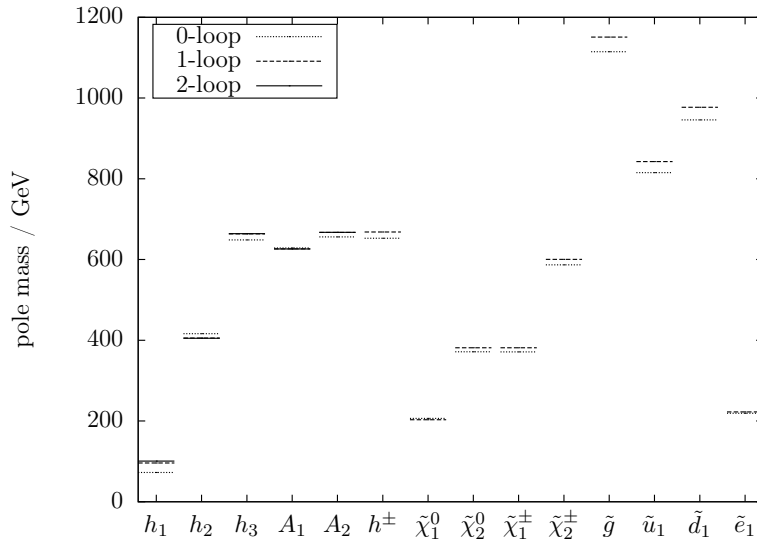


Figure 6.11: Influence of the self-energy and tadpole loop order on the pole mass spectrum in the NMSSM. The parameter point uses $m_0 = 125$ GeV, $M_{1/2} = A_0 = 500$ GeV, $\tan \beta = 10$, $\text{sign } \mu = +1$ and $\lambda(M_X) = 0.1$.

contributions to the Higgs pole mass were of the order 4 GeV, which demonstrates the need to include them when constraining on non-minimal SUSY models. Here, FlexibleSUSY provides an easy way to enable these contributions for MSSM- and NMSSM-like models.

6.4.4 Influence of GUT threshold corrections on the Higgs mass

In this section the influence of GUT threshold corrections on the predicted Higgs pole mass is studied with FlexibleSUSY for two different SUSY models. Since most SUSY models do not assume a specific GUT gauge group breaking mechanism, these threshold corrections are unknown and therefore ignored. However, they can affect the low-energy mass spectrum, which allows to constrain the possible size of the corrections from measured low-energy observables.

One important motivation for most SUSY models is the unification of gauge couplings, which allows to embed the low-energy gauge group into a simple GUT gauge group with a single gauge coupling. At the unification scale, M_X , the GUT gauge group is broken and the thereby emerging heavy fields are integrated out. As discussed in Section 3.1, integrating out heavy fields results in threshold corrections to the model parameters, in particular to the gauge couplings. The latter are of particular importance as they determine the value of the GUT scale by a condition of the form

$$g_1(M_X) = g_2(M_X) + \Delta g(M_X). \quad (6.62)$$

The GUT threshold corrections Δg have the general form [55]

$$\Delta g(M_X) = \frac{1}{(4\pi)^2} \sum_i \left(C_i \log \frac{m_i}{M_X} + D_i \right), \quad (6.63)$$

where the sum on the right-hand side runs over all fields that are integrated out. The constants C_i and D_i involve symmetry group invariants, charges and couplings and are of the order $O(1)$. However, the exact size of the constants C_i and D_i is unknown as long as no concrete GUT model is considered. For this reason Δg is set to zero in many SUSY models, as for example the CMSSM, NMSSM or CE_6SSM . However, one can gain information about the allowed size of the GUT threshold corrections from known low-energy observables. For example, in models with mSUGRA-inspired GUT boundary conditions, as the CMSSM or CE_6SSM , the GUT scale is a fundamental input scale where the soft-breaking parameters are fixed. A variation of the GUT scale due to non-zero threshold corrections will therefore translate to a variation of the low-energy phenomenology, which can be compared to experimental data.

In the following the influence of non-zero GUT threshold corrections on the lightest CP-even Higgs pole mass is studied with FlexibleSUSY. As models the CMSSM and the NUHM E_6SSM , from Section 6.4.2, are considered. For the study the threshold corrections are parametrized by a constant t_c and the GUT scale condition is written as¹⁵

$$g_1(M_X) = g_2(M_X) + t_c. \quad (6.64)$$

In the FlexibleSUSY model files for the CMSSM and E_6SSM this condition is realized by adding t_c to the input parameter block `EXTPAR` and changing the definition of the high-energy scale to

```
EXTPAR = { {100, tc} };
HighScale = g1 == g2 + tc;
```

A scan over t_c in the range $-0.1 \dots 0.1$ is performed for heavy CMSSM and E_6SSM scenarios, with $m_0 = M_{1/2} = A_0 = 5$ TeV, $\text{sign } \mu = +1$, $\lambda = \kappa = 0.1$ and $v_3 = \mu' = B\mu' = 10$ TeV. The chosen scan range for t_c is based on the following consideration: The overall size of t_c is given by the loop factor $(4\pi)^{-2} \approx 0.006$, the group invariants and the splitting of the mass spectrum at the GUT scale. Assuming $O(100)$ heavy particles¹⁶ with masses of the order $0.9 \dots 1.1M_X$ to be integrated out leads to a threshold correction of the order $t_c \approx 0.05$.

The left column in Figure 6.12 shows the lightest CP-even Higgs pole mass in the CMSSM and E_6SSM as a function of t_c for different values of $\tan \beta$. First, one finds that the overall variation of m_h^{pole} with t_c is larger in the CMSSM than in the E_6SSM .

¹⁵The case $t_c < 0$ in the CMSSM is equivalent to the so-called sub-GUT CMSSM [188, 189, 190], where the input scale for the soft-breaking parameters is chosen to be below the GUT scale.

¹⁶In the E_6SSM , for example, the fields which complete the $(\mathbf{27})'$, $(\mathbf{27})'$ and $(\mathbf{78})$ representations need to be integrated out, which results in $O(100)$ degrees of freedom.

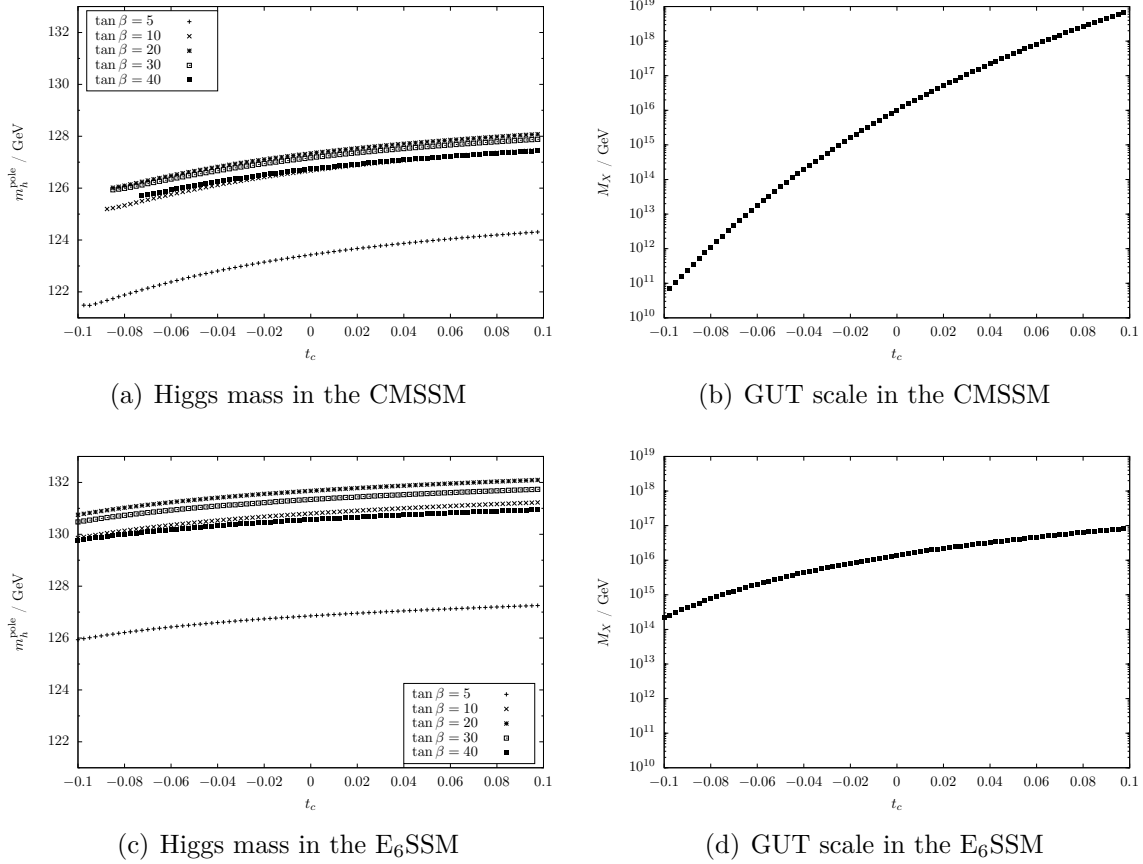


Figure 6.12: Higgs pole mass and GUT scale as a function of the GUT threshold corrections t_c in the CMSSM and E₆SSM. Both models use the common parameters $m_0 = M_{1/2} = A_0 = 5$ TeV and $\text{sign } \mu = +1$. In the E₆SSM the remaining free parameters are set to $\lambda = \kappa = 0.1$ and $v_3 = \mu' = B\mu' = 10$ TeV.

The reason is that in the CMSSM the GUT scale is more sensitive to t_c , see the plots in the right column. This sensitivity translates to a larger variation of the Higgs mass at the low-scale. The reason for the weaker dependency of $M_X(t_c)$ in the E₆SSM are the larger E₆SSM gauge coupling β -functions. As shown in Figure 6.13, they lead to a steeper slope of $g_i(M_X)$, which results in a weaker dependency of M_X on a deviation from exact coupling unification.

The overall variation of the Higgs mass is around 1...2 GeV in the CMSSM and around 1 GeV in the E₆SSM. It is thereby of the same order or smaller than the two-loop Higgs self-energy and tadpole corrections [166, 167]. The origin is a varying stop mass splitting, which is influenced by the value of the GUT scale at which the soft-breaking parameters are constrained. In the CMSSM this splitting is of the order 1 TeV for $t_c = -0.1$ and rises to 1.5 TeV when t_c is increased to 1.0.

Finally, it can be seen from Figure 6.12(b) that large negative threshold corrections ($g_1(M_X) < g_2(M_X)$) significantly decrease the GUT scale in the CMSSM. This can lead to a deformed Higgs potential at the low-scale, which prevents electroweak

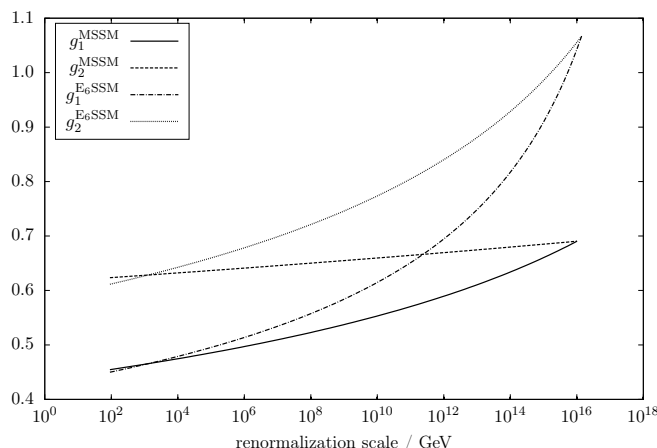


Figure 6.13: Running gauge couplings in the CMSSM and E_6 SSM. Both models use the common parameters $m_0 = M_{1/2} = A_0 = 5$ TeV, $\tan\beta = 10$ and $\text{sign}\mu = +1$. In the E_6 SSM the remaining free parameters are set to $\lambda = \kappa = 0.1$ and $v_3 = \mu' = B\mu' = 10$ TeV.

symmetry breaking from occurring. In the here studied case for $t_c \lesssim -0.08$ no real solution for the μ parameter which solves the EWSB equations exists. On the other hand, a large positive threshold correction $t_c \gtrsim 0.1$ can lead to a very high GUT scale of the order 10^{19} GeV or larger.

Conclusions

The influence of non-zero GUT threshold corrections on the predicted lightest CP-even Higgs pole mass was studied in the CMSSM and E_6 SSM for parameter scenarios with heavy spectra. The threshold corrections were varied in the wide range $-0.1 \dots 0.1$ to cover GUT models where large multiplets with $O(100)$ fields are integrated out. It was found that the variation of the Higgs pole mass can be up to 2 GeV in this range, which is due to a strong dependence of the GUT scale on the threshold correction. The size of this effect should therefore be kept in mind when considering GUT models with large multiplets. Furthermore, it could be seen that this study was easily possible with FlexibleSUSY, since only minimal modifications to existing CMSSM and E_6 SSM model files were needed to introduce a non-zero threshold correction.

6.5 Summary and conclusion

In this chapter FlexibleSUSY was presented, a Mathematica package which creates spectrum generators for minimal and non-minimal SUSY models in C++. It provides two levels to influence the generated source code: (i) The Mathematica meta code level, where the user can customize the model and the boundary conditions via a model file and (ii) the C++ level, where modular C++ classes are generated which allow for flexible reuse and extension. In addition FlexibleSUSY focuses on a short

run-time and provides interfaces for alternative boundary value problem solvers and towers of effective theories.

To demonstrate that the design goals have been achieved and to illustrate FlexibleSUSY's range of use four different applications were studied:

- A CMSSM spectrum generator run-time comparison was performed with the two hand-written programs SPheno and Softsusy and the automatically generated SPhenoMSSM. It was found that due to the fast linear algebra package and the used multi-threading FlexibleSUSY is faster by a factor 1.4–2.5 compared to Softsusy and SPheno, and faster by a factor 2.8–5 compared to SPhenoMSSM.
- The lightest CP-even Higgs pole mass was studied in the CMSSM, NMSSM, USSM and E_6 SSM. It was found that in the studied parameter regions the USSM and E_6 SSM can predict the largest Higgs masses.
- The influence of the loop order in the β -functions, self-energies, effective Higgs potential and threshold corrections was quantified in the CMSSM and NMSSM. Reduced loop orders or missing threshold corrections were found to shift the pole mass spectrum up to 80 GeV. The lightest Higgs mass was found to be sensitive to the used self-energy, tadpole and threshold corrections, which can amount to ± 5 GeV in the mass.
- The influence of non-zero GUT threshold corrections on the predicted Higgs pole mass was studied in a CMSSM- and E_6 SSM-like model. It was found that integrating out large field multiplets with $O(100)$ particles at the GUT scale can shift the Higgs mass up to 2 GeV at the low-energy scale.

These applications demonstrate that FlexibleSUSY can be used to create spectrum generators for minimal and non-minimal SUSY models and to constrain the parameter space by calculating the Higgs pole mass with leading two-loop precision. Furthermore, existing model files for the MSSM, NMSSM, USSM, E_6 SSM etc. can be easily modified at the Mathematica meta code level to allow studying model variants with different boundary condition set-ups. The generated C++ code is modular, which enables to exchange different modules easily by user-supplied routines and reuse components in existing programs.

Extensions of FlexibleSUSY are already planned which calculate sparticle and Higgs decays as well as the anomalous magnetic moment of the muon. The former is especially important in order to test SUSY models on experimental data. Furthermore, models with complex parameters will be allowed in the future, to study CP-violation for example.

FlexibleSUSY has been published in [114] and can be obtained from <https://flexiblesusy.hepforge.org>.

Chapter 7

Summary

Non-minimal supersymmetric models are attractive extensions of the Standard Model and the MSSM, as they provide solutions to the μ -problem, for example, can reduce the Higgs mass fine-tuning and introduce interesting new phenomenology. For phenomenological investigations of such models and to search for signals of SUSY particles in experimental data complicated consecutive computations must be carried out. The first step is usually to calculate the pole mass spectrum from a set of theory input parameters. This mass spectrum can then be used to calculate further observables, such as decays, cross sections, the dark matter relic density etc. Alternatively, the mass spectrum may be passed on to event generators and detector simulations to study how particle collisions manifest in a detector. This thesis makes four contributions in the field of non-minimal supersymmetry phenomenology, which increase the precision of the mass spectrum prediction and the $\overline{\text{DR}}$ parameters and allow to easily study new models with high accuracy.

The mass spectrum prediction in the CE_6SSM has been improved by calculating the E_6SSM gauge and Yukawa couplings taking one-loop radiative corrections from SUSY particles into account. They complement the partial gauge coupling threshold corrections to the Standard Model, which have been calculated earlier. Implementing these corrections into an existing CE_6SSM spectrum generator led to a more precise mass spectrum prediction and allowed one to re-evaluate the proposed benchmark points from the literature. A parameter scan was performed using the improved spectrum generator to confront the model with exclusion limits from current experiments. Parameter regions with light squarks have been found to be excluded by the gluino mass limit due to the characteristic gluino-sfermion hierarchy in the CE_6SSM . Regions which are not excluded by this limit can lead to the measured value of the Higgs mass due to large contributions from heavy stops and the extra D -term from the additional $U(1)_N$ gauge symmetry. The model is therefore still viable and can be probed by current experiments.

The β -functions of vacuum expectation values was calculated in a general and supersymmetric gauge theory in R_ξ gauge at the one- and two-loop level using an elegant background field formalism. The results reveal the general structure of the β -function of $\tan\beta$, which was found to be gauge-independent in the MSSM and NMSSM at the one-loop level due to an accidental cancellation. At the two-loop level the gauge dependence is manifest. The general expressions for the one- and two-loop VEV β -functions were specialized to the MSSM and NMSSM and implemented into

Softsusy. In addition, these general expressions are now available in SARAH since version 4.0.0 and are used to calculate the one- and two-loop β -functions of VEVs in any softly broken $N = 1$ SUSY model. The general SUSY spectrum generators SARAH/SPheno and FlexibleSUSY for example make use of these expressions to implement the renormalization group running of the VEVs in a user-defined SUSY model.

An NMSSM extension of Softsusy was created in order to calculate the pole mass spectrum and the $\overline{\text{DR}}$ parameters in the NMSSM with a high precision. As discussed, the NMSSM is a well-motivated SUSY model which solves the μ -problem of the MSSM and provides an interesting phenomenology with an extended Higgs sector which can be probed by the LHC. This extension is able to calculate the pole mass spectrum in the Z_3 -symmetric and Z_3 -violating NMSSM using full two-loop β -functions, one-loop self-energies and tadpoles as well as leading two-loop Higgs mass corrections. Softsusy thereby implements many precision corrections, which are neglected in NMSPEC. Among the advantages of having multiple spectrum generators for the same model, this enables to estimate the theory uncertainty of the predicted mass spectrum by comparing the output of the two programs.

FlexibleSUSY, a Mathematica package which creates spectrum generators for SUSY models, was written to allow studies of a wide range of non-minimal SUSY models to be carried out easily. The user defines a SUSY model at the Mathematica meta code level and specifies physical assumptions about the model in form of boundary conditions, as for example the electroweak symmetry breaking or universality conditions on the soft-breaking parameters at the gauge coupling unification scale. For a so-defined model FlexibleSUSY calls functions from SARAH to calculate β -functions, mass matrices, one-loop self-energies and tadpoles and converts these expressions into C++ classes with well-defined interfaces. In addition, leading two-loop Higgs mass contributions can be added in MSSM- and NMSSM-like models to enable a more precise mass prediction. Furthermore, one-loop expressions for the gauge coupling threshold corrections and Yukawa couplings are generated automatically to match the SUSY model to the Standard Model taking radiative corrections into account. The loop-corrected effective Higgs potential is constructed from the tadpole diagrams and electroweak symmetry breaking conditions and numerical routines are automatically created to find a minimum. All of these components are finally combined to a complete spectrum generator, which calculates the $\overline{\text{DR}}$ parameters and pole masses consistent with the user-defined boundary conditions. To solve the boundary value problem the standard two-scale fixed-point iteration algorithm used in the MSSM was generalized. It finds physical solutions consistent with an arbitrary number of constraints and can handle towers of effective field theories as well. FlexibleSUSY aims for a fast run-time, a modular structure and provides an interface for alternative boundary condition solvers to study parameter regions where the standard fixed-point iteration does not converge.

Using FlexibleSUSY it was possible to compare the lightest CP-even Higgs pole mass with leading two-loop accuracy in four different SUSY models, thereby studying the impact of extra matter fields and symmetries. It was found that especially in models with extra $U(1)$ gauge symmetries, such as the USSM and E_6 SSM, the

Higgs mass is significantly increased, which mitigates of the fine-tuning problem. In addition, the influence of non-zero GUT threshold corrections on the lightest CP-even Higgs pole mass was studied in CMSSM- and E₆SSM-like models. These corrections are ignored in many SUSY models due to an unspecified GUT gauge group breaking mechanism. However, these corrections can have a significant effect on the low-energy phenomenology in models where large multiplets with $O(100)$ particles are integrated out at the GUT scale, as is the case for example in the E₆SSM. In the studied range it was found that the lightest Higgs pole mass can vary up to 2 GeV, which is of the order or smaller than the two-loop Higgs mass corrections.

In summary, FlexibleSUSY provides a fast, precise, modular and easy to use spectrum generator framework. It allows the study of a wide range of non-minimal supersymmetric models and thereby can assist the SUSY community to search for supersymmetry at current experiments.

Appendix A

Group invariants

The group invariants used in Section 4 are defined as

$$C_{ab}^2(\text{S}) = T_{ac}^A T_{cb}^A, \quad (\text{A.1})$$

$$C_{ab}^2(\text{F}) = t_{ac}^A t_{cb}^A, \quad (\text{A.2})$$

$$C_2(\text{G})\delta^{AB} = f^{ACD} f^{BCD}, \quad (\text{A.3})$$

$$S_2(\text{S})\delta^{AB} = \text{Tr}[T^A T^B], \quad (\text{A.4})$$

$$S_2(\text{F})\delta^{AB} = \text{Tr}[t^A t^B], \quad (\text{A.5})$$

$$Y_{ab}^2(\text{S}) = \frac{1}{2} \text{Tr} \left(Y^{\dagger a} Y^b + Y^{\dagger b} Y^a \right), \quad (\text{A.6})$$

$$\Lambda_{ab}^2(\text{S}) = \frac{1}{6} \lambda_{acde} \lambda_{bcde}, \quad (\text{A.7})$$

$$H_{ab}^2(\text{S}) = \frac{1}{2} \text{Tr} \left(Y^a Y^{\dagger b} Y^c Y^{\dagger c} + Y^{\dagger a} Y^b Y^{\dagger c} Y^c \right), \quad (\text{A.8})$$

$$\bar{H}_{ab}^2(\text{S}) = \frac{1}{2} \text{Tr} \left(Y^a Y^{\dagger c} Y^b Y^{\dagger c} + Y^{\dagger a} Y^c Y^{\dagger b} Y^c \right), \quad (\text{A.9})$$

$$Y_{ab}^{2F}(\text{S}) = \frac{1}{2} \text{Tr} \left[C^2(\text{F})(Y^a Y^{\dagger b} + Y^b Y^{\dagger a}) \right]. \quad (\text{A.10})$$

The T_{ab}^A and t_{ab}^A are the generators of the gauge transformation of the scalar fields and Weyl spinors, respectively. The structure functions of the gauge group are denoted as f^{ABC} . The Yukawa couplings Y_{bc}^a and the scalar four-point couplings λ_{abcd} are normalized as in Eq. (4.9).

Appendix B

MSSM field content

The field content of the MSSM [20] in terms of chiral and vector superfields and their quantum numbers is listed in Table B.1. The decomposition of the superfields in terms of bosonic and fermionic component fields can be found in Table B.2. In this thesis the following R -parity conserving superpotential is used

$$\mathcal{W}_{\text{MSSM}} = \mu(H_1 H_2) - y_{ij}^e (H_1 L_i) \bar{E}_j - y_{ij}^d (H_1 Q_i) \bar{D}_j - y_{ij}^u (Q_i H_2) \bar{U}_j, \quad (\text{B.1})$$

where the bracket product $(AB) = \epsilon_{CD} A^C B^D$ denotes the $SU(2)$ invariant doublet product with $\epsilon_{CD} = -\epsilon_{DC}$ and $\epsilon_{12} = -1$.

Field	$SU(3)_c \times SU(2)_L \times U(1)_Y$	$SU(5)$
$Q_i = (Q_{u_i} \quad Q_{d_i})$	$(\mathbf{3}, \mathbf{2}, \frac{1}{6})_i$	} $(\mathbf{10})_i$
\bar{U}_i	$(\bar{\mathbf{3}}, \mathbf{1}, -\frac{2}{3})_i$	
\bar{E}_i	$(\mathbf{1}, \mathbf{1}, 1)_i$	
\bar{D}_i	$(\bar{\mathbf{3}}, \mathbf{1}, \frac{1}{3})_i$	} $(\bar{\mathbf{5}})_i$
$L_i = (L_{\nu_i} \quad L_{e_i})$	$(\mathbf{1}, \mathbf{2}, -\frac{1}{2})_i$	
?	$(\bar{\mathbf{3}}, \mathbf{1}, \frac{1}{3})$	} $(\bar{\mathbf{5}})$
$H_1 = (H_1^0 \quad H_1^-)$	$(\mathbf{1}, \mathbf{2}, -\frac{1}{2})$	
?	$(\mathbf{3}, \mathbf{1}, -\frac{1}{3})$	} $(\mathbf{5})$
$H_2 = (H_2^+ \quad H_2^0)$	$(\mathbf{1}, \mathbf{2}, \frac{1}{2})$	
V_g^a	$(\mathbf{8}, \mathbf{1}, 0)$	} $(\mathbf{24})$
?	$(\bar{\mathbf{3}}, \mathbf{2}, \frac{5}{6})$	
?	$(\mathbf{3}, \mathbf{2}, -\frac{5}{6})$	
V_W^i	$(\mathbf{1}, \mathbf{3}, 0)$	
V_Y	$(\mathbf{1}, \mathbf{1}, 0)$	

Table B.1: MSSM superfields and their gauge group representations (generation index $i = 1, 2, 3$). For the abelian group $U(1)_Y$ the charges $Y/2$ are listed. The ? placeholder represents fields that do not exist in the MSSM, but which would complete the fundamental $(\mathbf{5})$, $(\bar{\mathbf{5}})$ and $(\mathbf{24})$ representations of $SU(5)$.

Superfield	Component fields		
	Spin 0	Spin 1/2	Spin 1
$Q_i = (Q_{u_i} \quad Q_{d_i})^T$	$\tilde{q}_{iL} = (\tilde{u}_{iL} \quad \tilde{d}_{iL})^T$	$q_{iL} = (u_{iL} \quad d_{iL})^T$	
\bar{U}_i	\tilde{u}_{iR}^*	u_{iR}^C	
\bar{D}_i	\tilde{d}_{iR}^*	d_{iR}^C	
$L_i = (L_{\nu_i} \quad L_{e_i})^T$	$\tilde{\ell}_{iL} = (\tilde{\nu}_{iL} \quad \tilde{e}_{iL})^T$	$\ell_{iL} = (\nu_{iL} \quad e_{iL})^T$	
\bar{E}_i	\tilde{e}_{iR}^*	e_{iR}^C	
$H_1 = (H_1^0 \quad H_1^-)^T$	$h_1 = (h_1^0 \quad h_1^-)^T$	$\tilde{h}_{1L} = (\tilde{h}_{1L}^0 \quad \tilde{h}_{1L}^-)^T$	
$H_2 = (H_2^+ \quad H_2^0)^T$	$h_2 = (h_2^+ \quad h_2^0)^T$	$\tilde{h}_{2L} = (\tilde{h}_{2L}^+ \quad \tilde{h}_{2L}^0)^T$	
V_g^a		\tilde{g}^a	G_μ^a
V_W^i		\tilde{W}^i	W_μ^i
V_Y		\tilde{B}	B_μ

Table B.2: Component fields of the MSSM superfields (generation index $i = 1, 2, 3$). The charge conjugation of a spinor ψ is defined as $\psi^C := C \bar{\psi}^T$, where $C = i\gamma^2\gamma^0$.

Appendix C

The E_6 SSM

C.1 Gauge group

The Exceptional Supersymmetric Standard Model (E_6 SSM) is a supersymmetric gauge theory, that is inspired by Grand Unified Theories (GUTs) with an E_6 gauge symmetry. The E_6 gauge symmetry is broken at the GUT scale M_X via the Hosotani mechanism [191] to the direct product of the Standard Model gauge group and an extra $U(1)_N$ gauge group

$$SU(3)_c \times SU(2)_L \times U(1)_Y \times U(1)_N. \quad (\text{C.1})$$

This additional $U(1)_N$ arises from the step-wise breaking of the E_6 as [192, 193]

$$E_6 \rightarrow SO(10) \times U(1)_\psi \quad (\text{C.2a})$$

$$\hookrightarrow SU(5) \times U(1)_\chi \quad (\text{C.2b})$$

$$\hookrightarrow SU(3)_c \times SU(2)_L \times U(1)_Y, \quad (\text{C.2c})$$

where the two abelian gauge groups $U(1)_\chi \times U(1)_\psi$ are combined to

$$U(1)_N = U(1)_\chi \cos \theta + U(1)_\psi \sin \theta, \quad (\text{C.3})$$

with $\tan \theta = \sqrt{15}$. This choice of the mixing angle $\tan \theta$ leads to a pure gauge singlet, which can be assigned to the right-handed neutrino. For this gauge singlet a gauge invariant Majorana mass term is allowed, which enables a high-scale seesaw mechanism for the generation of neutrino masses.

C.2 Field content

The field content of the E_6 SSM fills three generations of complete fundamental $(\mathbf{27})$ representations of the E_6 group, see Table C.1. Anomaly cancellation is ensured hereby. In order to enable gauge coupling unification, the model is enhanced by two Higgs-like doublets H' and \bar{H}' , called survival Higgses. They originate from extra, incomplete $(\mathbf{27})'$ and $(\mathbf{27})'$ representations and do not spoil anomaly cancellation.

The Standard Model fermions and their superpartners fill the $SU(5) \times U(1)_N$ multiplets $(\mathbf{10}, 1)_i$ and $(\bar{\mathbf{5}}, 2)_i$. The $(\bar{\mathbf{5}}, -3)_i$ and $(\mathbf{5}, -2)_i$ representations contain three

Field	$G_{\text{SM}} \times U(1)_N$	$SU(5) \times U(1)_N$	E_6
$Q_i = (Q_{u_i} \quad Q_{d_i})$	$(\mathbf{3}, \mathbf{2}, \frac{1}{6}, 1)_i$	$(\mathbf{10}, 1)_i$	$(\mathbf{27})_i$
\bar{U}_i	$(\bar{\mathbf{3}}, \mathbf{1}, -\frac{2}{3}, 1)_i$		
\bar{E}_i	$(\mathbf{1}, \mathbf{1}, 1, 1)_i$		
\bar{D}_i	$(\bar{\mathbf{3}}, \mathbf{1}, \frac{1}{3}, 2)_i$	$(\bar{\mathbf{5}}, 2)_i$	
$L_i = (L_{\nu_i} \quad L_{e_i})$	$(\mathbf{1}, \mathbf{2}, -\frac{1}{2}, 2)_i$		
\bar{X}_i	$(\bar{\mathbf{3}}, \mathbf{1}, \frac{1}{3}, -3)_i$	$(\bar{\mathbf{5}}, -3)_i$	
$H_{1i} = (H_{1i}^0 \quad H_{1i}^-)$	$(\mathbf{1}, \mathbf{2}, -\frac{1}{2}, -3)_i$	$(\mathbf{5}, -2)_i$	
X_i	$(\mathbf{3}, \mathbf{1}, -\frac{1}{3}, -2)_i$		
$H_{2i} = (H_{2i}^+ \quad H_{2i}^0)$	$(\mathbf{1}, \mathbf{2}, \frac{1}{2}, -2)_i$	$(\mathbf{1}, 5)_i$	
S_i	$(\mathbf{1}, \mathbf{1}, 0, 5)_i$	$(\mathbf{1}, 0)_i$	
\bar{N}_i	$(\mathbf{1}, \mathbf{1}, 0, 0)_i$		
$H' = (H'^0 \quad H'^-)$	$(\mathbf{1}, \mathbf{2}, -\frac{1}{2}, 2)$	$\ni (\bar{\mathbf{5}}, 2)'$	$\ni (\mathbf{27})'$
$\bar{H}' = (\bar{H}'^+ \quad \bar{H}'^0)$	$(\mathbf{1}, \mathbf{2}, \frac{1}{2}, -2)$	$\ni (\mathbf{5}, -2)'$	$\ni (\mathbf{27})'$
V_g^a	$(\mathbf{8}, \mathbf{1}, 0, 0)$	$\ni (\mathbf{24}, 0)$	$\ni (\mathbf{78})$
V_W^i	$(\mathbf{1}, \mathbf{3}, 0, 0)$	$\ni (\mathbf{24}, 0)$	$\ni (\mathbf{78})$
V_Y	$(\mathbf{1}, \mathbf{1}, 0, 0)$	$\ni (\mathbf{24}, 0)$	$\ni (\mathbf{78})$
V_N	$(\mathbf{1}, \mathbf{1}, 0, 0)$	$\ni (\mathbf{1}, 0)$	$\ni (\mathbf{78})$

Table C.1: E_6 SSM superfields and their gauge group representations (generation index $i = 1, 2, 3$), where $G_{\text{SM}} \equiv SU(3)_c \times SU(2)_L \times U(1)_Y$. For the abelian groups $U(1)_Y$ and $U(1)_N$ the charges $Y/2$ and $N/2$ are listed.

generations of Higgs-like superfields H_{1i} , H_{2i} and exotic colored matter fields X_i , \bar{X}_i . The remaining $SU(5)$ singlets $(\mathbf{1}, 0)_i$ and $(\mathbf{1}, 5)_i$ represent right-handed neutrinos and singlet fields S_i , respectively. The complete list of E_6 SSM particles and their representations can be found in Table C.1 and C.2.

In an E_6 gauge symmetric theory the gauge bosons and their superpartners fill the adjoint $(\mathbf{78})$ representation of the E_6 . Under the breaking (C.2) and (C.3) the $(\mathbf{78})$ representation decomposes into

$$(\mathbf{78}) \rightarrow (\mathbf{8}, \mathbf{1}, 0, 0) + (\mathbf{1}, \mathbf{3}, 0, 0) + (\mathbf{1}, \mathbf{1}, 0, 0) + (\mathbf{1}, \mathbf{1}, 0, 0) + \dots \quad (\text{C.4})$$

The broken E_6 generators correspond to gauge bosons (and gauginos) with a mass of the order of the GUT scale M_X , which are assumed to be integrated out.¹ The four unbroken multiplets in (C.4) represent the eight gluons G^a (and gluinos \tilde{g}^a), the three $SU(2)_L$ gauge bosons W^i (and winos \tilde{W}^i), the $U(1)_Y$ gauge boson B (and the bino \tilde{B}) and the extra $U(1)_N$ gauge boson B' (and \tilde{B}'), respectively.

¹Integrating out heavy E_6 gauge bosons and gauginos can lead to significant threshold corrections to the gauge couplings at the GUT scale [55]. The presence of these corrections should be kept in mind when studying gauge coupling unification within a low-scale supersymmetric theory, such as the MSSM or E_6 SSM.

Superfield	Component fields		
	Spin 0	Spin 1/2	Spin 1
$Q_i = (Q_{u_i} \ Q_{d_i})^T$	$\tilde{q}_{iL} = (\tilde{u}_{iL} \ \tilde{d}_{iL})^T$	$q_{iL} = (u_{iL} \ d_{iL})^T$	
\bar{U}_i	\tilde{u}_{iR}^*	u_{iR}^C	
\bar{D}_i	\tilde{d}_{iR}^*	d_{iR}^C	
$L_i = (L_{\nu_i} \ L_{e_i})^T$	$\tilde{\ell}_{iL} = (\tilde{\nu}_{iL} \ \tilde{e}_{iL})^T$	$\ell_{iL} = (\nu_{iL} \ e_{iL})^T$	
\bar{E}_i	\tilde{e}_{iR}^*	e_{iR}^C	
\bar{N}_i	$\tilde{\nu}_{iR}^*$	ν_{iR}^C	
X_i	\tilde{x}_{iL}	x_{iL}	
\bar{X}_i	\tilde{x}_{iR}^*	x_{iR}^C	
$H_{1i} = (H_{1i}^0 \ H_{1i}^-)^T$	$h_{1i} = (h_{1i}^0 \ h_{1i}^-)^T$	$\tilde{h}_{1iL} = (\tilde{h}_{1iL}^0 \ \tilde{h}_{1iL}^-)^T$	
$H_{2i} = (H_{2i}^+ \ H_{2i}^0)^T$	$h_{2i} = (h_{2i}^+ \ h_{2i}^0)^T$	$\tilde{h}_{2iL} = (\tilde{h}_{2iL}^+ \ \tilde{h}_{2iL}^0)^T$	
S_i	s_i	\tilde{s}_i	
$H' = (H'^0 \ H'^-)^T$	$h' = (h'^0 \ h'^-)^T$	$\tilde{h}'_L = (\tilde{h}'_L^0 \ \tilde{h}'_L^-)^T$	
$\bar{H}' = (\bar{H}'^+ \ \bar{H}'^0)^T$	$\bar{h}' = (\bar{h}'^+ \ \bar{h}'^0)^T$	$\tilde{\bar{h}}'_L = (\tilde{\bar{h}}'_L^+ \ \tilde{\bar{h}}'_L^0)^T$	
V_g^a		\tilde{g}^a	G_μ^a
V_W^i		\tilde{W}^i	W_μ^i
V_Y		\tilde{B}	B_μ
V_N		\tilde{B}'	B'_μ

Table C.2: Component fields of the E_6 SSM superfields (generation index $i = 1, 2, 3$). The charge conjugation of a spinor ψ is defined as $\psi^C := C\bar{\psi}^T$, where $C = i\gamma^2\gamma^0$.

C.3 Superpotential

The most general renormalizable, E_6 invariant superpotential that can be formed out of the $(\mathbf{27})_i$ representations of the E_6 gauge group is given by the trace of the $(\mathbf{27})_i \otimes (\mathbf{27})_j \otimes (\mathbf{27})_k$. The invariance under the low-energy gauge group (3.1) of the E_6 SSM allows further terms. However, as in the case of the MSSM, the most general gauge $SU(3)_c \times SU(2)_L \times U(1)_Y \times U(1)_N$ invariant superpotential is phenomenologically not viable [42, 54], because it contains baryon number violating terms and could lead to unacceptably large non-diagonal flavor transitions. To conserve baryon number, avoid flavor changing neutral currents (FCNCs), and at the same time avoid stable exotic colored quarks [194, 195, 196], two discrete symmetries are imposed [42]:

1. An approximate Z_2^H symmetry, under which H_{13} , H_{23} and S_3 carry charge +1, and all other chiral superfields carry charge -1 .²³ This symmetry suppresses baryon number violating terms and avoids FCNCs.

²³Such a Z_2^H symmetry could be the result of a Δ_{27} family symmetry imposed at the GUT scale [197].

³As an alternative one might impose an exact \tilde{Z}_2^H symmetry and at the same time allow the exotic colored quarks to decay into matter fields from additional incomplete $(\mathbf{27})$ representations [198].

2. A symmetry analogous to R -parity in the MSSM, which avoids rapid proton decay, caused by the Z_2^H violating terms. This can either be
 - a) a Z_2^L symmetry, under which all chiral superfields carry charge $+1$, except for the leptons which carry charge -1 (Model I) or
 - b) a Z_2^B symmetry, under which the exotic quarks and leptons carry charge -1 , and all others superfields carry charge $+1$ (Model II).

The so constructed two possible E_6 SSM superpotentials read

$$\mathcal{W}_{E_6\text{SSM}}^{Z_2^H, Z_2^{L/B}} = \mathcal{W}_{E_6\text{SSM}}^{Z_2^H} + \mathcal{W}_{E_6\text{SSM}}^{Z_2^{L/B}}, \quad (\text{C.5})$$

where

$$\begin{aligned} \mathcal{W}_{E_6\text{SSM}}^{Z_2^H} &= -y_{ij}^e(H_{13}L_i)\bar{E}_j - y_{ij}^d(H_{13}Q_i)\bar{D}_j - y_{ij}^u(Q_iH_{23})\bar{U}_j \\ &\quad + \frac{1}{2}M_{ij}\bar{N}_i\bar{N}_j + h_{4j}^E(H_{13}H')\bar{E}_j + h_{4j}^N(H_{23}H')\bar{N}_j + \mu'(H'\bar{H}') \\ &\quad + \lambda_i S_3(H_{1i}H_{2i}) + \kappa_i S_3 X_i \bar{X}_i + f_{\alpha\beta} S_\alpha(H_{13}H_{2\beta}) + \tilde{f}_{\alpha\beta} S_\alpha(H_{1\beta}H_{23}), \end{aligned} \quad (\text{C.6})$$

$$\mathcal{W}_{E_6\text{SSM}}^{Z_2^L} = g_{ijk}^Q X_i (Q_j Q_k) + g_{ijk}^q \bar{X}_i \bar{D}_j \bar{U}_k, \quad (\text{C.7})$$

$$\mathcal{W}_{E_6\text{SSM}}^{Z_2^B} = g_{ijk}^N \bar{N}_i X_j \bar{U}_k + g_{ijk}^E \bar{E}_i X_j \bar{U}_k + g_{ijk}^D (Q_i L_j) \bar{X}_k. \quad (\text{C.8})$$

As can be seen from Eq. (C.7), in the Z_2^L symmetric case the scalar exotic quarks can decay into two quarks (they are diquarks), while in the Z_2^B symmetric case, Eq. (C.8), they decay into a lepton and a quark (they are leptoquarks).

To give masses to the gauge bosons, to the Standard Model fermions, to the exotic quarks and to the first two generation of Higgs-like doublets (so-called ‘‘inert Higgses’’) it is sufficient that the neutral scalar components of H_{13} , H_{23} and S_3 have non-zero vacuum expectation values

$$\langle h_{23}^0 \rangle = v_2/\sqrt{2}, \quad \langle h_{13}^0 \rangle = v_1/\sqrt{2}, \quad \langle s_3 \rangle = v_3/\sqrt{2}. \quad (\text{C.9})$$

To ensure this, the following hierarchy between the Yukawa couplings is imposed

$$\kappa_i \sim \lambda_3 \gtrsim \lambda_{1,2} \gg f_{\alpha\beta}, \tilde{f}_{\alpha\beta}, h_{4j}^E, h_{4j}^N. \quad (\text{C.10})$$

This hierarchy allows to approximate the E_6 SSM superpotential (C.5) as

$$\begin{aligned} \mathcal{W}_{E_6\text{SSM}} &\approx -y_\tau(H_{13}L_3)\bar{E}_3 - y_b(H_{13}Q_3)\bar{D}_3 - y_t(Q_3H_{23})\bar{U}_3 \\ &\quad + \lambda_i S_3(H_{1i}H_{2i}) + \kappa_i S_3 X_i \bar{X}_i + \mu'(H'\bar{H}'), \end{aligned} \quad (\text{C.11})$$

where the right-handed neutrinos are assumed to be integrated out and only dominant terms are kept. Note that in the superpotential (C.11), the singlet VEV generates an effective μ -term of the form $\mu_{\text{eff}} := \lambda_3 v_3/\sqrt{2}$, just as in the NMSSM, see Section 2.2.2. Further model details, as the Higgs potential, electroweak symmetry breaking conditions and mass eigenstates of all the particles have been presented in Ref. [54].

C.4 The constrained E_6 SSM

The Constrained Exceptional Supersymmetric Standard Model (CE₆SSM) [54] is a variant of the Exceptional Supersymmetric Standard Model (E₆SSM) where the soft squared masses m_k^2 of all $(\mathbf{27})_i$ scalars, the soft trilinear couplings A_i and the gaugino masses M_i unify at the GUT scale M_X (the scale where $\sqrt{5/3}g_Y = g_2$)

$$m_k^2(M_X) = m_0^2 \quad \text{for all scalars } k \text{ in } (\mathbf{27})_i, \quad (\text{C.12a})$$

$$A_i(M_X) = A_0, \quad (\text{C.12b})$$

$$M_i(M_X) = M_{1/2}. \quad (\text{C.12c})$$

These unification constraints are well-motivated by supergravity models of supersymmetry breaking [14]. The soft scalar masses of the survival Higgs bosons $m_{h'}^2, m_{\bar{h}'}^2$ are not assumed to be unified with m_0^2 , because they stem from incomplete $(\mathbf{27})'$ and $(\overline{\mathbf{27}})'$ representations of the E_6 . The soft bilinear term $B\mu'$ is also unconstrained.

Due to the simplified superpotential (C.11), the constraints (C.12), and VEVs (C.9) the CE₆SSM introduces the following 16 new parameters compared to the Standard Model⁴

$$g_N, \lambda_i \ (i = 1, 2, 3), \kappa_i \ (i = 1, 2, 3), \tan \beta, v_3, \quad (\text{C.13})$$

$$m_0^2, M_{1/2}, A_0, \mu', B\mu', m_{h'}^2, m_{\bar{h}'}^2,$$

where $\tan \beta = v_2/v_1$. Since the CE₆SSM is a GUT model, the new gauge coupling g_N is restricted at the GUT scale to unify with g_1 and g_2

$$g_1(M_X) = g_1'(M_X) = g_2(M_X) = g_3(M_X), \quad (\text{C.14})$$

where the GUT-normalized gauge couplings $g_1 := \sqrt{5/3}g_Y$ and $g_1' := \sqrt{40}g_N$ were introduced. The three non-zero vacuum expectation values of the Higgs fields lead to three electroweak symmetry breaking conditions

$$0 = \left. \frac{\partial V_{\text{Higgs}}}{\partial v_i} \right|_{h_{13}=h_{23}=s_3=0} \quad (i = 1, 2, 3), \quad (\text{C.15})$$

which demand that the scalar Higgs potential V_{Higgs} has an extremum. These conditions can fix further three of the parameters in (C.13). In Refs. [54, 57] these are chosen to be $m_0^2, M_{1/2}$ and A_0 . This leaves the following 12 free parameters in the CE₆SSM

$$\lambda_i \ (i = 1, 2, 3), \kappa_i \ (i = 1, 2, 3), \tan \beta, v_3, \mu', B\mu', m_{h'}^2, m_{\bar{h}'}^2. \quad (\text{C.16})$$

⁴The gauge couplings g_Y, g_2, g_3 as well as the Yukawa couplings y_t, y_b, y_τ are considered to be Standard Model parameters here. They are fixed by the known values of $\alpha_{\text{e.m.}}^{\text{SM}, \overline{\text{MS}}}(m_Z), \alpha_s^{\text{SM}, \overline{\text{MS}}}(m_Z), \theta_W^{\text{SM}, \overline{\text{MS}}}(m_Z), m_t^{\text{pole}}, m_b^{\text{SM}, \overline{\text{MS}}}(m_Z), m_\tau^{\text{pole}}$ [11].

C.5 Mass eigenstates

C.5.1 Higgs sector

The Higgs bosons in the E_6 SSM are written as

$$h_{pi} = \begin{pmatrix} h_{pi}^1 \\ h_{pi}^2 \end{pmatrix}, \quad s_i, \quad (\text{C.17})$$

where $i = 1, 2, 3$ is the generation index. The index $p = 1, 2$ labels the Higgs bosons which give masses to the down-type ($p = 1$) and up-type ($p = 2$) fermions, respectively. When the $SU(2)_L \times U(1)_Y \times U(1)_N$ is broken to $U(1)_{\text{em}}$ the third generation Higgs bosons get a vacuum expectation value

$$h_{13} = \begin{pmatrix} h_{13}^0 \\ h_{13}^- \end{pmatrix} \rightarrow \begin{pmatrix} \frac{v_1}{\sqrt{2}} + \Re h_{13}^0 + i \Im h_{13}^0 \\ h_{13}^- \end{pmatrix}, \quad (\text{C.18})$$

$$h_{23} = \begin{pmatrix} h_{23}^+ \\ h_{23}^0 \end{pmatrix} \rightarrow \begin{pmatrix} h_{23}^+ \\ \frac{v_2}{\sqrt{2}} + \Re h_{23}^0 + i \Im h_{23}^0 \end{pmatrix}, \quad (\text{C.19})$$

$$s_3 \rightarrow \frac{v_3}{\sqrt{2}} + \Re s_3 + i \Im s_3. \quad (\text{C.20})$$

The following abbreviations are introduced:

$$v := \sqrt{v_2^2 + v_1^2}, \quad \tan \beta := \frac{v_2}{v_1}, \quad \tan \phi := \frac{v}{2v_3} \sin 2\beta, \quad \mu_{\text{eff},i} := \frac{\lambda_i v_3}{\sqrt{2}}. \quad (\text{C.21})$$

From the real parts of h_{13}^0 , h_{23}^0 and s_3 three CP-even Higgs bosons are constructed. The diagonalization of the corresponding mass matrix is done in two steps. At first one transforms $\Re h_{13}^0$, $\Re h_{23}^0$ and $\Re s_3$ into intermediate states $(\mathbf{h}_1, \mathbf{h}_2, \mathbf{h}_3)$ as

$$\begin{pmatrix} \Re h_{13}^0 \\ \Re h_{23}^0 \\ \Re s_3 \end{pmatrix} = U_{\text{MSSM}} \frac{1}{\sqrt{2}} \begin{pmatrix} \mathbf{h}_1 \\ \mathbf{h}_2 \\ \mathbf{h}_3 \end{pmatrix} + \frac{1}{\sqrt{2}} \begin{pmatrix} v_1 \\ v_2 \\ v_3 \end{pmatrix}, \quad (\text{C.22})$$

where the mixing matrix U_{MSSM} has the form

$$U_{\text{MSSM}} = \begin{pmatrix} \cos \beta & -\sin \beta & 0 \\ \sin \beta & \cos \beta & 0 \\ 0 & 0 & 1 \end{pmatrix}. \quad (\text{C.23})$$

In the basis of $\mathbf{h} = (\mathbf{h}_1, \mathbf{h}_2, \mathbf{h}_3)^T$ the Lagrangian for the CP even Higgs masses reads

$$\mathcal{L}_{\text{even}} = -\frac{1}{2} \mathbf{h}^T M_{\text{MSSM}} \mathbf{h}, \quad (\text{C.24})$$

where the matrix M_{MSSM} is non-diagonal in general. Note that the above transformation is analogous to the MSSM, where the mixing angle in U_{MSSM} is β . In a

second step one diagonalizes the mass matrix M_{MSSM} by the unitary matrix U_{E_6} . The resulting CP-even Higgs mass eigenstates are labeled $h = (h_1, h_2, h_3)^T$. The diagonalization transformation reads

$$h = U_{E_6} \mathbf{h}, \quad M_{E_6} = U_{E_6}^* M_{\text{MSSM}} U_{E_6}^\dagger, \quad (\text{C.25})$$

where M_{E_6} is diagonal. From the gauge eigenstates $\mathbf{A} = (\Im h_{13}^0, \Im h_{23}^0, \Im s_3)^T$ one constructs three CP-odd Higgs boson mass eigenstates $A = (A_1, A_2, A_3)^T \equiv (G^0, G', A^0)^T$ as

$$\frac{1}{\sqrt{2}} A := U_A \mathbf{A}, \quad M_A = U_A^* M U_A^\dagger, \quad (\text{C.26})$$

where M_A is diagonal. The mixing matrix U_A is parametrized as

$$U_A = \begin{pmatrix} \cos \beta & -\sin \beta & 0 \\ -\sin \beta \sin \phi & -\cos \beta \sin \phi & \cos \phi \\ \sin \beta \cos \phi & \cos \beta \cos \phi & \sin \phi \end{pmatrix}. \quad (\text{C.27})$$

Analogous to the MSSM the charged Higgs and goldstone bosons $(h_i^\pm) = (G^\pm, h^\pm)^T$ are constructed from the gauge eigenstates h_{i3}^\pm as

$$h_i^\pm = U_{ij}^\pm h_{j3}^\pm \quad (i, j = 1, 2), \quad \text{where} \quad U^\pm = \begin{pmatrix} \cos \beta & -\sin \beta \\ \sin \beta & \cos \beta \end{pmatrix}. \quad (\text{C.28})$$

C.5.2 Inert Higgs sector

The first two generations ($i = 1, 2$; $p = 1, 2$) Higgs doublets in Eq. (C.17) are called inert Higgs bosons. For each generation $i = 1, 2$ the fields h_{1i}^0, h_{2i}^{0*} are mixed to mass eigenstates h_{ik}^0 with an unitary matrix U_{inert}^{0i} as

$$h_{ik}^0 = (U_{\text{inert}}^{0i})_{kl} \begin{pmatrix} h_{1i}^0 \\ h_{2i}^{0*} \end{pmatrix}_l, \quad U_{\text{inert}}^{0i} = \begin{pmatrix} \cos \theta_i^0 & \sin \theta_i^0 \\ -\sin \theta_i^0 & \cos \theta_i^0 \end{pmatrix}. \quad (\text{C.29})$$

Here $k, l = 1, 2$ enumerates the mass eigenstates and inter-generation mixing is neglected. Furthermore, for each generation $i = 1, 2$ the fields h_{1i}^-, h_{2i}^{+*} mix to mass eigenstates h_{ik}^- with an unitary matrix $U_{\text{inert}}^{\pm i}$ as

$$h_{ik}^- = (U_{\text{inert}}^{\pm i})_{kl} \begin{pmatrix} h_{1i}^- \\ h_{2i}^{+*} \end{pmatrix}_l, \quad U_{\text{inert}}^{\pm i} = \begin{pmatrix} \cos \theta_i^\pm & \sin \theta_i^\pm \\ -\sin \theta_i^\pm & \cos \theta_i^\pm \end{pmatrix}. \quad (\text{C.30})$$

Here $k, l = 1, 2$ enumerates again the mass eigenstates and inter-generation mixing is neglected. Furthermore, for each generation $i = 1, 2$ the higgsinos $\tilde{h}_{1iL}^0, \tilde{h}_{2iL}^0$ mix to mass eigenstates ψ_{li}^0 with an unitary matrix Z as

$$\psi_{li}^0 = Z_{ln} \begin{pmatrix} \tilde{h}_{1iL}^0 \\ \tilde{h}_{2iL}^0 \end{pmatrix}_n, \quad Z = \frac{1}{\sqrt{2}} \begin{pmatrix} 1 & 1 \\ -1 & 1 \end{pmatrix}. \quad (\text{C.31})$$

The Majorana mass eigenstates are then defined as

$$\tilde{h}_{i0}^0 = \begin{pmatrix} \psi_{i0}^0 \\ \psi_{i0}^{0T} \end{pmatrix}. \quad (\text{C.32})$$

The charged higgsinos $\tilde{h}_{1iL}^-, \tilde{h}_{2iL}^+$ are combined to mass eigenstates \tilde{h}_i^-

$$\tilde{h}_i^- = \begin{pmatrix} \tilde{h}_{1iL}^- \\ \tilde{h}_{2iL}^+ \end{pmatrix}. \quad (\text{C.33})$$

C.5.3 Survival Higgs sector

The neutral survival Higgs bosons h'^0, \bar{h}'^0 mix to mass eigenstates $h'_k{}^0$ with an unitary matrix U_{surv}^0 as

$$h'_k{}^0 = (U_{\text{surv}}^0)_{kl} \begin{pmatrix} h'^0 \\ \bar{h}'^{0*} \end{pmatrix}_l, \quad U_{\text{surv}}^0 = \begin{pmatrix} \cos \theta'^0 & \sin \theta'^0 \\ -\sin \theta'^0 & \cos \theta'^0 \end{pmatrix}. \quad (\text{C.34})$$

The charged survival Higgs bosons h'^-, \bar{h}'^+ mix to mass eigenstates $h'_k{}^-$ with an unitary matrix U_{surv}^\pm as

$$h'_k{}^- = (U_{\text{surv}}^\pm)_{kl} \begin{pmatrix} h'^- \\ \bar{h}'^{+*} \end{pmatrix}_l, \quad U_{\text{surv}}^\pm = \begin{pmatrix} \cos \theta'^\pm & \sin \theta'^\pm \\ -\sin \theta'^\pm & \cos \theta'^\pm \end{pmatrix}. \quad (\text{C.35})$$

The survival higgsinos obey the same mixing as the neutral and charged inert higgsinos in Section C.5.2. Their mass eigenstates are denoted as \tilde{h}'^\pm and $\tilde{h}'_i{}^0$ ($i = 1, 2$), respectively.

C.6 Self-energies

C.6.1 W boson

The W^\pm boson 1PI correlation function is decomposed into a transverse and longitudinal part as

$$\Gamma_{W_\mu^+ W_\nu^-}(p) = -g^{\mu\nu}(p^2 - m_W^2) - \left(g^{\mu\nu} - \frac{p^\mu p^\nu}{p^2} \right) \Pi_{WW,T}(p^2) - \frac{p^\mu p^\nu}{p^2} \Pi_{WW,L}(p^2). \quad (\text{C.36})$$

The $\overline{\text{DR}}$ renormalized transverse part is denoted as $\hat{\Pi}_{WW,T}(p^2)$, where the divergences $\Delta = 1/\epsilon - \gamma_E + \ln 4\pi$ are subtracted. In the E_6 SSM it reads

$$\frac{(4\pi)^2}{g_2^2} \hat{\Pi}_{WW,T}^{\text{E}_6\text{SSM}}(p^2) = \frac{1}{4} \sum_{i=1}^3 \sum_{k=1}^2 \left\{ (U_{ik}^{A*})^2 A_0(m_{A_i}) + (U_{ik}^{E_6*})^2 A_0(m_{h_i}) \right\}$$

$$\begin{aligned}
 & + \frac{1}{2}A_0(m_{h^\pm}) + \frac{1}{2}A_0(m_{G^\pm}) + m_W^2 \sum_{i=1}^3 \left(U_{i1}^{E_6^*} \right)^2 B_0(p^2, m_{h_i}, m_W) \\
 & - \sum_{i=1}^3 \sum_{j=1}^2 \left| U_{i1}^A U_{j1}^\pm + U_{i2}^A U_{j2}^\pm \right|^2 B_{22}(p^2, m_{A_i}, m_{h_j^\pm}) \\
 & - \sum_{i=1}^3 \sum_{j=1}^2 \left| \sum_{k=1}^3 U_{ik}^{E_6} \left(U_{1k}^{\text{MSSM}} U_{j1}^\pm - U_{2k}^{\text{MSSM}} U_{j2}^\pm \right) \right|^2 B_{22}(p^2, m_{A_i}, m_{h_j^\pm}) \\
 & + \sum_{i,l=1}^2 \left\{ \frac{1}{2} \left(|Z_{l1}|^2 + |Z_{l2}|^2 \right) H(p^2, m_{\tilde{h}_i^\pm}, m_{\tilde{h}_{li}^0}) \right. \\
 & \quad \left. - 2Z_{l1}Z_{l2}m_{\tilde{h}_i^\pm}m_{\tilde{h}_{li}^0} B_0(p^2, m_{\tilde{h}_i^\pm}, m_{\tilde{h}_{li}^0}) \right\} \\
 & - 2 \sum_{i=1}^2 \left\{ \cos^2(\theta_i^0 + \theta_i^\pm) \left(\tilde{B}_{22}(p^2, m_{h_{i1}^\pm}, m_{h_{i1}^0}) + \tilde{B}_{22}(p^2, m_{h_{i2}^\pm}, m_{h_{i2}^0}) \right) \right. \\
 & \quad \left. + \sin^2(\theta_i^0 + \theta_i^\pm) \left(\tilde{B}_{22}(p^2, m_{h_{i1}^\pm}, m_{h_{i2}^0}) + \tilde{B}_{22}(p^2, m_{h_{i2}^\pm}, m_{h_{i1}^0}) \right) \right\} \\
 & + \sum_{l=1}^2 \left\{ \frac{1}{2} \left(|Z'_{l1}|^2 + |Z'_{l2}|^2 \right) H(p^2, m_{\tilde{h}'_l}, m_{\tilde{h}'_l^0}) \right. \\
 & \quad \left. - 2Z'_{l1}Z'_{l2}m_{\tilde{h}'_l}m_{\tilde{h}'_l^0} B_0(p^2, m_{\tilde{h}'_l}, m_{\tilde{h}'_l^0}) \right\} \\
 & - 2 \sum_{i=1}^2 \left\{ \cos^2(\theta^0 + \theta^\pm) \left(\tilde{B}_{22}(p^2, m_{h'_{i1}^\pm}, m_{h'_{i1}^0}) + \tilde{B}_{22}(p^2, m_{h'_{i2}^\pm}, m_{h'_{i2}^0}) \right) \right. \\
 & \quad \left. + \sin^2(\theta^0 + \theta^\pm) \left(\tilde{B}_{22}(p^2, m_{h'_{i1}^\pm}, m_{h'_{i2}^0}) + \tilde{B}_{22}(p^2, m_{h'_{i2}^\pm}, m_{h'_{i1}^0}) \right) \right\} \\
 & + 4m_W^2 \frac{g_N^2}{g_2^2} \left\{ \left(\frac{N_{H13}}{2} + \frac{N_{H23}}{2} \right)^2 \sin^2 \beta \cos^2 \beta B_0(p^2, m_{h^\pm}, m_{Z'}) \right. \\
 & \quad \left. + \left(\frac{N_{H23}}{2} \sin^2 \beta - \frac{N_{H13}}{2} \cos^2 \beta \right)^2 B_0(p^2, m_{G^\pm}, m_{Z'}) \right\} \\
 & - s_W^2 \left(8\tilde{B}_{22}(p^2, m_W, 0) + 4p^2 B_0(p^2, m_W, 0) \right) \\
 & - \left\{ (4p^2 + m_Z^2 + m_W^2)c_W^2 - m_Z^2 s_W^4 \right\} B_0(p^2, m_Z, m_W) \\
 & - 8c_W^2 \tilde{B}_{22}(p^2, m_Z, m_W) \\
 & + \sum_{f_u/f_d} \left\{ \frac{1}{2} N_c^f H(p^2, m_u, m_d) - \sum_{i,j=1}^2 2N_c^f w_{fij}^2 \tilde{B}_{22}(p^2, m_{\tilde{u}_i}, m_{\tilde{d}_j}) \right\} \\
 & + \frac{1}{g_2^2} \sum_{i=1}^6 \sum_{j=1}^2 \left\{ f_{ijW} H(p^2, m_{\tilde{\chi}_i^0}, m_{\tilde{\chi}_j^+}) + 2g_{ijW} m_{\tilde{\chi}_i^0} m_{\tilde{\chi}_j^+} B_0(p^2, m_{\tilde{\chi}_i^0}, m_{\tilde{\chi}_j^+}) \right\}
 \end{aligned} \tag{C.37}$$

Analogous to [179] the symbol \sum_{f_u/f_d} sums over quark and lepton doublets and

$$(w_{fij}) = \begin{pmatrix} c_u c_d & c_u s_d \\ s_u c_d & s_u s_d \end{pmatrix}. \quad (\text{C.38})$$

The neutralino–chargino–W-boson couplings are given by

$$f_{ijW} = |a_{\tilde{\chi}_i^0 \tilde{\chi}_j^+ W}|^2 + |b_{\tilde{\chi}_i^0 \tilde{\chi}_j^+ W}|^2, \quad g_{ijW} = 2 \Re \left(b_{\tilde{\chi}_i^0 \tilde{\chi}_j^+ W}^* a_{\tilde{\chi}_i^0 \tilde{\chi}_j^+ W} \right), \quad (\text{C.39})$$

where the Feynman rule for the neutralino–chargino– W_μ vertex is written as $-i\gamma_\mu(aP_L + bP_R)$. The nonzero couplings in the E_6 SSM are the same as in the MSSM

$$a_{\tilde{\psi}_2^0 \tilde{\psi}_1^+ W} = b_{\tilde{\psi}_2^0 \tilde{\psi}_1^+ W} = -g_2, \quad a_{\tilde{\psi}_4^0 \tilde{\psi}_2^+ W} = -b_{\tilde{\psi}_3^0 \tilde{\psi}_2^+ W} = \frac{g_2}{\sqrt{2}}. \quad (\text{C.40})$$

The couplings to mass eigenstates for an incoming neutralino $\tilde{\chi}_i^0$ are

$$a_{\tilde{\chi}_i^0 \tilde{\chi}_j^+ W} = N_{ik}^* V_{jl} a_{\tilde{\psi}_k^0 \tilde{\psi}_l^+ W}, \quad b_{\tilde{\chi}_i^0 \tilde{\chi}_j^+ W} = N_{ik} U_{jl}^* b_{\tilde{\psi}_k^0 \tilde{\psi}_l^+ W}, \quad (\text{C.41})$$

while for an incoming chargino $\tilde{\chi}_j^+$ the couplings read

$$a_{\tilde{\chi}_i^0 \tilde{\chi}_j^+ W} = N_{ik} V_{jl}^* a_{\tilde{\psi}_k^0 \tilde{\psi}_l^+ W}, \quad b_{\tilde{\chi}_i^0 \tilde{\chi}_j^+ W} = N_{ik}^* U_{jl} b_{\tilde{\psi}_k^0 \tilde{\psi}_l^+ W}. \quad (\text{C.42})$$

C.6.2 Fermions

The general fermion 1PI correlation function can be decomposed as

$$\Gamma_{f\bar{f}}(p) = \not{p} \left[P_L \Gamma_{f\bar{f}}^L(p^2) + P_R \Gamma_{f\bar{f}}^R(p^2) \right] + P_L \Gamma_{f\bar{f}}^l(p^2) + P_R \Gamma_{f\bar{f}}^r(p^2) \quad (\text{C.43})$$

and the fermion self-energy is defined as

$$\Sigma_f(p^2) := \frac{1}{2} \left\{ m_f \left[\Gamma_{ff}^L(p^2) + \Gamma_{ff}^R(p^2) \right] + \Gamma_{ff}^l(p^2) + \Gamma_{ff}^r(p^2) \right\}. \quad (\text{C.44})$$

In the following the $\overline{\text{DR}}$ renormalized fermion self-energies $\hat{\Sigma}_f$ are listed, where the divergences $\Delta = 1/\epsilon - \gamma_E + \ln 4\pi$ are subtracted. In the E_6 SSM they are given by

$$\begin{aligned} (4\pi)^2 \frac{\hat{\Sigma}_t(p^2)}{m_t} &= \frac{4g_3^2}{3} \left\{ B_1(p^2, m_{\tilde{g}}, m_{\tilde{t}_1}) + B_1(p^2, m_{\tilde{g}}, m_{\tilde{t}_2}) - \left(5 + 3 \ln \frac{\mu^2}{m_{\tilde{t}}^2} \right) \right. \\ &\quad \left. - \sin(2\theta_t) \frac{m_{\tilde{g}}}{m_t} \left[B_0(p^2, m_{\tilde{g}}, m_{\tilde{t}_1}) - B_0(p^2, m_{\tilde{g}}, m_{\tilde{t}_2}) \right] \right\} \\ &\quad + \frac{y_t^2}{2} \sum_{i=1}^3 \left\{ \underline{A}_{ti}^2 \left[B_1(p^2, m_t, m_{h_i}) + B_0(p^2, m_t, m_{h_i}) \right] \right. \\ &\quad \left. + \underline{B}_{ti}^2 \left[B_1(p^2, m_t, m_{A_i}) - B_0(p^2, m_t, m_{A_i}) \right] \right\} \end{aligned}$$

$$\begin{aligned}
 & + \frac{1}{2} \left[(y_b^2 s_\beta^2 + y_t^2 c_\beta^2) B_1(p^2, m_b, m_{h^+}) + (g_2^2 + y_b^2 c_\beta^2 + y_t^2 s_\beta^2) B_1(p^2, m_b, m_W) \right] \\
 & + y_b^2 c_\beta^2 \left[B_0(p^2, m_b, m_{h^+}) - B_0(p^2, m_b, m_W) \right] - (ee_t)^2 \left(5 + 3 \ln \frac{\mu^2}{m_t^2} \right) \\
 & + \frac{g_2^2}{c_W^2} \left[(g_{t_L}^2 + g_{t_R}^2) B_1(p^2, m_t, m_Z) + 4g_{t_L} g_{t_R} B_0(p^2, m_t, m_Z) \right] \\
 & + \frac{1}{2} \sum_{i=1}^6 \sum_{j=1}^2 \left[f_{it\bar{t}_j} B_1(p^2, m_{\tilde{\chi}_i^0}, m_{\bar{t}_j}) + g_{it\bar{t}_j} \frac{m_{\tilde{\chi}_i^0}}{m_t} B_0(p^2, m_{\tilde{\chi}_i^0}, m_{\bar{t}_j}) \right] \\
 & + \frac{1}{2} \sum_{i,j=1}^2 \left[f_{it\bar{b}_j} B_1(p^2, m_{\tilde{\chi}_i^+}, m_{\bar{b}_j}) + g_{it\bar{b}_j} \frac{m_{\tilde{\chi}_i^+}}{m_t} B_0(p^2, m_{\tilde{\chi}_i^+}, m_{\bar{b}_j}) \right] \\
 & + g_N^2 \left[\left(\left(\frac{N_{t_L}}{2} \right)^2 + \left(\frac{N_{t_R}}{2} \right)^2 \right) B_1(p^2, m_t, m_{Z'}) + N_{t_L} N_{t_R} B_0(p^2, m_t, m_{Z'}) \right].
 \end{aligned} \tag{C.45}$$

The matrix elements \underline{A}_{fi} and \underline{B}_{fi} are defined as

$$\underline{A}_{fi} = \begin{cases} (U_{\text{MSSM}})_{2k} (U_{E_6})_{ik}^* & \text{if } f \text{ is up-type,} \\ (U_{\text{MSSM}})_{1k} (U_{E_6})_{ik}^* & \text{if } f \text{ is down-type,} \end{cases} \tag{C.46}$$

$$\underline{B}_{fi} = \begin{cases} (U_A)_{i2}^* & \text{if } f \text{ is up-type,} \\ (U_A)_{i1}^* & \text{if } f \text{ is down-type.} \end{cases} \tag{C.47}$$

In analogy to [179] the Feynman rules for the $\tilde{\chi}_i f \tilde{f}_j$ couplings are written as $-i(aP_L + bP_R)$ and the following abbreviations are defined:

$$f_{if\tilde{f}_j} = |a_{\tilde{\chi}_i f \tilde{f}_j}|^2 + |b_{\tilde{\chi}_i f \tilde{f}_j}|^2, \quad g_{if\tilde{f}_j} = 2 \Re(b_{\tilde{\chi}_i f \tilde{f}_j}^* a_{\tilde{\chi}_i f \tilde{f}_j}). \tag{C.48}$$

In the gauge eigenstate basis $\tilde{\psi}^0, \tilde{\psi}^+$ one has

$$a_{\tilde{\psi}_1^0 f \tilde{f}_R} = \frac{g_Y}{\sqrt{2}} Y_{f_R}, \quad b_{\tilde{\psi}_1^0 f \tilde{f}_L} = \frac{g_Y}{\sqrt{2}} Y_{f_L} \tag{C.49}$$

$$b_{\tilde{\psi}_2^0 f \tilde{f}_L} = \sqrt{2} g_2 \tau_3^{fL}, \quad a_{\tilde{\psi}_1^+ d \tilde{u}_L} = b_{\tilde{\psi}_1^+ u \tilde{d}_L} = g_2, \tag{C.50}$$

$$a_{\tilde{\psi}_3^0 d \tilde{d}_L} = b_{\tilde{\psi}_3^0 d \tilde{d}_R} = -b_{\tilde{\psi}_2^+ d \tilde{u}_L} = -b_{\tilde{\psi}_2^+ u \tilde{d}_R} = y_d, \tag{C.51}$$

$$a_{\tilde{\psi}_4^0 u \tilde{u}_L} = b_{\tilde{\psi}_4^0 u \tilde{u}_R} = -a_{\tilde{\psi}_2^+ u \tilde{d}_L} = -a_{\tilde{\psi}_2^+ d \tilde{u}_R} = y_u, \tag{C.52}$$

$$a_{\tilde{\psi}_6^0 f \tilde{f}_R} = \frac{g_N}{\sqrt{2}} N_{f_R}, \quad b_{\tilde{\psi}_6^0 f \tilde{f}_L} = \frac{g_N}{\sqrt{2}} N_{f_L}, \tag{C.53}$$

where the quantum numbers $Y_f/2$, $N_f/2$ and τ_3^f are listed in the Table C.1. The couplings to the mass eigenstates $\tilde{\chi}_i^0$ and $\tilde{\chi}_i^+$ are obtained by the rotations

$$a_{\tilde{\chi}_i^0 f \tilde{f}} = N_{ij}^* a_{\tilde{\psi}_j^0 f \tilde{f}}, \quad b_{\tilde{\chi}_i^0 f \tilde{f}} = N_{ij} b_{\tilde{\psi}_j^0 f \tilde{f}}, \tag{C.54}$$

$$a_{\tilde{\chi}_i^+ f \tilde{f}'} = V_{ij}^* a_{\tilde{\psi}_j^+ f \tilde{f}'}, \quad b_{\tilde{\chi}_i^+ f \tilde{f}'} = U_{ij} b_{\tilde{\psi}_j^+ f \tilde{f}'}. \tag{C.55}$$

To obtain the couplings to the sfermion mass eigenstates one rotates these couplings (both a - and b -type) by the sfermion mixing matrix,

$$\begin{pmatrix} a_{\tilde{\chi}f\tilde{f}'_1} \\ a_{\tilde{\chi}f\tilde{f}'_2} \end{pmatrix} = \begin{pmatrix} c_{f'} & s_{f'} \\ -s_{f'} & c_{f'} \end{pmatrix} \begin{pmatrix} a_{\tilde{\chi}f\tilde{f}'_L} \\ a_{\tilde{\chi}f\tilde{f}'_R} \end{pmatrix}. \quad (\text{C.56})$$

The self-energies for the other fermions are obtained from $\hat{\Sigma}_t$ by the substitutions

$$\hat{\Sigma}_\tau(p^2) = \hat{\Sigma}_t(p^2) \Big|_{t \rightarrow b, g_3=0}, \quad (\text{C.57})$$

$$\hat{\Sigma}_b(p^2) = \hat{\Sigma}_t(p^2) \Big|_{t \rightarrow b, c_\beta \leftrightarrow s_\beta}. \quad (\text{C.58})$$

In Eqs. (C.37) and (C.45) the Passarino-Veltman loop functions in the convention [179] are used. Finally, the one-loop bottom quark self-energy in the 5-flavour QCD reads

$$(4\pi)^2 \frac{\hat{\Sigma}_b^{(5)}(p^2)}{m_b^{(5)}} = -\frac{4g_3^2}{3} \left(5 + 3 \ln \frac{\mu^2}{m_b^2} \right). \quad (\text{C.59})$$

C.7 Gauge coupling threshold corrections

Gauge coupling threshold corrections Δg relate the gauge couplings between two different models. Here the E_6 SSM is considered to be a full theory and the Standard Model to be an effective theory, where all new E_6 SSM particles have been integrated out. In this setup the threshold corrections relate the E_6 SSM to the SM gauge couplings as

$$g_i^{\overline{\text{DR}}, E_6\text{SSM}}(\mu) = g_i^{\overline{\text{MS}}, \text{SM}}(\mu) + \Delta g_i(\mu) \quad (i = 1, 2, 3). \quad (\text{C.60})$$

As described in [57], the Δg_i can be calculated by matching all Green functions (and their derivatives), which are one-particle irreducible with respect to the light (Standard Model) fields l_i , at zero external momentum $k_i = 0$

$$\partial_{k_i}^n \Gamma_{l_{i_1} l_{i_2} \dots l_{i_n}}^{E_6\text{SSM}} \Big|_{k_i=0} = \partial_{k_i}^n \Gamma_{l_{i_1} l_{i_2} \dots l_{i_n}}^{\text{SM}} \Big|_{k_i=0}. \quad (\text{C.61})$$

These matching conditions will lead to relations between the model parameters of the E_6 SSM and the Standard Model. To obtain the threshold corrections for the gauge couplings, the following relations have to be imposed [57]

$$\partial_p \Gamma_{q_i \bar{q}_i}^{E_6\text{SSM}}(p, -p) \Big|_{p=0} = \partial_p \Gamma_{q_i \bar{q}_i}^{\text{SM}}(p, -p) \Big|_{p=0}, \quad (\text{C.62a})$$

$$\partial_{k^2} \Gamma_{G_\mu^a G_\nu^b}^{E_6\text{SSM}}(k, -k) \Big|_{k^2=0} = \partial_{k^2} \Gamma_{G_\mu^a G_\nu^b}^{\text{SM}}(k, -k) \Big|_{k^2=0}, \quad (\text{C.62b})$$

$$\Gamma_{G_\mu^a q_i \bar{q}_i}^{E_6\text{SSM}}(k, p, -(p+k)) \Big|_{p=k=0} = \Gamma_{G_\mu^a q_i \bar{q}_i}^{\text{SM}}(k, p, -(p+k)) \Big|_{p=k=0}, \quad (\text{C.62c})$$

$$\partial_{k^2}^n \Gamma_{W_\mu^+ W_\nu^-}^{\text{E}_6\text{SSM}}(k, -k) \Big|_{k^2=0} = \partial_{k^2}^n \Gamma_{W_\mu^+ W_\nu^-}^{\text{SM}}(k, -k) \Big|_{k^2=0} \quad (n = 0, 1), \quad (\text{C.62d})$$

$$\partial_{k^2}^n \Gamma_{Z_\mu Z_\nu}^{\text{E}_6\text{SSM}}(k, -k) \Big|_{k^2=0} = \partial_{k^2}^n \Gamma_{Z_\mu Z_\nu}^{\text{SM}}(k, -k) \Big|_{k^2=0} \quad (n = 0, 1), \quad (\text{C.62e})$$

$$\partial_{k^2} \Gamma_{A_\mu A_\nu}^{\text{E}_6\text{SSM}}(k, -k) \Big|_{k^2=0} = \partial_{k^2} \Gamma_{A_\mu A_\nu}^{\text{SM}}(k, -k) \Big|_{k^2=0}, \quad (\text{C.62f})$$

$$\Gamma_{Z_\mu A_\nu}^{\text{E}_6\text{SSM}}(k, -k) \Big|_{k^2=0} = \Gamma_{Z_\mu A_\nu}^{\text{SM}}(k, -k) \Big|_{k^2=0}, \quad (\text{C.62g})$$

$$\partial_p \Gamma_{\psi_{Li} \bar{\psi}_{Lj}}^{\text{E}_6\text{SSM}}(p, -p) \Big|_{p=0} = \partial_p \Gamma_{\psi_{Li} \bar{\psi}_{Lj}}^{\text{SM}}(p, -p) \Big|_{p=0}, \quad (\text{C.62h})$$

$$\partial_p \Gamma_{\psi_{Ri} \bar{\psi}_{Rj}}^{\text{E}_6\text{SSM}}(p, -p) \Big|_{p=0} = \partial_p \Gamma_{\psi_{Ri} \bar{\psi}_{Rj}}^{\text{SM}}(p, -p) \Big|_{p=0}, \quad (\text{C.62i})$$

$$\Gamma_{A_\mu \psi_i \bar{\psi}_j}^{\text{E}_6\text{SSM}}(k, p, -(p+k)) \Big|_{k=p=0} = \Gamma_{A_\mu \psi_i \bar{\psi}_j}^{\text{SM}}(k, p, -(p+k)) \Big|_{k=p=0}. \quad (\text{C.62j})$$

The field A_μ denotes the photon, Z_μ and W_μ^\pm are the gauge bosons of the weak interaction and ψ_i denote the Standard Model quarks and leptons. Evaluating the Eqs. (C.62) leads to the following gauge coupling threshold corrections:

$$\begin{aligned} \Delta g_1(\mu) = \frac{3}{5} \frac{g_1^3}{(4\pi)^2} & \left[-\frac{4}{3} N_c \sum_{i=1}^3 \left(\frac{Y_{X_i}}{2} \right)^2 \log \frac{m_{x_i}}{\mu} - \frac{1}{3} N_c \sum_{i=1}^3 \sum_{k=1}^2 \left(\frac{Y_{X_i}}{2} \right)^2 \log \frac{m_{\tilde{x}_{ik}}}{\mu} \right. \\ & - \frac{1}{3} N_c \sum_{i=1}^3 \sum_{k=L,R} \left\{ \left(\frac{Y_{\tilde{u}_{ik}}}{2} \right)^2 \log \frac{m_{\tilde{u}_{ik}}}{\mu} + \left(\frac{Y_{\tilde{d}_{ik}}}{2} \right)^2 \log \frac{m_{\tilde{d}_{ik}}}{\mu} \right\} \\ & - \frac{1}{3} \sum_{i=1}^3 \sum_{k=L,R} \left(\frac{Y_{\tilde{e}_{ik}}}{2} \right)^2 \log \frac{m_{\tilde{e}_{ik}}}{\mu} - \frac{1}{3} \sum_{i=1}^3 \left(\frac{Y_{\tilde{\nu}_{iL}}}{2} \right)^2 \log \frac{m_{\tilde{\nu}_{iL}}}{\mu} \\ & - \frac{1}{3} \sum_{i=1}^2 \sum_{p=1}^2 \sum_{j=1}^2 \left(\frac{Y_{h_{pi}^j}}{2} \right)^2 \log \frac{m_{h_{pi}^j}}{\mu} - \frac{1}{3} \sum_{j=1}^2 \left(\frac{Y_{h_{23}^j}}{2} \right)^2 \log \frac{m_h}{\mu} \\ & - \frac{2}{3} \sum_{i=1}^3 \sum_{p=1}^2 \sum_{j=1}^2 \left(\frac{Y_{\tilde{h}_{piL}^j}}{2} \right)^2 \log \frac{m_{\tilde{h}_{piL}^j}}{\mu} \\ & - \frac{1}{3} \sum_{j=1}^2 \left(\frac{Y_{h'^j}}{2} \right)^2 \log \frac{m_{h'^j}}{\mu} - \frac{2}{3} \sum_{j=1}^2 \left(\frac{Y_{\tilde{h}'_L{}^j}}{2} \right)^2 \log \frac{m_{\tilde{h}'_L{}^j}}{\mu} \\ & \left. - \frac{1}{3} \sum_{j=1}^2 \left(\frac{Y_{\tilde{h}''^j}}{2} \right)^2 \log \frac{m_{\tilde{h}''^j}}{\mu} - \frac{2}{3} \sum_{j=1}^2 \left(\frac{Y_{\tilde{h}''_L{}^j}}{2} \right)^2 \log \frac{m_{\tilde{h}''_L{}^j}}{\mu} \right], \quad (\text{C.63}) \end{aligned}$$

$$\begin{aligned} \Delta g_2(\mu) = \frac{g_2^3}{(4\pi)^2} & \left[\frac{1}{3} - \frac{1}{6} N_c \sum_{i=1}^3 \log \frac{m_{\tilde{q}_{iL}}}{\mu} - \frac{1}{6} \sum_{i=1}^3 \log \frac{m_{\tilde{\ell}_{iL}}}{\mu} - \frac{4}{3} \log \frac{m_{\tilde{W}}}{\mu} - \frac{1}{6} \log \frac{m_h}{\mu} \right. \\ & - \frac{1}{6} \sum_{i=1}^2 \sum_{p=1}^2 \log \frac{m_{h_{pi}}}{\mu} - \frac{1}{3} \sum_{i=1}^3 \sum_{p=1}^2 \log \frac{m_{\tilde{h}_{piL}}}{\mu} - \frac{1}{6} \log \frac{m_{h'}}{\mu} - \frac{1}{3} \log \frac{m_{\tilde{h}'_L}}{\mu} \\ & \left. - \frac{1}{6} \log \frac{m_{\tilde{h}''}}{\mu} - \frac{1}{3} \log \frac{m_{\tilde{h}''_L}}{\mu} \right], \quad (\text{C.64}) \end{aligned}$$

$$\begin{aligned}
 \Delta g_3(\mu) = \frac{g_3^3}{(4\pi)^2} & \left[\frac{1}{2} - 2 \log \frac{m_{\tilde{g}}}{\mu} - \frac{1}{6} \sum_{\tilde{q} \in \{\tilde{u}, \tilde{d}\}} \sum_{i=1}^3 \sum_{k=1}^2 \log \frac{m_{\tilde{q}_{ik}}}{\mu} \right. \\
 & \left. - \frac{2}{3} \sum_{i=1}^3 \log \frac{m_{x_i}}{\mu} - \frac{1}{6} \sum_{i=1}^3 \sum_{k=1}^2 \log \frac{m_{\tilde{x}_{ik}}}{\mu} \right].
 \end{aligned} \tag{C.65}$$

The μ -dependence in the above equations has been cross-checked against the difference of the E_6 SSM and SM gauge coupling β -functions and are in agreement with the general result [55].

Appendix D

NMSSM SLHA input template file

```
BLOCK MODSEL # Select model
  1 1 # mSUGRA
  3 1 # NMSSM
  6 0 # flavour violation
  8 2 # Higgs 2L corrections
  9 0 # dark matter relic density
 10 0 # no scan
 13 0 # calc decays
BLOCK SMINPUTS # Standard Model inputs
  1 1.279180000e+02 # alpha(-1) SM MSbar(MZ)
  2 1.166390000e-05 # G_Fermi
  3 1.189000000e-01 # alpha_s(MZ) SM MSbar
  4 9.118760000e+01 # MZ(pole)
  5 4.200000000e+00 # mb(mb) SM MSbar
  6 1.709000000e+02 # mtop(pole)
  7 1.777000000e+00 # mtau(pole)
BLOCK SOFTSUSY # SOFTSUSY specific inputs
  1 1.000000000e-04 # tolerance
  2 2.000000000e+00 # up-quark mixing (=1) or down (=2)
  5 1.000000000E+00 # 2-loop running
 18 0.000000000E+00 # use soft Higgs masses as EWSB output
BLOCK VCKMIN # input parameters for CKM matrix
  1 2.272000000e-01 # lambda
  2 8.180000000e-01 # A
  3 2.210000000e-01 # rhobar
  4 3.400000000e-01 # etabar
BLOCK MINPAR
  1 5.000000000e+03 # m_0
  2 5.000000000e+03 # m_12
  3 [0 .. 50] # tan(beta)
  4 1.000000000e+00 # sign(mu)
  5 -5.000000000e+03 # A_0
BLOCK EXTPAR
 61 0.1 # lambda
BLOCK QEXTPAR
 61 -1 # input lambda at Msusy
```


Appendix E

CMSSM speed test SLHA input template file

For the run-time comparison of the different CMSSM spectrum generators in Section 6.4.1 the following SLHA input template file was used:

```
Block MODSEL # Select model
  6 0 # flavour violation
  1 1 # mSUGRA
Block SMINPUTS # Standard Model inputs
  1 1.279180000e+02 # alpha(-1) SM MSbar(MZ)
  2 1.166390000e-05 # G_Fermi
  3 1.189000000e-01 # alpha_s(MZ) SM MSbar
  4 9.118760000e+01 # MZ(pole)
  5 4.200000000e+00 # mb(mb) SM MSbar
  6 1.709000000e+02 # mtop(pole)
  7 1.777000000e+00 # mtau(pole)
Block SOFTSUSY # SOFTSUSY specific inputs
  1 1.000000000e-04 # tolerance
  2 2 # up-quark mixing (=1) or down (=2)
  3 0 # printout
  5 1 # 2-loop running
  7 2 # EWSB and Higgs mass loop order
Block FlexibleSUSY
  0 1.000000000e-04 # precision goal
  1 0 # max. iterations (0 = automatic)
  2 0 # two-scale algorithm
  3 0 # calculate SM pole masses
  4 2 # pole mass loop order
  5 2 # EWSB loop order
  6 2 # beta-functions loop order
  7 1 # threshold corrections (1 = enabled)
Block SPhenoInput # SPheno specific input
  1 -1 # error level
  2 1 # SPA conventions
  11 0 # calculate branching ratios
  13 0 # include 3-Body decays
  31 -1 # dynamical GUT scale
  32 0 # Strict unification
  34 1.000E-04 # Precision of mass calculation
  35 40 # Maximal number of iterations
```

```

37 1          # Set Yukawa scheme
38 2          # 1- or 2-Loop RGEs
50 1          # use only positive masses
51 0          # Write Output in CKM basis
52 0          # Write spectrum in case of tachyons
55 1          # Calculate one loop masses
57 0          # Calculate low energy constraints
60 0          # Include possible, kinetic mixing
65 1          # Solution tadpole equation
75 0          # Write WHIZARD files
76 0          # Write HiggsBounds file
86 0.         # Max. width for invisible in h decays
510 0.        # tree level values for EWSB
515 0         # Write parameter values at GUT scale
520 0.        # Write effective Higgs couplings
525 0.        # Write loop contributions

```

For each parameter point a MINPAR block of the form

```

Block MINPAR
 1  [50..1000]          # m0(MX)
 2  [50..1000]          # m12(MX)
 3  [1..100]           # tan(beta)(MZ) DRbar
 4  {-1,+1}           # sign(mu)
 5  [-1000..1000]      # A0(MX)

```

was appended with concrete values for m_0 , $M_{1/2}$, $\tan\beta$, $\text{sign}\mu$ and A_0 .

Bibliography

- [1] S. R. Coleman and J. Mandula, *All Possible Symmetries of the S Matrix*, *Phys.Rev.* **159**, 1251 (1967).
- [2] R. Haag, J. T. Lopuszanski, and M. Sohnius, *All Possible Generators of Supersymmetries of the s Matrix*, *Nucl. Phys.* **B88**, 257 (1975).
- [3] S. Dimopoulos and S. Raby, *Supercolor*, *Nucl.Phys.* **B192**, 353 (1981).
- [4] E. Witten, *Dynamical Breaking of Supersymmetry*, *Nucl.Phys.* **B188**, 513 (1981).
- [5] M. Dine, W. Fischler, and M. Srednicki, *Supersymmetric Technicolor*, *Nucl.Phys.* **B189**, 575 (1981).
- [6] S. Dimopoulos and H. Georgi, *Softly Broken Supersymmetry and SU(5)*, *Nucl.Phys.* **B193**, 150 (1981).
- [7] N. Sakai, *Naturalness in Supersymmetric Guts*, *Z.Phys.* **C11**, 153 (1981).
- [8] R. K. Kaul and P. Majumdar, *Cancellation of Quadratically Divergent Mass Corrections in Globally Supersymmetric Spontaneously Broken Gauge Theories*, *Nucl.Phys.* **B199**, 36 (1982).
- [9] ATLAS Collaboration, G. Aad *et al.*, *Observation of a new particle in the search for the Standard Model Higgs boson with the ATLAS detector at the LHC*, *Phys.Lett.* **B716**, 1 (2012), 1207.7214.
- [10] CMS Collaboration, S. Chatrchyan *et al.*, *Observation of a new boson at a mass of 125 GeV with the CMS experiment at the LHC*, *Phys.Lett.* **B716**, 30 (2012), 1207.7235.
- [11] Particle Data Group, J. Beringer *et al.*, *Review of Particle Physics (RPP)*, *Phys.Rev.* **D86**, 010001 (2012).
- [12] L. Girardello and M. T. Grisaru, *Soft Breaking of Supersymmetry*, *Nucl.Phys.* **B194**, 65 (1982).
- [13] J. Wess and J. Bagger, *Supersymmetry and supergravity*, (1992).
- [14] A. H. Chamseddine, R. L. Arnowitt, and P. Nath, *Locally Supersymmetric Grand Unification*, *Phys.Rev.Lett.* **49**, 970 (1982).

- [15] M. Dine and A. E. Nelson, *Dynamical supersymmetry breaking at low-energies*, *Phys.Rev.* **D48**, 1277 (1993), hep-ph/9303230.
- [16] M. Dine, A. E. Nelson, and Y. Shirman, *Low-energy dynamical supersymmetry breaking simplified*, *Phys.Rev.* **D51**, 1362 (1995), hep-ph/9408384.
- [17] M. Dine, A. E. Nelson, Y. Nir, and Y. Shirman, *New tools for low-energy dynamical supersymmetry breaking*, *Phys.Rev.* **D53**, 2658 (1996), hep-ph/9507378.
- [18] L. Randall and R. Sundrum, *Out of this world supersymmetry breaking*, *Nucl.Phys.* **B557**, 79 (1999), hep-th/9810155.
- [19] G. F. Giudice, M. A. Luty, H. Murayama, and R. Rattazzi, *Gaugino mass without singlets*, *JHEP* **9812**, 027 (1998), hep-ph/9810442.
- [20] H. E. Haber and G. L. Kane, *The Search for Supersymmetry: Probing Physics Beyond the Standard Model*, *Phys.Rept.* **117**, 75 (1985).
- [21] S. P. Martin, *A Supersymmetry primer*, (1997), hep-ph/9709356.
- [22] G. R. Farrar and P. Fayet, *Phenomenology of the Production, Decay, and Detection of New Hadronic States Associated with Supersymmetry*, *Phys.Lett.* **B76**, 575 (1978).
- [23] S. Weinberg, *Supersymmetry at Ordinary Energies. 1. Masses and Conservation Laws*, *Phys.Rev.* **D26**, 287 (1982).
- [24] N. Sakai and T. Yanagida, *Proton Decay in a Class of Supersymmetric Grand Unified Models*, *Nucl.Phys.* **B197**, 533 (1982).
- [25] S. Dimopoulos, S. Raby, and F. Wilczek, *Proton Decay in Supersymmetric Models*, *Phys.Lett.* **B112**, 133 (1982).
- [26] H. Goldberg, *Constraint on the Photino Mass from Cosmology*, *Phys.Rev.Lett.* **50**, 1419 (1983).
- [27] J. R. Ellis, J. Hagelin, D. V. Nanopoulos, K. A. Olive, and M. Srednicki, *Supersymmetric Relics from the Big Bang*, *Nucl.Phys.* **B238**, 453 (1984).
- [28] M. Carena, G. Nardini, M. Quiros, and C. E. Wagner, *MSSM Electroweak Baryogenesis and LHC Data*, *JHEP* **1302**, 001 (2013), 1207.6330.
- [29] P. Bechtle *et al.*, *Constrained Supersymmetry after the Higgs Boson Discovery: A global analysis with Fittino*, (2013), 1310.3045.
- [30] Muon G-2 Collaboration, G. Bennett *et al.*, *Final Report of the Muon E821 Anomalous Magnetic Moment Measurement at BNL*, *Phys.Rev.* **D73**, 072003 (2006), hep-ex/0602035.

- [31] R. Benbrik *et al.*, *Confronting the MSSM and the NMSSM with the Discovery of a Signal in the two Photon Channel at the LHC*, *Eur.Phys.J.* **C72**, 2171 (2012), 1207.1096.
- [32] A. Arbey, M. Battaglia, A. Djouadi, and F. Mahmoudi, *The Higgs sector of the phenomenological MSSM in the light of the Higgs boson discovery*, *JHEP* **1209**, 107 (2012), 1207.1348.
- [33] P. Fayet, *Supergauge Invariant Extension of the Higgs Mechanism and a Model for the electron and Its Neutrino*, *Nucl.Phys.* **B90**, 104 (1975).
- [34] J. R. Ellis, J. Gunion, H. E. Haber, L. Roszkowski, and F. Zwirner, *Higgs Bosons in a Nonminimal Supersymmetric Model*, *Phys.Rev.* **D39**, 844 (1989).
- [35] M. Drees, *Supersymmetric Models with Extended Higgs Sector*, *Int.J.Mod.Phys.* **A4**, 3635 (1989).
- [36] C. Panagiotakopoulos and A. Pilaftsis, *Higgs scalars in the minimal nonminimal supersymmetric standard model*, *Phys.Rev.* **D63**, 055003 (2001), hep-ph/0008268.
- [37] U. Ellwanger, C. Hugonie, and A. M. Teixeira, *The Next-to-Minimal Supersymmetric Standard Model*, *Phys.Rept.* **496**, 1 (2010), 0910.1785.
- [38] J. P. Hall and S. F. King, *NMSSM+*, *JHEP* **1301**, 076 (2013), 1209.4657.
- [39] P. Fayet, *Spontaneously Broken Supersymmetric Theories of Weak, Electromagnetic and Strong Interactions*, *Phys.Lett.* **B69**, 489 (1977).
- [40] M. Cvetič, D. A. Demir, J. Espinosa, L. Everett, and P. Langacker, *Electroweak breaking and the mu problem in supergravity models with an additional $U(1)$* , *Phys.Rev.* **D56**, 2861 (1997), hep-ph/9703317.
- [41] J. Erler, P. Langacker, and T.-j. Li, *The $Z - Z'$ mass hierarchy in a supersymmetric model with a secluded $U(1)$ -prime breaking sector*, *Phys.Rev.* **D66**, 015002 (2002), hep-ph/0205001.
- [42] S. F. King, S. Moretti, and R. Nevzorov, *Theory and phenomenology of an exceptional supersymmetric standard model*, *Phys. Rev.* **D73**, 035009 (2006), hep-ph/0510419.
- [43] S. Dimopoulos and D. W. Sutter, *The Supersymmetric flavor problem*, *Nucl.Phys.* **B452**, 496 (1995), hep-ph/9504415.
- [44] G. D. Kribs, E. Poppitz, and N. Weiner, *Flavor in supersymmetry with an extended R -symmetry*, *Phys.Rev.* **D78**, 055010 (2008), 0712.2039.
- [45] P. Athron, S. King, D. Miller, S. Moretti, and R. Nevzorov, *Constrained Exceptional Supersymmetric Standard Model with a Higgs Near 125 GeV*, *Phys.Rev.* **D86**, 095003 (2012), 1206.5028.

- [46] C. Balazs, A. Mazumdar, E. Pukartas, and G. White, *Baryogenesis, dark matter and inflation in the Next-to-Minimal Supersymmetric Standard Model*, (2013), 1309.5091.
- [47] P. Binetruy, S. Dawson, I. Hinchliffe, and M. Sher, *Phenomenologically Viable Models From Superstrings?*, *Nucl.Phys.* **B273**, 501 (1986).
- [48] J. R. Ellis, K. Enqvist, D. V. Nanopoulos, and F. Zwirner, *Aspects of the Superunification of Strong, Electroweak and Gravitational Interactions*, *Nucl.Phys.* **B276**, 14 (1986).
- [49] L. E. Ibanez and J. Mas, *Low-energy Supergravity and Superstring Inspired Models*, *Nucl.Phys.* **B286**, 107 (1987).
- [50] E. Witten, *Dimensional Reduction of Superstring Models*, *Phys.Lett.* **B155**, 151 (1985).
- [51] E. Witten, *Symmetry Breaking Patterns in Superstring Models*, *Nucl.Phys.* **B258**, 75 (1985).
- [52] P. Candelas, G. T. Horowitz, A. Strominger, and E. Witten, *Vacuum Configurations for Superstrings*, *Nucl.Phys.* **B258**, 46 (1985).
- [53] A. Vilenkin, *Cosmic Strings and Domain Walls*, *Phys.Rept.* **121**, 263 (1985).
- [54] P. Athron, S. King, D. Miller, S. Moretti, and R. Nevzorov, *The Constrained Exceptional Supersymmetric Standard Model*, *Phys.Rev.* **D80**, 035009 (2009), 0904.2169.
- [55] L. J. Hall, *Grand Unification of Effective Gauge Theories*, *Nucl. Phys.* **B178**, 75 (1981).
- [56] A. Voigt, *The Calculation of Threshold Corrections to Renormalization Group Running in the Exceptional Supersymmetric Standard Model*, Diploma thesis, TU Dresden, 2010.
- [57] P. Athron, D. Stöckinger and A. Voigt, *Threshold Corrections in the Exceptional Supersymmetric Standard Model*, *Phys.Rev.* **D86**, 095012 (2012), 1209.1470.
- [58] H. Baer, J. Ferrandis, K. Melnikov, and X. Tata, *Relating bottom quark mass in DR-BAR and MS-BAR regularization schemes*, *Phys.Rev.* **D66**, 074007 (2002), hep-ph/0207126.
- [59] J. Vermaseren, S. Larin, and T. van Ritbergen, *The four loop quark mass anomalous dimension and the invariant quark mass*, *Phys.Lett.* **B405**, 327 (1997), hep-ph/9703284.
- [60] B. Allanach, *SOFTSUSY: a program for calculating supersymmetric spectra*, *Comput.Phys.Commun.* **143**, 305 (2002), hep-ph/0104145.

- [61] S. P. Martin and M. T. Vaughn, *Two loop renormalization group equations for soft supersymmetry breaking couplings*, *Phys.Rev.* **D50**, 2282 (1994), hep-ph/9311340.
- [62] Y. Yamada, *Two loop renormalization group equations for soft SUSY breaking scalar interactions: Supergraph method*, *Phys.Rev.* **D50**, 3537 (1994), hep-ph/9401241.
- [63] M. Sperling, D. Stöckinger, and A. Voigt, *Renormalization of vacuum expectation values in spontaneously broken gauge theories*, *JHEP* **1307**, 132 (2013), 1305.1548.
- [64] M. Sperling, D. Stöckinger, and A. Voigt, *Renormalization of vacuum expectation values in spontaneously broken gauge theories: Two-loop results*, *JHEP* **1401**, 068 (2014), 1310.7629.
- [65] ATLAS Collaboration, G. Aad *et al.*, *Search for gluinos in events with two same-sign leptons, jets and missing transverse momentum with the ATLAS detector in pp collisions at $\sqrt{s} = 7$ TeV*, *Phys.Rev.Lett.* **108**, 241802 (2012), 1203.5763.
- [66] ATLAS Collaboration, G. Aad *et al.*, *Search for long-lived stopped R-hadrons decaying out-of-time with pp collisions using the ATLAS detector*, *Phys.Rev.* **D88**, 112003 (2013), 1310.6584.
- [67] CERN Report No. ATLAS-CONF-2013-061, 2013 (unpublished).
- [68] ATLAS Collaboration, G. Aad *et al.*, *Combined search for the Standard Model Higgs boson using up to 4.9 fb^{-1} of pp collision data at $\sqrt{s} = 7$ TeV with the ATLAS detector at the LHC*, *Phys.Lett.* **B710**, 49 (2012), 1202.1408.
- [69] CMS Collaboration, S. Chatrchyan *et al.*, *Combined results of searches for the standard model Higgs boson in pp collisions at $\sqrt{s} = 7$ TeV*, *Phys.Lett.* **B710**, 26 (2012), 1202.1488.
- [70] P. Athron, S. King, D. Miller, S. Moretti, and R. Nevzorov, *LHC Signatures of the Constrained Exceptional Supersymmetric Standard Model*, *Phys.Rev.* **D84**, 055006 (2011), 1102.4363.
- [71] ATLAS Collaboration, *Search for squarks and gluinos using final states with jets and missing transverse momentum with the ATLAS detector in $\sqrt{s} = 7$ TeV proton-proton collisions*, (2012).
- [72] ATLAS Collaboration, *Hunt for new phenomena using large jet multiplicities and missing transverse momentum with ATLAS in $L = 4.7 \text{ fb}^{-1}$ of $\sqrt{s} = 7$ TeV proton-proton collisions*, (2012).

- [73] ATLAS Collaboration, *Further search for supersymmetry at $\sqrt{s} = 7$ TeV in final states with jets, missing transverse momentum and one isolated lepton*, (2012).
- [74] C. Rogan, *Kinematical variables towards new dynamics at the LHC*, (2010), 1006.2727.
- [75] CMS Collaboration, C. Collaboration, *Search for supersymmetry with the razor variables at CMS*, (2012).
- [76] CMS Collaboration, C. Collaboration, *Search for Supersymmetry in hadronic final states using MT_2 with the CMS detector at 7 TeV*, (2012).
- [77] ATLAS Collaboration, *Search for new phenomena using large jet multiplicities and missing transverse momentum with ATLAS in 5.8 fb^{-1} of $\sqrt{s} = 8$ TeV proton-proton collisions*, (2012).
- [78] ATLAS Collaboration, *Search for supersymmetry at $\sqrt{s} = 8$ TeV in final states with jets, missing transverse momentum and one isolated lepton*, (2012).
- [79] ATLAS Collaboration, *Search for Supersymmetry in final states with two same-sign leptons, jets and missing transverse momentum with the ATLAS detector in pp collisions at $\sqrt{s} = 8$ TeV*, (2012).
- [80] ATLAS Collaboration, *Search for squarks and gluinos with the ATLAS detector using final states with jets and missing transverse momentum and 5.8 fb^{-1} of $\sqrt{s} = 8$ TeV proton-proton collision data*, (2012).
- [81] CMS Collaboration, S. Chatrchyan *et al.*, *Search for narrow resonances in dilepton mass spectra in pp collisions at $\sqrt{s} = 7$ TeV*, *Phys.Lett.* **B714**, 158 (2012), 1206.1849.
- [82] ATLAS Collaboration, *Search for Scalar Top Quark Pair Production in Natural Gauge Mediated Supersymmetry Models with the ATLAS Detector in pp Collisions at $\sqrt{s} = 7$ TeV*, (2012).
- [83] ATLAS Collaboration, G. Aad *et al.*, *Search for scalar bottom pair production with the ATLAS detector in pp Collisions at $\sqrt{s} = 7$ TeV*, *Phys.Rev.Lett.* **108**, 181802 (2012), 1112.3832.
- [84] J. P. Hall and S. F. King, *Neutralino Dark Matter with Inert Higgsinos and Singlinos*, *JHEP* **0908**, 088 (2009), 0905.2696.
- [85] J. Hall *et al.*, *Novel Higgs Decays and Dark Matter in the $E(6)$ SSM*, *Phys.Rev.* **D83**, 075013 (2011), 1012.5114.
- [86] S. F. King and A. Merle, *Warm Dark Matter from keVins*, *JCAP* **1208**, 016 (2012), 1205.0551.

- [87] J. P. Hall and S. F. King, *Bino Dark Matter and Big Bang Nucleosynthesis in the Constrained E_6 SSM with Massless Inert Singlinos*, *JHEP* **1106**, 006 (2011), 1104.2259.
- [88] P. Athron, S. King, D. Miller, S. Moretti, and R. Nevzorov, *Predictions of the Constrained Exceptional Supersymmetric Standard Model*, *Phys.Lett.* **B681**, 448 (2009), 0901.1192.
- [89] CERN Report No. ATLAS-CONF-2013-051, 2013 (unpublished), Not published in the proceedings.
- [90] CERN Report No. ATLAS-CONF-2013-056, 2013 (unpublished).
- [91] S. Weinberg, *A Model of Leptons*, *Phys.Rev.Lett.* **19**, 1264 (1967).
- [92] A. Salam, *Weak and Electromagnetic Interactions*, *Conf.Proc.* **C680519**, 367 (1968).
- [93] S. Glashow, J. Iliopoulos, and L. Maiani, *Weak Interactions with Lepton-Hadron Symmetry*, *Phys.Rev.* **D2**, 1285 (1970).
- [94] P. W. Higgs, *Broken symmetries, massless particles and gauge fields*, *Phys.Lett.* **12**, 132 (1964).
- [95] F. Englert and R. Brout, *Broken symmetry and the mass of gauge vector mesons*, *Phys. Rev. Lett.* **13**, 321 (1964).
- [96] G. S. Guralnik, C. R. Hagen, and T. W. B. Kibble, *Global conservation laws and massless particles*, *Phys. Rev. Lett.* **13**, 585 (1964).
- [97] T. Kibble, *Symmetry breaking in nonAbelian gauge theories*, *Phys.Rev.* **155**, 1554 (1967).
- [98] G. 't Hooft, *Renormalization of Massless Yang-Mills Fields*, *Nucl.Phys.* **B33**, 173 (1971).
- [99] G. 't Hooft, *Renormalizable Lagrangians for Massive Yang-Mills Fields*, *Nucl.Phys.* **B35**, 167 (1971).
- [100] G. 't Hooft and M. Veltman, *Regularization and Renormalization of Gauge Fields*, *Nucl.Phys.* **B44**, 189 (1972).
- [101] B. Lee and J. Zinn-Justin, *Spontaneously Broken Gauge Symmetries. 1. Preliminaries*, *Phys.Rev.* **D5**, 3121 (1972).
- [102] B. Lee and J. Zinn-Justin, *Spontaneously broken gauge symmetries. 2. Perturbation theory and renormalization*, *Phys.Rev.* **D5**, 3137 (1972).
- [103] B. Lee and J. Zinn-Justin, *Spontaneously broken gauge symmetries. 3. Equivalence*, *Phys.Rev.* **D5**, 3155 (1972).

- [104] A. Freitas and D. Stöckinger, *Gauge dependence and renormalization of tan beta in the MSSM*, *Phys.Rev.* **D66**, 095014 (2002), hep-ph/0205281.
- [105] W. Siegel, *Supersymmetric Dimensional Regularization via Dimensional Reduction*, *Phys. Lett.* **B84**, 193 (1979).
- [106] D. Capper, D. Jones, and P. van Nieuwenhuizen, *Regularization by Dimensional Reduction of Supersymmetric and Nonsupersymmetric Gauge Theories*, *Nucl.Phys.* **B167**, 479 (1980).
- [107] P. H. Chankowski, S. Pokorski, and J. Rosiek, *Complete on-shell renormalization scheme for the minimal supersymmetric Higgs sector*, *Nucl.Phys.* **B423**, 437 (1994), hep-ph/9303309.
- [108] M. E. Machacek and M. T. Vaughn, *Two Loop Renormalization Group Equations in a General Quantum Field Theory. 1. Wave Function Renormalization*, *Nucl.Phys.* **B222**, 83 (1983).
- [109] M. E. Machacek and M. T. Vaughn, *Two Loop Renormalization Group Equations in a General Quantum Field Theory. 2. Yukawa Couplings*, *Nucl.Phys.* **B236**, 221 (1984).
- [110] M. E. Machacek and M. T. Vaughn, *Two Loop Renormalization Group Equations in a General Quantum Field Theory. 3. Scalar Quartic Couplings*, *Nucl.Phys.* **B249**, 70 (1985).
- [111] I. Jack and D. Jones, *Soft supersymmetry breaking and finiteness*, *Phys.Lett.* **B333**, 372 (1994), hep-ph/9405233.
- [112] F. Staub, *Automatic Calculation of supersymmetric Renormalization Group Equations and Self Energies*, *Comput.Phys.Commun.* **182**, 808 (2011), 1002.0840.
- [113] F. Staub, T. Ohl, W. Porod, and C. Speckner, *A Tool Box for Implementing Supersymmetric Models*, *Comput.Phys.Commun.* **183**, 2165 (2012), 1109.5147.
- [114] P. Athron, J.-h. Park, D. Stöckinger, and A. Voigt, *FlexibleSUSY – A spectrum generator generator for supersymmetric models*, (2014), 1406.2319.
- [115] L. D. Faddeev and V. N. Popov, *Feynman diagrams for the Yang-Mills field*, *Phys. Lett.* **B25**, 29 (1967).
- [116] C. Becchi, A. Rouet, and R. Stora, *Renormalization of Gauge Theories*, *Annals Phys.* **98**, 287 (1976).
- [117] R. K. Ellis, W. J. Stirling, and B. Webber, *QCD and collider physics*, *Camb.Monogr.Part.Phys.Nucl.Phys.Cosmol.* **8**, 1 (1996).
- [118] C. Itzykson and J. Zuber, *QUANTUM FIELD THEORY*, (1980).

- [119] E. Kraus and K. Sibold, *Rigid invariance as derived from BRS invariance: The Abelian Higgs model*, *Z.Phys.* **C68**, 331 (1995), hep-th/9503140.
- [120] M.-x. Luo, H.-w. Wang, and Y. Xiao, *Two loop renormalization group equations in general gauge field theories*, *Phys.Rev.* **D67**, 065019 (2003), hep-ph/0211440.
- [121] C. Becchi, A. Rouet, and R. Stora, *The Abelian Higgs-Kibble Model. Unitarity of the S Operator*, *Phys.Lett.* **B52**, 344 (1974).
- [122] C. Becchi, A. Rouet, and R. Stora, *Renormalization of the Abelian Higgs-Kibble Model*, *Commun.Math.Phys.* **42**, 127 (1975).
- [123] O. Piguet and S. Sorella, *Algebraic renormalization: Perturbative renormalization, symmetries and anomalies*, *Lect.Notes Phys.* **M28**, 1 (1995).
- [124] F. Brandt, N. Dragon, and M. Kreuzer, *All consistent Yang-Mills anomalies*, *Physics Letters B* **231**, 263 (1989).
- [125] J. Taylor, *Ward Identities and Charge Renormalization of the Yang-Mills Field*, *Nucl.Phys.* **B33**, 436 (1971).
- [126] A. Slavnov, *Ward Identities in Gauge Theories*, *Theor.Math.Phys.* **10**, 99 (1972).
- [127] G. 't Hooft and M. Veltman, *Combinatorics of gauge fields*, *Nucl.Phys.* **B50**, 318 (1972).
- [128] B. Lee and J. Zinn-Justin, *Spontaneously Broken Gauge Symmetries. 4. General Gauge Formulation*, *Phys.Rev.* **D7**, 1049 (1973).
- [129] R. Peccei and H. R. Quinn, *CP Conservation in the Presence of Instantons*, *Phys.Rev.Lett.* **38**, 1440 (1977).
- [130] M. Böhm, A. Denner, and H. Joos, *Gauge Theories of the Strong and Electroweak Interaction*, 3rd ed. (Teubner, Stuttgart, 2001).
- [131] M.-x. Luo and Y. Xiao, *Renormalization group equations in gauge theories with multiple $U(1)$ groups*, *Phys.Lett.* **B555**, 279 (2003), hep-ph/0212152.
- [132] R. M. Fonseca, M. Malinsky, W. Porod, and F. Staub, *Running soft parameters in SUSY models with multiple $U(1)$ gauge factors*, *Nucl.Phys.* **B854**, 28 (2012), 1107.2670.
- [133] R. M. Fonseca, M. Malinský, and F. Staub, *Renormalization group equations and matching in a general quantum field theory with kinetic mixing*, *Phys.Lett.* **B726**, 882 (2013), 1308.1674.
- [134] S. P. Martin and M. T. Vaughn, *Regularization dependence of running couplings in softly broken supersymmetry*, *Phys.Lett.* **B318**, 331 (1993), hep-ph/9308222.

- [135] D. Stöckinger and P. Varšo, *FeynArts model file for MSSM transition counterterms from DREG to DRED*, *Comput.Phys.Commun.* **183**, 422 (2012), 1109.6484.
- [136] B. Allanach, P. Athron, L. C. Tunstall, A. Voigt, and A. Williams, *Next-to-Minimal SOFTSUSY*, (2013), 1311.7659.
- [137] F. Staub, *SARAH 4: A tool for (not only SUSY) model builders*, (2013), 1309.7223.
- [138] S. Moretti, S. Munir, and P. Poulou, *125 GeV Higgs Boson signal within the complex NMSSM*, *Phys.Rev.* **D89**, 015022 (2014), 1305.0166.
- [139] J. Cao, F. Ding, C. Han, J. M. Yang, and J. Zhu, *A light Higgs scalar in the NMSSM confronted with the latest LHC Higgs data*, *JHEP* **1311**, 018 (2013), 1309.4939.
- [140] S. King, M. Muhlleitner, and R. Nevzorov, *NMSSM Higgs Benchmarks Near 125 GeV*, *Nucl.Phys.* **B860**, 207 (2012), 1201.2671.
- [141] J. F. Gunion, Y. Jiang, and S. Kraml, *The Constrained NMSSM and Higgs near 125 GeV*, *Phys.Lett.* **B710**, 454 (2012), 1201.0982.
- [142] BayesFITS Group, K. Kowalska *et al.*, *Constrained next-to-minimal supersymmetric standard model with a 126 GeV Higgs boson: A global analysis*, *Phys.Rev.* **D87**, 115010 (2013), 1211.1693.
- [143] T. Gherghetta, B. von Harling, A. D. Medina, and M. A. Schmidt, *The Scale-Invariant NMSSM and the 126 GeV Higgs Boson*, *JHEP* **02**, 032 (2013), 1212.5243.
- [144] D. G. Cerdeño, P. Ghosh, C. B. Park, and M. Peiró, *Collider signatures of a light NMSSM pseudoscalar in neutralino decays in the light of LHC results*, *JHEP* **1402**, 048 (2014), 1307.7601.
- [145] U. Ellwanger and C. Hugonie, *NMSPEC: A Fortran code for the sparticle and Higgs masses in the NMSSM with GUT scale boundary conditions*, *Comput.Phys.Commun.* **177**, 399 (2007), hep-ph/0612134.
- [146] F. Staub, *SARAH 3.2: Dirac Gauginos, UFO output, and more*, *Computer Physics Communications* **184**, pp. 1792 (2013), 1207.0906.
- [147] W. Porod, *SPheno, a program for calculating supersymmetric spectra, SUSY particle decays and SUSY particle production at e+ e- colliders*, *Comput.Phys.Commun.* **153**, 275 (2003), hep-ph/0301101.
- [148] W. Porod and F. Staub, *SPheno 3.1: Extensions including flavour, CP-phases and models beyond the MSSM*, *Comput.Phys.Commun.* **183**, 2458 (2012), 1104.1573.

- [149] B. Allanach *et al.*, *SUSY Les Houches Accord 2*, *Comput.Phys.Commun.* **180**, 8 (2009), 0801.0045.
- [150] S. Munir, *Novel Higgs-to-125 GeV Higgs boson decays in the complex NMSSM*, (2013), 1310.8129.
- [151] S. King, M. Mühlleitner, R. Nevzorov, and K. Walz, *Natural NMSSM Higgs Bosons*, *Nucl.Phys.* **B870**, 323 (2013), 1211.5074.
- [152] R. Barbieri, D. Buttazzo, K. Kannike, F. Sala, and A. Tesi, *Exploring the Higgs sector of a most natural NMSSM*, *Phys.Rev.* **D87**, 115018 (2013), 1304.3670.
- [153] M. Badziak, M. Olechowski, and S. Pokorski, *125 GeV Higgs and enhanced diphoton signal of a light singlet-like scalar in NMSSM*, (2013), 1310.4518.
- [154] D. T. Nhung, M. Muhlleitner, J. Streicher, and K. Walz, *Higher Order Corrections to the Trilinear Higgs Self-Couplings in the Real NMSSM*, *JHEP* **1311**, 181 (2013), 1306.3926.
- [155] B. Allanach and M. Bernhardt, *Including R-parity violation in the numerical computation of the spectrum of the minimal supersymmetric standard model: SOFTSUSY*, *Comput.Phys.Commun.* **181**, 232 (2010), 0903.1805.
- [156] B. Allanach, C. Kom, and M. Hanussek, *Computation of Neutrino Masses in R-parity Violating Supersymmetry: SOFTSUSY3.2*, *Comput.Phys.Commun.* **183**, 785 (2012), 1109.3735.
- [157] B. Allanach, S. Kraml, and W. Porod, *Theoretical uncertainties in sparticle mass predictions from computational tools*, *JHEP* **0303**, 016 (2003), hep-ph/0302102.
- [158] B. Allanach, A. Djouadi, J. Kneur, W. Porod, and P. Slavich, *Precise determination of the neutral Higgs boson masses in the MSSM*, *JHEP* **0409**, 044 (2004), hep-ph/0406166.
- [159] D. Jones, *Asymptotic Behavior of Supersymmetric Yang-Mills Theories in the Two Loop Approximation*, *Nucl.Phys.* **B87**, 127 (1975).
- [160] D. Jones and L. Mezincescu, *The Beta Function in Supersymmetric Yang-Mills Theory*, *Phys.Lett.* **B136**, 242 (1984).
- [161] P. C. West, *The Yukawa beta Function in $N = 1$ Rigid Supersymmetric Theories*, *Phys.Lett.* **B137**, 371 (1984).
- [162] Y. Yamada, *Two loop renormalization of gaugino masses in general supersymmetric gauge models*, *Phys.Rev.Lett.* **72**, 25 (1994), hep-ph/9308304.
- [163] V. D. Barger, M. Berger, and P. Ohmann, *The Supersymmetric particle spectrum*, *Phys.Rev.* **D49**, 4908 (1994), hep-ph/9311269.

- [164] A. Alexandrescu, *Modern C++ design : generic programming and design patterns applied* (Addison-Wesley, 2001).
- [165] A. Dedes and P. Slavich, *Two loop corrections to radiative electroweak symmetry breaking in the MSSM*, *Nucl.Phys.* **B657**, 333 (2003), hep-ph/0212132.
- [166] A. Dedes, G. Degrassi, and P. Slavich, *On the two loop Yukawa corrections to the MSSM Higgs boson masses at large tan beta*, *Nucl.Phys.* **B672**, 144 (2003), hep-ph/0305127.
- [167] A. Brignole, G. Degrassi, P. Slavich, and F. Zwirner, *On the $O(\alpha_t^2)$ two loop corrections to the neutral Higgs boson masses in the MSSM*, *Nucl.Phys.* **B631**, 195 (2002), hep-ph/0112177.
- [168] G. Degrassi and P. Slavich, *On the radiative corrections to the neutral Higgs boson masses in the NMSSM*, *Nucl.Phys.* **B825**, 119 (2010), 0907.4682.
- [169] B. Allanach, *SUSY Predictions and SUSY Tools at the LHC*, *Eur.Phys.J.* **C59**, 427 (2009), 0805.2088.
- [170] P. Minkowski, $\mu \rightarrow e\gamma$ at a Rate of One Out of 1-Billion Muon Decays?, *Phys.Lett.* **B67**, 421 (1977).
- [171] T. Yanagida, *HORIZONTAL SYMMETRY AND MASSES OF NEUTRINOS*, *Conf.Proc.* **C7902131**, 95 (1979).
- [172] M. Gell-Mann, P. Ramond, and R. Slansky, *Complex Spinors and Unified Theories*, *Conf.Proc.* **C790927**, 315 (1979), 1306.4669.
- [173] R. N. Mohapatra and G. Senjanovic, *Neutrino Mass and Spontaneous Parity Violation*, *Phys.Rev.Lett.* **44**, 912 (1980).
- [174] G. Guennebaud *et al.*, Eigen v3, <http://eigen.tuxfamily.org>, 2010.
- [175] T. Veldhuizen, *Expression Templates*, *C++ Report* **7**, 26 (1995).
- [176] P. Z. Skands *et al.*, *SUSY Les Houches accord: Interfacing SUSY spectrum calculators, decay packages, and event generators*, *JHEP* **0407**, 036 (2004), hep-ph/0311123.
- [177] The GNU Project, GSL – gnu scientific library, <https://gnu.org/software/gsl/>, 1996.
- [178] G. Passarino and M. Veltman, *One Loop Corrections for $e^+ e^-$ Annihilation Into $\mu^+ \mu^-$ in the Weinberg Model*, *Nucl.Phys.* **B160**, 151 (1979).
- [179] D. M. Pierce, J. A. Bagger, K. T. Matchev, and R.-j. Zhang, *Precision corrections in the minimal supersymmetric standard model*, *Nucl.Phys.* **B491**, 3 (1997), hep-ph/9606211.

- [180] D. Chowdhury, R. Garani, and S. K. Vempati, *SUSEFLAV: Program for supersymmetric mass spectra with seesaw mechanism and rare lepton flavor violating decays*, *Comput.Phys.Commun.* **184**, 899 (2013), 1109.3551.
- [181] F. E. Paige, S. D. Protopopescu, H. Baer, and X. Tata, *ISAJET 7.69: A Monte Carlo event generator for pp, anti-p p, and e+e- reactions*, (2003), hep-ph/0312045.
- [182] A. Djouadi, J.-L. Kneur, and G. Moultaka, *SuSpect: A Fortran code for the supersymmetric and Higgs particle spectrum in the MSSM*, *Comput.Phys.Commun.* **176**, 426 (2007), hep-ph/0211331.
- [183] G. Degrandi, P. Slavich, and F. Zwirner, *On the neutral Higgs boson masses in the MSSM for arbitrary stop mixing*, *Nucl.Phys.* **B611**, 403 (2001), hep-ph/0105096.
- [184] A. Brignole, G. Degrandi, P. Slavich, and F. Zwirner, *On the two loop sbottom corrections to the neutral Higgs boson masses in the MSSM*, *Nucl.Phys.* **B643**, 79 (2002), hep-ph/0206101.
- [185] A. Bednyakov, A. Onishchenko, V. Velizhanin, and O. Veretin, *Two loop $O(\alpha_s^2)$ MSSM corrections to the pole masses of heavy quarks*, *Eur.Phys.J.* **C29**, 87 (2003), hep-ph/0210258.
- [186] U. Ellwanger and C. Hugonie, *The Upper bound on the lightest Higgs mass in the NMSSM revisited*, *Mod.Phys.Lett.* **A22**, 1581 (2007), hep-ph/0612133.
- [187] P. Athron, S. King, D. Miller, S. Moretti, and R. Nevzorov, *Electroweak symmetry breaking in the $E(6)$ SSM*, *J.Phys.Conf.Ser.* **110**, 072001 (2008), 0708.3248.
- [188] J. R. Ellis, K. A. Olive, and P. Sandick, *Phenomenology of GUT-less supersymmetry breaking*, *JHEP* **0706**, 079 (2007), 0704.3446.
- [189] J. R. Ellis, K. A. Olive, and P. Sandick, *What if supersymmetry breaking appears below the GUT scale?*, *Phys.Lett.* **B642**, 389 (2006), hep-ph/0607002.
- [190] J. Ellis, F. Luo, K. A. Olive, and P. Sandick, *The Higgs Mass beyond the CMSSM*, *Eur.Phys.J.* **C73**, 2403 (2013), 1212.4476.
- [191] Y. Hosotani, *Dynamical Mass Generation by Compact Extra Dimensions*, *Phys.Lett.* **B126**, 309 (1983).
- [192] J. L. Hewett and T. G. Rizzo, *Low-Energy Phenomenology of Superstring Inspired $E(6)$ Models*, *Phys.Rept.* **183**, 193 (1989).
- [193] P. Langacker, *The Physics of Heavy Z' Gauge Bosons*, *Rev.Mod.Phys.* **81**, 1199 (2009), 0801.1345.

- [194] J. Rich, D. Lloyd Owen, and M. Spiro, *Experimental particle physics without accelerators*, *Phys. Rept.* **151**, 239 (1987).
- [195] P. F. Smith, *Terrestrial searches for new stable particles*, *Contemp. Phys.* **29**, 159 (1988).
- [196] T. K. Hemmick *et al.*, *A search for anomalously heavy isotopes of low z nuclei*, *Phys. Rev.* **D41**, 2074 (1990).
- [197] R. Howl and S. King, *Solving the Flavour Problem in Supersymmetric Standard Models with Three Higgs Families*, *Phys.Lett.* **B687**, 355 (2010), 0908.2067.
- [198] R. Nevzorov, *E6 Inspired SUSY Models with Exact Custodial Symmetry*, *Phys.Rev.* **D87**, 015029 (2013), 1205.5967.

Publications

The work in this thesis is based on research carried out at the Institut für Kern- und Teilchenphysik, Technische Universität Dresden.

The research described in this thesis was funded by the German Research Foundation DFG, through the Research Training Group 1504 and Grant No. STO876/2-1.

The research described in this thesis was carried out in collaboration with Prof. Dr. Benjamin Allanach, Dr. Peter Athron, Dr. Jae-hyeon Park, Dipl.-Phys. Marcus Sperling, Prof. Dr. Dominik Stöckinger, Dr. Lewis Tunstall, Prof. Dr. Anthony Williams.

Refereed Publications

1. Dominik Dannheim, Alexander Voigt, Karl-Johan Grahn, Peter Speckmayer, Tancredi Carli, *PDE-Foam: A probability density estimation method using self-adapting phase-space binning*, *Nucl. Instrum. Meth.* **A606**, 717 (2009) [arXiv:0812.0922]
2. Peter Athron, Dominik Stöckinger, Alexander Voigt, *Threshold Corrections in the Exceptional Supersymmetric Standard Model*, *Phys. Rev.* **D86**, 095012 (2012) [arXiv:1209.1470]
3. Marcus Sperling, Dominik Stöckinger, Alexander Voigt, *Renormalization of vacuum expectation values in spontaneously broken gauge theories*, *JHEP* **1307**, 132 (2013) [arXiv:1305.1548]
4. Marcus Sperling, Dominik Stöckinger, Alexander Voigt, *Renormalization of vacuum expectation values in spontaneously broken gauge theories: Two-loop results*, *JHEP* **1401**, 068 (2014) [arXiv:1310.7629]
5. B.C. Allanach, P. Athron, Lewis C. Tunstall, A. Voigt, A.G. Williams, *Next-to-Minimal SOFTSUSY*, *Comput. Phys. Commun.* **185**, 2322 (2014) [arXiv:1311.7659]

Preprints

6. Peter Athron, Jae-hyeon Park, Dominik Stöckinger, Alexander Voigt, *Flexible-SUSY — A spectrum generator for supersymmetric models*, submitted to: Computer Physics Communications, [arXiv:1406.2319]

Acknowledgments

First of all I thank Dominik Stöckinger for giving me the great opportunity to deeply research in the field of supersymmetry, quantum field theory and algebraic renormalization.

Special thanks go to Peter Athron for introducing me into the world of spectrum generators and SUSY phenomenology. I am very thankful for the exceptional supervision, all the physics explanations, weekend support, amusing e-mails, hours of testing and debugging and for motivating me to write clean code.

I am particularly thankful to Jae-hyeon Park for carefully reviewing my code and for hundreds of neat C++ tricks.

I am equally thankful to Ben Allanach for inviting me to the beautiful Cambridge and giving me the opportunity to give a talk at the joint DAMTP-Cavendish HEP phenomenology seminar.

Many thanks for the careful reading of this thesis and lots of helpful remarks go to Peter Athron, Marcus Sperling, Christoph Gnendiger and Philip Diessner.

Finally, I would like to express my deepest gratefulness to my family and all my friends for all the priceless support over the years. Without you all of this work would not have been possible. I am especially grateful to my sister for giving me the most beautiful gift in the world.

Erklärung

Hiermit versichere ich, dass ich die vorliegende Arbeit ohne unzulässige Hilfe Dritter und ohne Benutzung anderer als der angegebenen Hilfsmittel angefertigt habe. Die aus fremden Quellen direkt oder indirekt übernommenen Gedanken sind als solche kenntlich gemacht. Die Arbeit wurde bisher weder im Inland noch im Ausland in gleicher oder ähnlicher Form einer anderen Prüfungsbehörde vorgelegt.

Die vorliegende Arbeit wurde am Institut für Kern- und Teilchenphysik der Technischen Universität Dresden unter wissenschaftlicher Betreuung von Herrn Prof. Dr. Dominik Stöckinger angefertigt.

Es haben keine früheren erfolglosen Promotionsverfahren stattgefunden.

Hiermit erkenne ich die Promotionsordnung der Fakultät für Mathematik und Naturwissenschaften der Technischen Universität Dresden vom 23. Februar 2011 an.

Alexander Voigt
Dresden, 16.06.2014